Section 5: Technical Sessions

Frontal Crash Protection and Pedestrian Protection

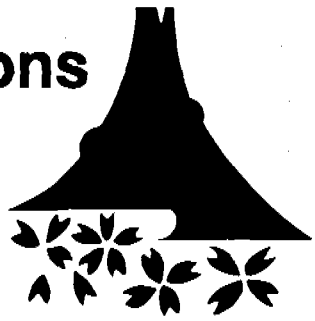

3661

Technical Session No. 1

Mr. Philip W. Davis, Chairman, United States

Compatibility and Passive Safety Terminology and Problematics

Dr. ULRICH BEZ and
Dr. WALTER SCHMID
Bayerisch Motoren Werke AG Germany

ABSTRACT

The different, semantic use of problem-relevant terms is proving an increasing obstacle to understanding among different experts and authors of technical literature. When is a vehicle safe, when is it compatible, what is risk of injury?

These are only a few of the fundamental terms whose meaning differs from author to author, from automobile manufacturer to automobile manufacturer, from country to country.

As a result of their work in various national and international bodies, the authors of this paper are constantly confronted with the problems resulting from different interpretation of such terms. Drawing on their own understanding of the problems involved and the effects of stipulations, the authors in their paper attempt to explain such terms on an application-oriented basis, to define them and to supplement, or at least round off, the "structure" by means of new terms. This paper is intended not only to be an aid to experts in informing others of their results but is also aimed at enabling the reader to understand what has become rather complex material.

INTRODUCTION

The subject of SAFETY IN ROAD TRAFFIC is as old as the invention of the wheel. In recent times—since 1970—efforts relating to this subject have intensified on a wide, international level.

Despite the age of this subject and the application of a massive engineering potential, there are problems of understanding on a national and international level—among experts and their discussion partners—greatly impeding the efficiency of all these efforts.

A study of the contents of literature meanwhile available regarding, e.g., COMPATIBILITY of vehicles in traffic accidents particularly reveals the problems involved.

What dominates is co-existence and ignorance.

The aim of this paper is to improve mutual understand-

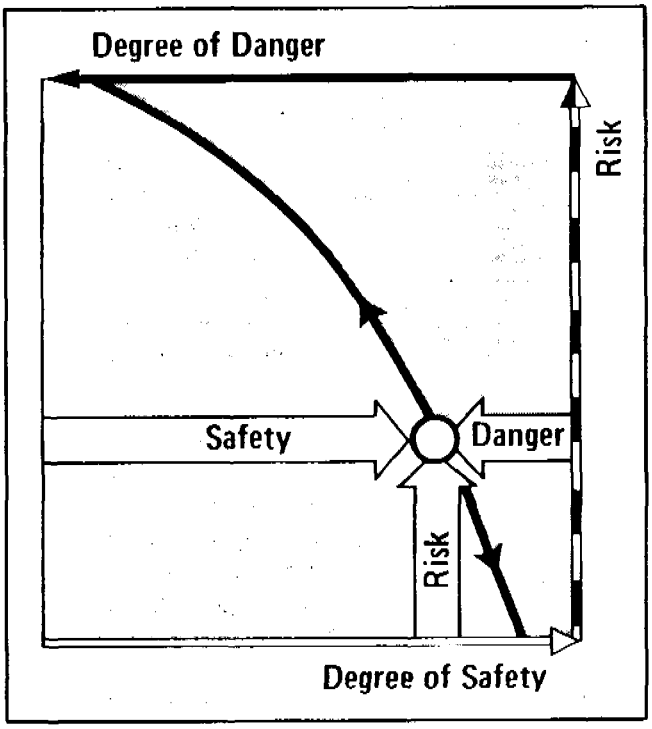

Figure 1. Scheme: Risk - Danger - Safety.

*Dr. Ing. h. c. F. Porsche AG until September 1982

ing between experts in industry and administration and to offer the experts a sound basis for a common goal-oriented approach.

Although the authors of this paper are aware of how difficult it is to change opinions once they have become ingrained and the problems which might confront common terminology, they nevertheless attempt to clarify the meaning of the terms PASSIVE SAFETY and COMPATIBILITY by means of a comprehensive consideration and then to define them relative to each other. For this consideration, it is necessary to somewhat delineate the meaning of terms in general usage such as DANGER, RISK or SAFETY.

SAFETY—DANGER—RISK

Life in itself is dangerous. The definition in DIN 31004 "SAFETY is the absence of DANGER" does admittedly imply a state of absolute safety. If, however, the focus of this consideration regarding SAFETY is humans with their health and wellbeing, an absolute level of safety is absolutely impossible for humans—due to the very nature of the matter.

As shown in Figure 1, there are only conditions described by a particular DEGREE OF SAFETY as well as by a DEGREE OF DANGER. It is not possible to transfer DEGREE OF SAFETY into AN OBJECT IS SAFE. Such statements are arbitrary.

This description of state does however enable a comparison to be made, e.g., of different means of transportation—whether expressed positively as DEGREE OF SAFETY or negatively as DEGREE OF DANGER. We can say, for instance, that means of transport A is safer than means of transport B. This necessitates laying down an absolute DEGREE OF SAFETY although it is sufficient to relate the objects under comparison to the same basis.

The term RISK is closely related to the DEGREE OF DANGER and thus to DEGREE OF SAFETY. A small RISK means a greater DEGREE OF SAFETY and smaller DEGREE OF DANGER.

- SAFETY is the probability of non-impairment of health and wellbeing of humans or non-damage to property.
- DANGER is the probability of impairment to health and wellbeing of humans or damage to property.
- The expressions SAFETY and DANGER are colloquial simplifications of DEGREE OF SAFETY and DEGREE OF DANGER. The term RISK is closely related to DANGER and SAFETY.
- Comparative considerations with the adjectives SAFE and DANGEROUS are possible, the prerequisite being: The same basis.
- The adjectives SAFE and DANGEROUS do not determine the actual state or behaviour of an object.

SAFETY IN ROAD TRAFFIC

Following the preceding section which was devoted to higher-order aspects dealing with terms, we now provide an overview of the complex known as road safety. A particular aim is to classify the terms PASSIVE SAFETY and COMPATIBILITY.

The four principal sectors determining safety in road traffic are:

The HUMAN
The VEHICLE
The ENVIRONMENT
The RESCUE SYSTEM

The human is a significant risk factor on the one hand as an active participant in traffic—being able to both avoid as well as to cause an accident as the result of his capabilities—and on the other hand in his capacity as a passive participant in an accident is the victim of the danger which he himself has frequently influenced. (Fig. 2.)

Depending on his constitution, his physical and psychic state, he represents a greater or smaller accident risk and consequently also an injury risk for himself and other humans, whether as driver of a vehicle or pedestrian by reacting, acting, judging in different ways.

The impairment of human health is influenced by the mechanical loads which can be sustained by head, thorax, pelvis and extremities. It can today be stated as a reliable

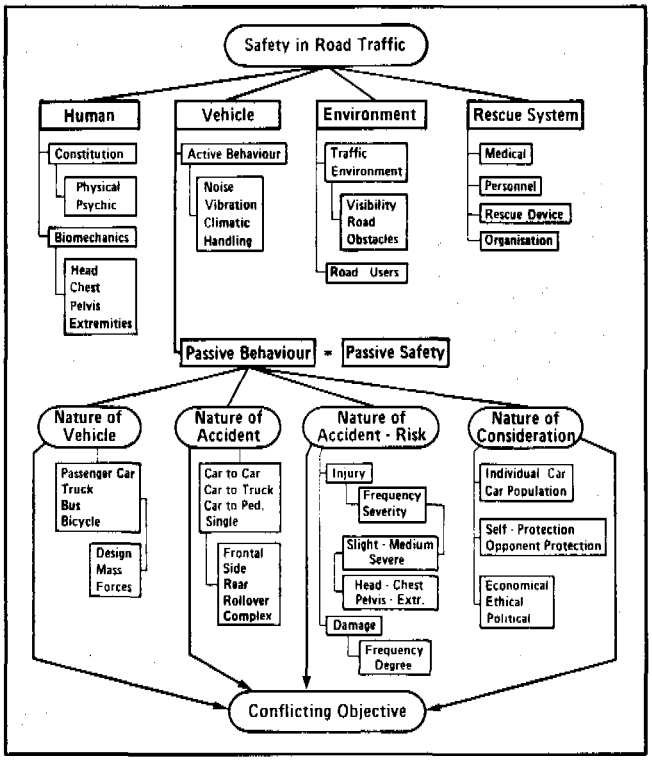

Figure 2. Structure of safety in road traffic.

fact that this load factor varies from human to human and is greatly dependent on age.

The behaviour of the vehicle is usually split up into an active and a passive sector.

In the active sector, a vehicle which is as quiet running as possible, dampens vibrations to the maximum extent possible and in which the air is properly conditioned provides the ideal requirements for maintaining the driver's concentration at a high level. Good road behaviour also comes under this sector. The terms PASSIVE SAFETY and COMPATIBILITY can be found under the heading of passive behaviour.

The environment affects vehicle safety inter alia by the visibility conditions existing, the condition of roads and any obstacles present. An essential factor is also the nature of other road users, e.g., other vehicles or pedestrians.

Rescue is significantly influenced by the human as rescuer and helper, by medicine (e.g., shock prophylaxis) by means of technical aids such as salvage tools or medical apparatus, as well as the organization set up to ensure that the right helpers are on the scene as rapidly as possible with the right equipment.

An attempt to change the degree of PASSIVE SAFETY results in fundamental conflicting objectives from the mutual influencing of the aforementioned principal sectors of passive safety, it being one of the principal tasks of the engineer to solve or reduce these conflicts.

Passive Safety

The definitions specified here are closely related to the terms elucidated.

- PASSIVE SAFETY deals with the effect of vehicle technology on the risk of injury to the human and property in defined accidents and with the biomechanical capacity of the human, which is assumed to be known.

The remarkable bandspread characterizing all known analyses of real traffic accidents is attributable primarily to the large bandspread of the biomechanical capacity of the human and the different accident conditions.

Measures to change PASSIVE SAFETY therefore require to be oriented on statistical characteristic values. Improvements to PASSIVE SAFETY result in a reduction in the ACCIDENT RISK by reducing INJURY SEVERITY and MATERIAL DAMAGE (Fig. 3.).

Using the designation, common in safety science, the severity of an accident becomes DEGREE OF DAMAGE S and the frequency of accident becomes PROBABILITY OF OCCURRENCE OF DAMAGE W and thus ACCIDENT RISK R.

$$R = S \cdot W$$

- PASSIVE SAFETY influences the degree of ACCIDENT SEVERITY primarily and independently

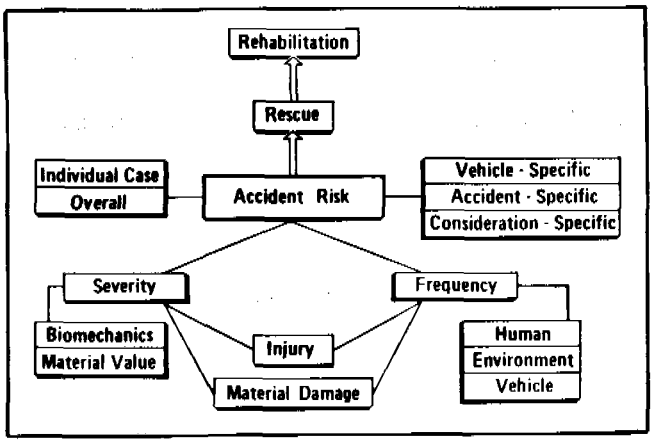

Figure 3. Structure of accident risk. Rescue as a filter function determines final rehabilitation.

of whom is involved in the damage or of how it is distributed.

Conflicts

Changing individual elements of the four principal sectors of PASSIVE SAFETY (Fig. 2) is still the method most widely used today to improve the degree of safety.

Development engineers in the automobile industry recognized early on, however, that a consequent reduction of the risk of injury, e.g., when impacting against a solid wall, can increase the risk of injury in other types of accidents, such as a head-on and side collision involving different vehicles.

It is therefore questionable in respect of a large number of legislative efforts based on individual elements—e.g., impact against wall, post laterally, etc.—whether they in fact increase PASSIVE SAFETY.

Solving such conflicts first of all demands researching the causes and mechanisms contributing to the occurrence of damage. It is then necessary to balance the attainable improvements on the one hand with any impairments which may have to be accepted on the other hand.

- Problems of the DISTRIBUTION OF ACCIDENT RISKS thus exist in the cases of conflicts.

Compatibility

Based on the knowledge of this problem of distribution, the following terminology is therefore proposed.

- COMPATIBILITY is concerned with the mutual influencing of elements of the four principal groups of PASSIVE SAFETY:

  Nature of collision
  Nature of vehicle
  Nature of risk
  Nature of consideration

Nature of collision is, e.g., single-vehicle collision, front-end, side or rear-end collision with other vehicles or rollover. Nature of risk of accident relates, e.g., to material damage or slight or severe injury to different parts of the body.

Apart from different types of private cars, we must reckon with collisions concerning trucks, buses and two-wheeled vehicles.

- COMPATIBILITY PROBLEMS are problems in which defined vehicle changes on the one hand increase PASSIVE SAFETY, reduce the risk of accident at that point while on the other hand increasing another ACCIDENT RISK.
- Compatibility influences the statistical accident risk of the entire number of all accidents via the distribution of the accident risk in the individual case and thus the DEGREE OF PASSIVE SAFETY.

In the same way as with the term SAFETY, a state of complete COMPATIBILITY is not possible since defined distributions are in themselves only variants which can only be assessed and arranged by employing further criteria. For this reason, the DEGREE OF COMPATIBILITY is decisively influenced by the criteria employed.

When dealing with compatibility problems, the viewpoint of the observer is of elementary significance. The primary consideration may be self protection, protection of other traffic users, losses to the economy or insurance economic aspects.

The conclusion to be drawn from this is that the strategy of the observer is of significant influence.

COMPATIBILITY STRATEGIES

If Chapters 1 to 3 are used in assessing technical literature—referred to in the Appendix—it can be stated that all the principal work can be arranged in the terminology stated. On the other hand, the statement and results differ due to the application of different strategies.

The strategy determines the results like a filter of spectral analysis, employed for input data with the same origin.

To aid understanding, it is urgently necessary in future for all authors, speakers, organizations, industry and authorities to clearly set out what is the strategy basis of their knowledge or requirements.

Figures 2 and 5 are an essential aid in this respect. Figure 5 presents the principal strategies and possibilities for mixing in a systematical form. Mixing takes place not only via the three circles MOTIVATION, FILTER, SPACE but also within each circle. It is seldom a matter of the PURE FORM of a strategy.

For instance, if the economic aspect dominates—whether national or private economic aspects—political (company or state) factors or humanitarian (moral or ethical) factors always play a role.

The middle circle, the FILTER CIRCLE, shows that the motivation aspects are filtered in a purely arbitrary manner or with focal points—e.g., dealing exclusively

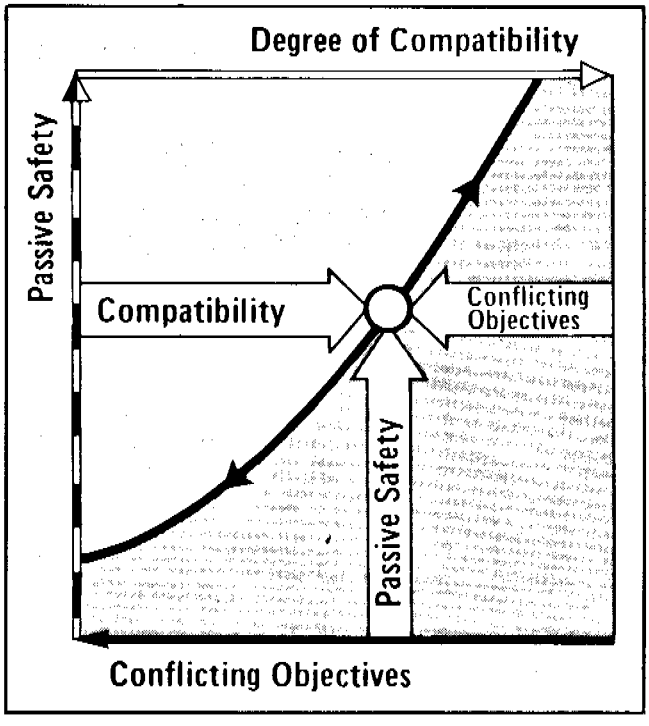

Figure 4. Scheme: Passive safety - Compatibility - conflicting objective.

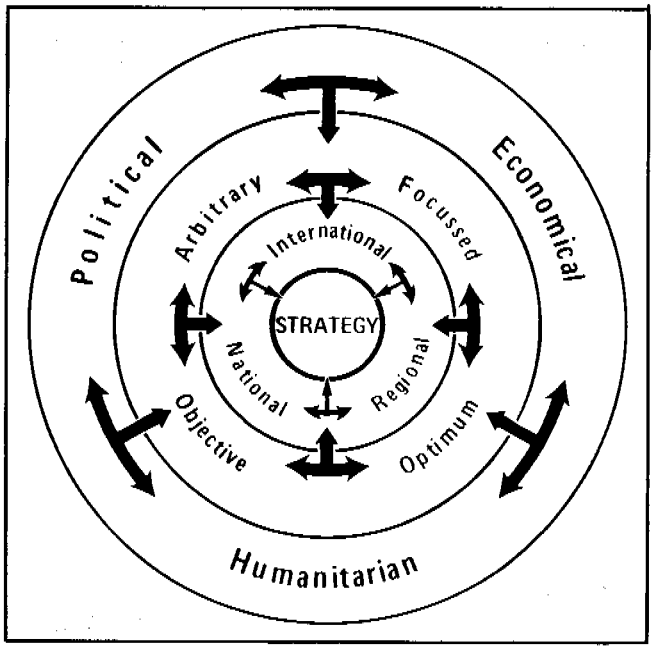

Figure 5. Presentation of important compatibility strategies and their correlation (motivation circle, selection circle, space limitation circle).

with car-to-car frontal accidents—or ideally with exclusive orientation to minimizing overall risk or objectivity—with as uniform possible distribution of risks.

The inner circle or SPACE LIMITATION CIRCLE finally provides information regarding regional, national or international applicability or interpretation of the criteria mentioned.

In the authors' view, the project supported by the German Ministry for Research and Technology, the abbreviated title of project Phase 1 being COMPATIBLE VEHICLES, pursues on the basis of this arrangement principle an

economically focused/optimum national strategy.

This eliminates any further RIGHT or WRONG in the discussion of compatibility, leaving only a co-existence of different approaches, which the individual author then must also explain.

Points of controversy are then no longer COMPATIBILITY PROBLEMS but the decision in favour of the criteria of the three STRATEGY CIRCLES to be employed.

SUMMARY

As a result of their work in various national and international bodies, the authors of this paper are constantly confronted with the problems involved from the different interpretation of terms. From their own knowledge of these problems and a study of the comprehensive technical literature meanwhile available, they explain the terms PASSIVE SAFETY and COMPATIBILITY on an application-oriented basis and define them relative to each other so as to cover all known terms. Only by introducing the term COMPATIBILITY STRATEGY and the variations which it offers is it possible to achieve a breakdown ensuring extraordinary transparency.

- PASSIVE SAFETY thus means effort to reduce the OVERALL ACCIDENT RISK.
- COMPATIBILITY means a proper distribution of unavoidable risks based on a specified strategy.

A Collection of Relevant Papers to the Term Compatibility

1. Appel, H.: Optimum deformation characteristics for front, rear and side structures of motor vehicles in mixed traffic; 2. ESV-Conference, Sindelfingen 1971
2. Appel, H.: Aggressivität von Fahrzeugen als Teilproblem der passiven Sicherheit; ATZ 75 (1973) 12
3. Appel, H.: Ergebnisse und Schlußfolgerungen aus dem ESV-RSV-Programm und der BMFT-Studie "Technologie für die Sicherheit im Straßenverkehr"; 4. Statussemin. Kfz- u. StV-Tech. BMFT, 2. Jtag. VDI-Gesell. Fz.Tech. 1976
4. Appel, H.: Hofmann, J.; Rau, H.: Entwicklung kompatibler Fahrzeuge—Analytische Abschätzung der Unfallmechanik der Unfallgruppen. 5. Statussemin. d. BMFT 1977
5. Scott, Basil Y.: Large and Small Car Accident Performance: A Large Scale Accident Data Base Analysis; SAE 750113
6. Beermann, H.J.: Verformungsverhalten von Personenkraftwagen an Unterfahrschutzeinrichtungen. Dt. Kraftfahrforsch. u. Straßenverkehrstech. H. 259 Düsseldorf
7. Bez, U.: Sicherheitsmaßnahmen imStraßenverkehr—Ergebnisse einer Nutzen/Kosten-Analyse von ausgewählten Maßnahmen. VDI-Berichte Nr. 418
8. Boehly, William A., Lombardo, Lois V.: Safety Consequences of the Shift to small cars in the 1980's; NHTSA, HS-805 506
9. BLMC: A house paper which describes a computer simulation of a car-to-car head-on impact to investigate vehicle aggressiveness.
10. Bühler, O.P.: Neue Chancen gegen Verkehrstod? Hydrauliksystem verbessert Unterfahrschutz an Lkw und Anhängern. Kfz-Anz. 32 (1979) 15
11. Carlson, W.L.: Crash injury and vehicle size mix. Conf. Amer. Assoc. for Automot. Med. and 7. Conf. Int. Assoc. for Accident and Traffic Med. Vol. 2
12. Carter, R.L.: Passive protection at 50 miles per hour. DOT HS 810 197
13. Chandler, E.: Car-to-car compatibility, a brief survey 4. ESV-Conference, Kyoto 1973
14. Chillon: The importance of vehicle aggressiveness in the case of a transversal impact; 1. ESV-Conference, Paris 71
15. Coquand: Vergleich der Sicherheit gewisser Klassen französischer Tourenfahrzeuge mit großer Verbreitung. Anhang IV zum Bericht vom 30. Juni 1972 (VDA Kommission für die Sicherheit von Fahrzeugen)
16. O'Day, James and Kaplan, Richard: How Much Safer Are You in a Large Car; SAE (Feb. 75) 750116
17. Davis, S.; Pierce, S.; Van Crashworthiness and Aggressivity Study; SAE 810090
18. S. Davis, R. Yee: Development of a Test Methodology for Evaluating Crash Compatibility and Aggressiveness DOT HS-805 063
19. Danner, M.: Entwicklung kompatibler Fahrzeuge—Bildung einer Rangreihe von Unfallgruppen anhand einer Untersuchung realer Unfälle; 5. Statussemin. d. BMFT 1977
20. Danner, M.; Langwieder, K.: Schwerpunkte des realen Unfallgeschehens und Auswirkungen auf Kompatibilitätsrelevante Einflußgrößen; BMFT-Statussemin. 1978

21. Langwieder, K.: Aspekte der Fahrzeugsicherheit anhand einer Untersuchung von realen Unfällen; HUK-Verband
22. Langwieder, K.: LKW-Kollisionen mit Personenwagen und Ansatzpunkte zur Verbesserung des Partnerschutzes TÜV-Rheinland
23. Fiat: Analysis of statistical data on road accidents in Italy (1969–1970); A Magara 2nd ESV-Conference 1971
24. Fiat: Technical presentation; 6. ESV-Conference in Wash.
25. Fischer, J.: Analyse der passiven Sicherheit: Partnerschaft auf italienisch. Der häufigste Unfall simuliert: Wagen mit 1100 kg gegen 800 kg mit je 40 km/h frontal und versetzt; Automob.-Rev. 74 (1979)
26. Fischer, R.G.: Occupant protection in car-to-car impacts 4. ESV-Conference, Kyoto 1973, SAE 740316
27. Fischer, J.: Frontal-Crash zwischen zwei extrem unterschiedlich großen Wagen. Analyse der passiven Sicherheit Automob.-Rev. 73 (1978)
28. Hutchinson, T.P.: On the relative frequencies of collisions between vehicles of different masses; Z. f. Verkehrssicherh. 25 (1979)
29. MacLaughlin, T.F.; Saul, R.A.; Daniels, S.: Causes and Measurement of Vehicle Aggressiveness in Frontal Collisions; SAE 801316
30. MacLaughlin, T.F.: Derivation and Application of Restraint Survival Distance in Motor Vehicle Collisions; SAE 810092
31. Makay, Murray; Ashton, Steve: Injuries in Collisions Involving Small Cars in Europe; SAE 730284
32. Middelhauve, V.; Breitbach, P.: Panzer der Straße? LKW-Unfallsimulation an der TU Berlin; Lastauto Omnibus 56 (1979) 6
33. Ragland, C.: Vehicle Aggressivity Measurement and Evaluation; SAE 790297
34. Randall, R.B.; Hee, J.: Cepstrum analysis; Bruel and Kjaer tech. Rev. (1981) 3
35. Renault: Point du probleme compatibilité (note RNUR)
36. Renault: A Method to Approach the Problems of Vehicle Compatibility; 3. Intern. Congress on Automotive Safety, San Francisco 1974
37. Renault: Compatibility between Vehicles in Frontal and Semifrontal Collisions; 5. ESV-Conference in London 1974
38. Renault: Classification des chocs. Compatibilité (note RNUR)
39. Ventre, P.: Homogeneous safety amid heterogeneous car population? 3rd Internat. Conference on ESV, Wash. 1972
40. Ventre, P.; Rullier, J.C.: Proposals for test evaluation of compatibility between very different passenger cars. 4. ESV-Conference, Kyoto 1973
41. Reidelbach, W.; Schmid, W: An Attempt to Define and Evaluate Vehicle Compatibility; 3. International Congress of Automotive Safety, San Francisco, 1974
42. Schmid, W.: Über Massenverhältnisse bei Fahrzeugunfällen im gemischten Straßenverkehr; Automobiltechnische Zeitschrift 77 (1975) 5
43. Reidelbach, W.; Schmid, W: Compatibility of Passenger Cars in Road Accidents; 6. ESV-Conference, Washington Oct. 76
44. Schmid, W.: Mathematical Modeling of Occupant Biomechanical Stress Occurring During a Side Impact; SAE 780670
45. Reidelbach, W.; Schmid, W.: Realistic Test Conditions for Evaluation of Passenger Car Occupant Protection 7th ESV-Conference, Paris, June 1979
46. Schmid, W.: Vermindertes Verletzungsrisiko bei Verkehrsunfällen durch Fahrzeug-Kompatibilität; FIS-ITA-Congress, Hamburg, Mai 1980
47. Schmid, W.: Minimum Risk of Injury on the Road, a Paradox; 8th ESV-Conference, Wolfsburg, Oct. 1980
48. Schmid, W.: The increase in the risk of injury in traffic accidents as a result of higher test impact speeds; 9. ESV Conference, Kyoto 1982
49. Panik, F.; Schmid, W.: Die 7. ESV-Konferenz—Überblick Automobiltechnische Zeitschrift 82 (1980) 1
50. Saul, R.A.; MacLaughlin, T.F.; Ragland, C.L.; Cohen, D.: Experimental Investigation of Crash Barriers for Measuring Vehicle Aggressiveness—Fixed Rigid Barrier Initial Results; SAE 810093
51. Searle, J.A.: The estimation of an aggressiveness coefficient from barrier impact test results. Working paper
52. Solomon, D.: Highway research and vehicle design for the 80s; SAE 770039
53. Stuhler, T.; Stankovic, P.: Vermeidbare Unfallfolgen? Z. f. Verkehrssicherh. 24 (1978) 4
54. Stcherbatchef, G.; Provensal, J. (F): Identification des facteurs de compatibilité des vehicules en choc lateral; VDI-Berichte Nr. 268, 1980
55. Stewart, J.R.; Stutts, J.C.: A Categorial Analysis of the Relationship between Vehicle Weight and Driver Injury in Automobile Accidents; HSRC/DOT HS-803 892
56. Stratmann, J.G.: ADAC-Untersuchung: Welche Vor- und Nachteile hat ein großes oder kleines Auto? ADAC-Mot.-Welt (1980) 10
57. Seiffert, U.: Crashworthiness regulations will be hard on small cars; SAE-Journal 4/73
58. VW: Realistic compatibility concepts and associated testing; 6. ESV-Conference in Washington
59. Seiffert, U., Hamilton, J. and Boersch, F.: Compatibility of traffic participants; 3. Intern. Congr. on Automotive Safety, San Francisco 1974
60. Seiffert, U.: Kompatibilität auf der Straße; ATZ 77 (1975)

61. Danckert, H.: Development of crash energy management solutions; SAE 760793
62. Weissner, R.: Fahrzeugtechnische Schwerpunkte zur Verminderung von Unfallfolgen; 4. Statussemin. Kfz- u. StV-Tech. BMFT, 2. Jtag. VDI-Gesell. Fz-Tech. 1976
63. Weissner, R.: Fahrzeugtechnische Möglichkeiten zum Schutz der Verkehrsteilnehmer; Kongr. d. Ärztl. Kraftfahrerverein. Österreichs, Wien 1977
64. Schimkat, H.: Entwicklung kompatibler Fahrzeuge—Zielsetzung und Arbeitsablaufplan; 5. Statussemin. d. BMFT 1977
65. Schimkat, H.: A concept of increasing compatibility of passenger cars; Int.Tech.Conf. on Exper.Saf.Veh. (US Dep.)
66. Weissner, R.: Kompatibilität von Personenkraftwagen unter Berücksichtigung unterschiedlicher Kollisionstypen Kongr.-Ber.Jtag. 1979 d. Dt. Gesell. f. Verkehrsmed. Unfall- u.Sicherh.Forsch. im Straßenverkehr
67. Bauer, A.; Richter, B.; Schimkat, H.; Weissner, R.: Entwicklung kompatibler Fahrzeuge—Grundlagen zur Erarbeitung von Maßnahmen für kompatible Fahrzeuge. BMFT-Statussemin. 1978
68. Zimmermann, P.; Oberdieck, W.; Richter, B.: Optimisation of energy absorbing structures for the improvement of the compatibility of passenger vehicles; 8. ESV-Conference, Wolfsburg 1980
69. Oberdieck, W.; Richter, B.; Zimmermann, P.: Optimierung von Deformationsstrukturen zur Verbesserung der Kompatibilität von Pkw; 18. int. FISITA-Kongr. Hamburg.
70. Oberdieck, W.; Richter, B.; Zimmermann, P.: Verbesserung der Kompatibilität von Fahrzeugen auf theoretischer Basis durch Einsatz eines Optimierungsverfahrens Automob.-Ind. 26 (1981)
71. Dreyer, W.; Richter, B.; Zobel, R.: Handling, Braking, and Crash-Compatibility Aspects of Small Front-Wheel Drive Vehicles; SAE 810792
72. Taylor, H.: Strukturverhalten der Kraftfahrzeuge bei Aufprall, Kompatibilität zwischen Fahrzeugen, Agressivität gegenüber anderen Verkehrsmitteln und Fußgängern. Akten d. Eur. Symp. f. Kraftfahrzeuge (1975), bd. 1 Brüssel
73. Thomas, C.; Faverjon, G.; Henry, C.; Got, C.; Patel, A. PSA, FR, Hop. Raymond Poincare: Comparative study of 1624 belted and 3242 non-belted occupants: Results on the effectiveness of seat belts; 24. Conf. of the Amer. Assoc. for Automot. Med. 1980
74. Wagner, R.: Market related passenger car design to improve collision protection for "own" vehicle and "other" vehicle; 7. ESV-Conference, Paris 1979
75. Warner, C.Y.; Peterson, R.: Automobile-attenuator compatibility in 1985: Some designer guidelines; 54. Annu. Meet., Transp. Res. Board
76. BMFT-Studie: Technologien für die Sicherheit im Straßenverkehr, Oktober 76
77. Verformungsverhalten von Fahrzeugstrukturen bei Unfällen VDA-Schriftenreihe 22 AUTO UND SICHERHEIT, 1976
78. TÜV-Rheinland, Köln: Partnerschutz vor Selbstschutz. Maßnahmen zur Verbesserung der äußeren Sicherheit an LKW Lastauto Omnibus 55 (1978)
79. Entwicklung kompatibler Fahrzeuge; BMFT- u. BMI-UBA-Semin. 1979
80. Dt. Verkehrswacht, Bonn: Verkehrswacht-Umfrage zur Sicherheit in kleineren Autos: Sparsam, leicht, lebensgefährlich? Autohaus (1980)
81. Evans, Leonard: Car Mass and Likelihood of Occupant Fatality; SAE 820807
82. Bez, U.; Hamm, L.; Hoefs, R.: Repräsentativität von Bezugsfahrzeugen und Wirkungsfeld von Sicherheitsmaßnahmen; Status-Seminar BMFT 1981, Ulm
83. Ardoino, P.L.: Capability of the Car to Minimize the Global Damage in Road Accidents; Course on Vehicle Design and Safety, Amalfi, May 82
84. Bez, U.; Rauser, M.: Specific energy absorption and vehicle weight criteria to be observed in body development for improved occupant protection and compatibility; 8. ESV-Conference 1980, Wolfsburg

NHTSA Frontal Structures Research

CARL L. RAGLAND
National Highway Traffic Safety Administration

ABSTRACT

A methodology is being developed to assess fleet safety in the frontal crash mode. While many individual safety contributions have been made in improving safety potential of one vehicle, few studies have successfully predicted net safety gains which may be obtained by relatively minor vehicle changes (in some cases) applied to large portions of the fleet. This study addresses the methodology for predicting the net gain in safety benefit by manipulation of input vehicle/fleet parameters (stiffness, weight, fleet distributions, accident distributions), and occupant injury predictive analysis. The application of this methodology is the identification of optimized vehicle structural input parameters which result in minimum risk to the population as a whole.

INTRODUCTION

Even though protection of occupants in frontal crashes has been a major focus of safety efforts in recent years, frontal crashes still continue to present the largest risk to passenger car occupants. For instance, 50% of all passenger car fatalities and 53% of all light vehicle serious injuries (AIS $\geq$ 3) result from frontal accidents. These data are obtained from NHTSA's Fatal Accident Reporting System and from the National Crash Severity Study.

To investigate this problem, NHTSA frontal structures research is undertaking a systems approach quantitatively identifying problem areas, conducting parameter studies to optimize structural/safety design and performance parameters, and finally recommending countermeasures that would be most effective in a specific fleet environment.

The first step of this approach is identifying all pertinent factors which influence occupant risk. These factors include exposure factors and physical factors such as stiffness, crash pulse shape, intrusion, and vehicle interior geometric and restraint data, all of which will be derived from various data sources including but not limited to:

—accident data
—crash test data
—registration data
—fleet weight data
—analytical studies
—vehicle studies

The next step will attempt to assess the effect of these risk factors to determine the potential for occupant harm. This risk assessment will be accomplished using simple but valid trend predicting analytical techniques. These techniques will relate the risk factors and changes in risk factors to overall fleet risk which allows the final step to be accomplished.

The final step in the approach utilizes an accounting model which sums the risk potential for all input scenarios to determine the optimum physical parameters for any given exposure which minimizes occupant risk. The output of one such study is shown in Figure 1. This study shows that for the range of input parameters there exists a minimum harm level associated with stiffness for every theoretical crash pulse shape. This result is very important in indicating the need for optimizing stiffness. However, the sample output shown here is not relatable to the real fleet because the definition used for stiffness is not applicable to car-to-car collisions and the crash pulse shapes are too theoretical (not linked to specific cars). This output is useful, though, to predict expected results from a more refined study. This paper will discuss the efforts to refine a methodology to assess present and future fleets and determine expected safety improvements associated with fleet/vehicle changes.

RISK FACTOR

Data Collection

The first step in the research approach is the collection and compilation of data necessary for input to the accounting methodology. As a major source for crash test and vehicle data, including weight, stiffness, geometry,

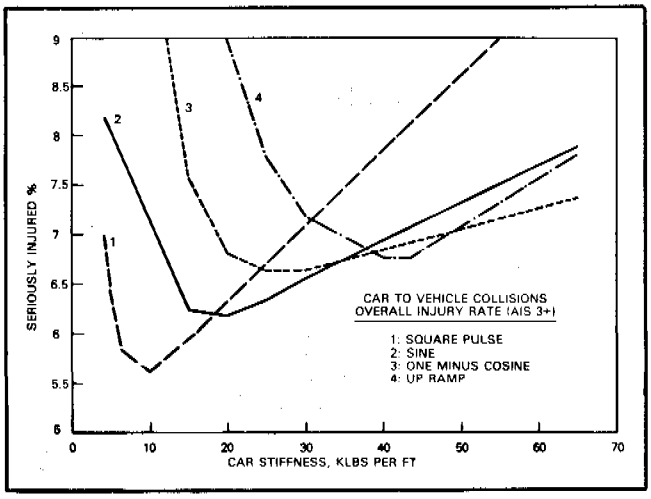

Figure 1. Injury frequency vs. stiffness by crash pulse shape.

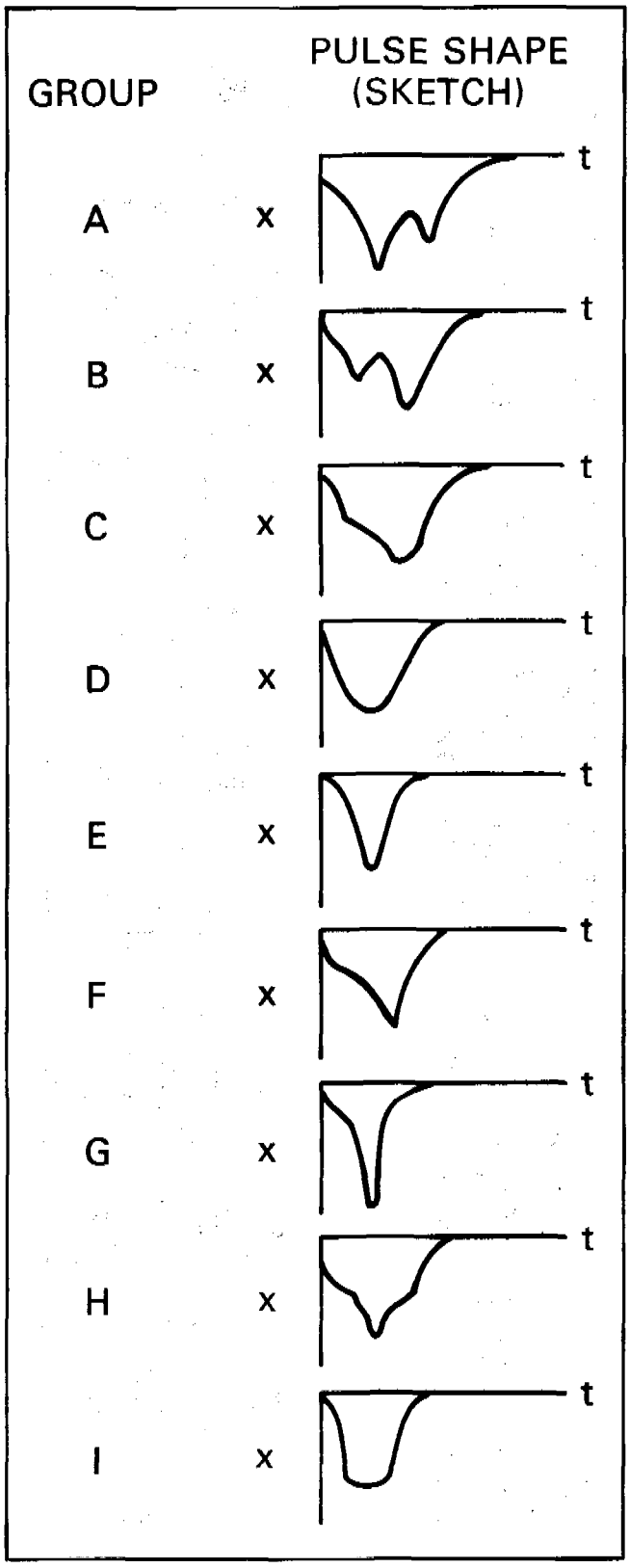

Figure 2. Generic crash pulse shapes.

etc., the NHTSA has collected in a data base system over 460 records of crash tests of various types performed over the past several years. Of these crash tests, approximately 240 include tests in which at least one of the vehicles were impacted with a predominantly frontal PDOF (principal direction of force). These records will be the primary emphasis of this study along with other necessary fleet properties, distributions of weights (current and projected), etc.

Collection and compilation of the crash test data are being performed to present the data in a format which is compatible with accident data. These data will be presented in tabular form showing distributions of delta V's, striking and struck car weights, collision types, and impact types. Comparisons will then be made with accident data to determine commonalities and voids in test data.

As shown in Figure 1 and in other research findings, crash pulse shape can have a significant influence on occupant frontal crash protection (1). Therefore one of the primary physical factors associated with occupant risk is crash pulse shape. This factor has been condensed from the 240 crash tests into 9 generic crash pulse shapes as shown in Figure 2 (2). These data will be useful as input to the accounting model for identifying one of the primary characteristics of the existing fleet.

From this sample of crash pulses it can be determined that, while variations of crash pulse shape are available, these variations may be narrowed down to perhaps 5 or 6 basic shapes. Future research work will concentrate on sales weighting these data to determine a representative fleet distribution.

Another structural parameter which can be linked to crash pulse shape is structural stiffness. Here stiffness is defined as the combination of factors influencing resistance to crash forces. Where specific stiffness is unique to each crash event, generally stiffness may best be derived from dynamic loads measured during a specified crash event such as a fixed load cell barrier test. The NHTSA has collected and compiled such force-crush curves using a NHTSA designed load cell barrier. This barrier, shown in Figure 3, is constructed of rigid supporting structure

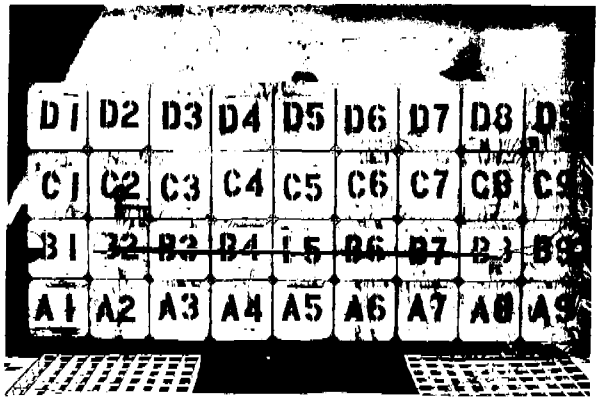

Figure 3. NHTSA load cell barrier face.

used to mount thirty-six, 50,000 pound capacity load cells, capable of measuring a 25,000 pound off-axis load when combined with a 25,000 inch pound moment. Extremely good data are being collected from this device. Integration of load-time histories indicates virtually no loss of load based on impulse-momentum balance. Additionally there is very negligible noise content in data.

Force-time data from the load cell barrier have been collected on a small sample of test vehicles. These data include approximately 14 model year 1980 cars, 12 model year 1980 cars, and 24 model year 1982 cars (1982 model year testing is currently in progress with approximately 10 model year 82 tests completed at date of writing). Utilization of these data has been primarily to determine stiffness of the crash tested cars and hence to extrapolate stiffness properties to the entire fleet.

A sample of the total load-time data digitally filtered at 300 Hz cut-off is shown in Figure 4.

Two secondary benefits have resulted from load cell barrier data. First, load data, unlike accelerometer data, have proven to have low susceptibility to noise and vibration. Therefore load-time data, can be used to "match" the best accelerometer response, when several redundant accelerometers are available in the vehicle compartment. Secondly, the actual structural response is measured with a high degree of precision. This allows assessment of repeatability of test car structures under similar test conditions. Load data, in this case, can identify structures that behave differently in tests due to manufacturing/ design changes, etc.

Complete load cell barrier data (load-time) are stored

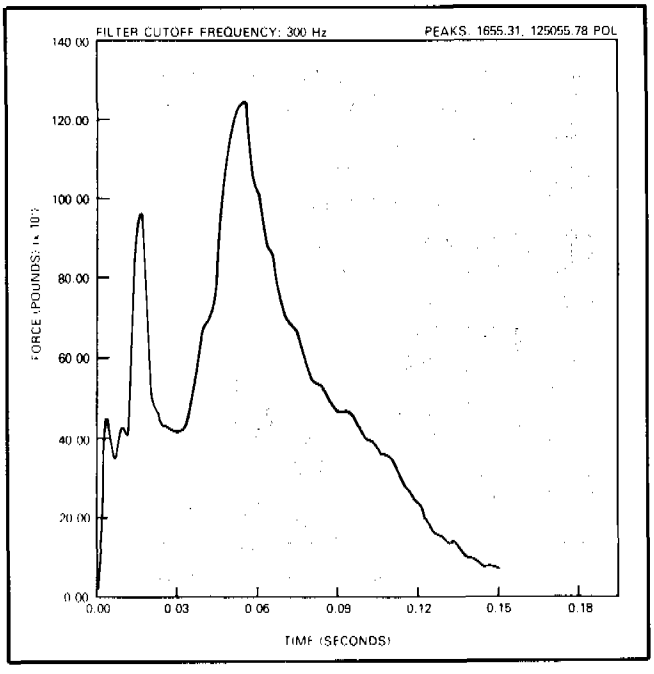

Figure 4. Load-time data filtered at 300 Hz. 1981 Mercury Marquis, 35 mph load cell barrier total force vs. time.

Table A. Stiffness comparison for 35 mph load cell barrier tests.

NHTSA TEST NO.	TEST VEHICLE WEIGHT	STIFFNESS, (LBS./FT.)
118	3066	55900
119	2404	69200
122	2314	58400
137	3714	80900
194	2707	75000
273	2456	77000
333	2214	73000
334	3417	87800
365	2650	57000
380	3965	52000
386	3930	93882
425	4615	89000
426	2641	60300
427	3880	84600
428	2767	58500
999*	3428	45600
999*	3060	65581
999*	2584	88000

* TO BE ASSIGNED

Table B. Stiffness comparison for 35 mph load cell barrier tests, 2100-2700 pound weight class.

NHTSA TEST NO.	TEST VEHICLE WEIGHT	STIFFNESS, K (LBS./FT.)
119	2404	69200
122	2314	58400
273	2456	77000
333	2214	73000
365	2650	57000
426	2641	60300
999*	2584	88000

* TO BE ASSIGNED

Table C. Stiffness comparison for 35 mph load cell barrier tests, 2700-3300 pound weight class.

NHTSA TEST NO.	TEST VEHICLE WEIGHT	STIFFNESS, K (LBS./FT.)
118	3066	55900
194	2707	75000
428	2767	58500
999*	3060	65581

* TO BE ASSIGNED

in the NHTSA data base. Table A presents one form of comparing these data using the definition that stiffness, K, is the maximum force divided by the dynamic crush which occurs at the same time as that maximum force value. While this straight line force-crush is not totally representative of overall stiffness, it serves as a reasonable approximation in most cases for classifying the selected test cars by stiffness. A weight breakdown of this small sample of data is presented in Tables B through E. Future attempts will be made to expand this sample size to include a cross section of cars in terms of stiffness. Then, association of crash pulse shapes with stiffness will be used as input to the accounting methodology to be described in the following section.

Other data required to analytically assess the frontal crash environment include interior geometry of occupant compartments, fleet weight distributions for current fleets as well as projected fleets, closing velocity frequency distributions, and relationships between occupant injury severity with both intrusion and occupant impact speed (with interior vehicle components). Interior geometry can

Table D. Stiffness comparison for 35 mph load cell barrier tests, 3300-3900 pound weight class.

NHTSA TEST NO.	TEST VEHICLE WEIGHT	STIFFNESS, K (LBS./FT.)
137	3714	80900
334	3417	87800
427	3880	84600
999*	3428	45600

* TO BE ASSIGNED

Table E. Stiffness comparison for 35 mph load cell barrier tests, over 3900 pound weight class.

NHTSA TEST NO.	TEST VEHICLE WEIGHT	STIFFNESS, K (LBS./FT.)
380	3965	52000
386	3930	93882
425	4615	89000

most simply be expressed as a frequency distribution of the shortest distance between an occupant's head or chest and interior components. An example is shown in Table F. More sophisticated dimensions may be required for more detailed occupant studies. Fleet distributions are available from many sources such as fuel economy data for projected fleets, Polk Data, and accident data sources such as NCSS (National Crash Severity Study) and NASS (National Accident Sampling System). One compilation of 1985 weight projections is shown in Figure 5 while overall NCSS passenger car weight distribution is shown in Figure 6 (3,4). Frequency of closing velocity distributions and accident types is obtained also from NCSS and NASS data along with occupant injury relationships. It is anticipated that exposure data as currently obtained will not significantly be altered in future fleets, except weight-frequency distribution changes. Other data being compiled for possible input to the analytical accounting model are interior data necessary to exercise an analytical 2-D or 3-D occupant model. These data may include input for intrusion in the model, various occupant sizes, various seating positions, etc. It is anticipated that the more complex approach to occupant modeling will not, however, be a part of the initial research effort.

ASSESSMENT OF RISK FACTORS

The primary factors which are related to risk and are practical to control by vehicle designs are vehicle structures and occupant protection countermeasures. Since nu-

Table F. Occupant spacing frequency distribution.

X_n (INCHES)	F (%)
6	34
12	50
18	8
24	8

X_n=MINIMUM SPACING BETWEEN OCCUPANT AND INTERIOR SURFACE

F=FREQUENCY OF OCCURRENCE OF A GIVEN OCCUPANT SPACING

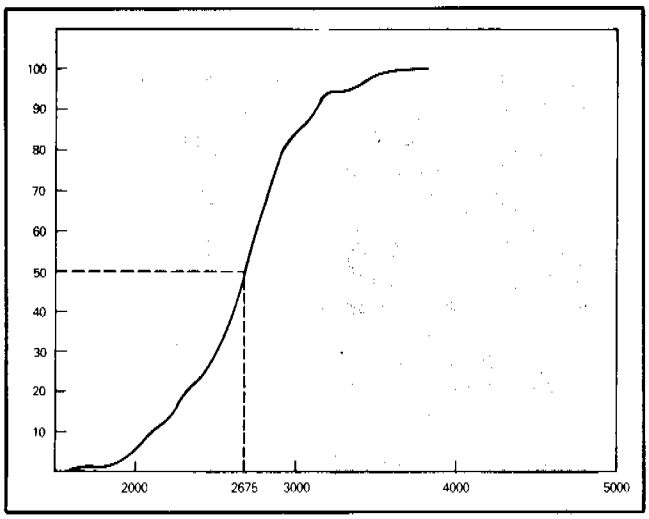

Figure 5. 1985 passenger car weight distribution by sales.

merous other studies have addressed occupant protection countermeasures in the vehicle interior, this paper will concentrate on assessing factors relating to vehicle frontal structures for design optimization purposes. Assessment of occupant risk requires understanding of general effects on the occupant due to changed structural parameters. A simple occupant model will be employed.

The direction for assessment of structures/occupant response is to adequately predict trends of occupant protection by varying structural parameters. For instance, predictions of occupant harm for unrestrained occupants will be based on the difference between the velocity of a free flying single mass object representing an occupant and the compartment velocity at the time the one-mass occupant contacts with interior. Time of interior contact is determined based on the difference between the integration of the occupant velocity and the compartment

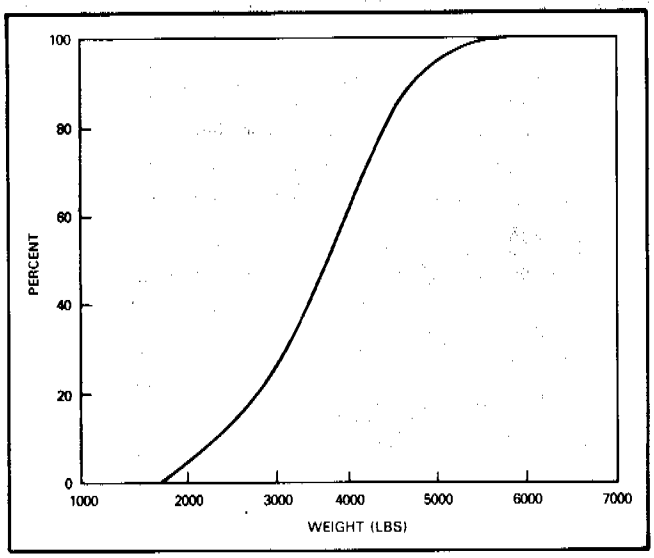

Figure 6. NCSS passenger car weight distribution.

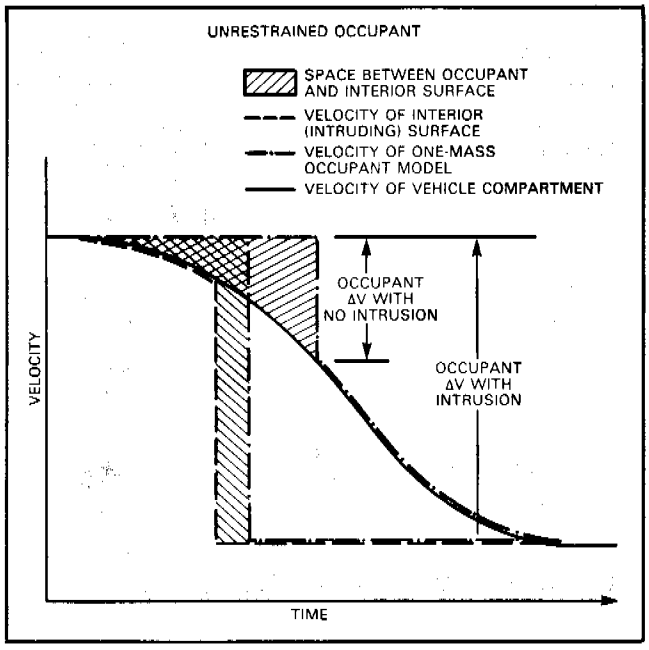

Figure 7. Unrestrained occupant velocity-time relationships.

velocity. Figure 5 shows the various occupant velocities which will be used to assess occupant harm. Likewise determination of contact speed is determined (if it occurs) for a restrained occupant as shown in Figure 6. Additionally, intrusion is considered very simply as a rigid coupling between the front bumper and the intruding surface (dash, steering assembly, etc.). Therefore, when intrusion begins it is assumed the intruding surface immediately undergoes the entire delta V of that crash event as shown by the theoretical representation of the interior intruding surface velocity profile in Figures 7 and 8. Furthermore it has been experimentally shown from crash test data that intrusion begins at approximately the time the crush reaches 80% of the value of the measured

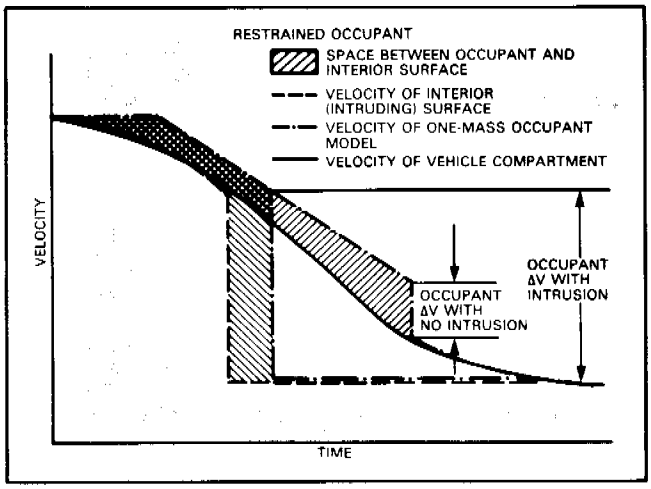

Figure 8. Restrained occupant velocity-time relationships.

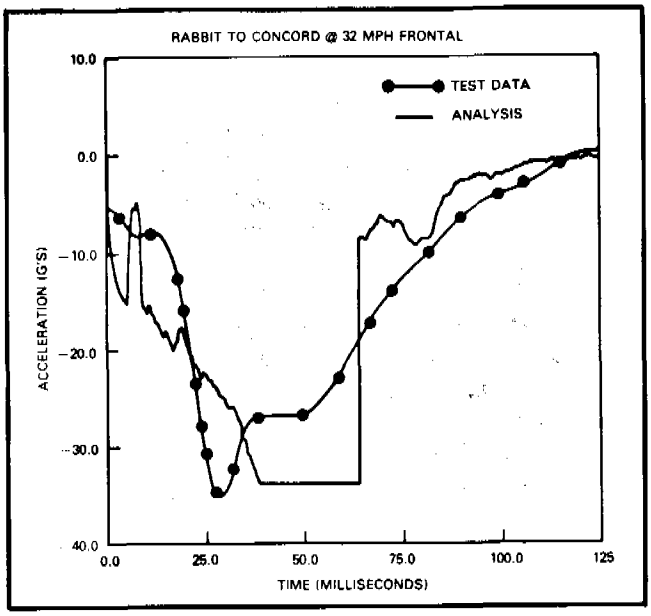

Figure 9. Acceleration time history for Rabbit from Rabbit-to-Concord crash test and from analytical prediction.

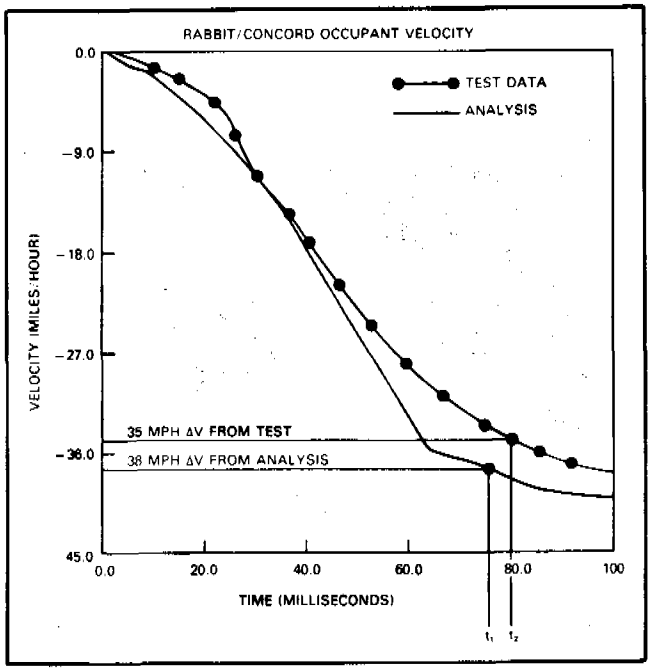

Figure 10. Velocity-time history of theoretical one-mass occupant, test vs. prediction.

distance between the engine and the front bumper. These distances on existing cars in the crash test data base may be obtained and assessed relative to occupant safety.

While these occupant injury relationships are simply conceived and are not expected to accurately predict crash protection potential of an individual vehicle in the fleet, it is expected that general "good" and "bad" structural characteristics (crash pulse, stiffness, engine placement) of individual vehicles and vehicle fleets can be identified.

To produce the multitude of crash pulses that can be generated from various car-to-car, object, etc., collisions an analytical crash model was developed. This analytical tool is used to predict occupant compartment response. By using this method, vehicle crush as well as time occurrence of crush is predicted. Therefore, all of the simplified occupant parameters as previously described can be defined. An example output is compared to actual crash data for a car-to-car collision in Figures 9 to 12. Note this shows the most difficult prediction in which two cars of incompatible structures collide head on. Particularly encouraging is the reasonable accuracy of the dynamic crush, see Figure 12. Compared parameters are presented in Table G. Note from Figures 11 and 12, intrusion begins substantially before the occupant would have contacted the interior surface (without intrusion). Therefore, as can be seen by referring to previous Figure 7, the occupant undergoes the total vehicle delta V as reported in the table.

The basis of this crash analysis is a comparative method by which structural crushing forces generated in two-car crash tests are compared at each time increment of the crash event to determine how each car is crushing due to its lower force level and to predict the resulting crash pulse. Part of the computational software assumes a constant force crush of the "weaker" car when its peak crush is reached. This plateau can be seen in Figure 9. Adjustments are then made to the duration of impact to obtain a theoretical impulse/momentum balance. Refinement of this methodology is still ongoing to validate results against crash data in all impact conditions. Also consideration is being given to the question of whether

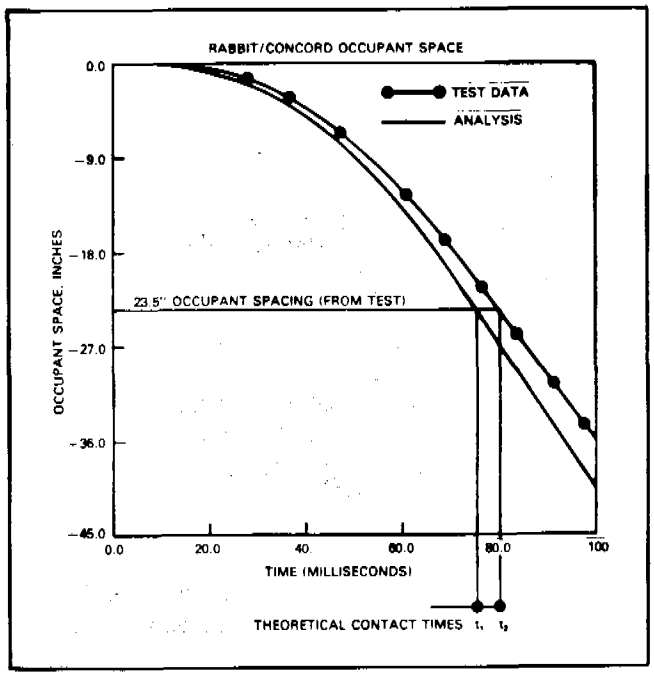

Figure 11. Rabbit unrestrained occupant spacing vs. contact time, test vs. prediction.

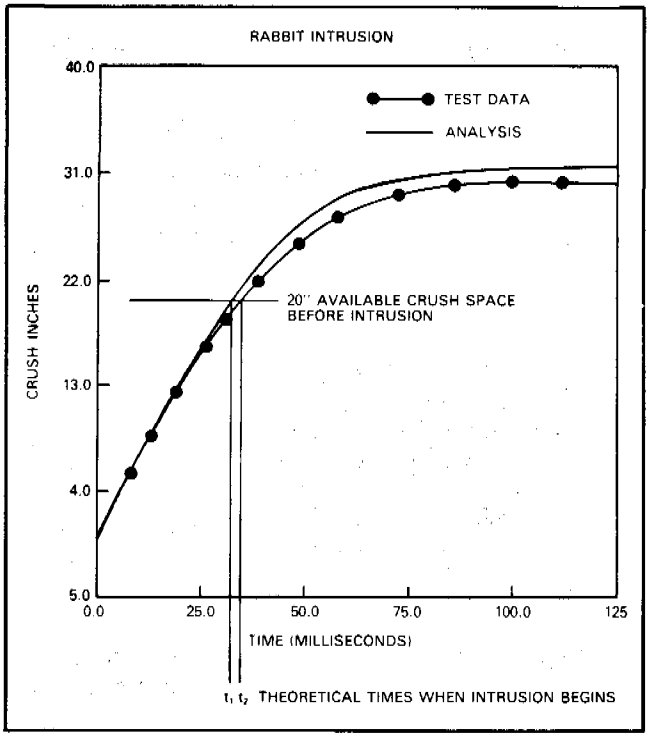

Figure 12. Rabbit displacement-time history to predict intrusion, test vs. prediction.

accelerometer generated force data can be used rather than currently used load cell data which have restricted availability.

PARAMETER STUDIES AND OPTIMIZATION

A methodology is currently being developed to account for all of the above parameters and predict their combined effect on occupant harm. The basis of this methodology was developed by Dr. A. C. Malliaris. A sample of the output generated was shown in Figure 1. Results were encouraging from the initial exercise of the methodology, but several refinements are required to include "best" available input data as previously discussed.

One of the major refinements to the model replaces empirically derived equations to predict occupant response and separate equations to predict crush and intrusion with the structural crash model as previously discussed.

Other refinements to the accounting methodology will include the ability to analyze a nonhomogeneous fleet of varying stiffness and crash pulse shapes.

As far as input refinements, all input parameters are being validated and changed as necessary using latest and best available data. One of the major refinements is in the area of structural data, which includes stiffness properties and crash pulse shapes. Other areas include weight, crash velocity, and occupant injury data as previously discussed.

EXPERIMENTAL APPROACH

Once an analytical method successfully predicts trends for improved structural crash performance, an experimental technique needs to be developed to verify results of this prediction. Currently the accepted method of evaluating crashworthiness is by flat rigid barrier. While this method has proven valuable in advancing state-of-the art in crashworthiness, particularly with regards to restraint development, it has done very little to advance improvements in compatibility as evidenced by extreme variations in stiffness (Table A). Shortcomings in assessment of crashworthiness and compatibility using the flat rigid barrier are twofold. First of all the intrusion aspect of crashworthiness is not evaluated on a comparable scale. This assessment can be readily visualized when one considers that in barrier crash testing, intrusion is proportional only to kinetic energy, meaning intrusion could be just as severe for large and small cars alike. In the accident environment, however, it is recognized that intrusion is typically a greater problem for small car occupants. Also, accident data show greater intrusion than crash test data at comparable delta V's. This latter observation is due to the crash environment of usually less than full frontal engagement resulting in lower acceleration (force) and greater extent of crush. The second shortcoming of the rigid barrier is the assumption that actual objects crashed into by a car will have the same force-crush properties as the car or will be non-yielding.

This assumption, while reasonable if stiffness of the car is "average," may result in ineffective restraint designs if the structural properties of the car versus those of the fleet are not considered. Note that car-to-car force inter-

Table G. Comparison of Rabbit data from Rabbit-to-Concord test and analysis.

	TEST DATA	ANALYTICAL SIMULATION
PEAK ACCELERATION	35 g's	34 g's
VELOCITY CHANGE OF OF VEHICLE	42 MPH	42 MPH
MAXIMUM CRUSH, RESIDUAL	28.6 INCHES	28 INCHES
VELOCITY WHEN OCCUPANT HITS INTRUDING SURFACE	42 MPH* (CALCULATED)	42 MPH*
VELOCITY WHEN OCCUPANT HITS NON-INTRUDING SURFACE	35 MPH (CALCULATED)	38 MPH

* SAME AS ΔV

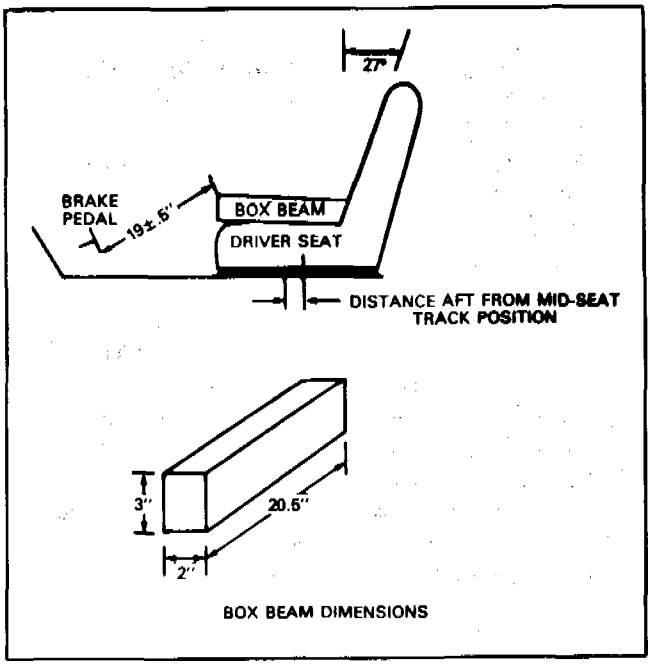

Figure 13. Seat positioning method used in deformable moving barrier testing.

actions are emphasized here because only 40% of the AIS $\geq$ 3 injuries are associated with fixed object collisions with a very small percentage of that number being a truly rigid, flat surface. The remaining 60% frontal AIS $\geq$ 3 injuries result from car-to-car collisions with a relatively large share, especially the more severe crashes, associated with front-to-front collisions. Thus the largest percentage of accidents, in which peak accelerations approach the peak dynamic force capability of the structure (divided by the mass), are accidents involving reasonably symmetric front-to-front collisions.

Therefore the crash environment initially chosen for experimental structure crashworthiness and compatibility evaluation, is one that creates maximum acceleration and maximum intrusion under a delta V environment which is inversely proportional to test car weight. Intrusion is also intended to be inversely proportional to structural stiffness of the test car, unlike the rigid barrier environment, in which intrusion is proportional to kinetic energy or energy dissipated by the cars structural collapse.

The means of testing cars in this crash environment is performed with a deformable moving barrier. Incidentally, load cells are mounted behind the deforming element to enhance knowledge of the structural behavior of the test car. This barrier is constructed of aluminum honeycomb and is the same barrier developed for side impact testing (5). It is designed to absorb energy roughly equivalent to that of a 1600 pound car impacting a rigid barrier at 35 mph. The purpose of this design is to force larger cars to absorb more energy for compatibility assessment and intrusion assessment.

Results of dummy response parameters using Part 572 dummies are shown in Table H. To eliminate variability in these tests the restraints were fixed at the "D" ring, thus eliminating restraint spool-out. Also for comparative analysis the seats were placed identically, as shown in Figure 13, to represent an intuitively average seating position. One more deformable barrier test is planned in the near future using a Fiat Strada. Analysis of the data has not been completed and will be presented at a later date.

CONCLUSIONS

This study is based on the premise that occupant risk is dependent not just on the singular properties of a vehicle but on the properties of the entire fleet. Research studies have shown that occupant response is indeed related to crash pulse shapes. It may also be rationalized that crash pulse shapes are dependent upon stiffness and on the combination of stiffness in car-to-car events. Therefore occupant response is also dependent on stiffness as it indirectly affects the crash pulse shape. Stiffness also affects the occupant harm environment directly by either preventing or allowing intrusion, particularly in car-to-car collisions.

NHTSA research will continue to quantify the effects

Table H. Dummy response using frontal deformable moving barrier.

CAR	TEST TYPE	HIC		CHEST G's 3 MSEC		FEMUR LOADS			
						DRIVER		PASSENGER	
		DRIVER	PASSENGER	DRIVER	PASSENGER	LEFT	RIGHT	LEFT	RIGHT
CITATION	DMB	483	418	40	30	255	750	1700	300
VOLVO	DMB	352	361	29	35	500	2000	200	750
MARQUIS	DMB	313	269	27	28	800	600	600	600
CONCORD	DMB	806	523	58	38	1825	1100	675	525
CUTLASS	DMB	1101	751	48	35	520	225	1585	1800
RABBIT	DMB	2250	707	59	39	550	400	650	400

of these and other parameters that affect occupant response. Finally, this research is intended to identify the structural properties which are optimal for occupants protection in the real world environment. Initially the effort will consist of a simplified analytical approach. Follow up studies may employ more sophisticated techniques such as the Fiat Methodology (6) or the Safety System Optimization Model.

REFERENCES

1. Cohen, D.S., Jettner, E. and Smith, W.E., "Light Vehicle Frontal Impact Protection," SAE Paper No. 820243, Warrendale, Pennsylvania, February, 1982.
2. Dimasi, P., "Generic Crash Pulse Study and Preliminary Data on Characterization of Generically Similar Kinematic Response in X vs X Plane," (A Progress Report) Transportation Systems Center, September 1982.
3. Segal, D.J. and Miller, P.M., "Methodology for Recommending Side Impact Moving Barrier Weight," October 1979, Progress Report, MGA Report No. 69-003-V-1
4. Jatras, K. and Carlson, W., "Frequency Distributions of Passenger Cars by Weight and Wheelbase by State—July 7, 1976," Report No. DOT-HS-803-382, June 1978.
5. Davis, S. and Ragland, C., "Development of a Deformable Side Impact Moving Barrier," Eighth International Technical Conference on Experimental Safety Vehicles, October 1980, Wolfsburg, Germany.
6. Shaw, L. M. and Ragland, C., "Application of the Fiat Methodology for Characterizing Vehicle Structural Responses in Side Impacts" to be published in the proceedings of the Ninth International Technical Conference on Experimental Safety Vehicles, November 1982, Kyoto, Japan.

Frontal Crash Protection in a Modern Car Concept 3663

RUNE ALMQVIST, HUGO MELLANDER, MAGNUS KOCH

Volvo Automotive Safety Centre Volvo Car Corporation

ABSTRACT

Volvo's Safety Engineering Philosophy is described in detail starting with Volvo traffic accident investigations as one of the most important inputs to the safety characteristics specified for a new Volvo car. How the safety characteristics are transformed to measurable properties in laboratory environment is then explained and exemplified. The car specification is further broken down to system and subsystem specifications suitable and understandable to the engineer at the drawing board. The engineering follow-up procedure, including Crashworthiness Design Review Meetings and at the end certification tests and production control tests, is discussed.

How variations in test results affect the engineering procedure and methods to set engineering limits to be used during the different design phases are discussed.

How this Safety Engineering Philosophy is implemented into the development of a new Volvo car is then described step by step and exemplified by different technical solutions and test results.

INTRODUCTION

With the Volvo Safety Engineering Philosophy as a background this paper describes how the crashworthiness characteristics at the very first beginning of a project are built into a new car and how this is controlled through the total development programme.

VOLVO SAFETY ENGINEERING PHILOSOPHY

One of the primary characteristics of a Volvo car has for a long time been safety and with the safety characteristics Volvo has always meant safe transportation in the real traffic environment.

Volvo Safety Engineering Philosophy can be explained by a circle as in Figure 1.

As safety in the traffic environment is the primary goal, it is important to know the real performance of our cars in actual accidents.

Accident Analysis

Since 1965 Volvo has carried out traffic accident research on Volvo cars and the knowledge from this research is used to set up our own safety requirements.

Volvo's Traffic Accident Research consists of two main parts

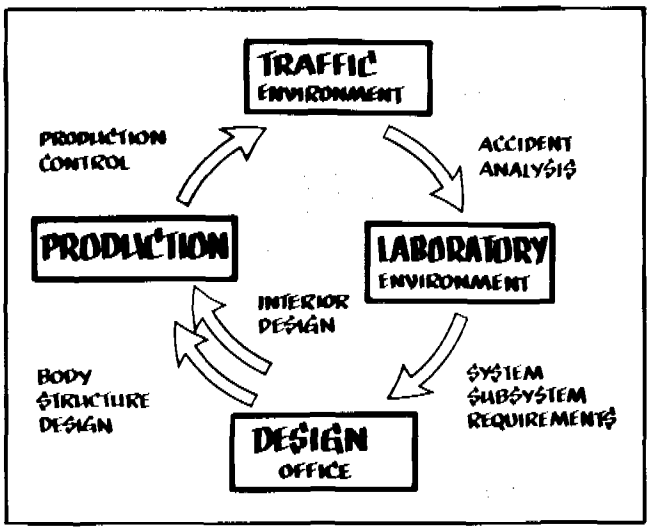

Figure 1. Volvo Safety Engineering Philosophy.

—multidisciplinary accident investigations
—data collection and statistical analysis

The multidisciplinary accident team is on call round the clock, seven days a week. All accidents with occupant injuries in a Volvo car, truck or bus are investigated. On the scene of the accident, the investigator looks for all information which can be of importance during his later analysis. This analysis consists of finding the cause of the accident and the consequences to the occupants and the vehicle. The medical expert of Volvo's investigation team gets in touch with his colleagues at the hospital to which the injured persons have been taken. With the help of data from the vehicle and information concerning the sustained injuries, it is possible to relate the pattern of injuries to the type of impact which caused them.

To get a material large enough to be used in a statistical analysis Volvo's unique insurance system has for a long time been used. All Volvo cars sold in Sweden are covered by a three-year motor vehicle damage warranty. This damage warranty is administrated by Volvo's insurance company. Through this motor vehicle warranty system Volvo has access to all data concerning the accidents. Each year, about 45,000 such accidents are reported to the warranty department. About 5,000 of the more seriously damaged vehicles are inspected by Volvo's staff of 12 damage assessors who are placed throughout the country. The basic information for our statistical accident research comes from this group of serious accidents.

Our own data in combination with data from different accident data files from all over the world are the basic background for setting our priorities.

Laboratory Requirement

The first step in the engineering procedure is to transform the accident scene to a controlled laboratory environment. The complex accident has to be transformed to a test which is repeatable and reproducible. Examples of these tests are frontal impacts into a rigid barrier, movable deformable barrier for side collisions and rollover simulations.

The occupants in the car have to be simulated with test dummies. These dummies are of course not in every detail copies of the human being but they are anthropometric and anthropomorphic. Dummies of different sizes are available (such as 5th percentile female, 50th percentile male, 95th percentile male and many different sizes of child dummies). Several different injury criteria are connected to the dummies, e.g., head injury criterion, chest injury criterion, femur injury criterion. These criteria have been found through biomechanical research. Within our function analysis staff Volvo has an expert in biomechanics who monitors this research in detail.

Engineering Requirements

Having the functional laboratory requirements on the complete car is not enough. The car must be divided into various systems and the system into various subsystems. With this technique the complete car requirement for different collisions could be broken down into a set of system and subsystem requirements which can be checked in laboratories and which are understandable to the draftmen and engineers.

The requirements on systems and subsystems form the basis for our development technique within the safety engineering procedure. The two major systems are the body structure system and the interior system. The body structure system covers the "body in white" and drive line (engine-transmission) and the interior system covers all the interior of the car such as instrument panel, steering wheel, seats and safety belts.

The requirements for the structure system are built up around a measuring technique using barrier tests, "body tests" and component tests. During the entire development procedure analytical tools such as structural mass/spring models and finite-element calculations are used to further optimize the mechanical engineering.

Two very important requirements for the structural system are intrusion and deceleration characteristics in the different crash tests. The reason is that these characteristics form the inputs to the interior system. The basic development technique for the interior system is a crash simulator in which the intrusion and deceleration can be reproduced. In this way the development of the interior is not depending on the possibilities to crashtest complete cars. As for the structure system the interior system uses several subsystem tests and in parallel calculations in mathematical models are made.

After a couple of loops between the structure and interior engineering departments in which an optimization of performance, weight and cost is done, the complete

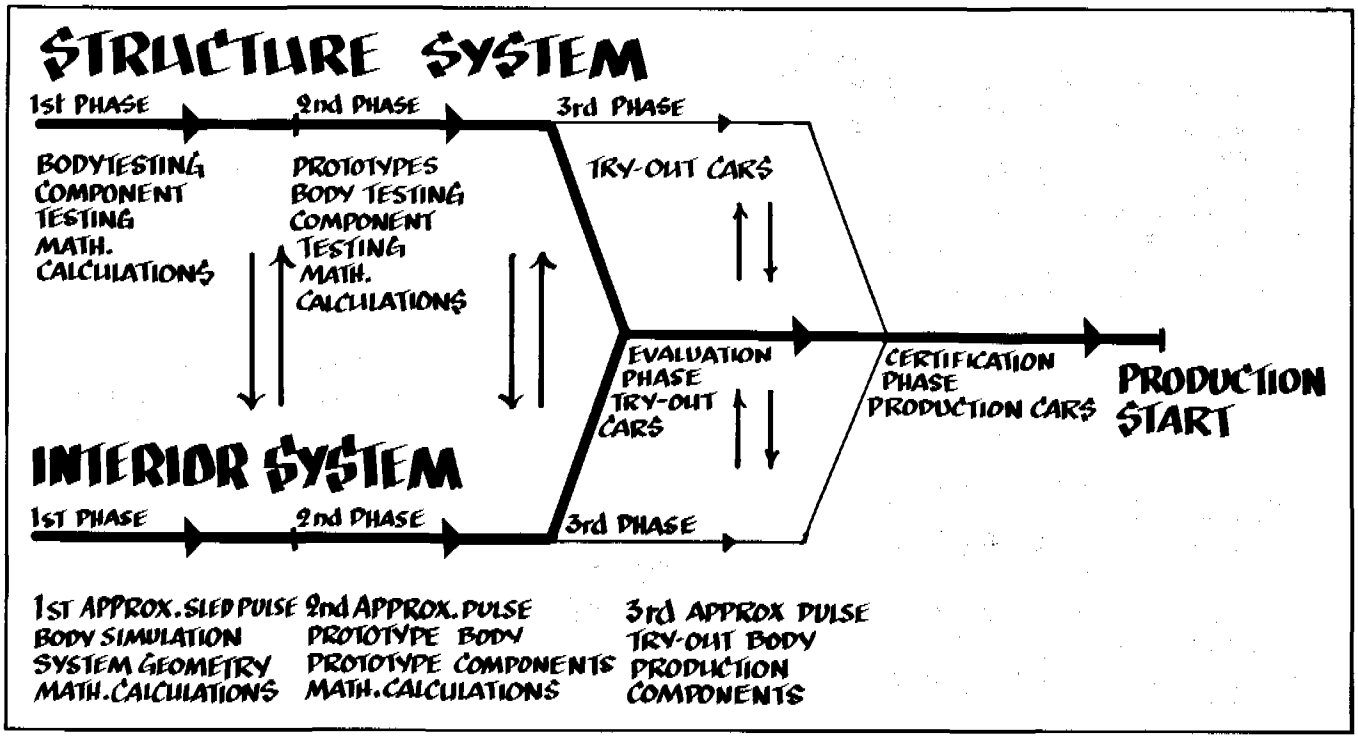

Figure 2. Development cycle for a new car.

car is ready for the evaluation and certification phase. In this phase complete cars (try-out and preproduction cars) are tested with the specified test methods and controlled against the specified criteria. A few extra loops back to structure and interior system may be necessary during the evaluation phase. Certification tests against legal requirements are then made, sometimes with representatives from the authorities witnessing the actual tests. Figure 2 shows a typical development cycle for a new car.

Production Control

During the development many different types of documentation are produced to ensure the production quality. A special documentation system for Vital Safety Parts (VSP) is used to

- —guide product engineering, manufacturing and assembly in accordance with government requirements
- —demonstrate compliance with government requirements
- —limit the number of vehicles affected by recall action in case of non-compliance or safety defect
- —limit product liability exposure and demonstrate that due care has been exercised

During production control many systems and subsystems (e.g. safety belts, windshields, seats, sunvisor) are tested and complete cars are taken as samples for crash tests.

The circle (see Figure 1) is closed and the new car is ready for the actual traffic environment. The Volvo Traffic Accident Research can start its investigations to evaluate the safety performance and to gain more knowledge for further improvements.

FRONTAL COLLISION PERFORMANCE FOR THE NEW VOLVO 760

The above described engineering philosophy will now be repeated and the special considerations during the development of the new Volvo 760 will be accounted for.

From all international traffic accident statistics as well as our own (refs 1, 2) it is obvious that frontal collisions are the type of collision with the highest number of accidents as well as the highest total cost for the society.

This has since a long time been recognized by Volvo and since the early fifties Volvo has gradually introduced different kinds of technical solutions to improve frontal crash protection (ref 3). When the work to specify a new Volvo for the eighties started, one of the highest priorities was to engineer a car with outstanding performance in frontal collision.

Test Method

The first step in our safety engineering procedure was to transform the overall specifications to functional requirements measurable in laboratory environment. Different safety regulations have since a long time used impacts against fixed barriers as their test procedures. Of course these test procedures are very simple simulations

of actual accidents and must be combined with careful analysis by experienced test engineers as well as by accident investigators. To limit development cost it was nevertheless decided to use these procedures (impact against a fixed barrier 0°, ± 30°) as the main laboratory tests as they must be used in the certification phase. It was decided to test at 35 mph.

Test Dummies

What type of dummies to use was the next decision to be taken. During the development of the Volvo 240/260 most of the tests were made with the Part 572 (50 percentile) male dummy. From our own experiences (ref 4) as well as others (ref 5) it is obvious that the total measurement chain with a dummy as "sensor" is a very complicated one and large variations in test results are to be expected. Careful analysis of test signals together with studies of the behaviour of the dummy during the test must be used to overcome the shortcomings of the dummy. As no other well documented dummies were available the Part 572 dummy was chosen.

Injury Criteria

The conventional measurements to be taken in the dummies are head and chest acceleration and femur forces. From these readings special injury criteria such as HIC, SI, Max Chest acceleration etc. can be derived.

In spite of heavy criticism the criteria stipulated in FMVSS 208, namely HIC, peak chest acceleration (3 ms) and maximum femur forces, are frequently used.

The protection levels of these criteria, HIC 1000, 60 g and 2250 lbf (10 kN) respectively have also been questioned, in particular the level of the HIC value. Patrick et al. (ref 6) suggested in 1974 that HIC of 3000 was below the acceptable limit and Walfish et al. (ref 7) recommends a tolerance limit of 1500.

To have consistency with all our previous experimental work it was nevertheless decided to use HIC 1000, chest acceleration 60 g and femur force 10 kN as protection levels.

During later years the problem of detecting submarining or penetration of lap belt into the abdomen has been focused. Our experience is that an optimal restraint system is heavily depending on the performance of the seat. One way to evaluate this performance is to measure submarining or submarininglike behaviour. Even if submarining is not a great problem in real life the benefits of a good support from the seat cushion in experimental work have been documented by several authors (refs 8–10).

Transducers on the iliac crest were therefore used in combination with high speed film analysis to evaluate the performance of the belt system.

Vehicle Related Criteria

Vehicle criteria were also set up, such as FMVSS 212 Windshield Retention, FMVSS 219 Windshield Zone Intrusion, and FMVSS 301 Fuel System Integrity.

ENGINEERING METHODOLOGY

System and Subsystem Requirements

Having the functional requirements on the complete car was not enough. The draftsman at the drawing table cannot design for example a front side member only knowing that certain injury criteria in a dummy should be below a specified level. The car must be divided into various main systems and the main systems into various subsystems. For the frontal collision two main systems are body structure system and interior system (Figure 3).

The body structure system covers the "body in white" and driveline and the interior system covers all the interior such as instrument panel, steering wheel, seats and safety belts.

By using mathematical modelling technique, structural mass/spring models, finite element calculations as well as different models of occupant simulations, the complete car functional requirements were broken down into requirements for the two main systems.

Body Structure System

The body structure system was specified for example by body deceleration curves for 0° and 30° barrier tests, intrusion limits for different parts of the body such as floor pan, instrument panel and steering wheel intrusion and vertical movement. These requirements formed an

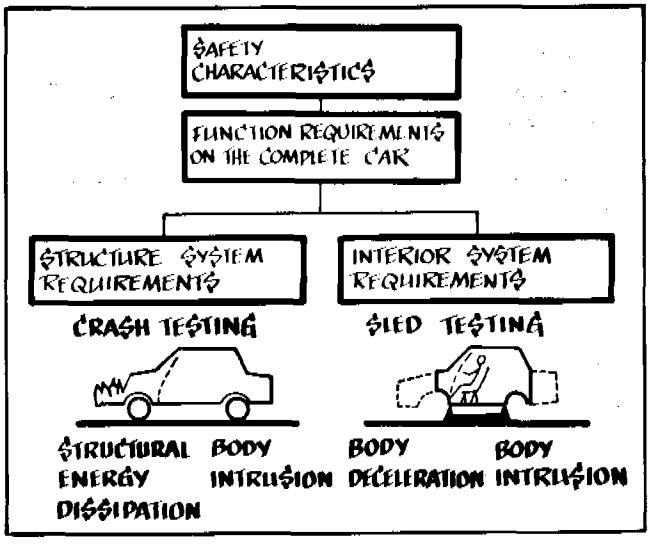

Figure 3. Body structure and interior system engineering methodology.

input to the body engineers for a further procedure broken down into subsystem requirements.

These systems and subsystems requirements were then controlled with test techniques such as component testing, subsystem testing, "body tests" and prototype tests. The "body test" is a technique used during early stages of development when no prototypes are available. By taking an existing car body and replacing specific parts in front of the A-pillar with prototype body concepts early test results such as force/deflection curves can be obtained. Our experiences from these body tests are that they are very useful both when different body concepts are to be evaluated as well as during the process of optimization between the structure design and material selection (ref 11).

Interior System

For the interior system the barrier test requirements are broken down to a sled test deceleration curve (the same as the body deceleration curve) and intrusion limits for body and interior parts such as the instrument panel and the steering wheel.

These requirements are the inputs to the interior engineering process which uses a HYGE crash simulation sled as an evaluation tool. From our early experiences of the use of the HYGE sled a good correlation between barrier tests and their simulations on the sled can be achieved at test speeds up to 30 mph (ref 12). Testing at higher velocities has however shown the need of further development of the simulation technique. Due to the higher test speed the body deceleration characteristics also in the vertical direction (pitch) and dynamic intrusions of body and interior panel including the steering wheel play an important role for the results in the dummies. Different techniques are used (max intrusion, intrusion at contact between dummy and interior, pitch simulations) but still much development has to be done to get an optimal simulation at speeds higher than 30 mph. In the meantime careful evaluation of test results from sled tests and a detailed comparison with results from barrier tests must be done during the development process. The importance of not being lost in these highly simplified simulations of actual traffic accident is obvious. For that reason our traffic accident analysis experts are involved also in the test evaluation process to ensure that not only good test results but also good performance in accidents will be achieved.

During both the structure and the interior engineering process mathematical calculations are used to back up the engineering and test work. Mathematical calculations have proven to be very helpful in concept evaluations and parameter optimizations.

The body structure and interior systems are developed in parallel during the early phases of a complete car project (see Figure 2). Several loops between the two systems are done in which performance, weight and cost are optimized. During the complete car evaluation phase tryout and preproduction cars are tested with specified test methods and controlled against specified criteria. A few extra loops back to the structure and interior systems may be necessary.

The number of complete cars crashed during the development of the Volvo 760 have been 50 and added to that around 70 body and component tests and 150 sled tests.

Crashworthiness Design Review Meeting

The safety characteristics influence more or less all the systems and subsystems in the car and consequently all departments in the organization have to be involved. Therefore a special steering committee meeting "Crashworthiness Design Review Meeting" was formed to control the implementation of the Volvo Safety Engineering Philosophy into the design process.

The responsibility to chair these meetings was given to the Crashworthiness Functional Analyst. The Functional Analyst is a person in the organization responsible for converting the crashworthiness characteristics set by the Product Planning Department into Functional Requirements of the complete vehicle.

In the case of crashworthiness the Functional Analyst is also responsible for the Volvo Automotive Safety Test Centre including Volvo Traffic Accident Research which ensures that neither test result nor actual traffic accident results are neglected during the development process.

The meetings have taken place every month and participants have been all of the managers in the line organization including representatives for Engine and Transmission Engineering, heads of different safety test departments, traffic accident experts and also representatives from Legal Requirement and Product Liability department.

The Crashworthiness Design Review Meeting was proven to be a very effective way to follow and control the development of the car safety characteristics during all stages of development. Optimization problems between different engineering areas have been possible to solve at the earliest possible time in the project.

ENGINEERING LIMITS

The various national and international requirements on safety characteristics are usually expressed as a maximum limit that no cars are allowed to exceed.

This implies that the average performance of the manufactured cars must be engineered with a margin to the limits.

The margin must include allowance for a number of factors. Some of these are

—uncertainty in the parameters that are used by the engineer in his work

—inaccuracies in the measurement techniques and data evaluation in the crash test
—unrepeatability of nominally identical crash test executions
—difference between prototype cars and production cars
—difficulties in making statistical inference from a small number of laboratory tests

Note that a single test outcome above the limit does not imply that the actual car value is outside the limit. It might equally well have been random fluctuations in the laboratory test procedures that have given this result.

A thorough treatment of the statistical consequences of some of these factors is given by Versace (ref 13). He has illustrated how the engineering limit can be related to the regulatory limit, by paying attention to all the above factors.

As input during the early stages of a new car project experience data from crash tests of previous models, data from the accident research and predictions on future technologies are used. If there is a larger technological step, say for instance a proposed change from belt restraints to airbag systems, due respect must be paid to the uncertainty concerning the behaviour of the new system. Based upon this, requirements are formulated which require the first tests with the prototype to exhibit values well below a limit. As the development continues and the test data accumulates for the new concept, the confidence increases in the soundness of the new product. This increased confidence makes it possible to revise the requirements so that the average performance is closer to the requirement than first permitted, even while the risk of having one car exceeding the limit is kept low.

It must be noted here that the requirement during development work is not, as some technicians may think, a more severe requirement than the requirement on the production cars. It is only an augmented and reformulated requirement on the engineers' work that must be achieved in order to get just the performance of the final car that the customers expect and the regulations require (ref 14).

TECHNICAL SOLUTIONS

The overall dimension and weight requirements for the 760 car were as such a challenge. The length from bumper to A-pillar was to be decreased some 10 cm as compared with the 240/260 car. The kerb weight should also be lowered some 50 kg. As a high crash performance was to be designed into the 760 car these goals demanded a thorough optimization between structure and interior engineering.

Structure

The 760 concept is a front engine, rear wheel drive, five-seat passenger car.

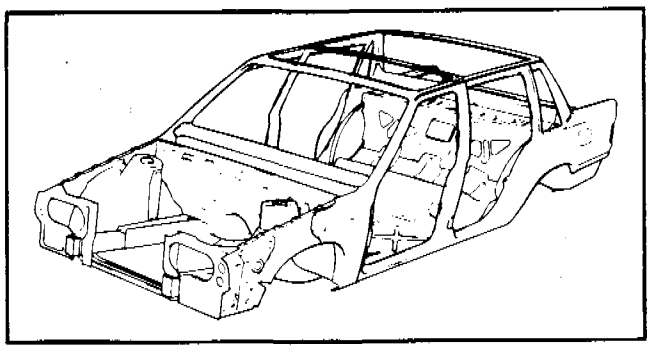

Figure 4. Structure design concept 760.

To optimize the stiffness and weight relationship, member design, sectional properties, welded joints and other joints have, for the monocoque body, been carefully calculated, analyzed and compared with experiences gained from previous designs (Figure 4).

The front side members (Figure 5) are designed as closed sections and from the front and backwards they form a continuously increasing cross section. The side members run under the floor with an outward angle and are connected to the doorsills with a cross member in order to distribute forces.

The front wheel housing and the suspension strut form together with the side member an integrated structure welded to the compartment.

The system is able to effectively absorb the kinetic energy in a frontal crash. The side members are at the front provided with "trigger swages" to initiate and control the buckling during deformation.

The aim has been to construct a body which, despite a large body area, weighs less than its predecessor. High strength steel (HSLA) has therefore been used in the front section of the front side members and sheet metal thickness has in different parts of the body been varied in order to optimize strength and weight.

Interior

The interior restraint systems are engineered not only to meet the overall safety requirements but also to improve the systems performance in the following areas: belt comfort, webbing guidance to eliminate problems with pi-

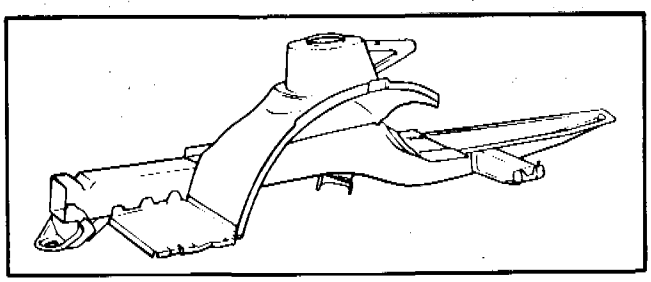

Figure 5. Front member system.

voting webbing guides, seat cushion yieldingness for front and rear seats optimizing the balance of the forces acting on the restrained occupant in a crash.

For the front seats a three-point manual belt with lower anchorage points in the seat frame was chosen. The system incorporates one reel and webbing guide fully covered behind a panel. The webbing guide in the B-pillar is inclined "aligned" and bolted to the pillar hereby giving consistent performance in crash testing.

The lower belt anchorages are located in the seat structure giving constant belt geometry of the lap belt independent of the seat position. The dynamic forces in a crash are transmitted through the rails which are engineered to withstand this extra loading.

The seat structure shown in Figure 6 has a special tube under the frontal part of the cushion which limits the vertical movement of the occupant during a crash.

To minimize steering wheel intrusion during a crash the system has at two locations a collapsible shaft, one for bending moments and one for axial loadings, in combination with a, for rearward forces, strong mounting of the upper shaft bearing.

Forces generated by chest impacts of unbelted occupants in a crash will be absorbed at a tolerable force level by deforming the steering wheel and the bracket for the upper shaft bearing.

The steering wheel with its four spokes, padded rim and hub is designed to mitigate head and face injuries on belted occupants in case of contact with the steering wheel during a crash.

The primary goal has been to keep the instrument panel away from the belted occupant during a crash. This has put special demands on the fire-wall and scuttle area as well as the attachments of the instrument panel.

At the same time efforts have been made to design an instrument panel without protruding parts, projecting a "clean" surface towards the occupant.

Sheet metal structure and padding characteristics have been combined to give tolerable forces if, in spite of all, a head contact would occur.

The three-point belt in the rear seat has the same fixed, inclined webbing guide as described above. The floor under the seat cushion has a special ridge which prevents excessive vertical movement and submarining during a crash. This design was built on the experience from the Volvo Concept Car (ref 12).

All belt geometries have within the limits of existing regulations been elaborated to give good protection and comfort for occupants spanning from 5th female to 95th male percentile.

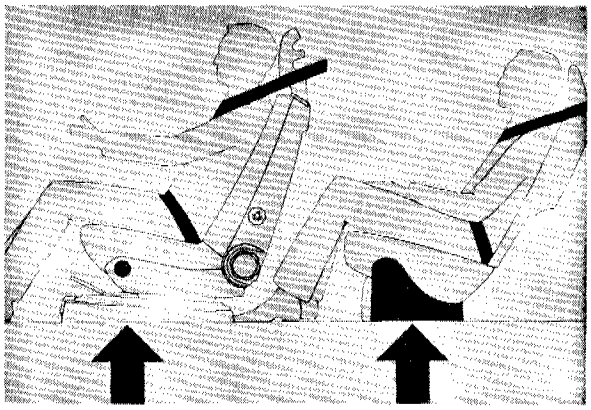

Figure 6. The interior design concept in the Volvo 760.

TEST RESULTS

During the complete development procedure (see Figure 2) a lot of testing was done at component, subsystem, system and complete car level.

At the end of the development it was decided to run three identical frontal barrier tests at 35 mph. The number of tests was chosen as a compromise between cost and the need to cover the repeatability and reproducibility problem. These three tests were run at MIRA (Motor Industry Research Association, England). They are identified by the numbers 227-229 in the following result presentation.

For comparison two previous tests done at the Volvo crash test laboratory are presented. The Volvo tests are taken from some early test series and the cars are prototypes not completely identical with the MIRA cars. The test numbers are 225 and 226. The test results are shown to illustrate the variation in test results during development.

TEST PROCEDURES

The tests were run according to the test procedure specified in FMVSS 208. Both MIRA and Volvo crash test laboratories have a long experience with this test procedure and fullfill all instrument requirements including a well organized dummy calibration procedure. The main difference between the two laboratories is the propulsion system used. MIRA uses an electrical linear motor directly connected to the car and Volvo uses a tyristor controlled electrical rotational motor and an endless wire connected to the car.

The test cars were Volvo 760 GLE with automatic transmission (see Figure 7).

Test weight was as specified in FMVSS 208 (unloaded vehicle weight plus its rated cargo and luggage capacity weight plus two Part 572 dummies) which for the Volvo 760 means 1630 kg (3590 lb).

A total of 50 signals cover both the dummies and different car related measurements as well as a segmented force measuring barrier. The tests were covered by eight high speed cameras.

The dummies were calibrated before every single test.

Table 1 shows some test parameters.

Figure 7. The Volvo 760 GLE.

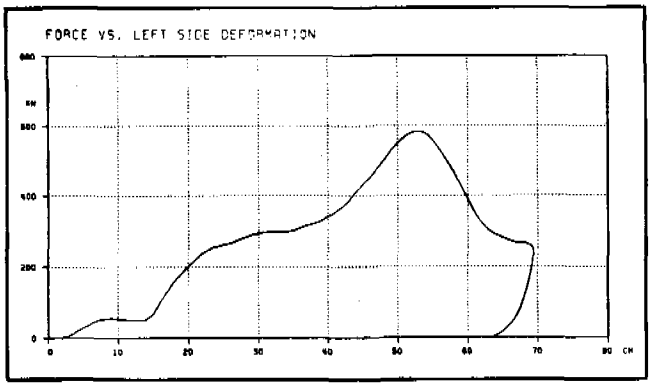

Figure 8. Body deceleration pulse.

Structure Related Test Results

A typical body deceleration pulse is shown in Figure 8.

A typical force/deflection curve is shown in Figure 9.

The following structure related regulations were checked: FMVSS 212 Windshield Retention, FMVSS 219 Windshield Zone Intrusion and FMVSS 301 Fuel System Integrity.

Table 2 shows results of the test.

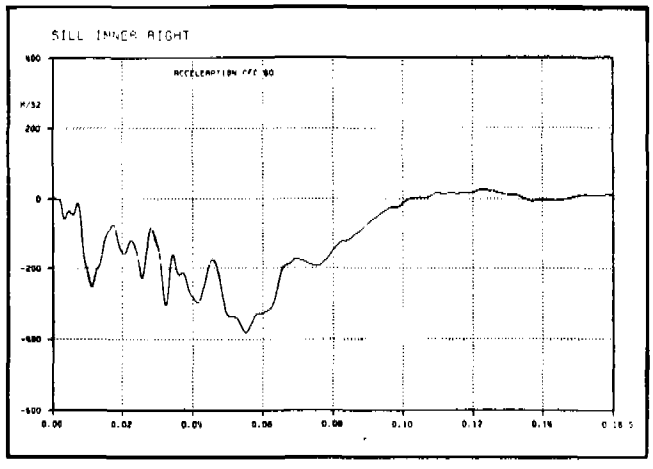

Figure 9. Dynamic Force/Deflection Curve during 35 mph barrier test.

Table 1. Test parameters.

	MIRA 227	MIRA 228	MIRA 229	Mean Value	SD*)	Volvo 225	Volvo 226
Test Weight kg	1630	1630	1630	1630	0.0	1630	1630
Test Speed mph	35.3	35.3	35.2	35.27	0.006	35.2	35.4
Test Temp °C	22.0	22.0	22.0	22.0	0.0	19	20

*) SD = standard deviation defined as SD = $\sqrt{\frac{\sum xi2 - n\bar{x}^2}{n-1}}$

Table 2. FMVSS 212, 219 and 301 test results.

Regulation	MIRA 227	MIRA 228	MIRA 229	Volvo 225	Volvo 226
FMVSS 212 % Retention	100	100	100	100	100
FMVSS 219 Penetration	OK	OK	OK	OK	OK
FMVSS 301 Leakage gram	0	0	0	0	0

Interior Related Test Results

The occupant crash protection was evaluated by measuring dummy signals as required in FMVSS 208.

Chest Injury Criteria

In Table 3 two chest injury criteria are shown.—Resultant chest acceleration duration longer than 3 ms, g_{3ms} and Chest Severity Index, CSI, (weighted time integral of chest resultant during crash).

Head Injury Criteria

Table 4 shows the Head Injury Criteria calculated as defined in FMVSS 208 (HIC) and also the same calculation but during head contact (HIC_c).

Femur Injury Criteria

In Table 5 femur injury criteria as defined in FMVSS 208 are presented.

Seat Belt Loads

Seat belt loads in the lap belt and shoulder belt were also measured and are listed in Table 6.

30° Barrier Test Results

Two tests were also done to evaluate the 30° barrier performance. One test 30° right—first contact passenger side and one test 30° left—first contact driver side and both tests at a velocity of 35 mph.

Requirements in FMVSS 212 Windshield Retention, FMVSS 219 Windshield Zone Intrusion and FMVSS 301 Fuel System Integrity were all met.

Dummy test results as for FMVSS 208 can be seen in Table 7.

CONCLUSIONS

This work has demonstrated that by integrating the desired safety properties from the very beginning of a new

Table 3. Dummy results—Chest injury criteria.

Chest Injury Criteria	MIRA 227	MIRA 228	MIRA 229	Mean Value	SD	Volvo 225	Volvo 226
Driver							
g_{3ms}	46.4	50.0	47.0	47.8	1.9	54.0	49.2
CSI	370	427	417	405	30	455	428
Passenger							
g_{3ms}	41.6	45.0	45.0	43.9	2.0	45.8	41.4
CSI	283	311	323	306	21	345	372

Table 4. Dummy results—Head injury criteria.

Head Injury Criteria	MIRA 227	MIRA 228	MIRA 229	Mean Value	SD	Volvo 225	Volvo 226
Driver							
HIC	945	697	820	821	124	898	825
HIC_c	645	676	820	714	93	898	825
Passenger							
HIC	729	890	990	870	132	1030	1290
HIC_c	27	209	87	108	93	349	686

Table 5. Dummy results—Femur injury criteria.

Femur Force kN	MIRA 227	MIRA 228	MIRA 229	Mean Value	SD	Volvo 225	Volvo 226
Driver							
F_L (Left)	4.96	4.74	4.24	4.65	0.37	5.8	4.4
F_R (Right)	0.61	1.76	1.07	1.15	0.58	2.0	1.3
Passenger							
F_L (Left)	3.91	5.52	3.36	4.26	1.12	3.6	3.1
F_R (Right)	1.31	2.98	0.87	1.72	1.11	1.0	2.3

Table 6. Dummy results—seat belt loads.

Belt load kN	MIRA 227	MIRA 228	MIRA 229	Mean Value	SD	Volvo 225	Volvo 226
Driver							
Lap	6.3	7.9	7.5	7.2	0.8	7.0	6.1
Shoulder	7.4	8.2	7.5	7.7	0.4	5.2	7.7
Passenger							
Lap	7.3	7.0	7.9	7.4	0.5	7.4	7.5
Shoulder	7.6	6.8	6.7	7.0	0.5	7.8	7.7

Table 7. Dummy results—30° barrier.

Test Parameters				
Velocity: 36.5 mph Right; 36.2 mph Left Weight: 1630 kg.				
	30° Right/MIRA		30° Left/MIRA	
	Driver	Passenger	Driver	Passenger
Chest g_{3ms}	35.0	31.0	47.0	44.0
CSI	216	227	388	315
HIC	418	517	762	570
HIC_c	285	258	361	73
Femur Forces			3.2	1.4
F_L kN	1.4	2.8		
F_R kN	2.8	2.4	2.6	0.8
Belt Loads			4.2	8.9
Lap kN	5.9	2.2		
Shoulder kN	6.9	5.1	6.8	7.6

car project and by continuously following up the engineering process it is possible to achieve an increased level of safety.

It has pointed out the inherent complexity of crash testing and the need to use statistical methods in order to make qualified judgments during a car development process.

Emphasis has also been placed on the necessity to use experience from field accidents in order to complement the laboratory simulation.

REFERENCES

1. H. Norin et al. Injury reducing effect of seat belts on rear seat passengers. ESV-Conference Wolfsburg 1980.
2. Fatal Accident Reporting System 1979. United States Department of Transportation.
3. N. J. Bohlin. Refinements of Restraint System Design—A Primary Contribution to Seat Belt Effectiveness in Sweden. International Symposium on Occupant Restraint. Toronto June 1981.
4. G. O'Connel, R. Almqvist. A Survey Concerning the Quality of Part 572 Hybrid II Dummies as measuring instruments for crash testing. SAE 770263.
5. V. Seiffert, H. Leyer. Dynamic Dummy Behaviour under Different Temperature Influence. SAE 760804.
6. L. M. Patrick, A. Andersson, N. J. Bohlin. Three-point Harness Accident and Laboratory Data Comparison. 18th STAPP Car Crash Conference 1974.
7. G. Walfisch et al. Human Head Tolerance to Impact: Influence of the Jerk on the Occurrence of Brain Injuries. IRCOBI 1981.
8. L. G. Svensson. Means for Effective Improvement of the Three-Point Seat Belt in Frontal Crashes. 22th STAPP Car Crash Conference 1978.
9. D. Adomeit, H. Appel. Influence of Seat Design on the Kinematics and Loadings of the Belted Dummy. IRCOBI 1979.
10. B. Lundell et al. Safety Performance of a Rear Seat Belt System with Optimized Seat Cushion Design. SAE Passenger Car Meeting 1981, SAE 810796.
11. S. Runberger. Dynamic Test Method for Crash Testing of Front Structures. To be presented at Open University, Milton Keynes UK November 1982.
12. H. Mellander, M. Koch. Restraint System Evaluation—A Comparison Between Barrier Crash Tests, Sled Tests and Computer Simulation. SAE Passenger Car Meeting 1978. SAE 780605.
13. J. Versace. Safety Test Performance Level. 6th Experimental Safety Vehicle Conference. Washington DC 1976.
14. M. Koch, A. Nilsson-Ehle. Setting Realistic Design Limits in Vehicle Safety Development. To be presented at the 1983 SAE International Congress and Exposition, Detroit February/March 1983.

Computer Modeling of Occupant Dynamics in Very Severe Frontal Crashes

SHERMAN E. HENSON
Ford Motor Company

3664

ABSTRACT

Computer simulations of occupant dynamics in frontal crashes have pretty much been done like sled tests, in that crash-induced deformation of the interior—which may be significant for the occupant—has usually not been accounted for. The object of occupant dynamics simulation studies is often to assess the effect of changes in vehicle front-end parameters on occupant response. But these parameter variations may influence the amount of interior deformation. In order to simulate more accurately occupant dynamics in very severe crashes, the interior deformation caused by engine intrusion should concurrently be simulated. Crash test results over a range of speeds were used in a computer simulation study of occupant compartment intrusion in high speed barrier crash tests. It was found that intrusion has a significant effect on occupant response and where appropriate should be included in crash simulations. For the crash conditions simulated, intrusion increased the restrained occupant's head and chest accelerations while no clear trend emerged for the unrestrained occupant.

INTRODUCTION

This paper describes the use of a computer model to simulate dummy dynamics in very severe frontal car crashes—crashes that are similar to running a car into a wall at speeds ranging from 35 to 50 mph. Figures 1 and 2 are photographs of vehicles which were in real accidents of approximately the range of severity of the simulations discussed in this paper. These high speed crashes tend to use up all of the energy-absorbing capability built into the front structure of the car and so the front of the passenger compartment gets pushed closer to the occupant. The effect of this passenger compartment deformation on the loads imposed on the occupant in severe crashes is not very well understood. Computer simulations of occupant dynamics in frontal crashes have usually been done like sled tests, in that crash-induced deformation of the interior—which may be significant for the occupant—has not been accounted for. The object of such simulation studies is often to assess the effect of changes in vehicle front-end parameters on occupant response. But these parameter variations may influence the amount of interior deformation. In order to simulate more accurately occupant dynamics in very severe crashes, interior deformation caused by engine intrusion should concurrently be simulated.

In the study reported here, results of high speed barrier crash tests run by NHTSA were used to estimate occupant compartment intrusion as a function of time for input to a computer simulation model of occupant dynamics. Simulations were run both with and without intrusion to study the effect of intrusion isolated from other crash variables.

METHODOLOGY

The study utilized a computer model called MVMA-2D that was developed by the University of Michigan Highway Safety Research Institute with funding from the Motor Vehicle Manufacturers Association. The model is a lumped mass multi-degree-of-freedom dynamics model which represents an occupant, his restraint system, and the vehicle interior, as shown in Figure 3. The windshield, steering column, instrument panel, and floor pan are represented by line segments. In order to simulate the effects of occupant compartment intrusion, the movement of these components as a function of time relative to the occupant's seating position was needed as an input to the model.

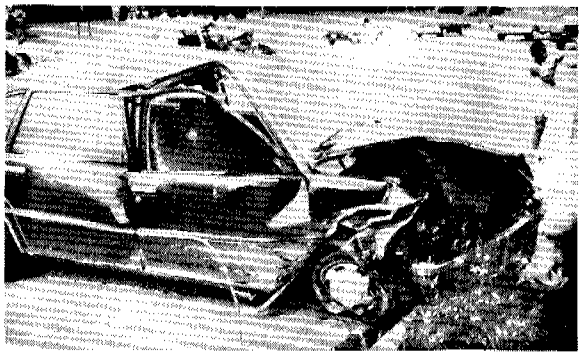

Figure 1. Actual severe crash.

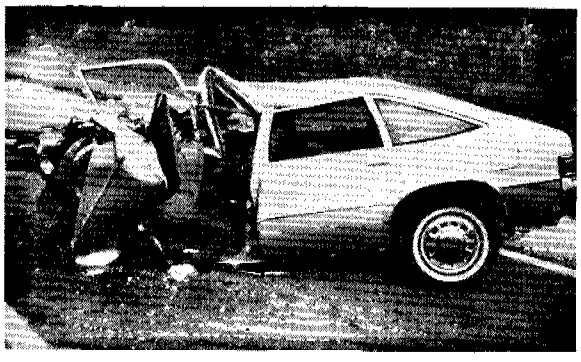

Figure 2. Actual severe crash.

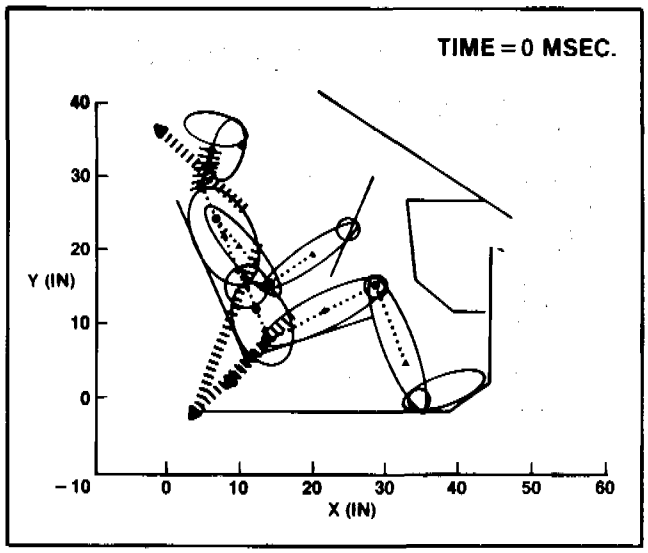

Figure 3. MVMA-2D computer model.

To estimate the movement of the intruding components into the passenger compartment, films of crash tests run by the NHTSA on Chevrolet Citations at 35, 40, and 48 mph were analyzed. The availability of test data at these high speeds was the main reason for choosing the Citation for this simulation study. High speed film analysis was used to determine the relative engine movement as a function of time in these three crashes because the engine, in effect, forced the intruding components rearward into the passenger compartment. Figure 4 shows the results of the film analysis, the average dynamic engine intrusion in inches as a function of time in milliseconds at the three speeds. The maximum intrusion varies from about 3 in. at 35 mph to about 22 in. at 48 mph and reaches the maximum at about 90 to 120 ms.

Knowing the engine movement as a function of time, and the Chevrolet Citation interior dimensions, the vehicle interior deformation was estimated for these crashes. The maximum rearward movement of the windshield, A-pillar, and upper instrument panel were gotten from post-crash vehicle photographs and from post-crash measurements included in the crash reports. The above components were assumed to begin relative movement at the time when engine intrusion began and to reach maximum deformation at the time of maximum vehicle crush. Displacement of each component between these two times was assumed to increase linearly with time. It had to be assumed that the lower instrument panel, dash panel, steering wheel, and floor pan displacement-time relationships were identical to that of the engine intrusion since the data were not available from the test to establish the intrusion precisely as a function of time and the area was hidden from the high speed camera coverage. It is recognized that the lower instrument panel rearward movement may not be identical to that of the engine, but the assumption was necessary in this case and the error introduced by this assumption is believed to be small. During model validation at 48 mph, the maximum rearward displacement of the steering wheel was adjusted somewhat to improve simulation fidelity. Figure 5 shows an outline of the maximum deformation of the passenger-side windshield and instrument panel at the three speeds as well as the undeformed location. The windshield position at 35 mph is the same as the undeformed position. A line drawing of the seat is shown for reference. Notice how the instrument panel and windshield move back and rotate as the crash speed is increased. Figure 6 shows the same thing for the driver side, except the steering wheel maximum deformation is included. As in Figure 5, the

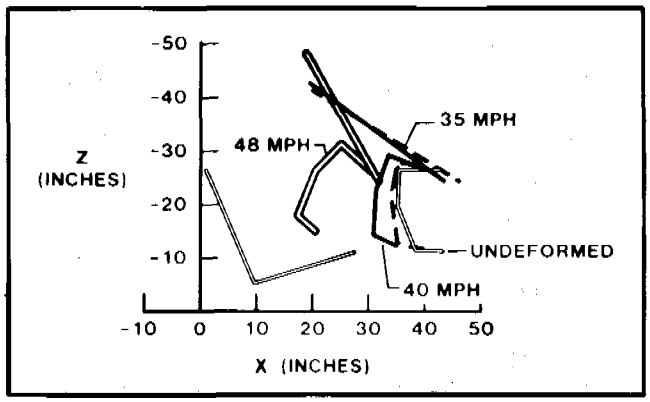

Figure 5. Passenger side interior deformation.

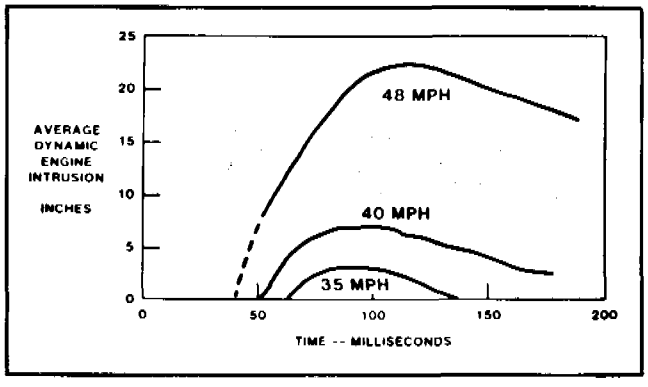

Figure 4. Average dynamic engine intrusion *vs.* time.

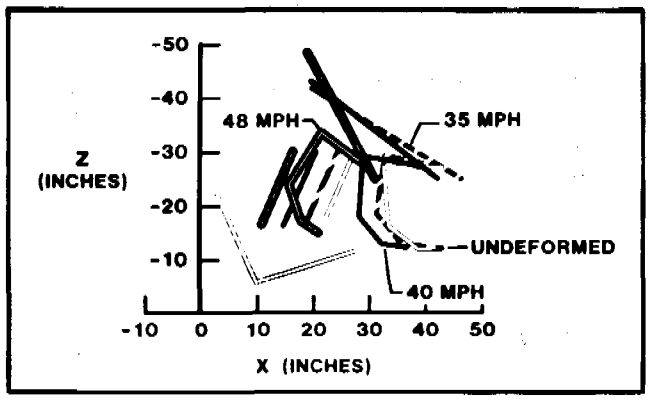

Figure 6. Driver side interior deformation.

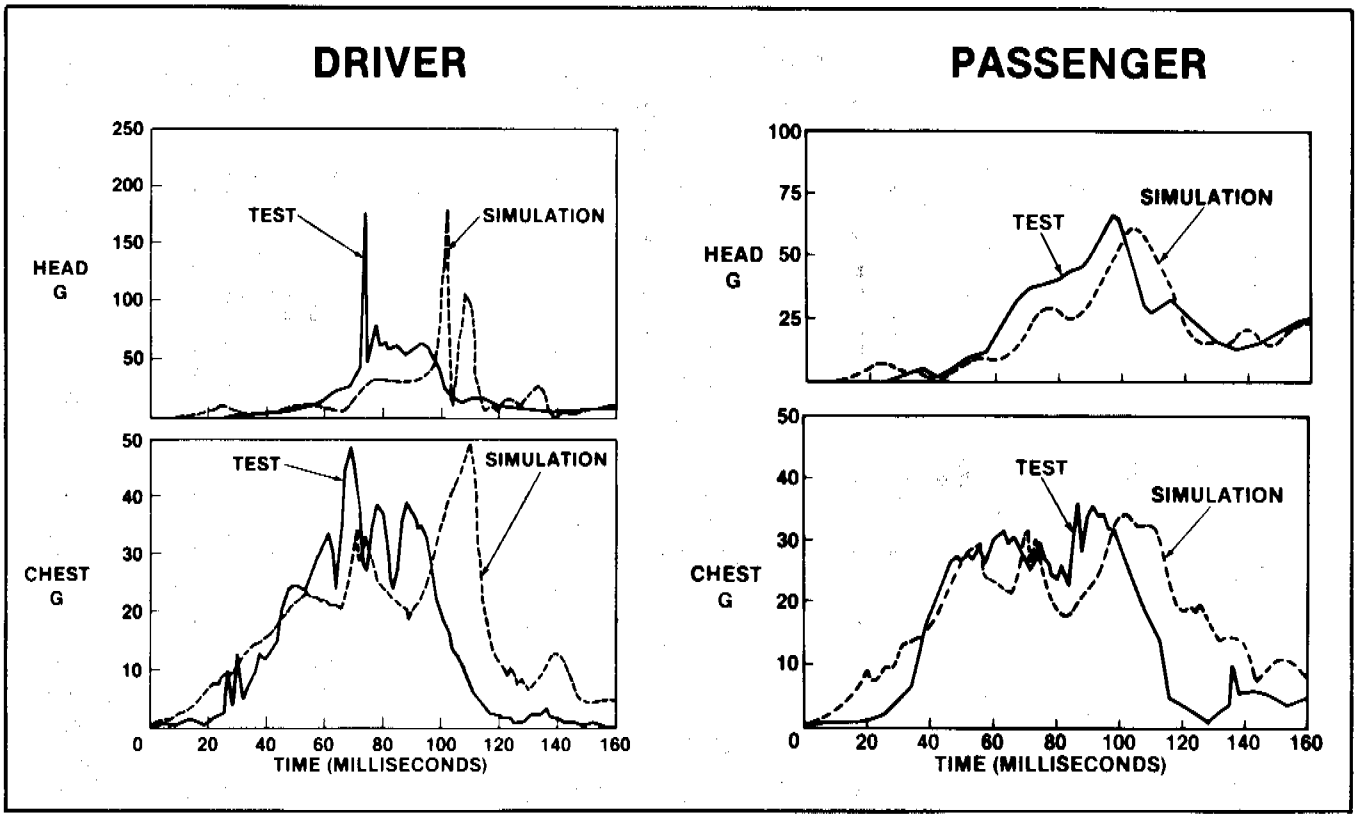

Figure 7. Model validation at 35 mph.

windshield is not deformed at 35 mph. The steering wheel position shown is the expected position without occupant loading. Figures 5 and 6 show the *maximum* deformation of the components, but for input into the model, the positions as a function of time for not only these components but the floor pan and toe board were required. To get the component positions as a function of time, functional relationships for the movement of all of these components were derived from the test results and the functions were inputted into the model as tables of surface displacement as a function of time.

The MVMA-2D model was set up to represent a 50th percentile male in a Citation package. The belt-restrained occupant is shown in Figure 3, but an unrestrained occupant was also simulated. Exercising these models is a very complex and time-consuming procedure, since hundreds of input variables are required to describe the occupant and vehicle interior. For each of the panels that can be contacted by the occupant such as the windshield, instrument panel, and seat, force-deflection characteristics are inputted into the model in either tabular or polynomial format. Belt restraint material properties have to be inputted as well as the acceleration-time pulse of the occupant compartment. Once all the input data were gathered and put into the computer correctly, several runs were made and the results were compared to those of the Citation tests to see if the model was a reasonable simulation of the event. The following section describes the model validation.

VALIDATION

Figure 7 shows a comparison of the dummy head and chest acceleration as a function of time for a driver and right front passenger in a 35 mph barrier crash. The solid lines are the test values from the Chevrolet Citation tests and the dashed lines are the simulation results. The results of the simulations compare reasonably to the test results especially when the large test-to-test variability of barrier crashes is considered. The same comparison at 40 mph is shown in Figure 8. The match again is reasonable except that, as in Figure 7, the peak head g's in the simulation occur somewhat later than in the test. The comparison at 48 mph in Figure 9 again shows that the simulation peaks occur later than the test.

Although there is room for improvement in the simulation, overall, the results were considered acceptable for the present study. Matching peak accelerations over the wide range of crash severity represented here proved to be more difficult than tuning a model to a single, less severe crash. The model predictions could not be compared to test results for the unrestrained occupant because a comparable set of tests has not been run.

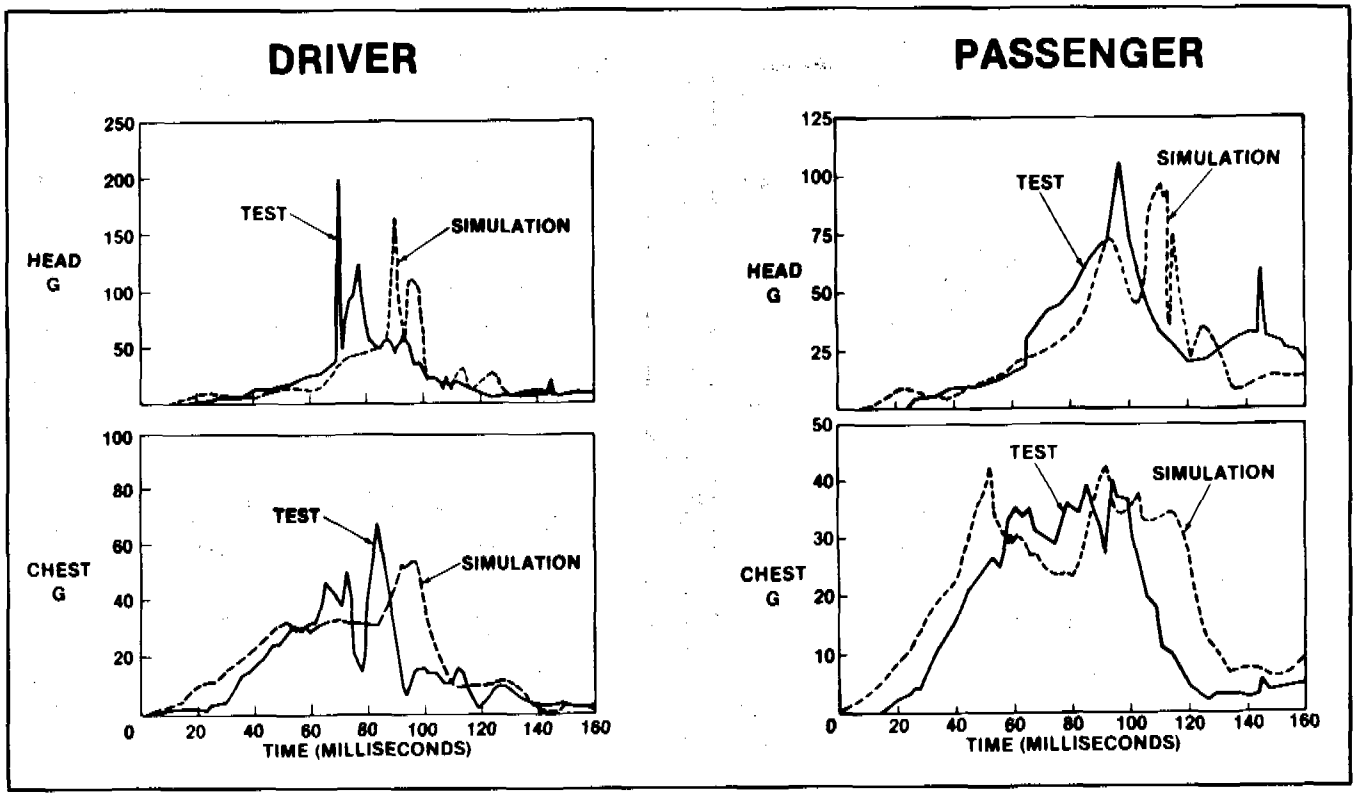

Figure 8. Model validation at 40 mph.

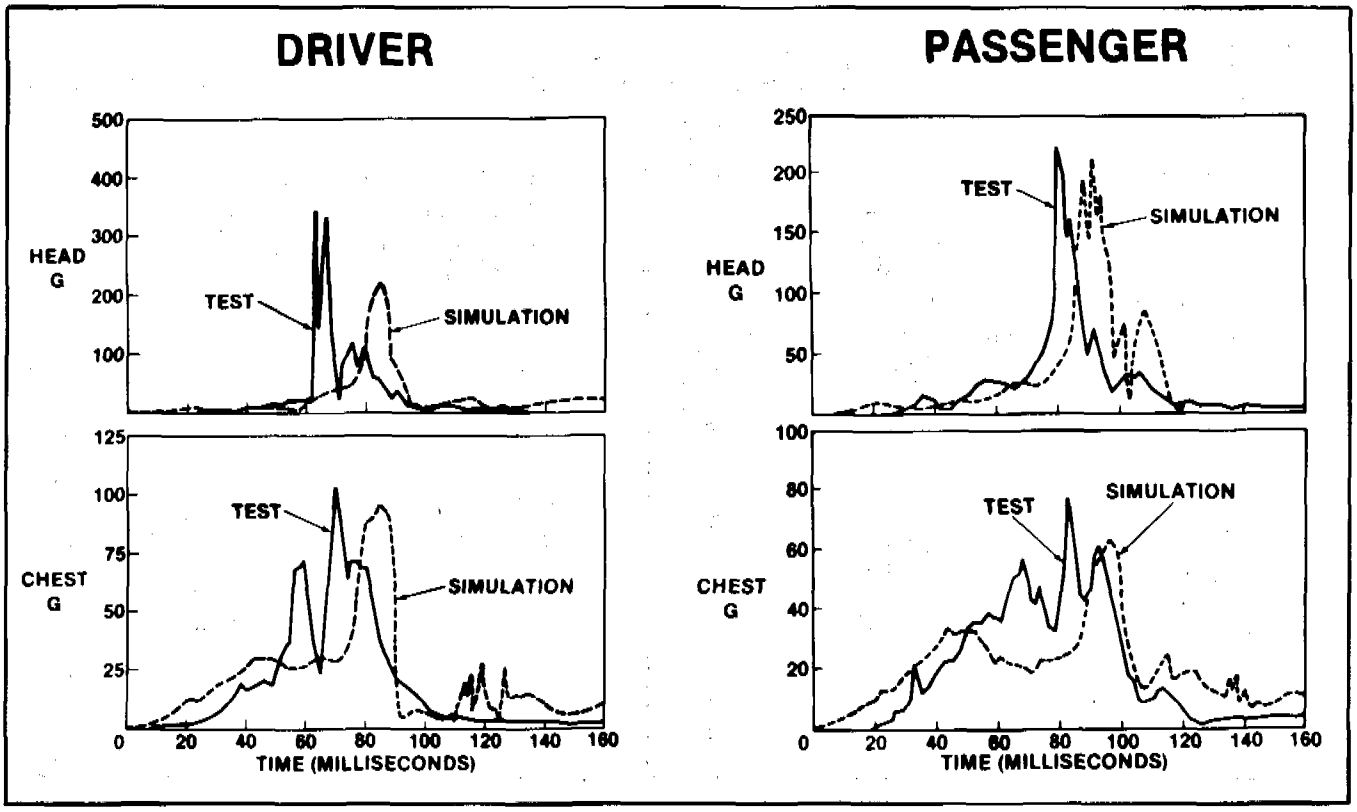

Figure 9. Model validation at 48 mph.

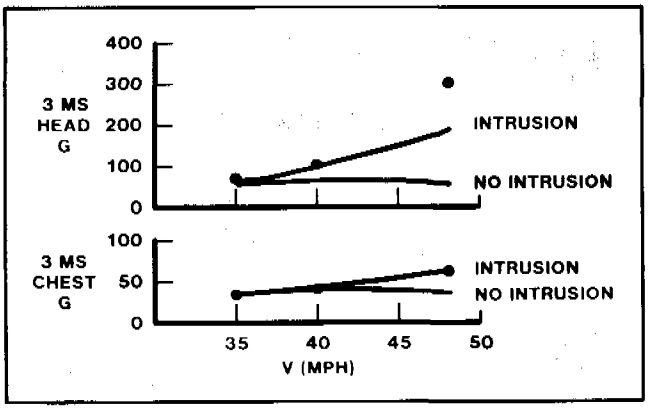

Figure 10. Intrusion effects on restrained passenger.

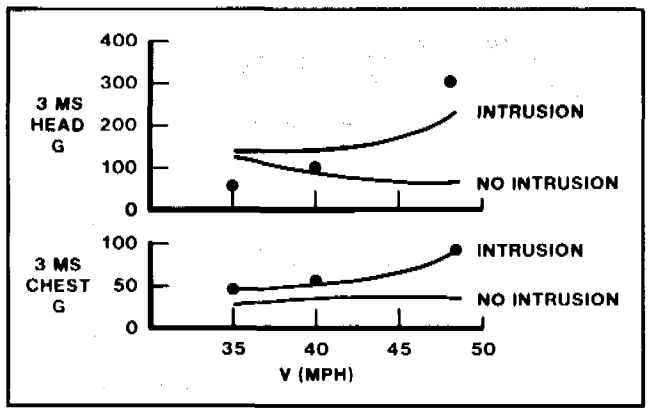

Figure 12. Intrusion effects on restrained driver.

PRELIMINARY RESULTS

Once the model was validated, computer runs were made to explore the effect of intrusion on dummy dynamics. This was done by simply repeating the simulations of the Citation barrier crash tests at the three speeds without the occupant compartment deformation. Figure 10 shows the maximum head acceleration of the restrained right front dummy for the three crash speeds with intrusion and with no intrusion. The dots on the graph are the values from the Citation tests. It is apparent that eliminating the intrusion for the restrained occupant has little effect at 35 mph where the intrusion is small, but the effect increases with speed and the head acceleration is much larger at 48 mph. Without intrusion, the dummy responses are nearly constant as speed increases. The constant response occurs because at these large values of structural crush, the crush resistance is nearly constant and so the vehicle average deceleration is nearly constant over the range from 35 to 48 mph.

Figure 11 shows the occupant kinematics for the same simulations as Figure 10. The upper set shows the occupant position at about the time of maximum forward movement, which is about 100 ms, for the three crash speeds when intrusion was included in the simulations.

It can be seen in the upper figures, the ones where intrusion was simulated, that the occupant strikes the instrument panel more forcefully as the crash speed is increased because the instrument panel and floor pan are moving closer to him. It was shown in Figure 4 that maximum engine intrusion occurs at about the same time, 100 ms. In the lower set of figures, the case with no intrusion, the occupant moves nearly the same distance forward even as speed increases and never hits the instrument panel because the panel remains in the same relative position.

The peak head and chest accelerations for the restrained driver are shown in Figure 12. As in the case of the restrained passenger, head and chest accelerations are lower when there is no intrusion. The apparent decrease in head acceleration is an artifact due to the 3 ms cutoff; the absolute peak acceleration actually increases slightly with speed.

The restrained driver position at 100 ms is shown in Figure 13 for the simulations with intrusion and with no intrusion. It is again apparent from the figures that the occupant loads the intruding components more forcefully when there is intrusion, resulting in higher head and chest accelerations.

While eliminating intrusion appears to be an attractive

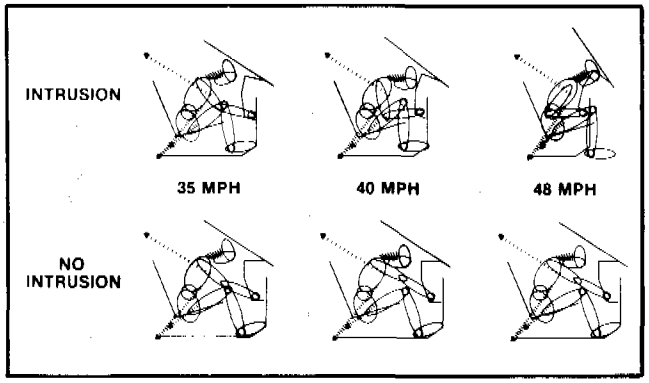

Figure 11. Intrusion effects on restrained passenger at 100 milliseconds.

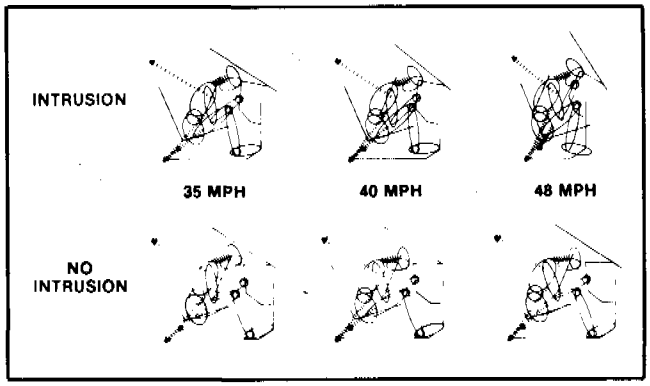

Figure 13. Intrusion effects on restrained driver at 100 milliseconds.

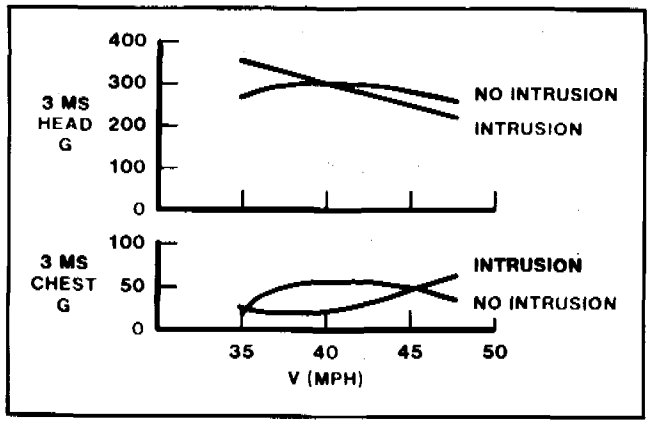

Figure 14. Intrusion effects on unrestrained passenger.

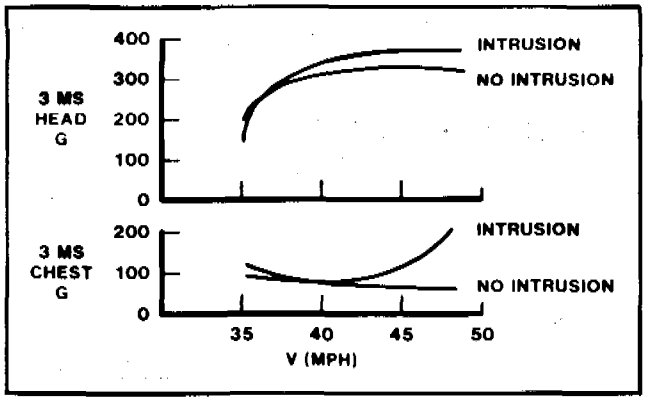

Figure 16. Intrusion effects on unrestrained driver.

way to reduce occupant loads for both driver and passenger, it is difficult in practice. In order to eliminate intrusion in these very severe crashes, the front structure would have to be made either very stiff, or the front of the car would have to be made very long. If the structure were stiffened, the vehicle acceleration would increase and the occupant in the bottom set of pictures in Figures 11 and 13 would move farther forward and probably strike the instrument panel like the occupant in the upper pictures where intrusion is included. Increasing the length, on the other hand, of the front of the car by the large amount necessary to eliminate intrusion in these very severe collisions would be impractical.

Figure 14 is similar to Figure 10 except the results are for the unrestrained passenger. The unrestrained model is identical to the validated restrained model except the belts were removed. There is no clear difference between the simulations with intrusion and those with no intrusion either for head or chest accelerations. There is an interesting effect, however, for the head acceleration in the case of intrusion. The head acceleration decreases somewhat as the crash speed increases. This is probably due to an effect known as ride-down, where the relative speed that the head contacts the windshield decreases at higher impact speeds because the windshield is moving closer to the occupant.

Figure 15 shows the kinematics for the unrestrained occupant. Notice that the occupant kinematics confirm the conclusion drawn from Figure 14, that there is very little difference in the unrestrained occupant response whether or not there is intrusion. The final occupant position in the simulations with intrusion shown in the upper figures looks almost like the bottom row of figures where no intrusion was included.

The head and chest acceleration results for the unrestrained driver are shown in Figure 16. Head acceleration is somewhat lower for the case with no intrusion, but is quite high in both cases. There is little difference in chest acceleration for intrusion compared to no intrusion except in the extremely severe 48 mph collision where the simulated steering column bottoms out. The validity of the simulation in this region is not known since test results for unrestrained occupants were not available. The high chest acceleration is determined by the assumed force-deflection characteristic of the steering system in the region beyond the normal collapse zone. Because force-deflection characteristics for the steering column were not available under these severe conditions, the simulation

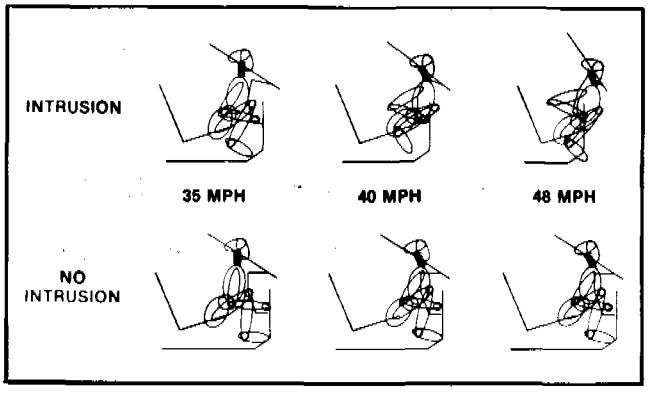

Figure 15. Intrusion effects on unrestrained passenger at 100 milliseconds.

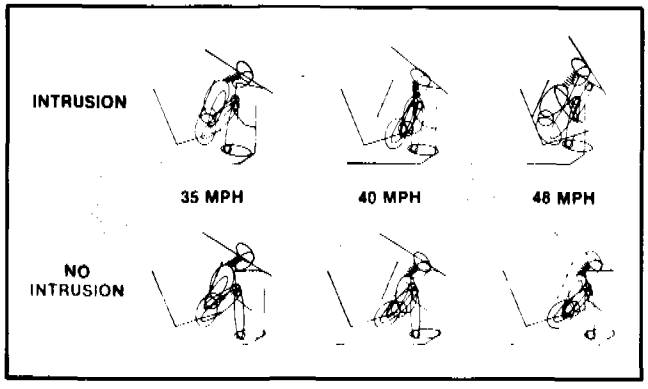

Figure 17. Intrusion effects on unrestrained driver at 100 milliseconds.

results could be considerably in error. The kinematics of the unrestrained driver are shown in Figure 17.

DISCUSSION AND CONCLUSIONS

The results of the computer simulation study indicate that simulations, whether by mathematical model or by impact sled, of severe collisions should take intrusion into account. Including intrusion is most important for the restrained occupant where intrusion may make the difference between contacting or not contacting the instrument panel or windshield, or where intrusion may have a large influence on the force generated by the contact.

In all the restrained occupant simulations, the effect of intrusion was to increase occupant acceleration. The effect of intrusion on the unrestrained dummy was not as clear as for the restrained dummy. In some cases intrusion reduced accelerations while in other simulations, accelerations were increased by intrusion.

The results of the simulations discussed above should not be generalized and applied to all accidents. Only a small fraction of frontal collisions were simulated in this study. Offset and angular collisions with other size occupants could produce different results. Also, while it is easy to eliminate intrusion in mathematical models, it is not so simple in practice. Using today's technology, major structural changes would be required (particularly for the higher speed crashes) which, even if possible, would greatly increase weight, cost, and fuel consumption and could adversely affect the safety of vehicles now on the road through increased aggressiveness in car-to-car collisions. A major challenge for the future is to determine through systems analysis tradeoff studies, the optimal balance of vehicle structure characteristics.

ACKNOWLEDGEMENT

The simulations described in this paper were set up and run by John Dueweke. Matthew Huang developed the program which created the computer graphics of the MVMA-2D occupant. Assistance and consultation by other MVMA-2D users at Ford is gratefully acknowledged.

REFERENCES

1. Bowman, B. M., Bennett, R. O., and Robbins, D. H., "MVMA Two-Dimensional Crash Victim Simulation, Version 4," Volume 1 (UM-HSRI-79-5-1) and Volume 2 (UM-HSRI-79-5-2), Highway Safety Research Institute, The University of Michigan, June 29, 1979.
2. Bowman, B. M., Bennett, R. O., Robbins, D. H., and Becker, J. M., "MVMA Two-Dimensional Crash Victim Simulation, Version 4," Volume 3 (UM-HSRI-79-5-3), Highway Safety Research Institute, The University of Michigan, June 29, 1979.
3. Levan, W. E., and Alianello, D. A., *"New Car Assessment and Standards Enforcement Indicant Testing*—FMVSS Nos. 212, 219, and 301-75, General Motors Corporation 1980 Chevrolet Citation 5-Door Hatchback, NHTSA 308-T1-430," Report No. 6525-V-1, (39.93 Mph), Calspan Corporation, Buffalo, N.Y., June 6, 1979.
4. Levan, W. E., and Alianello, D. A., *"New Car Assessment and Standards Enforcement Indicant Testing*—FMVSS Nos. 212, 219, and 301-75, General Motors Corporation 1980 Chevrolet Citation 5-Door Hatchback, NHTSA 308-T2-431," Report No. 6525-V-2, (48.0 Mph), Calspan Corporation, Buffalo, N.Y., June 7, 1979.
5. Levan, W. E., and Alianello, D. A., *"New Car Assessment and Standards Enforcement Indicant Testing*—FMVSS Nos. 212, 219, and 301-75, General Motors Corporation 1980 Chevrolet Citation 5-Door Hatchback, NHTSA 308-T3-432," Report No. 6525-V-3, (35.0 Mph), Calspan Corporation, Buffalo, N.Y., June 12, 1979.

Possible Future Trends Towards Increasing Occupant Protection in Frontal Impacts

3665

G. JONES
Austin Rover Group Ltd.

ABSTRACT

Over the past decade or so of ESV/RSV activity it has been a priority to improve occupant protection in frontal impacts and there is evidently a need to continue research towards establishing maximum protection in this mode of impact.

In the ESV program we have seen developments aimed at making larger heavier cars more accommodating to the smaller lightweight cars in collision situations. We have also seen that there are big problems in reducing the aggressiveness of the larger heavier vehicles.

Future developments, particularly for lightweight cars, may therefore have to be based on the assumption that

it is not always possible to achieve the ideal of little or no intrusion matched to a restraint system which ideally attenuates the vehicle deceleration.

In these circumstances there appears to be considerable merit in the concept that the occupant be held much more rigidly in the seating position by seat belts considerably stiffer than those currently used.

Recent tests using a typical 30 mph barrier crash pulse show that reduced injury levels and much reduced forward displacement to avoid or reduce the effects of secondary impact, are obtained when adopting this concept.

With a more severe pulse the latter advantages are retained and injury levels, though higher, are still below accepted tolerable levels.

Bearing in mind the fact that a high proportion of frontal impacts are assymetric, producing relatively lower deceleration values but with more intrusion, the overall trade-off would appear to favour the system with reduced forward displacement.

INTRODUCTION

This paper concerns an investigation into the possibility of obtaining increased protection from seat belts in frontal impacts.

It is well known that belts as currently provided, and when correctly worn, do enable occupants to survive impacts of much greater severity than would be so if the occupants were unrestrained. However, there is evidently a need to continue the search for further improvements in restraint system performance particularly in view of the fact that initiatives towards producing a degree of compatibility between large and small vehicles in frontal impacts has proved to be much less fruitful than was expected at the start of the ESV program.

Accident data show that in some impacts the most serious injuries are as a result of the occupant striking forward interior components such as the steering wheel or facia partly because the restraint itself can allow considerable forward displacement and partly because of intrusion.

These injuries are generally more severe than those produced by the belts themselves.

The tests described in this paper were therefore carried out to determine the effect of having a restraint system which very much reduced the forward displacement of the occupant.

ACCIDENT DATA

The most recent data which indicate the general effectiveness of seat belts in the United Kingdom have been provided by the Transport and Road Research Laboratory and by the University of Birmingham Accident Research Unit.

One of the conclusions in a TRRL report by Hobbs (1) was that a seat belt wearing rate of 100% would give an estimated further saving of over 12,000 fatal and serious casualties per year. If only 85% wearing rate were achieved, which is a more realistic figure, the potential further saving would be 9,000. An estimate by the University of Birmingham Accident Research Unit, based on detailed studies of fatal accidents (2) suggests that in the United Kingdom about 800 people each year die needlessly in their cars simply because they do not use the seat belts available to them. These people represent 12% of all road accident fatalities, because car occupant fatalities comprise only about one-third of the total road deaths.

Note that the overall average seat belt wearing rate in Britain during the period covered by these statements has been about 30%.

Frontal impacts, even for those wearing seat belts, do however present the greatest risk of serious injury though this risk is much lower than for those not wearing belts.

One of the TRRL findings was that where injuries due to direct seat belt loading occurred they were mainly of minor severity.

It was also reported that the head was the most commonly injured region of the body and, because of the presence of the steering wheel, there were more drivers with serious injures (AIS3–6) than there were front seat passengers within the same injury range.

However, the difference was not statistically significant. Similar general statements on the TRRL findings were reported by Hobbs in a more recent paper (3).

In-depth investigations have also been carried out by the University of Birmingham Accident Research Unit and findings (4) were similar to those of the TRRL with regard to belted drivers suffering more severe head injuries than belted front seat passengers in frontal impacts.

Using the University of Birmingham data it is calculated that for injuries AIS3–6 the difference between drivers and front seat passengers was not statistically significant in this study also. When moderate injuries are included so that the range is AIS2–6 the difference, as reported, is statistically significant.

For drivers, the head and face was the most frequently injured body area, followed by the legs and the chest. For front seat passengers the head and face was the most frequently injured body area but its importance was much reduced compared with drivers and the chest was almost as important followed by the legs.

As would be expected, head or facial contacts were much more frequent where there was headspace intrusion, there being severe head space intrusion in accidents involving under-run and significant intrusion compromising belt performance in partial overlap impact configurations.

Although chest injuries were almost as important as head and face injuries for front seat passengers, it is noted that in the absence of intrusion and additional loading

from rear seat passengers, or luggage, no occupant sustained a chest injury more severe than AIS3, that is they were non-life-threatening.

A later publication by the University of Birmingham Accident Research Unit (5) deals specifically with steering wheel induced head injuries amongst drivers restrained by seat belts and a paper by Mackay (6) has emphasised the fact that injury producing contacts with the steering wheel and other forward components are subjects for further investigation in the search for better protection in frontal impacts.

BASIC CONCEPTS AND PRACTICAL REALITIES

One currently popular concept for obtaining increased occupant protection is to assume that there is little significant intrusion into the passenger compartment and to provide a restraint system which attenuates the vehicle deceleration to produce minimum forces on the occupant. Such a concept relies on inelastic deformation of the restraint system and use of all available space.

In cases where intrusion is small it is natural to endeavour to produce the ideal by allowing the restraint system to make full use of the forward displacement available before the occupant contacts the facia or steering wheel, etc.

However, current safety belt systems are not sufficiently inelastic or in other words the displacement is not sufficiently plastic as to produce attenuation. In fact there is usually a degree of magnification as associated with the performance of a damped elastic system.

Whilst this may indicate that future developments towards providing a more plastic restraint system deformation would be beneficial, field experience shows that there is little intrusion only in a limited proportion of real crash events.

Therefore good energy absorption qualities need to be linked to the practical limitations of available space when intrusion occurs.

An alternative concept, based on acceptance of the fact that considerable intrusion does occur in a proportion of the more severe frontal impacts, is to restrain the occupant so that he or she experiences little displacement within the passenger compartment and is subject to substantially the same deceleration pulse as the vehicle itself, virtually all of the energy-absorption being exterior to the occupant compartment.

In theory even when there is no intrusion the occupant should at least be better off than with an elastic restraint system in that there should be no magnification of deceleration.

The Battelle Memorial Institute proposed such a system as a near-term recommendation in their 1970 report 'The Evaluation of Phase I Reports on the Experimental Safety Vehicle Program' (7)—the recommendation being based mainly on reducing occupant mass sensitivity problems associated with elastic restraint systems, and concerned with vehicles in which there would be little intrusion.

In the context of the present study there are obvious advantages when considerable intrusion occurs.

TEST PROGRAMME

To obtain some facts related to this concept a series of tests was carried out on the 'Hyge' sled at the Motor Industry Research Association. These were to compare the performance of a typical inertia reel belt system with a belt system broadly in accordance with the Battelle recommendations, i.e., an elongation rate 10 to 20 percent of current belts under comparable loading.

This stiffer belt system consisted of a laminate of four thicknesses of current webbing for the lap and diagonal section, and for test purposes it was a static system with the shoulder belt terminating the 'B' post anchorage, to also minimise the effective belt length.

We estimate that at comparable loading the elongation of this system was in the order of 5 to 10 percent of that for the inertia reel system.

FIRST TEST SERIES

Figure 1 shows the 'Hyge' pulse used for the initial series of tests,—it is similar to the crash signatures from some medium size UK cars subjected to 30 mph barrier tests.

In this initial series of tests the Part 572 manikin was installed on the sled in a rigid seat as normally used for ECE 16 type seat belt tests.

Comparative forward displacements and injury criteria for the Part 572 manikin are shown in Table 1.

With standard inertia reel belts the mean maximum forward displacement of the head was 460 mm and with the stiff belts the figure was 300 mm.

The mean chest 'g' value exceeded for a cumulative

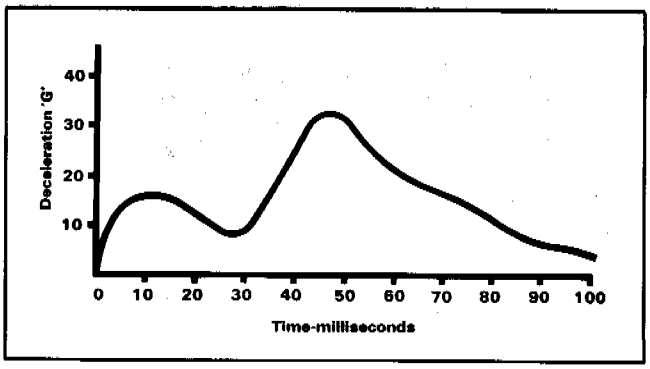

Figure 1. 'HYGE' test pulse-first series of tests.

Table 1. Results from part 572 manikin-first series.

Injury Criteria	Mean Test Results	
	Standard inertia reel belt	Special stiff belt system
Maximum Forward Displacement of Head—mm	460	300
Chest 'G' Exceeded for Cumulative 3 milliseconds	36.2	32.6
Chest Peak Resultant Deceleration 'G'	40.0	35.0
Head Injury Criteria	635	424
Head 'G' Exceeded for Cumulative 3 milliseconds	55.0	47.0
Head Peak Resultant Deceleration 'G'	57.6	50.0

3 m sec period was 36.2 for the standard inertia reel belt system and 32.6 with the stiff belt system.

Although many regard measured head injury criteria as being of no consequence when there is no contact between the head and any vehicle component, it is of interest to note that in these tests, in which there were no components to contact, the mean HIC was 635 with the standard belts and 424 with the stiff belt system.

It will be noted that with the stiff belt system the maximum forward displacement—that is, at the head—is approximately 65 percent of that which occurs with the standard belt system and at the same time the numerical injury values are less.

A further point noted was the tendency for the torso of the manikin to roll out of the diagonal section of the standard inertia reel belts.

This tendency was less evident with the stiff belts.

SECOND TEST SERIES

A further series of tests was carried out using a 'Hyge' pulse which lies within the ECE 16 envelope and which is shown in Figure 2.

This series of tests was carried out to determine the effect of using a differently shaped pulse, i.e., one having a more rapid build-up to peak 'g'.

As in the initial test series the ECE 16 seat and the Part 572 manikin were used.

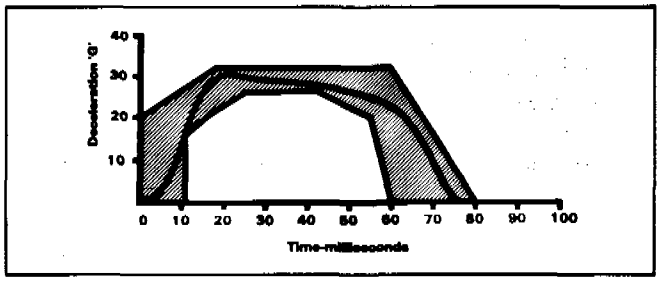

Figure 2. 'HYGE' test pulse-second series of tests.

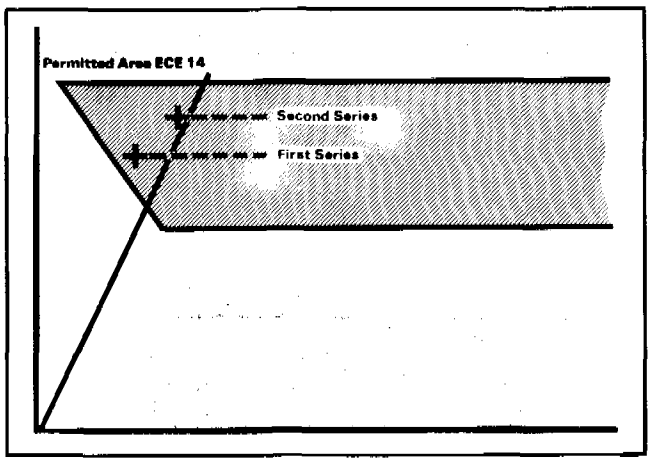

Figure 3. Shoulder anchorage point positions.

For this further series of tests the shoulder anchorage point was also raised in an endeavour to reduce the torso roll-out which had occurred particularly when standard inertia reel belts were used in the initial series. The respective anchorage points are shown in Figure 3.

The raised anchorage point still complies with the requirements of Regulation ECE 14 but the belt fit was more suited to the Part 572 manikin and there was no tendency to roll out.

Figure 4 shows comparative forward displacements of the manikin.

In this case with standard inertia reel belts the maximum forward displacement of the head was 530 mm and with the stiff belts the figure was 310 mm, i.e., less than 60 percent of the amount with standard belts.

Table 2 shows forward displacements relative to the ECE regulation requirements, this time at chest level. Head displacement is also shown for comparison.

Compared with the ECE 16 range of between 100 and 300 mm, measurements at chest level were 310 and 135 mm respectively for standard inertia reel and stiff belt system.

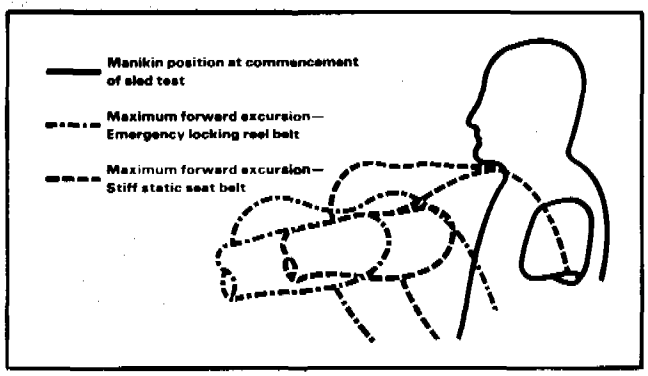

Figure 4. Forward movement of manikin restrained by emergency locking reel belt and by stiff static seat belt.

Table 2. Forward displacement of manikin-second series.

	ECE 16 Requirement	Mean Test Results mm: Standard inertia reel belt	Special stiff belt system
Head Displacement	None	530	310
Torso Displacement	Between 100 & 300	310	135
Pelvis Displacement	Between 80 & 200	170	95

It is of interest to note that although the Part 572 manikin is quite different from that used in testing belts to Regulation ECE 16 the forward displacements with standard reel belts are in the region of the higher ECE 16 values whereas with stiff belts they are near the lower values.

The comparative mean measured injury values from the Part 572 manikin are shown in Table 3. In this test series the mean chest 'g' value exceeded for a cumulative 3 m sec period was 44.5 for the standard reel belt system and 54.3 for the stiff system.

Comparable peak resultant chest values were 48.8 and 59.6 'g' respectively.

Note that whereas in the initial series of tests the values for the stiff system were lower, the values in this second series are higher.

However the results from these tests, using a pulse which some regard as being excessively severe, do show that even the peak resultant chest value does not exceed the 60 'g' which is accepted as being tolerable for a cumulative period of no more than 3 m sec.

With regard to head injuries it may again be pointed out that the quoted values may be of no consequence in the absence of head contact.

Even if they were considered to be of consequence the slightly higher results from the stiff belt system are not significant.

Table 3. Results from part 572 manikin-second series.

Injury Criteria	Mean Test Results: Standard inertia reel belt	Special stiff belt system
Chest 'G' Exceeded for Cumulative 3 milliseconds	44.5	54.3
Chest Peak Resultant Deceleration 'G'	48.8	59.6
Head Injury Criteria	521	582
Head 'G' Exceeded for Cumulative 3 milliseconds	60.2	63.5
Head Peak Resultant Deceleration 'G'	62.2	66.2

CONCLUSIONS

The results of the tests indicate that the forward movement of the occupant in an impact can be significantly reduced by the use of seat belts which at a comparable loading have much less elongation than current reel belt systems. This is particularly significant in the case of the driver whose space available for forward movement is limited by the steering wheel and also when in more severe impacts there is intrusion into the passenger compartment.

Though there is some trade-off in chest injury when the more severe test pulse is used, it must be noted that no special attention was paid to damping properties and it is possible that an increased amount would be an advantage.

Belt tensioning and webbing clamping devices are known developments towards the objective of reducing forward movement of the occupant. Low elongation webbing of minimum length, possibly in combination with a suitably developed webbing clamping system may be the most practical means of producing further improvements in reel belt systems. Any future developments along these lines must however run in parallel with developments towards providing maximum possible levels of comfort and convenience.

ACKNOWLEDGEMENTS

The writer would like to thank colleagues in the Austin Rover Group of BL Cars for assistance in preparing this paper.

Management are also thanked for permission to publish this paper.

REFERENCES

1. Hobbs C. A. The Effectiveness of Seat Belts in Reducing Injuries to Car Occupants. Department of Transport TRRL Report LR811. Crowthorne, 1978 (Transport and Road Research Laboratory).
2. Mackay G. M. University of Birmingham Accident Research Unit—Press Statement, May 1981.
3. Hobbs C. A. Car Occupant Injury Patterns and Mechanisms. Transport and Road Research Laboratory. Crowthorne, paper at Eighth International Technical Conference on Experimental Safety Vehicles—Wolfsburg, 1980.
4. Rattenbury S. J. et al.: The Biomechanical Limits of Seat Belt Protection. The American Association for Automotive Medicine. Kentucky, 1979.
5. Gloynes P. F. et al.: Steering Wheel Induced Head and Facial Injuries Amongst Drivers Restrained by Seat Belts. Sixth IRCOBI Conference, France, 1981.

6. Mackay G. M. Seat Belts In Europe—Their Use and Performance in Collisions. International Symposium on Occupant Restraint. Ontario, Canada, June 1981.

7. The Evaluation of Phase 1 Reports on the Experimental Safety Vehicles Program. Battelle Memorial Institute—Columbus Laboratories, Ohio, 1970.

3666

Occupant Protection from Impact with the Steering Assembly

JOHN B. MORRIS, LEE STUCKI, RICHARD M. MORGAN and NANCY BONDY
National Highway Traffic Safety Administration

ABSTRACT

This paper will discuss areas of NHTSA research relating to the accident environment of the driver impacting the steering assembly. These include:

- Accident analyses to define the problem.
- Development of biomechanical criteria for assessment of injury severity on test surrogates.
- Laboratory testing of steering assemblies to determine the safety performance.
- Computer modeling for reconstructing accidents and assessing the effects of changes to steering assembly characteristics on driver responses.

The accident analyses quantify the problem in terms of injuries and fatalities sustained by drivers as a result of impacting the steering assembly. Relationships will be developed between frequency and severity of injury and source of injury, affected body regions, crash direction and severity, and steering assembly response parameters.

Biomechanical injury criteria on blunt thoracic impact is available and may be applicable to chest impact with steering wheel hubs.

A program was recently completed which evaluated the safety performance of several production steering assemblies and, also, one improved steering assembly constructed from components with desirable safety attributes. The performance was evaluated via component tests and dynamic sled tests with instrumented Hybrid III dummies.

A computer program entitled "*S*teering *C*olumn and *O*ccupant *RE*sponse *S*imulation" (SCORES) has been developed to model the various interactions of a driver impacting a steering assembly in a frontal collision. The SCORES model is used to predict the occupant/steering assembly response when certain assembly characteristics are changed, i.e., column force deflection properties, and to reconstruct actual accident cases.

A joint effort by NHTSA and Transportation Systems Center (TSC) is being conducted to reconstruct the accident environment of occupants injured by the steering assembly. The SCORES model will be exercised for various make/model vehicles, occupant sizes, and accident configurations which essentially comprise this accident environment. Countermeasures will be introduced into the SCORES model and the effect on injury and fatality reduction will be assessed.

BACKGROUND

The steering column is responsible for producing more injuries and fatalities than any other vehicle component. In an effort to alleviate the harm caused by the steering assembly, the automobile industry started designing and developing energy absorbing steering assemblies in the late 1950's (1). Methods were also devised to prevent rearward intrusion of the steering column during the crash event. In 1965, the Society of Automotive Engineers (SAE), recognizing the need for a test procedure for this new device, issued Recommended Practice J944 (2). This practice describes the laboratory test procedure for evaluating the characteristics of steering control systems under simulated driver impact conditions. It consists of a body form weighing 75 pounds that impacts a steering assembly mounted in the production configuration. A load cell mounted between the wheel and column is used to measure the force imparted to the system.

In 1966, the General Services Administration (GSA) issued a steering assembly protection rule (GSA Standard 515/4a) which became effective in October 1967 (3)(4). All passenger cars purchased by GSA after the effective date were required to comply with this standard. The standard specified that the force imparted to the SAE J944 body form must not exceed 2,500 pounds when impacting the steering assembly at 15 mph. The intrusion prevention portion of the standard specified that the rearward horizontal displacement of the upper end of the column must not exceed 5 inches during a 30 mph frontal barrier test.

In 1967, NHTSA adopted the GSA standard but separated the energy absorption and rearward displacement requirements into two standards, FMVSS Nos. 203 and 204. These standards became effective on January 1, 1968 (5). Federal Motor Vehicle Safety Standard (FMVSS) No. 203, "Impact Protection for the Driver From the Steering Control System," specifies requirements for minimizing chest, neck, and facial injuries by providing steering systems that yield forward, cushioning the impact of the driver's chest by absorbing much of his impact energy in

frontal crashes. FMVSS No. 204, "Steering Control Rearward Displacement," specifies requirements limiting the rearward displacement of the steering control into the passenger compartment to reduce the likelihood of chest, neck, or head injuries.

Compliance with these standards has resulted in various designs for absorbing the energy of the occupant impacting the steering assembly, usually an energy absorbing device in the column (FMVSS No. 203). The prevention of column intrusion into the occupant compartment is usually accomplished by a shear capsule (FMVSS No. 204). The standards were subsequently extended to light trucks and vans effective September 1, 1981.

Many accident analyses have been conducted to assess the effect of post-1968 steering assemblies. Garrett (6), Huelke (7), Nahum (8), Levine (9), O'Day (10), and McLean (11) all reported a reduction in severe injuries as a result of the energy absorbing steering column. Two studies have been conducted by NHTSA to determine the effectiveness of post-1968 steering assemblies. One study was conducted by Kahane (4)(12), and the other which is included in the rulemaking support paper for FMVSS Nos. 201, 203, and 204 Extension to Light Trucks and Vans (13).

Kahane (4) reported that in pre-standard cars in the National Crash Severity Study (NCSS), 58 percent of the drivers who were killed or hospitalized in frontal crashes were seriously injured by contacts with the steering assembly. This is in agreement with a study by Nahum (8) based on 1960-1966 model cars. Kahane also reported that the pre-standard steering column entered into the passenger compartment in 3.5 percent of the towaway accidents. There also was column displacement in 20 percent of the cases involving steering assembly contact and 75 percent of the driver fatalities (14).

Using data from the Fatal Accident Reporting System (FARS), Kahane concluded that energy absorbing steering systems reduced the risk of driver fatalities in frontal crashes by 12 percent. Using NCSS data the study also concluded that energy absorbing systems reduced by 38 percent the risk of serious injury due to the steering assembly. Also observed was that post-standard steering system reduced the incidence of column intrusion into

Table 1. Harm to car occupant as a function of contact point.

	Contact	Body Region	Harm % of Total
1	Steering assembly	Chest	11.90
2	Steering assembly	Abdomen	9.41
3	Side interior surface	Chest	4.94
4	Windshield	Head and face	4.68
5	A-Pillars	Head and face	4.04
6	Instrument panel	Lower extremities	3.43
7	Steering assembly	Head and face	3.13
8	Roof edge	Head and face	3.02
9	Side interior surface	Abdomen	2.36
10	Instrument panel	Chest	2.06
11	Instrument panel	Abdomen	1.85
12	Roof	Head and face	1.80
13	Instrument panel	Head and face	1.65
14	Instrument panel	Upper extremities	1.40
15	Arm rests	Abdomen	1.25
16	Glove comp. area	Abdomen	1.23
17	Steering assembly	Upper extremities	1.16
18	Mirrors	Head and face	1.08
19	Glove comp. area	Chest	0.84
20	Window glass	Head and face	0.79
21	Window frame	Head and face	0.77
22	Front seat backs	Abdomen	0.76
23	Side interior surface	Lower extremities	0.71
24	Floor	Lower extremities	0.69
25	Roof edge	Neck	0.57
	All the above		65.52
	All other interior contacts		14.74
	All non-contact		7.91
	All exterior contacts		11.83
	All		100.0

Malliaris (15)

the passenger compartment by 68 percent. It should be noted that since it is difficult to separate the effects of FMVSS Nos. 203 and 204 on injury reduction, the above estimates are based on the combined effectiveness of the two standards.

Despite the apparent safety improvements of steering assemblies since 1968, the steering assembly remains the major source of injury. Using NCSS data, Malliaris (15) ranked source of injury (contact point) by percent of harm. Four of the top 17 most harmful body region/contact point interactions are produced by the steering assembly. Table 1 presents harm to the occupant as a function of contact point/body region.

Cohen (16) in analyzing NCSS data concluded that the steering assembly is responsible for 27 percent of all serious (AIS 3-6) injuries. The body areas involved and their percentage of total serious injury is shown in Table 2. As can be seen, steering assembly impacts with the chest and abdomen account for nearly 20 percent of all serious injuries. A tabulation of the distribution of steering assembly injury by body region is shown in Table 3. Serious to fatal injuries attributed to the steering assembly occur predominately to the chest (54%) and abdomen (25%). Cohen also investigated the effect of delta V on injury produced by the steering assembly. Figure 1 illustrates the results of this analysis. The mean delta V for serious chest injury is approximately 27 mph and 32 mph for the abdomen. Additional analysis of the accident data as it relates to the steering column will follow later.

Table 2. Percent of all AIS 3-6 injuries caused by steering assemblies.

Steering assembly/all body parts 27.3%		(698)
Steering assembly/chest	14.5	
Steering assembly/abdomen	6.6	
Steering assembly/upper extremity	1.8	
Steering assembly/head and face	1.7	
Steering assembly/pelvis	1.4	

Cohen (16)

Table 3. Distribution of steering assembly injuries (AIS 3-6) by body part and impact direction.

Body Part	Frontal	Non-Frontal
Chest	53.5%	51.8%
Head and face	6.6	5.5
Abdomen	24.9	22.1
Pelvis	5.8	4.5
Upper extremity	5.0	11.1
Lower extremity	2.2	2.5
Total AIS 3-6 Injuries	499	199

Cohen (16)

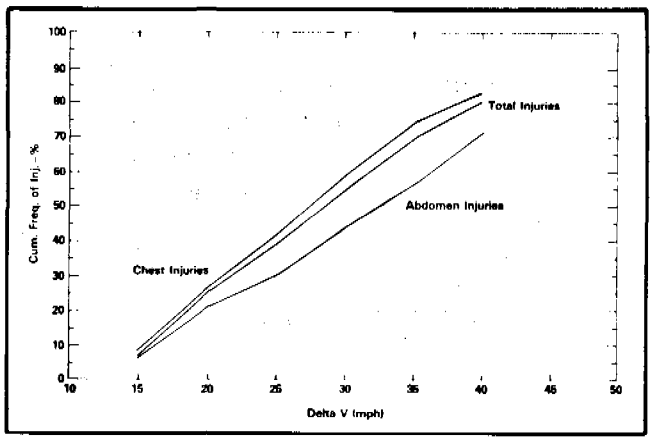

Figure 1. Distribution of steering assembly injuries—AIS 3-6 injuries—for drivers in frontal impacts by delta V.

As reported by Stucki (17) several issues have been raised regarding the adequacy of the FMVSS No. 203 test procedures. Key among these issues are:

- The test device does not physically simulate the driver impacting the steering assembly in actual crash simulations.
- The test device is not a good human surrogate and the performance criteria are not adequate indicators of injury severity.
- The inability of the test and/or performance criteria to distinguish "good" and "bad" design steering assemblies as a result of the previous inadequacies.

Observations of the inability of the current test procedure to address the effects of accident-induced steering column behavior were made by Gloyns (18) and Garrett (19).

Stucki also noted that the FMVSS No. 203 force criteria do not account for load distribution and that improvements to the safety of the steering assembly such as load distribution features are not rewarded by the performance criteria. Ways to realistically evaluate the safety performance of the steering assembly will be addressed later in this paper.

ACCIDENT ANALYSIS

The National Crash Severity Study (NCSS) contains 12,050 accidents in which a passenger car, light truck, or van had to be towed. Accidents were sampled from seven areas throughout the United States from January 1977 to March 1979. The NCSS file reports 67,559 weighted drivers in towaway passenger cars, of which 14,512 had a known contact source. Of the 14,512 drivers 5,902 or 40.7% had contact with the steering assembly of which 154 or 2.69% were fatally injured. The data presented in this section consist of only those drivers in passenger cars having contact with the steering assembly.

Table 4 shows the distribution of driver injury severity in terms of AIS, by crash mode. Crash mode is defined by the variable 'General Area of Deformation' which is the second component of the Collision Deformation Classification (CDC) and describes the general area of impact to the vehicle. The most severe impact to the vehicle was used to define crash mode.

Table 4 shows that 72% of the drivers having steering assembly contact were in frontal impacts. Almost 74% of the injuries caused by steering assembly contact were minor injuries (AIS 1). Note: in right and left impacts, there are almost the same number of drivers contacting the steering assembly.

Table 5 shows the distribution of AIS for drivers having contact with the steering assembly by delta V. Delta V is defined as the change in velocity which occurs during the collision.

Deleting the 'other' category, Table 5 shows that 76% of the drivers were occupants of passenger cars having a delta V between 1-20 miles per hour. Approximately 82% of the AIS 1 and 2 injuries occur at the delta V between 1-20 mph. The severe injuries AIS 3-6, increase proportionally as the delta V increases.

Table 6 describes the injuries sustained by drivers contacting the steering assembly in terms of body region and AIS.

Table 6 shows that over 60 percent of the injuries to drivers contacting the steering assembly are to the body regions face and chest, followed by upper extremities, head and abdomen. Note: the majority of these injuries are of low severity; however, over 40 percent of the injuries to the abdomen and one-fourth of the injuries to the chest are AIS 3 and above.

The National Accident Sampling System—Continuous Sampling Subsystem (NASS-CSS) is a random sample of police-reported accidents in 10 sites throughout the United States. These accidents when weighted produce national estimates. Because the potential error in many of the estimates is large, these numbers should be used as estimates, not as precise counts.

Table 4. AIS for drivers having contact with the steering assembly by crash mode (NCSS).

Frequency Percent Row % Column %							
AIS	Front	Right	Left	Back	Top	Other*	Total
	3113	264	246	213	106	420	4362
	52.75	4.47	4.17	3.61	1.80	7.12	73.91
1	71.37	6.05	5.64	4.88	2.43	9.63	
	73.21	71.16	66.49	89.50	75.71	79.10	
	558	53	60	11	9	65	756
	9.45	0.90	1.02	0.19	0.15	1.10	12.81
2	73.81	7.01	7.94	1.46	1.19	8.60	
	13.12	14.29	16.22	4.62	6.43	12.24	
	325	33	32	13	19	33	455
	5.51	0.56	0.54	0.22	0.32	0.56	7.71
3	71.43	7.25	7.03	2.86	4.18	7.25	
	7.64	8.89	8.65	5.46	13.57	6.21	
	99	7	17	0	2	8	133
	1.68	0.12	0.29	0	0.03	0.14	2.25
4	74.44	5.26	12.78	0	1.50	6.02	
	2.33	1.89	4.59	0	1.43	1.51	
	90	8	9	1	3	2	113
	1.53	0.14	0.15	0.02	0.05	0.03	1.91
5	79.65	7.08	7.96	0.88	2.65	1.77	
	2.11	2.16	2.43	0.42	2.14	0.38	
	16	2	2	0	0	0	20
	0.27	0.03	0.03	0	0	0	0.34
6	80.00	10.00	10.00	0	0	0	
	0.38	0.54	0.54	0	0	0	
Injured	51	4	4	0	1	3	63
Severity	0.86	0.07	0.07	0	0.02	0.05	1.07
Unknown	80.95	6.35	6.35	0	1.59	4.76	
	1.20	1.08	1.08	0	0.71	0.56	
Total	4252	371	370	238	140	531	5902
	72.04	6.29	6.27	4.03	2.37	9.00	100

*Other includes undercarriage, unclassifiable, and unknown.

Table 5. AIS for drivers having contact with the steering assembly by delta V (NCSS).

Frequency Percent Row % Column %	Delta V (miles per hour)								
AIS	1-10	11-20	21-30	31-40	41-50	51-60	61-99	Other*	Total
	823	1351	358	46	9	2	0	1773	4362
	13.94	22.89	6.07	0.78	0.15	0.03	0	30.04	73.91
1	18.87	30.97	8.21	1.05	0.21	0.05	0	40.65	
	88.59	75.35	60.58	25.56	18.37	14.29	0	75.80	
	80	275	89	37	6	1	0	268	756
	1.36	4.66	1.51	0.63	0.10	0.02	0	4.54	12.81
2	10.58	36.38	11.77	4.89	0.79	0.13	0	35.45	
	8.61	15.34	15.06	20.56	12.24	7.14	0	11.46	
	20	107	87	46	13	2	1	179	455
	0.34	1.81	1.47	0.78	0.22	0.03	0.02	3.03	7.71
	4.40	23.52	19.12	10.11	2.86	0.44	0.22	39.34	
3	2.15	5.97	14.72	25.56	26.53	14.29	14.29	7.65	
	1	28	27	19	7	1	1	49	133
	0.02	0.47	0.46	0.32	0.12	0.02	0.02	0.83	2.25
4	0.75	21.05	20.30	14.29	5.26	0.75	0.75	36.84	
	0.11	1.56	4.57	10.56	14.29	7.14	14.29	2.09	
	0	15	25	25	13	6	4	25	113
	0	0.25	0.42	0.42	0.22	0.10	0.07	0.42	1.91
5	0	13.27	22.12	22.12	11.50	5.31	3.54	22.12	
	0	0.84	4.23	13.89	26.53	42.86	57.14	1.07	
	0	1	0	4	1	1	1	12	20
	0	0.02	0	0.07	0.02	0.02	0.02	0.20	0.34
6	0	5.00	0	20.00	5.00	5.00	5.00	60.00	
	0	0.06	0	2.22	2.04	7.14	14.29	0.51	
Injured	5	16	5	3	0	1	0	33	63
Severity	0.08	0.27	0.08	0.05	0	0.02	0	0.56	1.07
Unknown	7.94	25.40	7.94	4.76	0	1.59	0	52.38	
	0.54	0.89	0.85	1.67	0	7.14	0	1.41	
Total	929	1793	591	180	49	14	7	2339	5902
	15.74	30.38	10.01	3.05	0.83	0.24	0.12	39.63	100
%AIS ≤ 3	2.3	8.5	23.7	53	69.4	77	100		

*Other includes unknown and not applicable.

Since the weighting factors assigned to actual accident cases are large in order to extrapolate to national estimates, this magnifies differences between cells with no actual cases and those with only a few cases. As more cases are collected by NASS, this discrepancy should be somewhat corrected.

The NASS-CSS file reports, for 1979 and 1980 combined, 17,703,387 drivers of passenger cars of which 821,732 or 4.6% had contact with the steering assembly. Of the 821,732 drivers 10,353 or 1.3% were fatally injured.

Table 7 shows the distribution of AIS for drivers contacting the steering assembly by crash mode.

Table 7 shows that 60% of the drivers having contact with the steering assembly were in frontal impacts. Almost 85% of the injuries to these drivers were minor injuries (AIS 1). These results are in agreement with the NCSS file.

Table 8 shows the distribution of AIS by delta V.

Excluding the 'other' category, Table 8 shows that 76.7% of the drivers contacting the steering assembly were occupants of passenger cars having a delta V between 1-20 mph. About 80% of the AIS 1 and 2 injuries occurs at delta V between 1-20 mph. The severe injuries, AIS 3-6, increase proportionally as the delta V increases with the exception of delta V '51-60.' The discrepancy is most likely due to the small number of actual cases that fall into the '51-60' category.

Table 9 describes the injuries to drivers in terms of body region and AIS.

Table 9 shows that half of the injuries to drivers are to the body regions, face and chest followed by upper extremities, abdomen, and head. The majority of the injuries are of low severity (AIS 1 and 2); however, almost one-fourth of the injuries to the abdomen and one-sixth of the injuries to the chest are AIS 3 and above. These

Table 6. AIS for drivers having steering assembly contact by body region (NCSS).

Frequency Percent Row % Column %	AIS							
Body Region	1	1	3	4	5	Injured Severity 6	Unknown	Total
*Upper Extremities	682 11.56 84.0 15.64	78 1.32 9.61 10.32	43 0.73 5.30 9.45	9 0.15 1.11 6.77	0 0 0 0	0 0 0 0	0 0 0 0	812 13.76
Chest	1046 17.72 65.62 23.98	144 2.44 9.03 19.05	276 4.68 17.31 60.66	41 0.69 2.57 30.83	60 1.02 3.76 53.09	17 0.20 1.07 85.00	10 0.17 0.63 15.87	1594 27.01
Face	1723 29.19 83.00 39.50	318 5.39 15.32 42.06	29 0.49 1.40 6.37	5 0.08 0.24 3.76	0 0 0 0	0 0 0 0	1 0.02 0.05 1.59	2076 35.17
Head	218 3.69 58.13 5.00	97 1.64 25.87 12.83	13 0.22 3.47 2.86	3 0.05 0.80 2.26	9 0.15 2.40 7.96	1 0.02 0.27 5.00	34 0.58 9.07 53.97	375 6.35
Knee	84 1.42 84.00 1.93	12 0.20 12.00 1.59	4 0.07 4.00 0.88	0 0 0 0	0 0 0 0	0 0 0 0	0 0 0 0	100 1.69
Abdomen	189 3.20 54.94 4.33	2 0.03 0.87 0.26	28 0.47 8.14 6.15	64 1.08 18.60 48.12	44 0.75 12.79 38.94	1 0.02 0.29 5.00	16 0.27 4.65 25.40	344 5.83
Pelvis	71 1.20 57.26 1.63	16 0.27 12.90 2.12	35 0.59 28.22 7.69	1 0.02 0.81 0.75	0 0 0 0	0 0 0 0	1 0.02 0.81 1.59	124 2.10
Shoulder	168 2.85 71.19 3.85	60 1.02 25.42 7.94	7 0.12 2.97 1.54	0 0 0 0	0 0 0 0	0 0 0 0	1 0.02 0.42 1.59	236 3.99
Thigh	88 1.49 73.95 2.02	12 0.20 10.08 1.59	14 0.23 11.76 3.08	5 0.08 4.20 3.76	0 0 0 0	0 0 0 0	0 0 0 0	119 2.02
Other Unknown	93 1.58 76.23 2.13	17 0.29 13.93 2.25	6 0.10 4.92 1.32	5 0.08 4.09 3.76	0 0 0 0	1 0.02 0.82 5.00	0 0 0 0	122 2.07
Total	4362 73.91	756 12.81	455 7.71	133 2.25	113 1.91	20 0.34	63 1.07	5902 100

*Includes arm, elbow, forearm, and wrist/hand.

Table 7. AIS for drivers contacting the steering assembly by crash mode (NASS).

Frequency Percent Row % Column %							
AIS	Front	Right	Left	Back	Top	Other*	Total
	413779	22080	39209	24459	12388	183047	694962
	50.35	2.69	4.77	2.98	1.51	22.28	84.57
	59.54	3.18	5.64	3.52	1.78	26.34	
1	83.12	75.64	70.46	78.99	82.68	94.78	
	45756	4850	6942	6015	999	8606	73168
	5.56	0.59	0.84	0.73	0.12	1.05	8.90
2	62.54	6.63	9.49	8.22	1.37	11.76	
	9.11	16.62	12.48	19.43	6.67	4.45	
	24110	1850	8749	491	1596	1485	38281
	2.93	0.23	1.06	0.05	0.19	0.18	4.66
3	62.98	4.83	22.85	1.28	4.17	3.88	
	4.84	6.34	15.72	1.59	10.65	0.77	
	6194	110	276	0	0	0	6580
	0.75	0.01	0.03	0	0	0	0.80
4	94.13	1.67	4.19	0	0	0	
	1.24	0.38	0.50	0	0	0	
	4514	0	0	0	0	0	4514
	0.55	0	0	0	0	0	0.55
5	100.00	0	0	0	0	0	
	0.91	0	0	0	0	0	
	1498	299	0	0	0	0	1797
	0.18	0.04	0	0	0	0	0.22
6	83.36	16.64	0	0	0	0	
	0.30	1.02	0	0	0	0	
Injured	1961	0	469	0	0	0	2430
Severity	0.24	0	0.07	0	0	0	0.30
Unknown	80.70	0	19.30	0	0	0	
	0.39	0	0.84	0	0	0	
Total	497812	29189	55645	30965	14983	193138	821732
	60.58	3.55	6.77	3.77	1.82	23.50	100

*Other includes undercarriage, unknown, and unclassified.

results are similar to those shown in Table 6 from the NCSS. Differences which appear are primarily due to the small number of actual cases sampled.

SUMMARY

The NCSS and NASS files both indicate that drivers are more likely to contact the steering assembly in frontal impacts than in any of the other impacts. The severity of the impact defined by delta V shows that the severity of the injuries (AIS 3-6) increases as the delta V increases. The common injuries sustained by drivers contacting the steering assembly primarily to the face and chest, followed by upper extremities, head, and abdomen. The majority of these injuries are AIS 1 and 2, however, the severe injuries, AIS 3-6 occur to the body regions, abdomen and chest.

INJURY CRITERIA

In order to assess the protective capability of a steering assembly a criterion for estimating injury is required. As noted previously the two most prevalent body regions injured by the steering assembly are the thorax and the abdomen. In the following section a review of previous studies addressing thoracic and abdominal injury tolerance is undertaken, and the most appropriate continuous injury criteria for frontal thoracic and abdominal impact are presented.

THORAX INJURY CRITERIA—A variety of kinematic parameters have been utilized in the literature for predicting the results of a blow to the thorax—thoracic acceleration, force, deflection, power, etc. The data bases for these approaches also vary extensively in type of subject tested—cadavers, porcine subjects, squirrel monkeys,

Table 8. AIS for drivers having contact with the steering assembly by delta V (NASS).

Frequency Percent Row % Column %	Delta V (miles per hour)							
AIS	1-10	11-20	21-30	31-40	41-50	51-60	Other*	Total
	89174	126837	34646	7583	2175	2522	432022	694959
	10.85	15.44	4.22	0.92	0.26	0.31	52.58	84.57
1	12.83	18.25	4.99	1.09	0.31	0.36	62.17	
	92.35	86.51	67.59	56.18	40.28	71.26	85.57	
	5275	15423	7355	3327	0	782	41009	73171
	0.64	1.88	0.90	0.40	0	0.10	4.99	8.90
2	7.21	21.08	10.05	4.55	0	1.07	56.04	
	5.46	10.52	14.35	24.65	0	22.10	8.12	
	1204	1830	6688	551	2110	235	25653	38271
	0.15	0.22	0.81	0.07	0.26	0.03	3.12	4.66
3	3.15	4.78	17.48	1.44	5.51	0.61	67.03	
	1.25	1.25	13.05	4.08	39.08	6.64	5.08	
	0	1418	1993	0	0	0	3169	6580
	0	0.17	0.24	0	0	0	0.39	0.80
4	0	21.55	30.29	0	0	0	48.16	
	0	0.97	3.89	0	0	0	0.63	
	0	666	0	1801	635	0	1411	4513
	0	0.08	0	0.22	0.08	0	0.17	0.55
5	0	14.76	0	39.91	14.07	0	31.26	
	0	0.45	0	13.34	11.76	0	0.28	
	0	440	399	235	0	0	724	1798
	0	0.05	0.05	0.03	0	0	0.09	0.22
6	0	24.47	22.19	13.07	0	0	40.27	
	0	0.30	0.78	1.74	0	0	0.14	
Injured	911	0	180	0	479	0	861	2431
Severity	0.11	0	0.02	0	0.06	0	0.10	0.30
Unknown	37.47	0	7.40	0	19.70	0	35.42	
	0.94	0	0.35	0	8.87	0	0.17	
Total	96564	146614	51261	13497	5399	3539	504849	821723
	11.75	17.84	6.24	1.64	0.65	0.43	61.44	100
%AIS ≤ 3	1.3	3.0	17.7	19.2	55.8	6.6		

*Other includes unknown and not applicable.

rhesus monkeys, baboon, etc. Each of these data bases has difficulties associated with its use. Using cadavers, the muscle tension and lung inflation (as compared to living subjects) must be considered. Animal tests must be scaled to account for size, shape, and anatomical differences.

The approach taken herein is based on two facets: [1] the injury criteria must be continuous and [2] only data sets composed of human cadavers or porcine subjects shall be utilized and other animal species shall be used only to guide the analysis. Porcine subjects are used based on the understanding that the circulatory, respiratory, and skeletal systems of the pig are important human analogues which establish the pig as structurally a very similar animal species to man (20).

The first body of experiments to be considered is the Kroell data (21, 22). These data are comprised of 24 cadavers which received frontal blunt thoracic impacts. The Kroell data (where the cadaver weights were 90-209 pounds) are shown in Figure 2. The numbers in the center of the figure are the associated injury (using the 1971 AIS scale). The ΔV term for the Kroell data should be the maximum change-of-velocity between the sternum and a point on the spine, say fourth thoracic vertebra. In actuality, that number is often not available and the ΔV of the impactor is substituted. This turns out to be a reasonable approximation for the Kroell data because the sternum pulse is over by the time the spine pulse begins (21). In Reference 23, the average ratio of first integral of the sternal spike pulse to the contact velocity of the impactor is 1:11.

Where this approximation breaks down is when the

Table 9. AIS for drivers having steering assembly contact by body region (NASS).

Frequency Percent Row % Column %	AIS							
Body Region	1	2	3	4	5	Injured Severity 6	Unknown	Total
*Upper Extremities	103258	21818	1458	1087	0	0	0	127621
	12.56	2.66	0.18	0.13	0	0	0	15.53
	80.91	17.10	1.14	0.85	0	0	0	
	14.86	29.82	3.81	16.52	0	0	0	
Chest	165235	11641	26981	3379	2097	1350	1050	211741
	20.11	1.42	3.28	0.41	0.26	0.17	0.13	25.77
	78.04	5.50	12.74	1.60	0.99	0.64	0.50	
	23.78	15.91	70.48	51.34	46.46	75.53	43.21	
Face	267544	28082	746	0	0	0	0	296377
	32.56	3.42	0.09	0	0	0	0	36.06
	90.27	9.48	0.25	0	0	0	0	
	38.50	38.38	1.95	0	0	0	0	
Head	25905	3721	424	0	0	0	0	30050
	3.15	0.45	0.05	0	0	0	0	3.66
	86.21	12.38	1.41	0	0	0	0	
	3.73	5.08	1.11	0	0	0	0	
Knee	24165	709	0	0	0	0	0	24874
	2.94	0.09	0	0	0	0	0	3.03
	97.15	2.85	0	0	0	0	0	
	3.48	0.96	0	0	0	0	0	
Abdomen	33057	511	6151	2115	2417	0	469	44720
	4.02	0.06	0.75	0.26	0.29	0	0.06	5.44
	73.92	1.14	13.75	4.73	5.40	0	1.05	
	4.76	0.70	16.07	32.14	53.54	0	19.30	
Shoulder	31396	3533	0	0	0	0	911	35840
	3.87	0.43	0	0	0	0	0.11	4.36
	87.60	9.86	0	0	0	0	2.54	
	4.52	4.83	0	0	0	0	37.49	
Thigh	27962	0	0	0	0	0	0	27962
	3.40	0	0	0	0	0	0	3.40
	100.00	0	0	0	0	0	0	
	4.02	0	0	0	0	0	0	
Other	16440	3154	2522	0	0	440	0	22556
	2.00	0.38	0.31	0	0	0.05	0	2.74
	72.89	13.98	11.18	0	0	1.95	0	
	2.37	4.31	6.59	0	0	24.47	0	
Total	694962	73169	38282	6581	4514	1798	2430	821736
	84.57	8.90	4.66	0.80	0.55	0.22	0.30	100

*Includes arm, elbow, forearm, and wrist/hand.

impactor mass is very light which is the case for a handful of the Kroell data. (In those few cases, momentum calculations were made to better estimate the sternum ΔV.)

Two models—to define the dependent variable, AIS, as a function of the response parameters—were considered. These were:

$$AIS = f(\Delta V, P/D, Age)$$

and

$$AIS = g(P/D, Age)$$

where

ΔV = impact velocity (fps),
P = penetration,
D = depth of chest,
P/D = normalized total deflection,

and

AGE is in years.

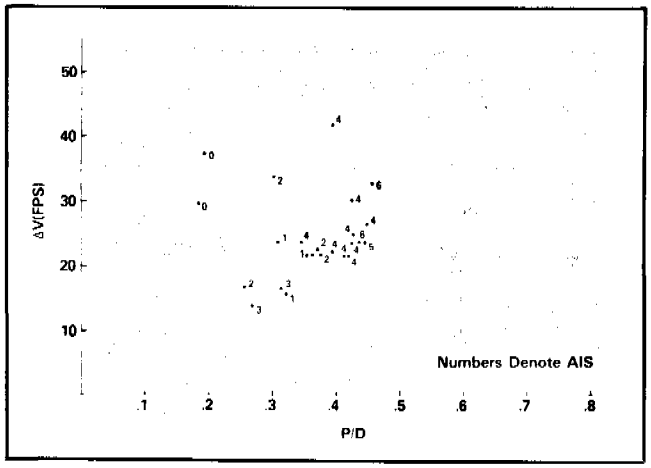

Figure 2. GM cadaver frontal impacts to the thorax.

The following equation is the AIS predictive expression as a function of P/D and AGE:

$$AIS = 17.4\ P/D + 0.0313\ AGE - 5.15 \quad (1)$$

where

R = multiple correlation coefficient = .87
SE = standard error of estimate = .87

This is Neathery's equation from Reference 22. Naturally, this regression equation is only good for values of P/D and AGE which lie within the region covered by the original data (24); e.g., this equation is not to be used for a 5-year-old child because children were not included in the original data set.

For the regression analysis on AIS = f (ΔV, P/D, AGE), the coefficient in front of the ΔV term is not significant. In other words, ΔV is not a good independent parameter for the GM cadaver tests. This point bears further consideration.

Recently, Eppinger (25) used a combination of digital convolution theory and least-squares approximation techniques to predict relative velocity and deflection based on accelerometer readings from side impacts of human cadavers. Eppinger found a relationship which suggests that the magnitude or severity of the resulting trauma is not only the result of the maximum deflection the thorax experiences but also a function of the rate at which the thoracic deflection is produced.

In 1975, Fayon et al. (26) investigated frontal crash simulations with 3 point seat belts. Results were presented for 31 cadavers in dynamic tests and 7 other in static tests. Fayon concluded that it is not possible to specify a tolerance level for thorax deflection without specifying the deflection speed which the thorax undergoes.

Jonsson (27) exposed anesthetized rabbits to controlled compression blunt impact on the right side. The results of this study suggest that velocity, as well as compression, might be a primary factor in nonpenetrating thoracic injury mechanisms. Predominantly fatal injuries were observed at velocities > 39 fps and input compressions of 20-30%, whereas compression of 50-60% were required for a lethal outcome at velocities < 39 fps.

The apparent injury mechanism was different for impact velocities above and below the 39 fps impact velocity region. In the higher velocity exposures the lung lesions resembled those found in blast injury.

Twenty-one living and post mortem porcine subjects were exposed to blunt thoracic impact by GM (20, 28). The impactor was a 46.3 pound mass with a flat contact surface traveling at 9.8 to 34.8 fps. The contacting interface was an unpadded, 6-inch-diameter wooden block with a half-inch edge radius to prevent localizing loading at the perimeter. The GM argued that a comprehensive review of comparative anatomy between the swine and man would indicate that the cardiovascular, respiratory, and thoracic skeletal systems of the pig are anatomically and functionally a good parallel of similar structures in man. During the impacts, the force was applied in the horizontal direction through the vertically aligned contact block and was centered midsagitally over the sternum.

In their most recent swine experiments (29), the GM team concluded that—while chest compression is clearly an important factor related to injury in severe blunt thoracic impact—there is a specific role for velocity as well. In other words, for a given level of thoracic compression, a higher average loading velocity represents a potentially more damaging exposure.

There is a possible reason ΔV is not a significant independent variable for the Kroell data. Figure 3 shows the GM swine data, or Viano data, for blunt thoracic impact. (The weight of the swine varied from 102-154 pounds). The Viano data have points of high ΔV and low P/D while the cadaver data do not.

The Viano data suggest that the magnitude of the resulting trauma is not only the result of the maximum deflection the thorax experiences but is also a function of the rate at which the thoracic deflection is produced.

Finally, chest deflection was used for a Highway Safety

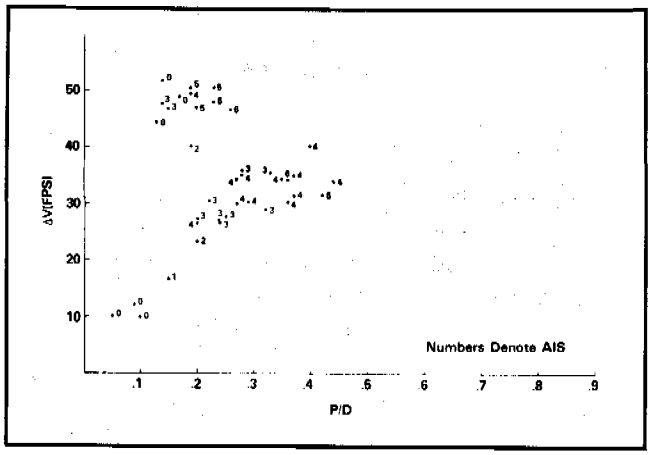

Figure 3. GM swine frontal impact to the thorax.

Research Institute (HSRI) study (30) as the indicator of injury.

The whole of the GM, HSRI, Fayon, Jonsson, and Eppinger work suggests that the most appropriate continuous injury criteria for frontal impact to the thorax should be based on at least two kinematic parameters: maximum deflection of the thorax and the rate at which the thoracic deflection is produced.

At this time, the *best continuous injury criteria* is:

(1) The Neathery equation

$$AIS = 17.4\ P/D + 0.0313\ AGE - 5.15$$

Plus (both parts are to be used together)

(2) The following restriction on the rate at which the thoracic deflection is produced as suggested by Figure 4 if

$\Delta V \leq 30$ fps, use Neathery equation

if $30 \text{ fps} \leq \Delta V \leq 40$ fps,
use Greater of AIS = 3 or Neathery equation

if $40 \text{ fps} < \Delta V \leq 50$ fps,
use Greater of AIS = 4 or Neathery equation

if $50 \text{ fps} < \Delta V$,
use Greater of AIS = 5 or Neathery equation

The duration over which the rate of thoracic deflection is calculated should not exceed 120 msec.

ABDOMEN INJURY CRITERIA—The mechanisms of injury to various abdominal organs are not well understood. Biomechanical studies by Stalnaker et al. (31) have defined tolerance values or injury severity as function of a dimensionless parameter involving force magnitude, duration of impact, mass of the impacted subject, and the area of contact. Melvin et al. (32) have established a loading rate sensitivity of the isolated liver and kidney to injury. In a recent study of closed blunt impacts delivered to anesthetized rabbits, Lau and Viano (33) also demonstrated that injury severity of the liver was velocity dependent.

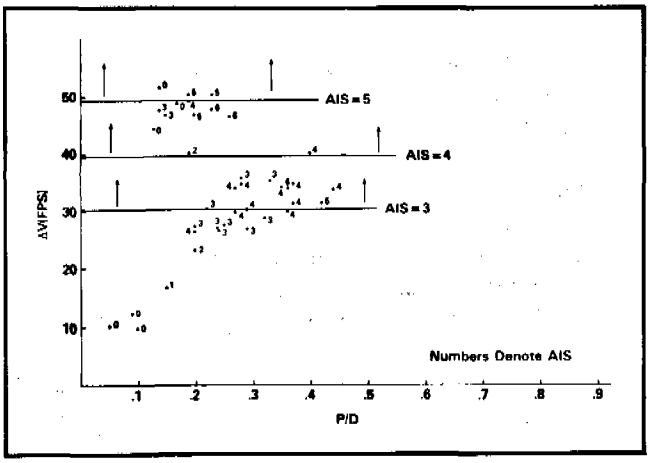

Figure 4. Velocity layers for frontal impact to the thorax.

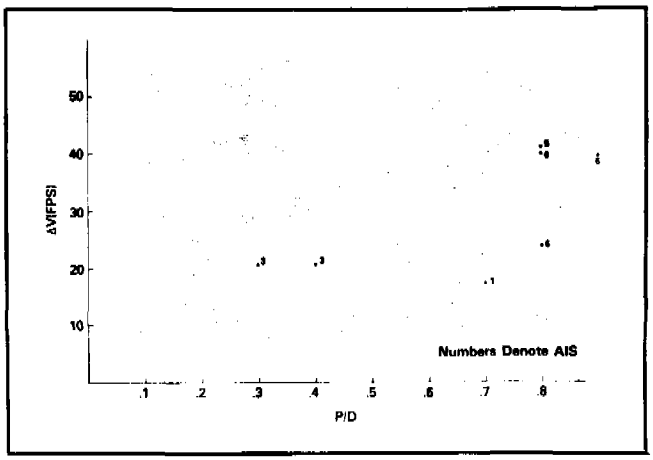

Figure 5. Winquist's swine frontal impact to the abdomen.

One of the earliest studies to try to relate kinematic parameters to abdominal injury level is a 1953 report by Winquist et al. (Discussed in Reference 34.). They employed upright seated swine to examine the effects of frontal abdominal impacts against objects that might be struck in an aircraft cockpit. These objects were a control wheel, a stick-like protrusion—struck end-on—and a large, flat surface similar to a radio box. The animals received impacts in both their midriff and lower abdominal regions at velocities of 20 and 40 fps. All of the high velocity exposures were fatal. These data are shown in Figure 5. These swine weighed from 95-187 pounds.

A regression analysis of these data results in a lower correlation coefficient for AIS as a function of P/D alone.

This lower correlation coefficient is probably due to the AIS = 1 at P/D = .7. The impactor in that event was the stick-like protrusion. What may have happened—as suggested by the second author of Reference (34) in personal communication—is that the rod went in at a lower speed and allowed the midriff organs to avoid the main thrust.

In Reference (35), 15 swine (43–65 pounds) were exposed to controlled frontal abdominal impact. The rigid impactor weighed 30 pounds and had a 3-inch-diameter circular impacting surface.

The swine test data are shown in Figure 6. Regression models for this data have a correlation coefficient of about 0.75.

The data for abdominal impact suggest a dependence of injury on normalized abdominal penetration and upon rate of change of the penetration. The data are not abundant enough to allow the exact understanding of these parameters (or of possible age effects).

The equation for abdominal impact to the HSRI swine (frontal) and Winquist swine (frontal) shows some similarity to the GM work for frontal impact to the thorax.

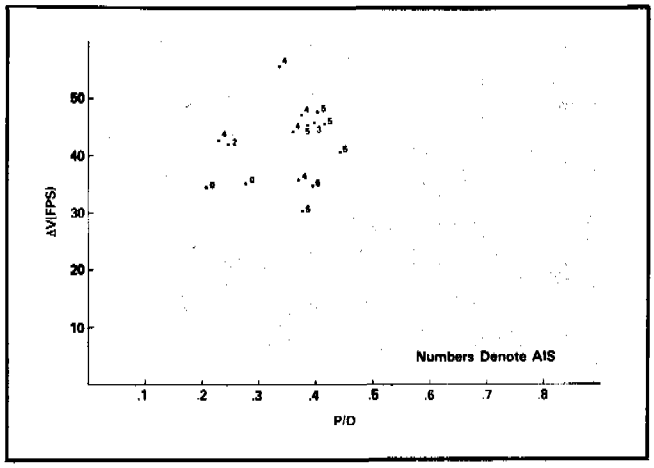

Figure 6. HSRI swine frontal impact to the abdomen.

If the assumption is made that severe injury begins to appear after 30 percent normalized total penetration (the same as in the thorax for frontal impact), then an injury criteria can be hypothesized.

The *most appropriate continuous injury criteria* for frontal abdominal impact are:

(1)

$P/D \leq .1$	$AIS = 0$
$.1 < P/D \leq .5$	$AIS = .15\ P/D - 1.5$
$.5 < P/D$	$AIS = 6$

plus (both parts are to be used together)

(2)

if $\Delta V \leq 30$ fps, use equation in (1) above
if 30 fps $< \Delta V \leq 40$ fps, use Greater of AIS = 3 or equation above
if 40 fps $< \Delta V \leq 50$ fps, use Greater of AIS = 4 or equation above
if 50 fps $< \Delta V$, use Greater of AIS = 5 or equation above

The duration over which the rate of thoracic deflection is calculated should not exceed 120 msec.

RECENT AND CURRENT RESEARCH

Several programs recently completed or currently in progress will advance our understanding of the role of the steering assembly in causing injury during an accident. A program which was the subject of an SAE paper entitled "Study of Steering Assemblies for Evaluation and Rating of Safety Performance" (17) investigated the performance of several production steering assemblies via static component and dynamic systems tests. The selection of steering assembly types was based on acquiring a cross section of production available types of energy absorbers as shown in Table 10. Since publication of this paper additional research was conducted in this same program. An improved dynamic systems test was developed where the complete Hybrid III dummy is impacted into a stationary assembly. Tests were conducted on four make's types of steering assemblies (Ford Fairmont, Chevy Citation, Volvo, and a hybrid type) in the frontal mode at 20 and 25 mph and 30° oblique at 25 mph.

The hybrid steering assembly was constructed from components which yielded the best results based on earlier testing: a Ford Fairmont column and energy absorber and Volvo steering wheel. Table 11 shows the results of the dynamic testing.

As discussed previously in the biomechanics section and in References 23, 26, and 29, it appears that chest deflection correlates better with injury than does spinal chest acceleration for blunt impact. If this is used as a performance criteria, the hybrid steering assembly would rank as the best of those tested.

Two other innovations were developed during this program. A device which uses electrical switches to give a rough estimate of the area in contact between the dummy and the impacted surface was developed and included in the later tests. An abdomen form which replaces the standard insert was constructed of Styrofoam and following impact will show the maximum penetration of the wheel rim, or other component into the abdomen. Both of these techniques will provide measurements which will be useful in determining the injury severity.

This device for measuring contact area was further refined under a NHTSA contract (36) to improve the accuracy. The switching array was expanded to 180 switches, monitored discretely, arranged on a 180 square inch area. The discrete method has numerous advantages over the parallel method originally used on the device, such as improved electronic accuracy and the potential to identify the specific location of each closed switch. The device was built into a vest which can be worn over the chest of a dummy. Since the area monitoring method used a discrete switching pattern of 1 inch squares, the accuracy of the device is very dependent on both size and shape of the contact surface. Based on geometric analysis and static and dynamic testing using common shapes (circles, squares, etc.), the accuracy appears to vary from 10% or less for larger areas (greater than 20 square inches) up to 30% for small areas (less than 4 square inches) when sufficient pressure is applied to close the switches.

A computer model has been developed to specifically address the unrestrained driver impacting the steering assembly in a frontal collision. This model entitled

Table 10. Steering column types.

Make/Model	EA Types	Other Features
Chevrolet Citation	Ball-tube	Cowl bracket guide
Volvo	Convoluted jacket	Self-aligned wheel
Ford Fairmont	Ring-tube	
Mercedes	Convoluted hub	EA unit in lower column
Honda	Hook bends plate	
Chrysler K-car	Mesh-Mandrel	

Table 11. Dynamic test results (phase II).

Column Test No. (inches)	Column	Mode	Speed (mph)	Peak Chest Acceleration (Gs)	Maximum Chest Deflection (inches)	Maximum Stroke
2251	Citation	Frontal	19.8	38.4	3.1	0.94
2254	Citation	Frontal	24.6	46.5	2.6	3.75
2282	Citation	Oblique	24.9	35.5	20.5	3.42
2260	Volvo	Frontal	19.0	28.7	1.6	3.50
2262	Volvo	Frontal	25.0	49.4	2.5	3.1
2278	Volvo	Oblique	24.9	40.5	1.92	2.2
2357	Fairmont	Frontal	20.0	39.7	1.6	3.05
2362	Fairmont	Frontal	25.0	61.1	2.9	3.8
2287	Fairmont	Oblique	25.0	50.6	2.7	1.8
2237	Hybrid	Frontal	19.7	34.0	1.6	2.5
2350	Hybrid	Frontal	25.0	47.9	1.95	4.5
2288	Hybrid	Oblique	25.1	36.6	1.76	1.2

SCORES (Steering Column and Occupant Response Simulation) was the subject of an SAE paper by Stucki and Fitzpatrick (37).

As noted in the report more work was needed to validate the model and to add the capability of modeling occupant impact with the windshield and/or header. As part of a larger computer modeling effort which was awarded in September 1982, the first task will be to incorporate the windshield and header into the current SCORES model and to validate these additions.

A program is currently being conducted at NHTSA's Safety Research Laboratory (SRL) to validate the SCORES model. Two passenger cars (Ford Fairmont and Chevrolet Citation) were selected for the study. All inputs for the modeling will be obtained from available sources such as vehicle and dummy specification, through direct measurement and from testing of dummies and steering assembly components. Frontal sled tests at 20 and 25 mph were conducted on both vehicles. The unrestrained driver dummy is the same Hybrid III which was used in the component tests to ensure consistent responses. These sled tests will be used as cases for the validation study, comparing dummy and steering assembly responses predicted by the SCORES model to the measured responses in the sled tests.

FUTURE PROJECTS

A project was recently started by the NHTSA to give a better understanding of harm resulting from steering assembly impact and methods of alleviating the problem. The following tasks, to be conducted, will contribute towards these objectives:

A. Establish relationship between injury and occupant and vehicle response measurements.
B. Extrapolate this analysis to a national representative accident environment such as that predicted by the NASS and/or NCSS files.
C. Propose countermeasures to reduce injuries and fatalities which will be applied to the predicted accident environment.
D. Analyze the effects of these countermeasures on injury and fatality, nationwide and select the most viable candidates for further development through sled and crash testing.

The spectrum of accidents will be those in which an injury to the occupant was caused from impact with the steering assembly. The form of the accident data will be a multi-element array of the following parameters:

(a) Body region injured.

(b) AIS level: 1 through 6.
(c) Vehicle Make/model, 1975 and later.
(d) Occupant size and sex: A maximum of 3 categories for each.
(e) Principle Direction of Force (PDOF): 11, 12, and 1 o'clock.
(f) Object contacted: Other vehicle or fixed object.
(g) Velocity change: Either 5 or 10 mph increments from 5 to 35 mph.

The SCORES computer model will be exercised for each cell of this matrix, i.e., for each make/model vehicle, occupant size, and sex, PDOF, object contacted, and velocity change SCORES will predict responses for each body region (for SCORES this is limited to head, chest, abdomen, and femurs). These responses will be converted to injury level (AIS) by the applicable biomechanical criteria for the particular body region. The outcome of this exercise will be an AIS level for each cell in the multi-element array. The frequency of occurrence can be applied to each cell and summed to give overall frequency of each AIS level for comparison with the actual accident file. If the AIS distributions are not similar between the SCORES prediction and the actual accident data, adjustments will be made to the SCORES inputs until good agreement is achieved.

One of the major efforts of this project is to acquire the inputs necessary to exercise SCORES on each cell of the matrix. The Transportation Systems Center (TSC) has responsibility for providing all vehicle dimensions for approximately 40 post-1974 passenger car lines which account for more than 90% of the passenger cars produced in this period (one car line will generally include several models). These measurements include dimensions such as steering column angle, wheel location, etc., and force-deflection properties of the wheel rim and energy absorber unit in the column.

TSC is also generating vehicle crash pulses for different velocity change, PDOFs, and object contacted. The final requirement for input is the anthropometric and biomechanical properties of the various occupant sizes for each sex. Much of this information currently exists for certain size occupants and may have to be extrapolated to other size occupants using engineering judgment.

The output of the SCORES model will be verified by checking against results of other models, such as the MVMA-2D, and sled and crash test results. The input parameters will continually be upgraded by this verification process and by the latest biomechanical criteria.

One of the primary injury risks to occupants involved in collisions is the relative velocity at which the occupant strikes interior contact surfaces. The SCORES output will provide the information, in terms of body part velocities and responses, needed to construct relationships between body part response (which can be converted to an injury level) and impact velocity. Figure 7 shows this relationship for the chest impacting the steering wheel hub, where the given responses are the most probable indicators of chest injury level. This is a preliminary analysis based on several SCORES runs with a 50th percentile male occupant and 1979 Volvo dimensions and properties. Once relationships such as these have been developed, countermeasures, which will lower the injury risk, in this case impact velocity, can be investigated using the SCORES Model.

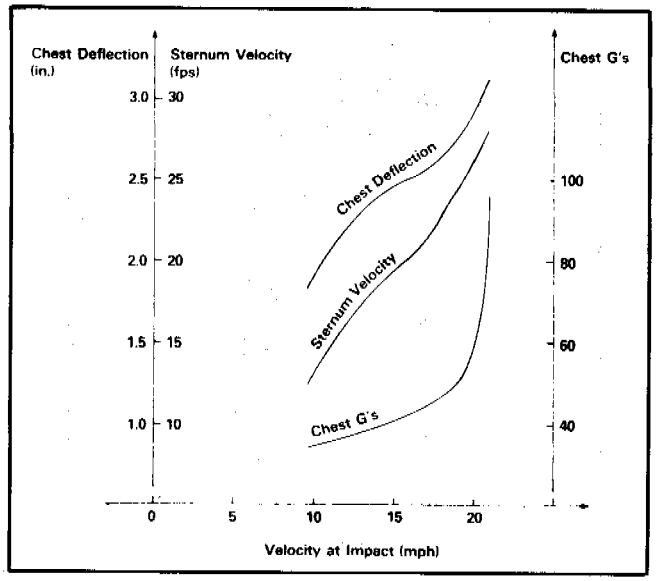

Figure 7. Chest/steering wheel hub impact.

SUMMARY

The steering column is responsible for producing more injuries and fatalities than any other vehicle component: 27% of all serious to fatal (AIS 3-6) injuries. Steering assembly impact with the chest and abdomen accounts for over 20% of all serious injuries.

The most appropriate continuous injury criteria for frontal impact to the thorax are based on maximum deflection and the rate at which the thorax deflection is produced. The most appropriate injury criteria for abdominal impact are abdominal penetration and rate of change of penetration.

An improved dynamic systems test has been developed and the performance of several steering assemblies evaluated.

A steering assembly computer model has been developed and is being validated.

We are establishing the relationship between injury and occupant and vehicle response measurements, investigating countermeasures, and analyzing the effects of these countermeasures on injury reduction.

REFERENCES

1. Marquis, D.P., "The General Motors Energy Absorbing Column" SAE Report 670039, Society of Automotive Engineers.
2. Recommended Practice J944, *1981 SAE Handbook*, Society of Automotive Engineers.
3. *Federal Register*, Vol. 31, National Archives, Washington, D.C., July 15, 1966, pg. 9631-2.
4. Kahane, C. J., "An Evaluation of Federal Motor Vehicle Safety Standards for Passenger Car Steering Assemblies; Standard No. 203—Impact Protection for the Driver, Standard No. 204—Rearward Column Displacement," DOT Report No. DOT-HS-805 705, 1981.
5. *Federal Register*, Vol. 32, National Archives, Washington, D.C., February 3, 1967, pg. 2414.
6. Garrett, J. W., "A First-Look-Differences in Injuries in 1968 and Pre-1968 Automobiles," Society of Automotive Engineers Report No. 680542, August 1968.
7. Huelke, D. F., and Chewning, W. A., "The Energy Absorbing Steering Column," Highway Safety Research Institute, Report B10-7, 1968, (DOT-HS-002 615).
8. Nahum, A. M., Siegal, A. W., and Brooks, S., "The Reduction of Collision Injuries; Past, Present, and Future," Society of Automotive Engineers, Report No. 700895, 1970.
9. Levine, D. N., and Cambell, B. J., "Effectiveness of Lap Belts and the Energy Absorbing Steering Systems in the Reduction of Injuries," Highway Safety Research Center, November 1971, (DOT-HS-011 537).
10. O'Day, J., and Creswell, J. S., "Can The Effect of Changes in Vehicle Design be Seen in Mass Accident Data?" *HIT LAB Reports*, University of Michigan, February 1971 (DOT-HS-009 811).
11. McLean, A. J., "Collection and Analysis of Collision Data for Determining the Effectiveness of Some Vehicle Systems" Motor Vehicle Manufacturers Association, 1974.
12. Kahane, C. J., "Evaluation of Current Energy Absorbing Steering Assemblies" Society of Automotive Engineers, Report No. 820473, 1982.
13. *Federal Register*, Vol. 44, No. 321, National Archives, Washington, D.C., November 29, 1979.
14. Huelke, D. F., and Gikas, P. W., "How Do They Die? Medical Engineering Data From On-Scene Investigation of Fatal Automobile Accidents" Highway Vehicle Safety, Society of Automotive Engineers, 1968.
15. Malliaris, A. C., Hitchcock, R., and Hedlund, J., "A Search For Priorities In Crash Protection", Society of Automotive Engineers, Report No. 820242, 1982.
16. Cohen, D. S., Jettner, E., and Smith, W. E., "Light Vehicle Frontal Impact Protection", Society of Automotive Engineers, Report No. 820243, 1982.
17. Stucki, S.L., and Hannemann, N., "Study of Steering Assemblies for Evaluation and Rating of Safety Performance", Society of Automotive Engineers, Report No. 820476, 1982.
18. Gloyns, P. F., and Mackay, G. M., "Impact Performance of Some Designs of Steering Assembly in Real Accidents and Under Test Conditions", SAE Paper 741176, Proceedings of the Eighteenth Stapp Car Crash Conference, 1974.
19. Garrett, J. W., and Hendricks, D. L., "Factors Influencing the Performance of the Energy Absorbing Steering Column in Accidents", 5th International Conference on Experimental Safety Vehicles, London, England, June 1974.
20. Viano, D. C., and Warner, C. Y., "Thoracic Impact Response of Live Porcine Subjects", 20th Stapp Car Crash Conference, October 1976.
21. Kroell, C. K., Schneider, D. C., and Nahum, A. M., "Impact Tolerance and Response of the Human Thorax II", 18th Stapp Car Crash Conference, December 4-5, 1974.
22. Neathery, R. F., Kroell, C. K., and Mertz, H. J., "Prediction of Thoracic Injury from Dummy Responses", 19th Stapp Car Crash Conference, November 17-19, 1975.
23. Nahum, A. M., Schneider, D. C., and Kroell, C. K., "Cadaver Skeletal Response to Blunt Thoracic Impact", 19th Stapp Car Crash Conference, November 17-19, 1975.
24. Draper, N. R., and Smith, H., "Applied Regression Analysis", Second Edition, John Wiley and Sons, Inc., New York, 1981, pg. 8.
25. Eppinger, R. H., and Chan, H. S., "Thoracic Injury Prediction via Digital Convolution Theory", 25th Stapp Car Crash Conference, October 1981.
26. Fayon, A., Tarriere, C., Walfisch, G., Got, C., and Patel, A., "Thorax of 3-Point Belt Wearers During a Crash (Experiments with Cadavers)", 19th Stapp Car Crash Conference, November 17-19, 1975.
27. Jonsson, A., Clemedson, C. J., Sundquist, A. B., and Arvebo, E., "Dynamic Factors Influencing the Production of Lung Injury in Rabbits Subjected to Blunt Chest Wall Impact", Aviation, Space, and Environment Medicine, Vol. 50, No. 4, April 1979, pp. 325–337.
28. Viano, D. C., Kroell, C. K., and Warner, C. Y., "Comparative Thoracic Impact Response of Living and Sacrificed Porcine Siblings", 21st Stapp Car Crash Conference, October 19–21, 1977.
29. Kroell, C. K., et al., "Interrelationship of Velocity and Chest Compression in Blunt Thoracic Impact to Swine", 25th Stapp Car Crash Conference, September 28–30, 1981.
30. Melvin, J. W., Mohan, D., and Stalnaker, R. L., "Occupant Injury Assessment Criteria", Warrendale, Pennsylvania, SAE Paper No. 750914, 1975.
31. Stalnaker, R. L., et al., "Door Crashworthiness Cri-

teria", Final Report for Contract No. DOT-HS-031-2-382, September 1973.
32. Melvin, J. W., et al., "Impact Injury Mechanisms in Abdominal Organs", 17th Stapp Car Crash Conference, November 1973.
33. Lau, V. K., and Viano, D. C., "Influence of Impact Velocity on the Severity of Nonpenetrating Hepatic Injury", *Journal of Trauma*, Vol. 21, November 2, 1981.
34. Mertz, H. J., and Kroell, C. K., "Tolerance of Thorax and Abdomen", *Impact Injury and Crash Protection*, Charles C. Thomas, Springfield, Illinois, 1970.
35. Beckman, D. L., et al., "Impact Tolerance—Abdominal Injury", Report No. DOT-HS-800 549, June 30, 1971.
36. Broadhead, W. G., Final Report, Contract No. DTNH22-82-P-07024, "Development of a Measuring Device for Chest Contact Area", June 30, 1982.
37. Stucki, S. L., and Fitzpatrick, M. U., "A Computer Model for Simulating an Unrestrained Driver in Frontal Collisions", Society of Automotive Engineers Report No. 820469, 1982.

A Study on the Ride-Down Evaluation

HIROSHI KATOH and RYOJI NAKAHAMA
Passenger Car Engineering Center
Mitsubishi Motors Co., Ltd.

3667

ABSTRACT

The injury of occupants restrained by seat belt is dominantly affected by the vehicle crash characteristics and seat belt effectiveness. Matching both performances is essential in attaining occupant's safety with most reasonable weight and cost.

Hitherto the efficiency of occupant's energy disposal has been evaluated in terms of a concept of Ride-Down, a ratio of energy absorbed vicariously by the vehicle to the occupant's initial kinetic energy.

This long established idea, however, has a certain limit for further analysis. In this paper, a new method of assessing relative effectiveness of vehicle structure and seat belt system is proposed to enable to attain a balanced approach as a whole.

The Ride-Down efficiency is decomposed to one that concerns vehicle structure and the other that relates to restraint system. The former is determined as relative Ride-Down efficiency when the simulated system of the vehicle is subjected to collision with a standard restraint system. The latter is obtained in the relation of conventional and the newly obtained method.

The two-way Ride-Down approach paves the way to indicating straightforwardly the most effective direction in which occupant protection is harmoniously attained in each vehicle design.

INTRODUCTION

The trend toward smaller car and weight reduction of automobiles has progressed increasingly to save energy and material.

To make down-sizing and safety compatible, it is well known to be important to utilize Ride-Down phenomena effectively.

Many studies (Refs. 1-8) have been made regarding what kind of vehicle crash characteristics or seat belt one can decrease occupant injury with.

However, there seems no study to clarify the effect of seat belt and vehicle crash characteristics on Ride-Down efficiency. It is difficult to separate the effect of seat belt and that of vehicle body, since Ride-Down phenomena consist of a combined effect of vehicle crash characteristics and seat belt ones.

Here an idea, which we call "Ride-Down index," is introduced and utilizied for safety design to evaluate each effect of vehicle body and seat belt separately.

RELATIONSHIP BETWEEN RIDE-DOWN EFFICIENCY AND PASSENGER CHEST DECELERATION

Figure 1 shows the macrosocopic model of vehicle collision against fixed barrier. K is a spring which denotes seat belt and is assumed constant.

Passenger energy absorption is written in equation (1).

$$1/2M\ Vo^2 = M\ddot{X}_1 dX_2 + 1/2\ K\ (X_1 - X_2)^2 \quad (1)$$

where M : Passenger mass
Vo : Velocity at collision
$\ddot{X}_1$: Passenger deceleration
$\ddot{X}_1$: Passenger displacement
X_2 : Vehicle displacement
K : Spring constant of seat belt

The first term of right hand of equation (1) denotes the energy which vehicle body vicariously absorbs and is generally called Ride-Down energy. The rate of Ride-Down energy to initial passenger kinetic energy (1/2 M Vo^2) is called Ride-Down efficiency. That is

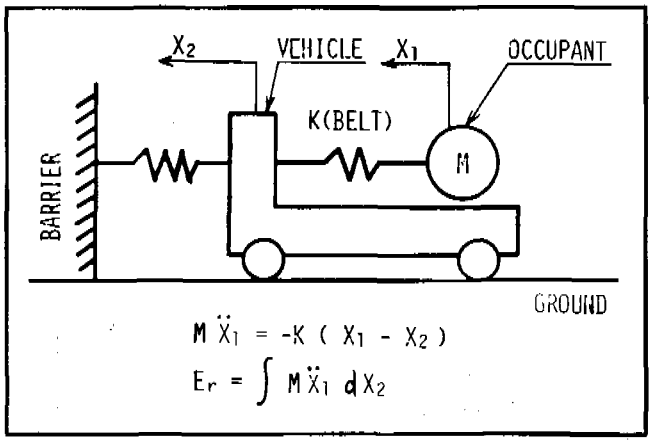

Figure 1. Macroscopic model of collision.

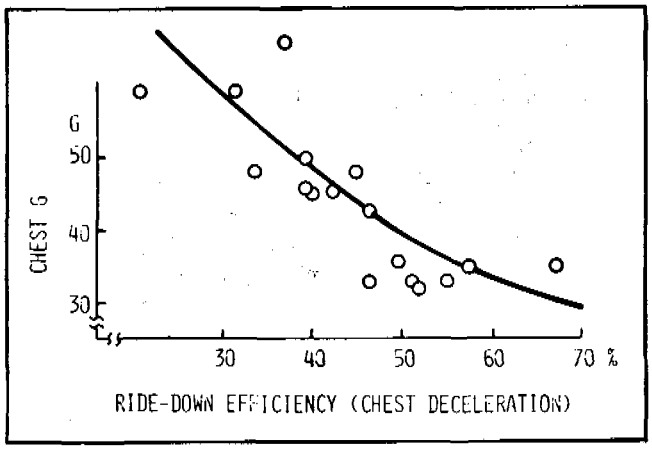

Figure 2. Passenger chest G and Ride-Down efficiency.

Ride-Down energy:

$$Er = \int_0^{X_2 max} M\ddot{X}_1 dX_2 \qquad (2)$$

Ride-Down efficiency:

$$\eta_t = \frac{\int_0^{X_2 max} M\ddot{X}_1 dX_2}{1/2\ M\ Vo^2}$$

where X_2max : Maximum vehicle displacement

Furthermore, it is well known that Ride-Down efficiency is closely related to occupant injury value. Figure 2 shows this relationship between Ride-Down efficiency and passenger chest deceleration of frontal collision tests at 35 mph. Here Ride-Down efficiency is calculated according to equation (2) where $\ddot{X}_1$ is replaced with fore and aft component of passenger chest deceleration. These data are based on 35 mph collision tests performed on various vehicles since 1978 as a part of NCAP (New Car Assessment Program) by NHTSA (National Highway Traffic Safety Administration) in U.S.A.

Figure 2 clearly indicates the relationship that passenger chest deceleration decreases as Ride-Down efficiency increases.

However, since Ride-Down efficiency, as shown in Figure 1 and equation (2), is the result of a combined effect of both vehicle body and seat belt, each effect cannot be estimated separately. But from the standpoint of safety design, if each effect of vehicle body and seat belt can be estimated independently, it is very useful.

INTRODUCTION OF "RIDE-DOWN INDEX"

Considering the collision model shown in Figure 1, we assume that seat belt has the characteristics shown in Figure 3(A), where spring rate K is constant and initial slack δ_0 is chosen as a parameter of seat belt characteristics. Besides vehicle crash characteristics are defined by sine wave deceleration time history shown in Figure 3(B), and maximum deceleration Gm is selected as a parameter of vehicle body characteristics. Because the collision velocity is constant (35 mph), Gm·Tt becomes constant.

In this simple model, Ride-Down efficiency ηt becomes a function of two variables (Gm, δ_0). In order to obtain each effect of vehicle body and seat belt, we keep either Gm or δ_0 constant and vary the other. Then "Ride-Down index of vehicle body" ηv is for convenience defined as a function of Gm (while δ_0 = const.). Similarly "Ride-

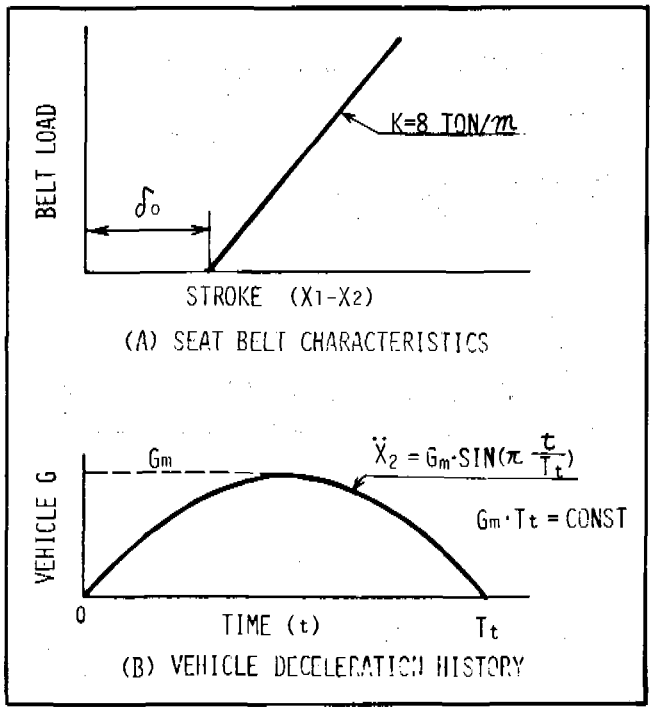

Figure 3. Conditions used for calculation.

Down index of seat belt" ηb is defined as a function of δ_0 (while Gm = const.). That is

$$\text{Ride-Down efficiency} \quad \eta t = f(\delta_0, \text{Gm})$$

$$\text{Ride-Down index of vehicle body} \quad \eta v = f(\delta_{0B}, \text{Gm});\ \delta_{0B} = \text{const. (5 mm)} \qquad (3)$$

$$\text{Ride-Down index of seat belt} \quad \eta b = f(\delta_0, \text{Gm}_B);\ \text{Gm}_B = \text{const. (17G)}$$

where

δ_0 : seat belt slack

δ_{0B} : the slack of the standard seat belt (5 mm)

Gm : maximum vehicle deceleration

Gm_B: maximum vehicle deceleration of the standard vehicle (17 G)

The value of δ_{0B}, Gm_B is selected practically as the most optimum value after various attempts were made.

Then, simulation calculation results in the constant ηt curves shown in Figure 4. Now ηt is divided into ηb and ηv. Therefore we can estimate each effect of vehicle body and seat belt on the Ride-Down efficiency ηt, and the most cost-benefit direction on the improvement of ηt can be indicated. The change in ηt due to the variation in ηv or ηb can be respectively estimated using Figure 4. For example, in case of ηt = 30% and ηb = 40%, ηv is shown to be large, about 80%. Therefore to increase ηt, it seems more practical to improve ηb rather than ηv. On the other hand,in case of ηt = 30%, ηv = 40%, it seems better to improve ηv rather than ηb.

Figure 5 shows the flow chart of actual improvement method.

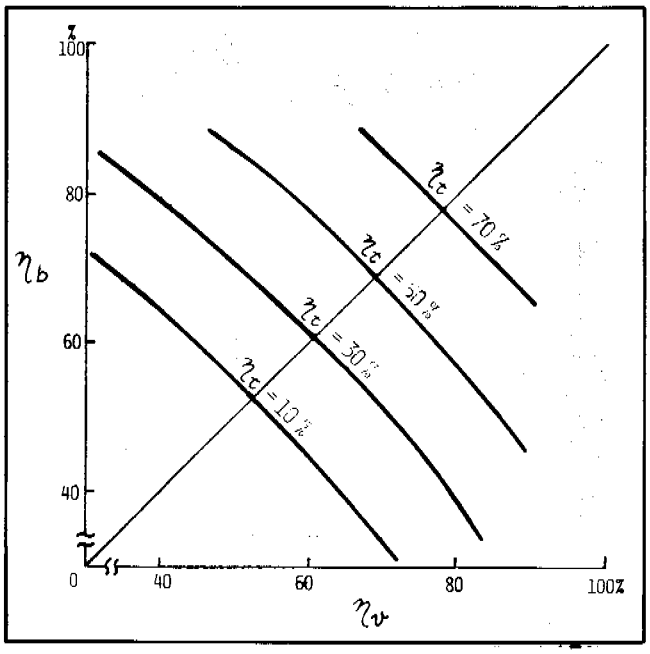

Figure 4. Constant value lines of ηt.

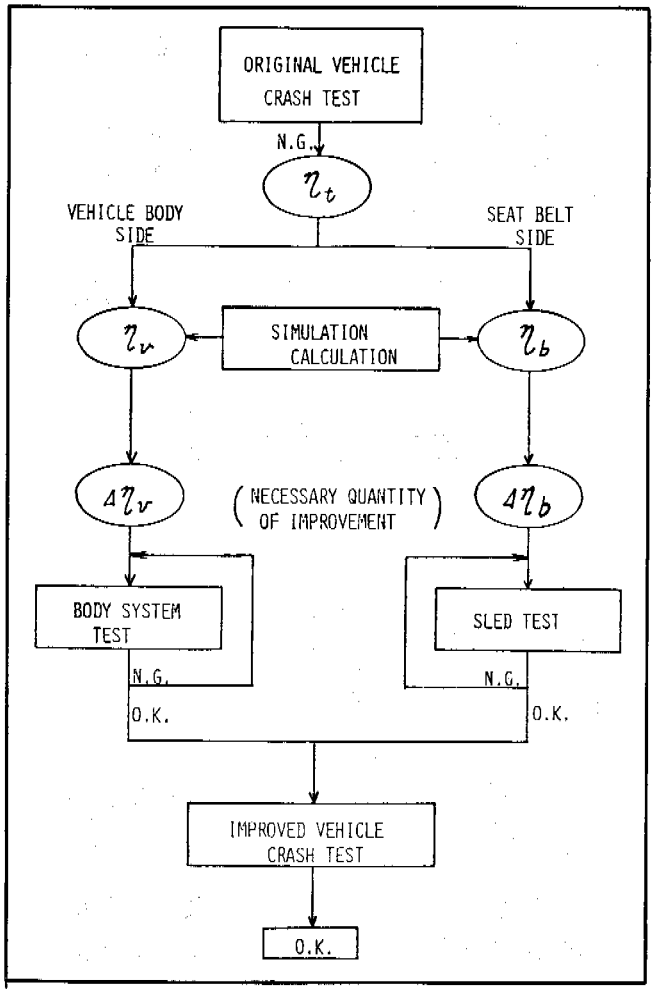

Figure 5. Flow chart of improvement method.

THE METHOD TO OBTAIN ηb AND ηv IN ACTUAL TEST

First, ηt is obtained from actual test data by substituting the fore and aft component of passenger chest deceleration as $\ddot{X}_1$ into equation (2).

In order to obtain ηv, two-dimensional simulation model shown in Figure 6 is used. Here seat belt characteristics shown in Figure 7 are applied for all vehicles, and for vehicle crash characteristics, vehicle deceleration time history of the actual test is used. Then ηv is obtained.

Two-dimensional simulation model is used here instead of one-dimensional model shown in Figure 1 because the chest deceleration can be calculated in two-dimensional model. Then ηv using the chest deceleration in two-dimensional simulation becomes comparable with ηt substituting the chest deceleration measured in actual test as described above.

Accordingly ηb can be known when ηt, ηv are plotted on Figure 4. Now the effect of vehicle crash characteristics and seat belt characteristics on Ride-Down efficiency in actual test can be obtained separately.

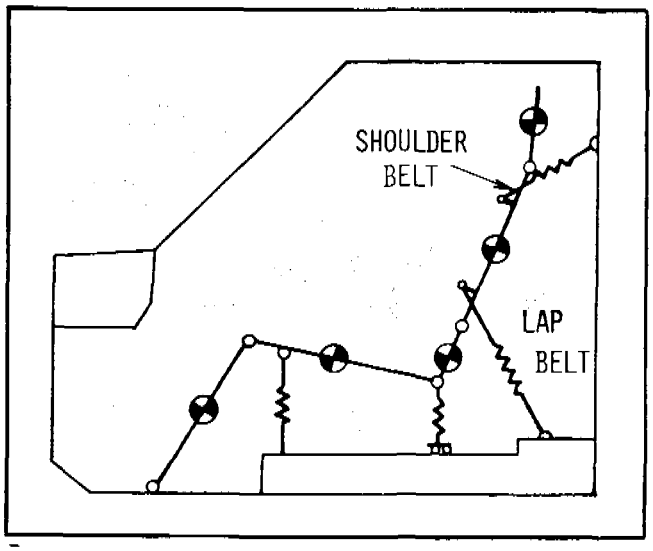

Figure 6. Two-dimensional simulation model.

Here a consideration must be given to the fact that ηv and ηb are not really independent, so evaluation by ηv and ηb are not absolute but relative. However, within the scope of actual vehicle collision, ηv and ηb are considered to be of practical significance in evaluating each functions of the various vehicles relatively.

ηb can be approximately obtained by the following simple method. As we take δ_0 as a parameter of seat belt characteristics, consider the seat belt slack δ_{100}, which indicates relative displacement between passenger and vehicle when shoulder belt load reaches 100 kg (220 lb.).

δ_{100}: relative displacement between passenger and vehicle when shoulder belt load reaches 100 kg (220 lb.).

Here δ_{100} is chosen instead of δ_0 in Figure 3(A), because it is difficult to obtain δ_0 in actual test.

Figure 8 shows the relationship between ηb and δ_{100}. It can be said that they are mutually related. From Figure 8, ηb can be approximately obtained if δ_{100} is known.

APPLICATION TO TEST DATA

Figure 9 shows the summary of ηv, ηb for various vehicles subjected to NCAP crash tests at 35 mph. The data are classified based on whether the vehicle passed injury criteria of FMVSS 208 or not.

To pass injury criteria, $\eta t \geqq 50\%$ becomes a necessary condition.

Furthermore, improvement direction and quantity can be easily obtained from Figure 9. For example, ηv of vehicle A is almost the same as that of vehicle B, but ηb is considerably different and as a result vehicle B could not pass injury criteria. If vehicle B were equipped with the same seat belt as vehicle A, vehicle B could be expected to pass the criteria. Keeping ηb at the same value, and increasing ηv up to 83%, a similar result could be expected.

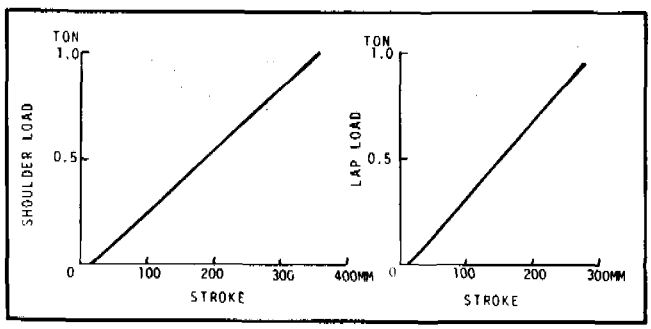

Figure 7. Seat belt characteristics used for calculation.

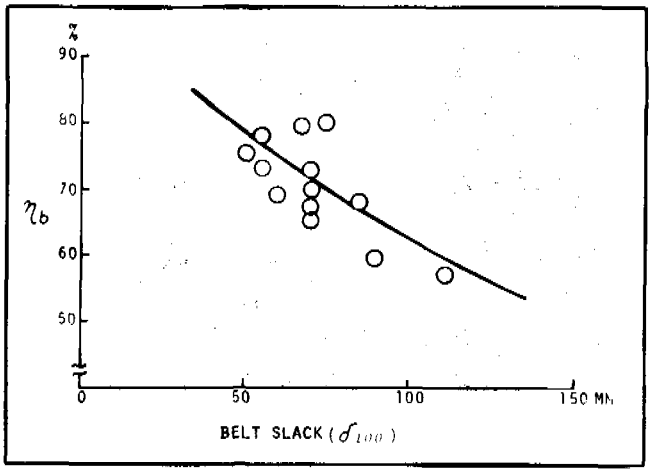

Figure 8. Seat belt slack and ηb.

EXAMPLE OF ACTUAL IMPROVEMENT

Figure 10 shows a result of improvement on vehicle C_1 in Figure 9. As ηv of vehicle C_1 is relatively high, im-

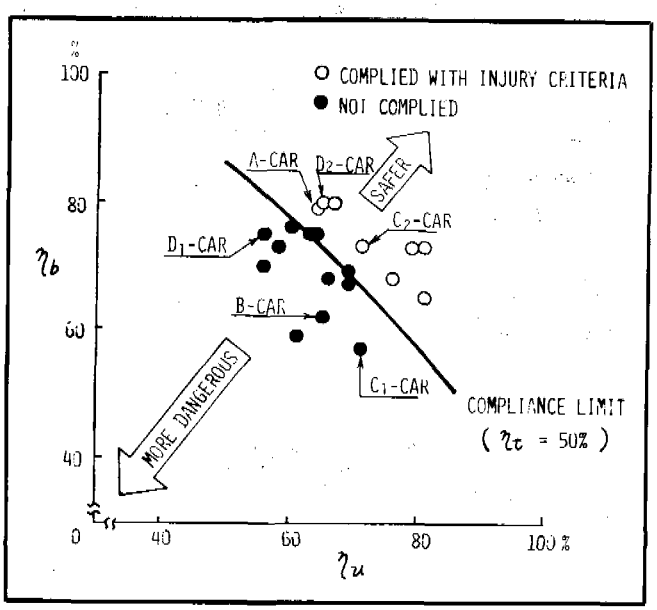

Figure 9. Test data arranged by ηv and ηb.

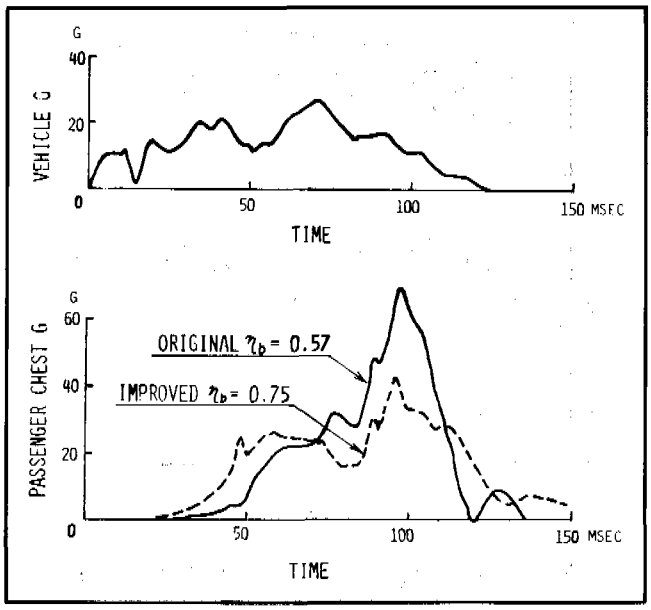

Figure 10. Example improved by increasing ηb (C_1 and C_2 car in Figure 9).

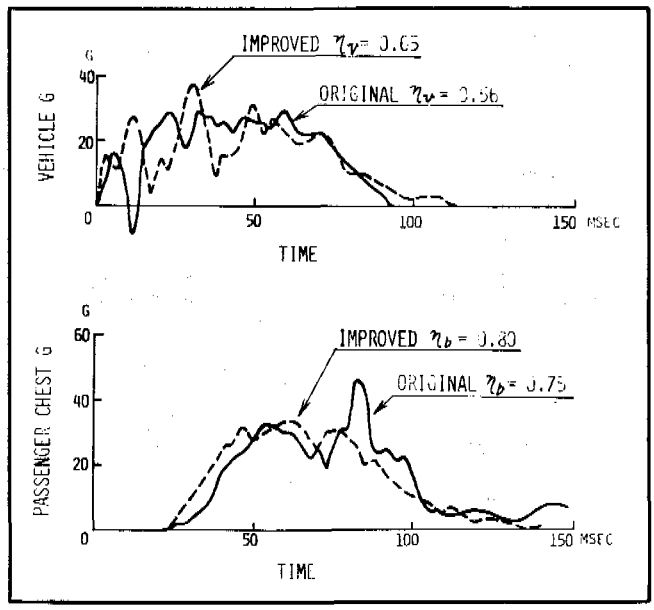

Figure 12. Example improved by increasing both ηv and ηb (D_1 and D_2—car in Figure 8).

provement of ηb was made. In original test (C_1) δ_{100} = 120 mm and ηb = 57%. To pass injury criteria, ηb must be increased up to 75% and seat belt slack δ_{100} must be shortened by about 60 mm from Figure 8. Therefore seat belt retractor was modified to minimize the spool-effect or spool-out due to squeezed winding around the spool, and the favorable result (C_2) is obtained.

Figure 11 also shows the example of seat belt improvement on another vehicle at 30mph collision.

Figure 12 shows the case of improvement made on both vehicle body and seat belt. This case is expressed as vehicle D_1 (original) and D_2 (improved) in Figure 9.

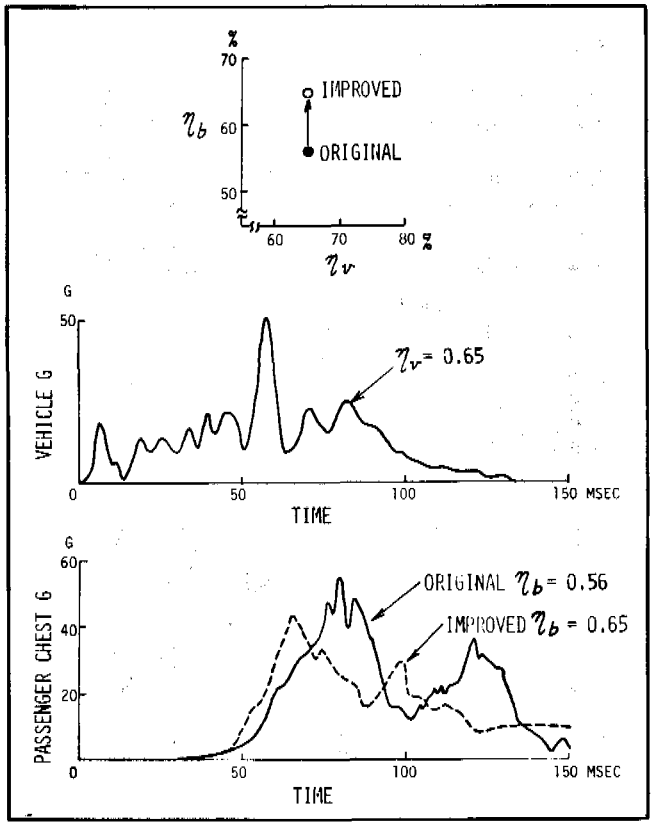

Figure 11. Example improved by increasing ηb (at 30 mph).

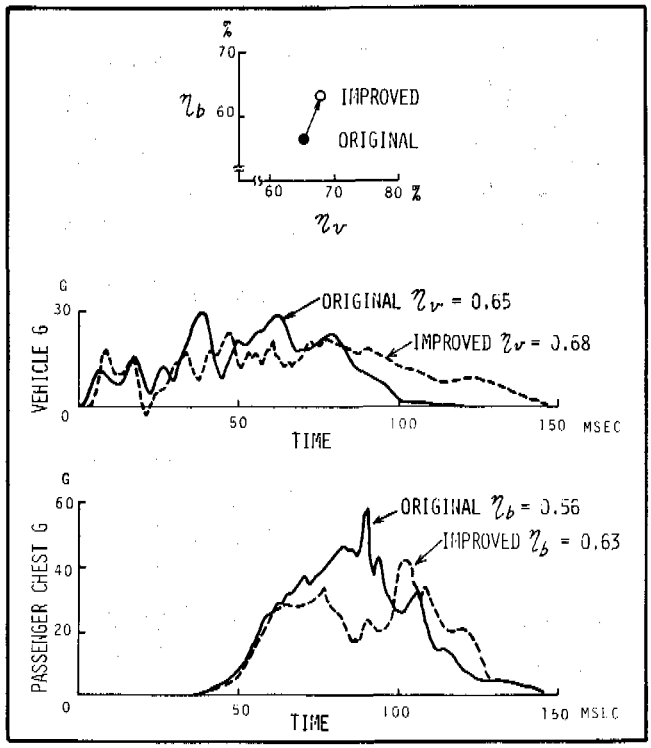

Figure 13. Example improved by increasing both ηv and ηb (at 30 mph).

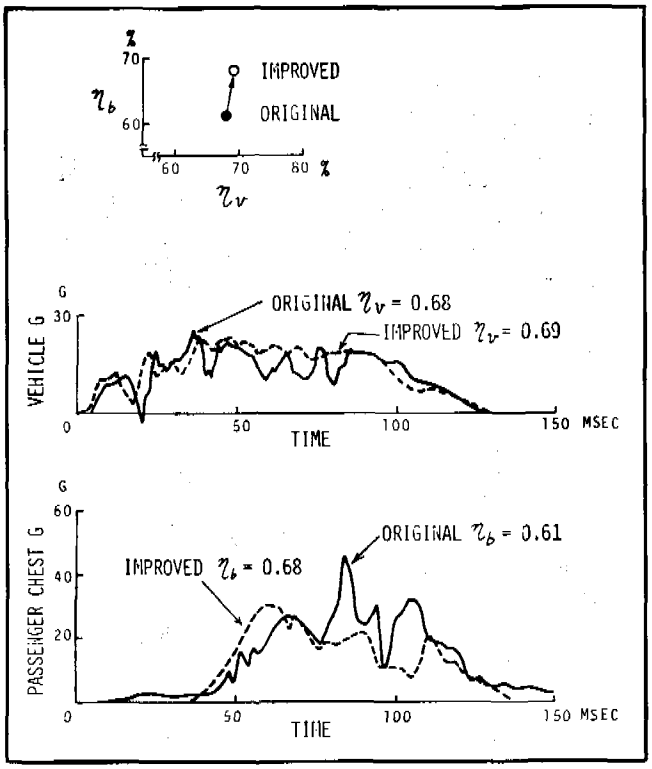

Figure 14. Example improved by increasing both ηv and ηb (at 30 mph).

Figures 13 and 14 also show the test results of the similar improvement made on both vehicle body and seat belt. Generally, if the base body structure is unchanged, it seems very hard to increase ηt without changing the front side member layout largely.

CONCLUSION

(1) Ride-Down efficiency ηt has a close relation to the occupant injury value in the vehicle frontal collision.
(2) The new idea to separate the effect of seat belt and vehicle body on the Ride-Down efficiency (ηt) is proposed.
(3) The vehicle crash characteristics can be evaluated by Ride-Down index of vehicle body (ηv) which is obtained by using the mathematical simulation with the standard seat belt.
(4) The seat belt characteristics can be evaluated by Ride-Down index of seat belt (ηb) which is obtained by using the mathematical simulation with the standard vehicle body.
(5) By using ηb and ηv, the problem of which side and how much improvement of vehicle body and seat belt should be made is easily clarified. This idea of Ride-Down index is practically useful for safety design.

REFERENCES

1. R. McHenry et al., "Computer Simulation of the Crash Victim—A Validation Study", SAE 660792.
2. H. Furusho, "Effect of Vehicle Body Crush Characteristics on Occupant Second Collision", JSAE VOL 22, No. 8, 1968.
3. D. F. Moore, "Minimization of Occupant Injury by Optimum Front-End Design", 1970 International Automobile Safety Conference Compendium.
4. R. McHenry, "Analysis of the Dynamics of Automobile Passenger-Restraint System", 7th Stapp Car Crash Conference.
5. K. Higuchi, "Characteristics of Body Energy Absorption and Restraint System", 5th International Technical Conference on E.S.V.
6. N. Aya, "A Method How to Estimate the Crashworthiness of Body Construction", 6th International Technical Conference on E.S.V.
7. N. Bohlin, "Safety and Comfort Factors in Volvo Occupant Compartment Packaging", SAE 780135.
8. H. Nakaya, "Collision Safety Design by Structural Analysis", JSAE VOL 34, No. 9, 1980.

Optimizing Knee Restraint Characteristics for Improved Air Bag System Performance of a Small Car

HIDEO TAKEDA and SABURO KOBAYASHI
Honda R & D Co., Ltd.

3668

ABSTRACT

The two known systems for restraining vehicle occupants in a crash situation are the seat belt and the air bag. A series of head-on crash tests against a barrier indicated that these restraining devices present widely different G waveforms for the chest of a dummy seated behind the steering wheel as the crash pulse becomes more severe. The dummy chest, when restrained by a seat belt, showed a gentle G waveform, while with an air bag, it presented another waveform with unusual spikes.

An analysis of the test findings reveals that spikes in chest G are always accompanied by similar spikes in G for the pelvis. It was found that this is attributable to a substantial shock when the dummy's upper leg contacts the molded pelvic structure. This suggests that the existing dummy might have some structural deficiency. This con-

tact occurs when the restraining force for the upper torso of the dummy is much less than that for the pelvis.

An air bag was used to restrain the driver's upper torso and a knee restraint to hold the pelvis. The restraining force for the upper torso was limited by the characteristics of the bag. Therefore, use of a softer knee bolster appeared to be the only available alternative for keeping the upper and lower restraining forces well-balanced.

Another series of crash tests was conducted on an improved air bag system using softer knee bolsters. The findings indicate that the improved system can allow gentle G waveforms even with severe crash pulses despite the shortcoming of the existing dummy.

INTRODUCTION

A series of head-on crash tests against a barrier was conducted to develop a suitable air bag for small cars. When the vehicle crash speed was increased from 30mph to 35mph and the vehicle structure modified accordingly, unusual spikes began to appear frequently in chest G for the driver side dummy. Available data were analyzed by various methods to find why such spikes occur and how they could be precluded. This report discusses the research efforts that have successfully solved the chest G spike problem.

AIR BAG/SEAT BELT-RESTRAINED DRIVER CHEST G

Figures 1 and 2 present typical chest G for the driver dummy restrained by two alternative methods—an air bag and a seat belt—in 30mph and 35mph head-on crash tests against a barrier. The dummy chest, when restrained by a seat belt, continued to show a gentle G waveform with no appreciable change even if the crash speed was increased to 35mph, while with an air bag, it presented another waveform with unusual spikes at 35mph crash speed.

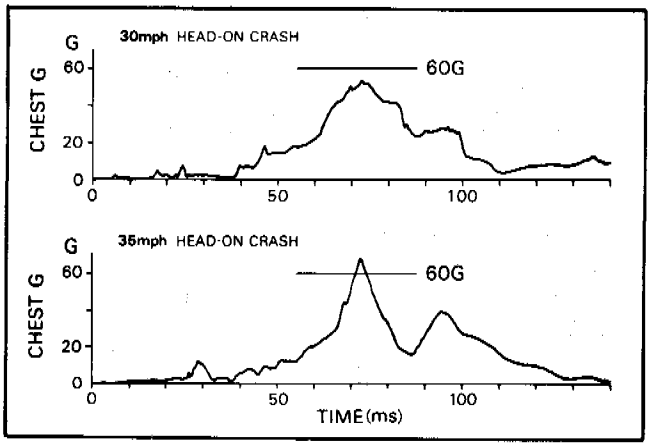

Figure 1. Air bag-restrained driver dummy chest G.

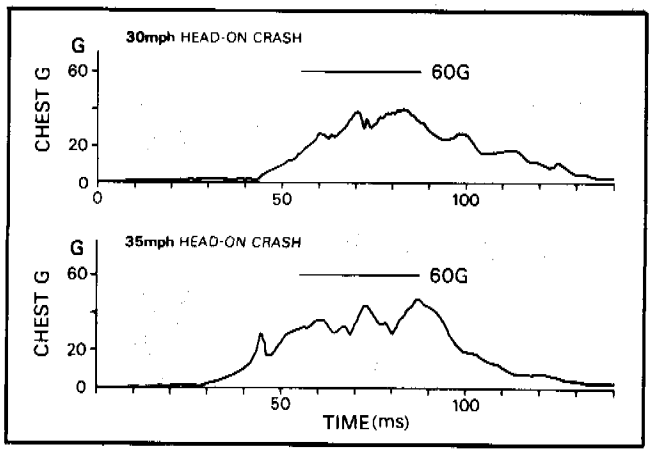

Figure 2. Seat belt-restrained driver dummy chest G.

CONCEIVABLE CAUSES OF UNUSUAL CHEST G SPIKES

Initially, we simply attributed the unusual spikes in chest G to inadequate energy-absorbing capability of the air bag system. Therefore a variety of techniques were developed to increase the energy-absorbing capability including the use of a larger air bag, increased gas generator capacity, and a longer stroke for the energy-absorbing column. None of them resulted in any appreciable improvement.

Longitudinal, vertical, and lateral G traces were separately analyzed in relation to the position of the dummy from high speed films. The analysis revealed that a vertical G spike always appeared immediately preceding a longitudinal G spike. The findings led to the assumption that unusual spikes in chest vertical G create big longitudinal G with high peaks and deep valleys. (See Fig. 3.) The dummy's behavior was carefully examined with particular attention given to the movement of its pelvis because this region is the only conceivable source of vertical G input.

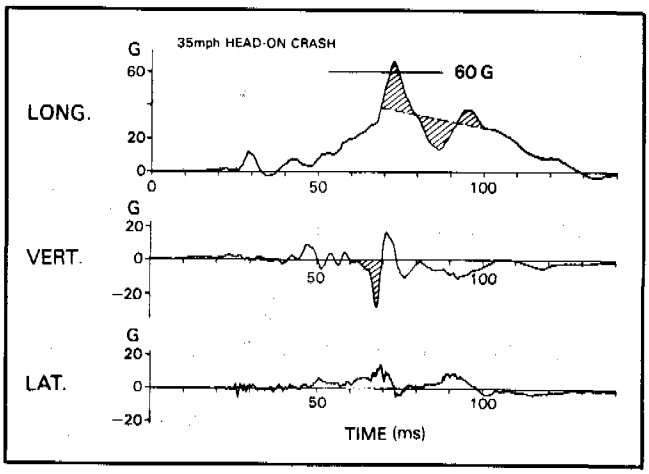

Figure 3. Typical measured chest G with unusual spike.

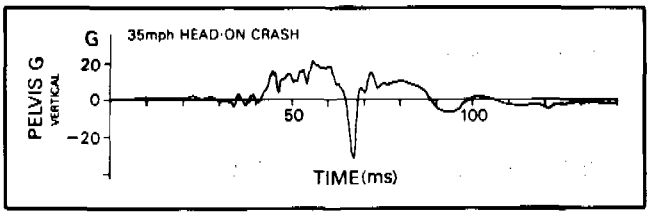

Figure 4. Typical measured pelvis G.

As shown in Figure 4, it was found that the vertical G for the pelvis has similar spikes as those in the chest vertical G.

Figure 5 shows another important finding: these spikes occur when the hip joints reach their maximum angle due to the upper leg segments firmly contacting the molded pelvic structure. Unlike the dummy, we can bend over until our thighs touch the abdomen. This suggests that the existing dummy might have some structural deficiency. The impact occurring under this condition is presumably transmitted to the chest through the steel cable which forms the central core of the lumbar spine as shown in Figure 5.

RESEARCH EFFORTS TO REDUCE CHEST G SPIKES

Chest G spikes might occur, as noted earlier, when the dummy's hip joints are bent to the utmost limit. It was assumed therefore that the spikes could be removed simply by reducing the extent to which the hip joints bend in a crash test.

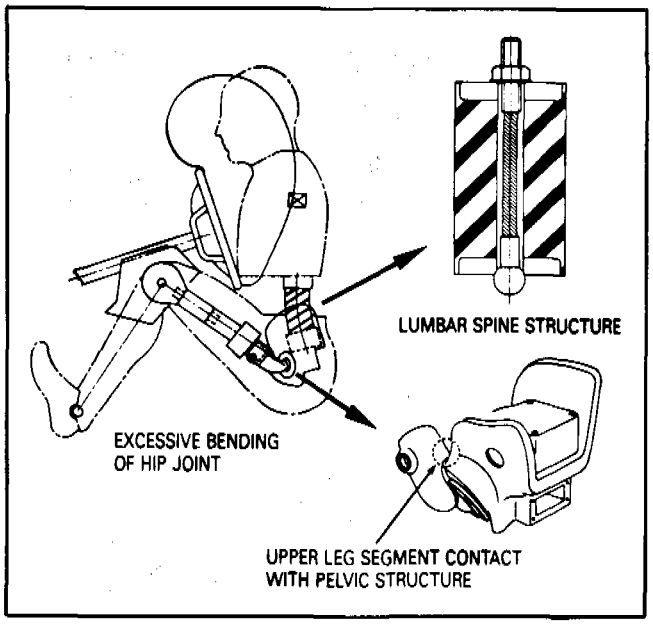

Figure 5. Excessive bending of hip joint.

Major Factors of Large Hip Joint Bending

In our crash tests on air bag systems, the dummy's upper torso was restrained by an air bag, while pelvis was held by a knee bolster. The sharp bending of the hip joints is attributable to a large difference between these two systems in developing restraining force. (See Fig. 6.)

The air bag cannot develop a restraining force as quickly as the knee bolster since the gas inside the bag has to be compressed by the dummy to some extent to produce a sufficient reaction force. The difference between these systems' initial restraining forces permits the upper torso of the dummy to move forward substantially more than the lower part in a crash situation. This is probably why the hip joints bend sharply.

As noted earlier, unusual spikes in chest G began to appear after the vehicle crash speed was increased to 35mph and the vehicle structure stiffened as required. In other words, a crash of a stiffer vehicle structure at a speed 5mph faster than the previous level reduced the crash pulse duration. As the crash pulse becomes more severe, the imbalance in restraining forces between the air bag and knee bolster systems becomes greater. This is a significant factor affecting hip joint bending.

System Improvements to Reduce Hip Joint Bending (Table 1)

The following paragraphs discuss the system improvements we made to reduce sharp hip joint bending and the problems we faced in working out such improvements.

Several attempts were made to improve the unfavorable characteristics of the air bag in developing a restraining force. These improvement efforts included the use of a larger bag and increased gas generator capacity for faster bag deployment. As discussed earlier, however, a series of tests revealed that none of these changes resulted in any appreciable improvement and at the same time tended to increase air bag deployment noise.

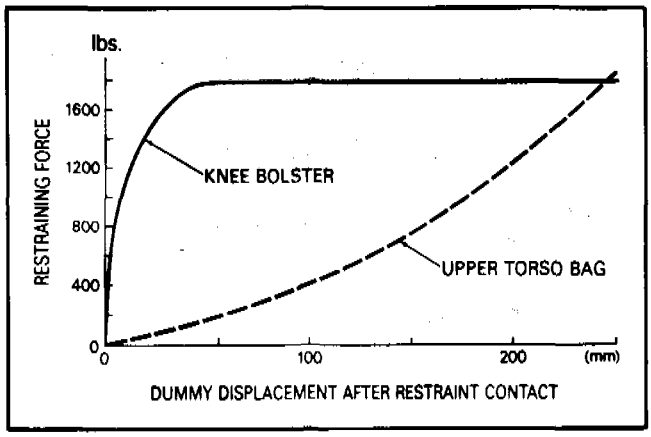

Figure 6. Typical restraining force of knee bolster and upper torso bag.

Table 1. Causes and remedies of sharp hip joint bending.

	Causes	Remedies	Problems
1	Inadequate air bag capability to quickly develop a restraining force	Use of a larger bag and faster deployment system	Larger noises during bag deployment
2	Greater restraining force of the knee bolster	Reduction of the knee bolster's restraining force by increasing its crush	Reduced passenger leg space in a small automobile

We concluded that the only available means to ensure well-balanced restraining forces for the upper and lower parts of the dummy would be to reduce the knee bolster's restraining force. Our improvement efforts were then concentrated on the development of a modified knee bolster.

KNEE BOLSTER MODIFICATION

A series of 35mph head-on crash tests against a barrier using a buck was conducted with knee bolsters of different hardness levels and sizes installed at different distances from the occupant. The findings may be summarized as follows: As shown in Figure 7, a greater forward displacement of the pelvis results in lower chest G. In other words, favorable results can be achieved if the knees sink deeper into the bolster. However, when a smaller, harder knee bolster is used to minimize the required space and is installed farther away from the occupant to allow a greater forward displacement of the pelvis, spikes in chest G still occur if the bolster's collapsing load exceeds a 1400 lb. level in femur load equivalent. A knee bolster installed closer to the occupant to immediately produce a restraining force also fails to preclude chest G spikes because it stops the forward movement of the dummy's pelvis too early and causes sharp hip bending. These findings suggest that a satisfactory solution to the chest G spike problem requires the use of a larger, softer knee bolster which has a much smaller collapsing load than the allowable femur load limit as specified in FMVSS 208. The knee bolster must be installed at a proper distance from the occupant to allow sufficient forward displacement of the pelvis.

Figure 8 shows typical examples of chest G curves recorded at average femur loads of 1720 lb., 1350 lb., and 1100 lb. As is apparent from the diagram, vertical chest G spikes become smaller, reducing the maximum resultant chest G, as femur load decreases.

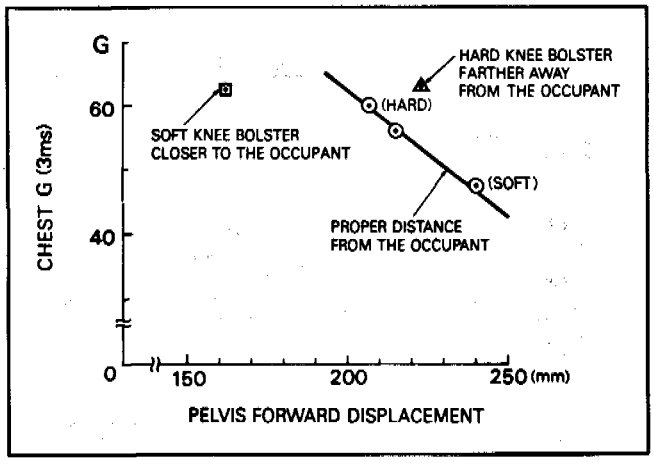

Figure 7. Pelvis forward displacement vs. chest G.

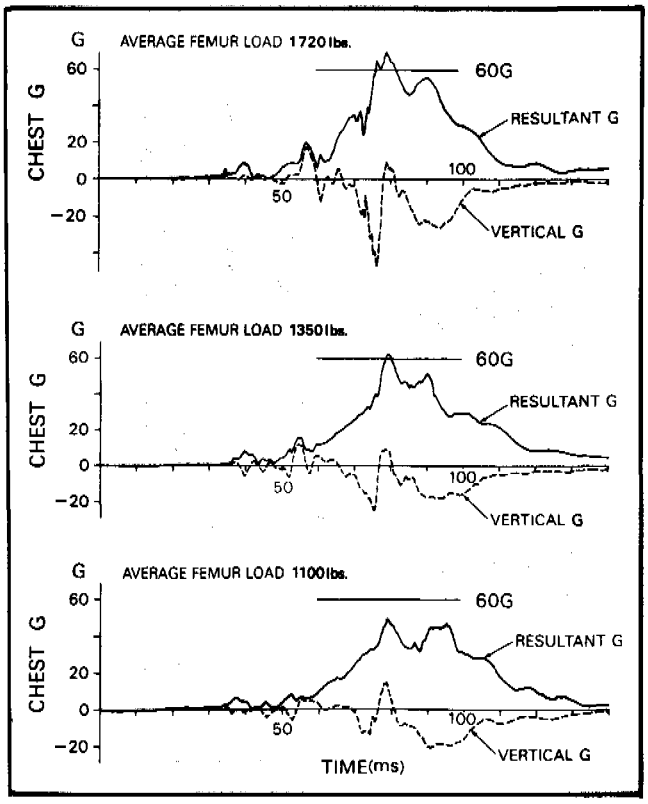

Figure 8. Typical chest G with different femur load.

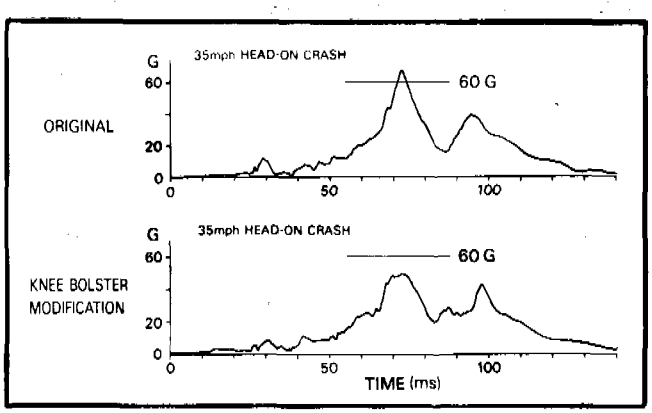

Figure 9. Effects of knee bolster modification on chest G.

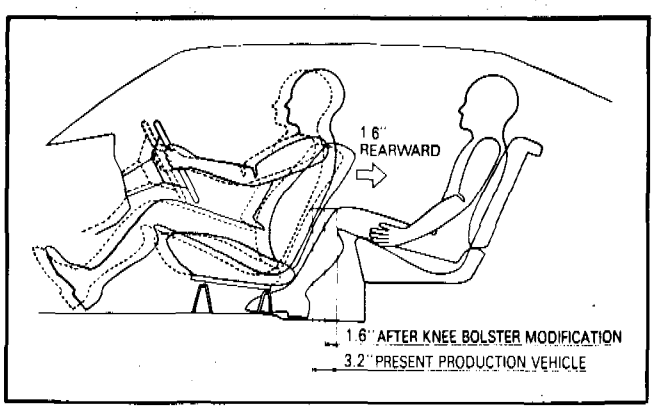

Figure 10. Required seat positioning.

FULL-SCALE CRASH TESTS

Some full-scale crash tests were performed to demonstrate the effects of the above remedies for chest G spikes. Figure 9 shows the chest G traces recorded before and after the improvements were made in the knee bolster. As expected, the results are similar to those of the buck tests; no unusual spikes appeared in chest G. The improved restraint system produced acceptable head and chest G and femur loads in a 35 mph head-on crash test against a barrier. (See Table 2.)

CONCLUSION

The modification of knee bolster characteristics enabled us to prepare an experimental vehicle with a driver air bag system that produced good results. Unusual spikes in chest G traces appearing when the dummy's hip joints are bent to the utmost limit are very likely to occur in small automobiles that have severe crash pulses. The improvement of the restraint system discussed in this report required the use of a larger knee bolster. Therefore the front seats had to be moved rearward to give the driver sufficient leg space to freely to operate the control pedals. This unfavorably affected the interior layout of the car as the rear leg space was reduced substantially. (Fig. 10) Installing an air bag system in an existing small vehicle design will drastically impact its basic layout and utility.

Table 2. Test results with air bag system—research stage (35 mph head-on crash).

Driver			
HIC	Chest G	Femur load [lbs]	
		Left	Right
465	50.5	1526	1854
859	58.5	1790	1416
437	47.2	1557	1438
364	55.8	1616	1447

REFERENCES

1. D. Theodore Zinke, "Small Car Front Seat Occupant Inflatable Restraint System, Volume II—Citation Air Bag Systems".
2. H. T. E. Hertzberg, "The Anthropology of Anthropomorphic Dummies", 13th STAPP Car Crash Conference.
3. Gerald W. Nyquist and Clarence J. Murton, "Static Bending Response of the Human Lower Torso", 19th STAPP Car Crash Conference.
4. Naveen K. Mital, Richard Cheng, Robert S. Levine and Albert I. King, "Dynamic Characteristics of the Human Spine During — G_x Acceleration", 22nd STAPP Car Crash Conference

3669

On the Optimum Parameters of a Seat Belt Pre-loading Device

KOJI KURIMOTO, HAYAO HIRAI and
TSUTOMU SUGAWARA
Toyo Kogyo Co., Ltd.

ABSTRACT

The effectiveness of occupant restraint system is generally reduced as the impact velocity of vehicle increases. The addition of a pre-loading device to seat belt system has been proposed as one of useful measures to this kind of degradations.

This paper proposes the optimum selection of activation time and level of load produced by the assumed pre-loading device in case of 2-point diagonal seat belt system with knee bolster on the frontal impact at 40mph.

The two dimensional, five mass occupant mathematical model is developed and the validation of the model is carried out by adjusting various parameters of the model in comparison of the simulated results with those of the actual sled test, where a typical pre-loading device is employed.

The set of optimum parameters of pre-loading device is derived in relation to the level of HIC (head injury criteria) and the displacement of occupant through the computer simulation of this kinematic model.

PREFACE

On frontal collision at higher impact speed, so called "spool out" and additional elongation of the webbing reduce the restraint capability of seat belt system with retracting device. As one of the measures to avoid this, a pre-loading device is proposed which retracts a certain length of webbing during the first few milliseconds of a crash (1).

The effectiveness of pre-loading device, in correspondence to a target velocity where its maximum effectiveness is obtainable, varies substantially depending on such parameters as its activation time and the level of load produced. In this respect, this paper discusses the selection of these optimum parameters at the impact velocity of 40 mph, as the improvements of the restraint capability could be attainable with rather conventional manner below this speed.

As a typical case, a 2-point diagonal seat belt system with knee bolster is considered, where the anchorage locations are selected based on a certain 4-door sedan. In addition, the vehicle deceleration profile selected is a half-sine curve simulating a result of actual crash test of the vehicle that does not tend to undergo a large peak deceleration in the passenger compartment around the end of vehicle deformation.

The conventional anthropomorphic dummy is treated as a two dimensional, five mass mathematical model, whose validation is made as follows. First, various parameters of the mathematical model are adjusted to obtain agreement with the actual sled test results, for the case where the dummy is restrained by the 2-point diagonal seat belt without pre-loading device. Second, the results by the computer simulation with the parameters thus determined and those by the actual sled test are compared for the case where the pre-loading device is activated, resulting that the computed results are in good agreement with test results. Then, computer simulations are made to find the optimum parameters for the pre-loading device, employing the mathematical model of the aforementioned characteristics.

MATHEMATICAL MODELING

General Description

A two dimensional, five mass model is employed, the schematic of which is shown in Figure 1, since a dummy makes a virtually two dimensional movements on frontal collision, and a modeling of unnecessarily complicated design would make characterization and input to the model excessively complex. Here, the front seat passenger is dealt, since it is generally difficult for the driver to avoid impact against the steering wheel, making it necessary to consider the energy absorption of steering system by the occupant.

This mathematical model is provided with toe board, seat, and knee bolster. These surfaces are to make interaction with parts of the dummy expressed as circular segments, generating friction force on contact. The characteristics of seat belt are mathematically adjusted on two dimensional plane by designating the relative anchorage locations and the actual elongation of the webbing. The seat belt on the mathematical model is to contact with the dummy model at two points, generating friction force at respective point.

Dummy Characteristics

By referring to the geometric, inertial, and joint characteristics of Part 572 Hybrid II dummy described in publications (2–3), and by conducting some measurements, dummy characteristics are determined. The neck joint characteristic, as a representative example, is shown in Figure 2, where the torque versus rotational movement is nonlinearly represented with angular velocity depend-

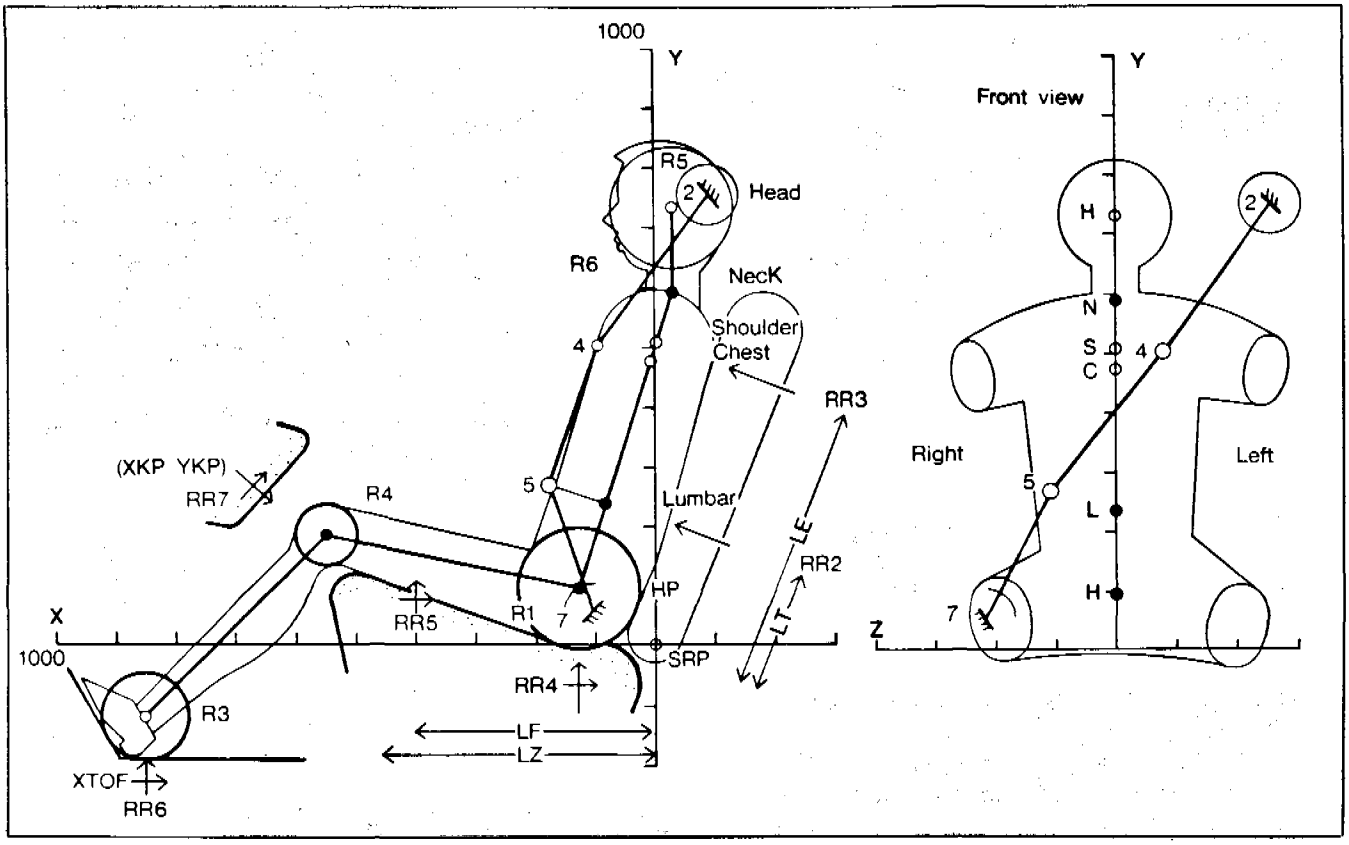

Figure 1. Schematic of mathematical model.

ent hysteresis. Similar approaches are made in determining the characteristics of other joints.

Characteristics of Restraint Components

The seat cushion is represented by a plate on two vertical nonlinear resistances, one of which is fixed at the front end of the plate. The other is connected at the bottom of the dummy's hip, making it possible to move forward with the hip displacement. These characteristics, whose typical examples are shown in Figure 3, are determined by pressing the seat cushion with hip-shaped ram.

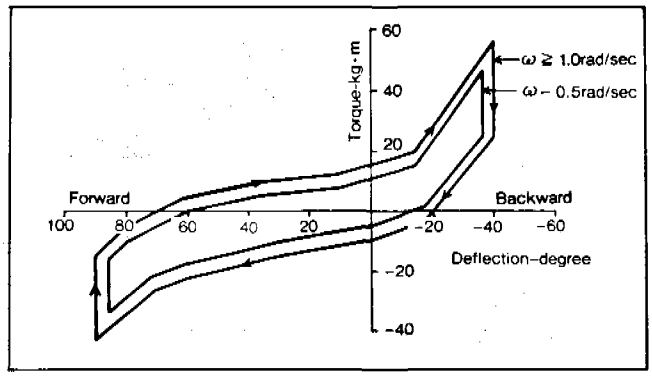

Figure 2. Representative neck joint characteristic.

The knee bolster is represented by a plate, where the force versus deflection is nonlinearly represented with hysteresis. A typical characteristic is shown in Figure 4,

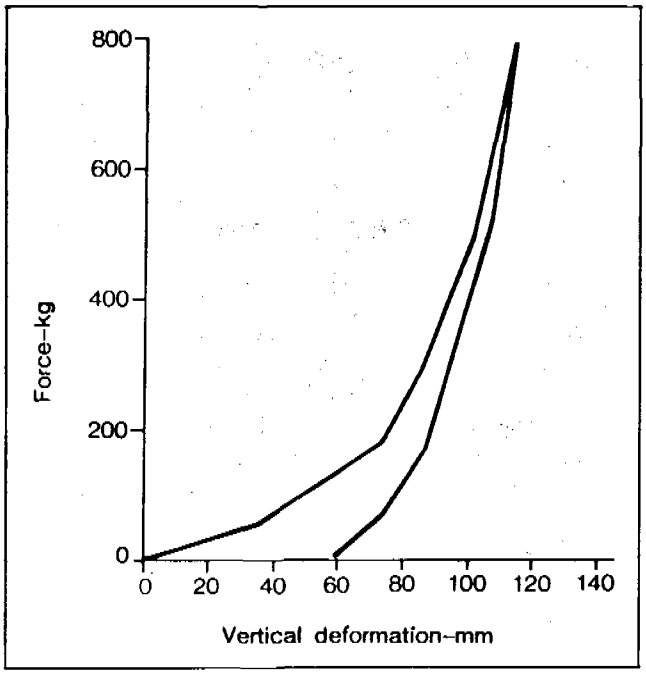

Figure 3. Representative seat cushion (rear part) characteristic.

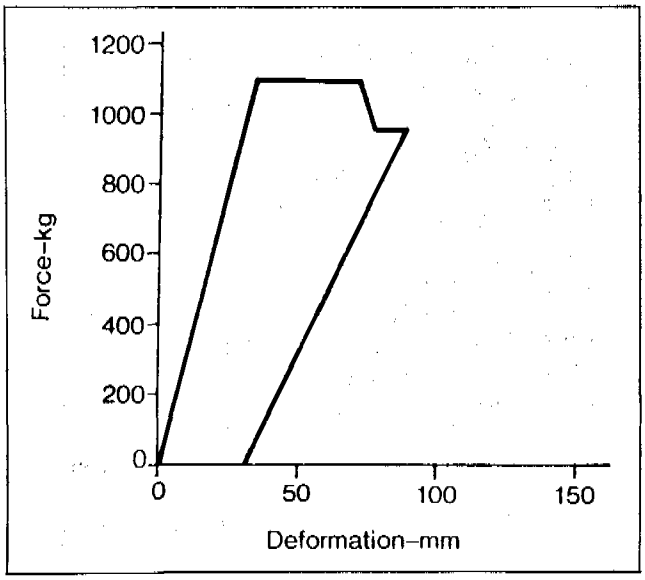

Figure 4. Representative knee bolster characteristic.

which is determined by pressing a knee-shaped ram on a knee bolster.

The load versus elongation characteristics of the seat belt webbing between upper and lower anchorages is also nonlinearly represented with hysteresis. This characteristic is determined as the combination of the following three characteristics, whose typical example is shown in Figure 5:

—Elongation characteristic of seat belt webbing is determined by the method stipulated in FMVSS 209.
—The "spool out" of seat belt webbing taken up in the retractor is determined by measuring the actual spool out characteristics.
—Deflection characteristic of chest on interaction with seat belt at Part 572 Hybrid II dummy is determined by such method as described in the literature (4).

VALIDATION OF MATHEMATICAL MODEL

Seat Belt System Without Pre-loading Device

A computer simulation is executed at 33.5 mph with the aforementioned characteristics, resulting smaller head displacement and larger HIC value compared to actual sled test results at the same velocity. The reason for this is substantially because, in actual test, the dummy's rotational movement toward sideways causes the head to move forward, whose effects is not taken into account on this mathematical model.

To compensate this inconsistency the elongation characteristic of the seat belt is partially adjusted. As the consequence, the computation yields results in good agreement with those by the actual test, as shown in Figure 6.

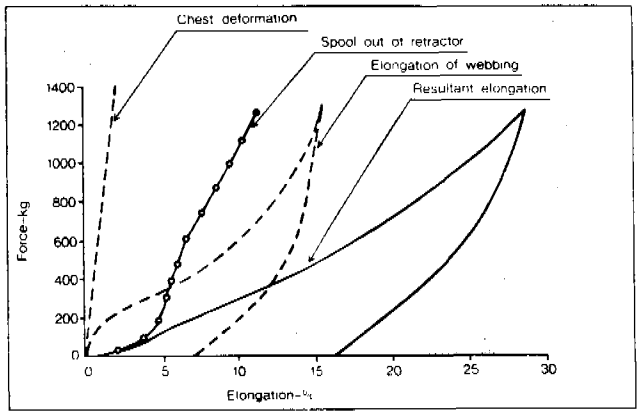

Figure 5. Representative seat belt system characteristics.

Seat Belt System with Pre-loading Device

As a result of the aforementioned mathematical computation for the case without pre-loading device, the time sequence can be plotted on the load versus elongation characteristics of a seat belt system as shown in Figure 7. Respective time on the plot is utilized to specify the activation time of a pre-loading device. Once this acti-

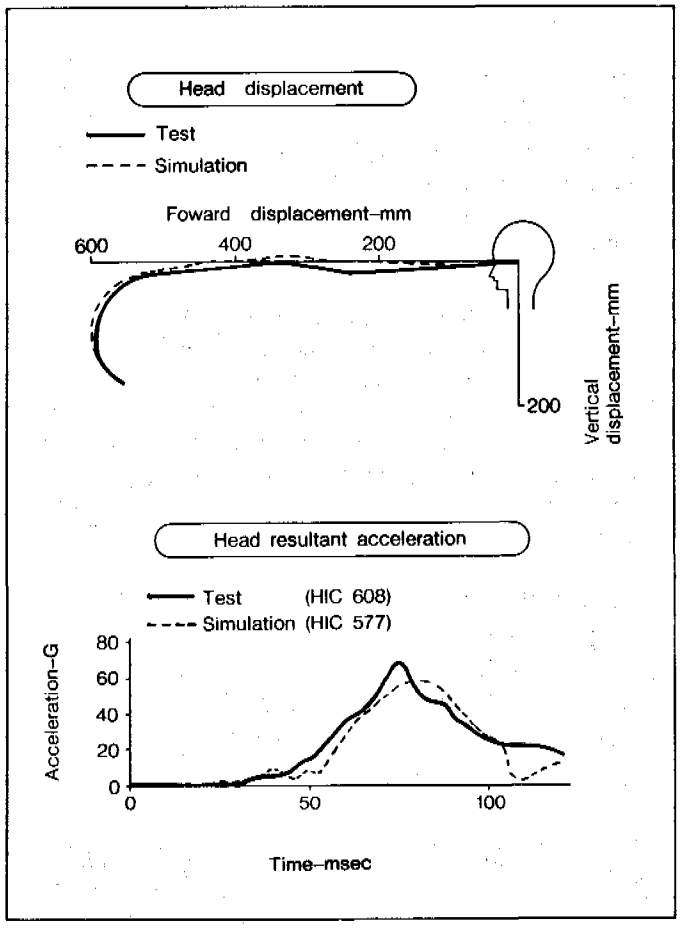

Figure 6. Comparison of the results between simulation and test (without pre-loading device).

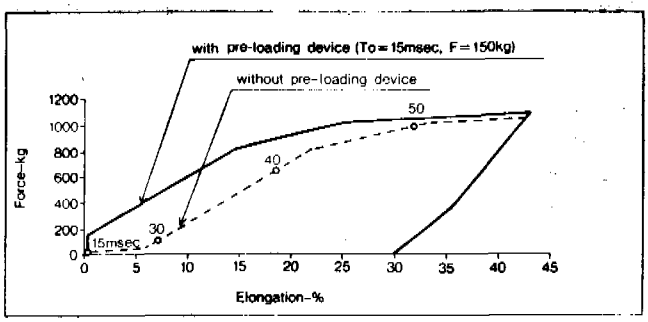

Figure 7. Representative seat belt system characteristics (with and without pre-loading device).

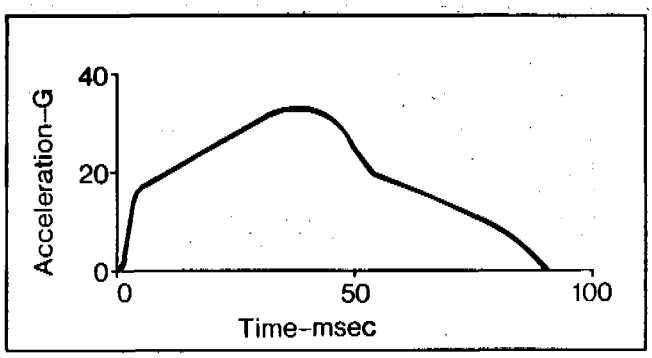

Figure 9. Crash pulse.

vation time and a particular extraction force produced by a pre-loading device are specified, the characteristic curve is shifted along the horizontal axis as the elongation increases in correspondence with the load.

This procedure is used to provide the load versus elongation characteristics of the seat belt system with a given pre-loading device of specific parameters. Figure 7 also presents an example of the characteristics of the case where the activation time is 15 msec and the extraction force is 150 kg.

To compare the results by computation with those by experiment, an actual sled test is run at 36.3 mph, where a typical pre-loading device which produces the maximum load of 150 kg is installed as shown in Figure 8 and activated at 15 msec. Then, Computer Simulation with the aforementioned parameters is executed at 36.3 mph, where a half-sine acceleration profile similar to the actual crash pulse for the test above is set as shown in Figure 9. The results thus obtained show in good agreement with those by the actual sled test, some typical examples of which are shown in Figure 10.

OPTIMUM PARAMETERS AT 40 MPH

Computer Simulations at 40 mph are carried out with various combinations of activation time and load of the pre-loading device, thus to clarify the influence of parameters on HIC level and head displacement, the results of which are shown in Figure 11. Figure 11 also indicates the shaded horizontal lines which implies the target HIC level and the permissible head displacement short of contacting a forward interior object. Here, the target HIC level is specified at 800 and the permissible head displacement is set at 600 mm, assuming probable contact with the instrument panel beyond this value.

Since this simulation model is made without instrument panel, the calculated HIC level registered is low, even when head displacement exceeded the permissible level. In actual situations, however, a higher level as shown by broken line in Figure 11 would be assumed to result, once when the head is brought into strong contact with the instrument panel. Consequently, it is important to hold the head displacement to below the permissible level.

It is observed, in Figure 11, that both HIC and head displacement are decreased as the activation time is reduced and the load of the pre-loading device is increased.

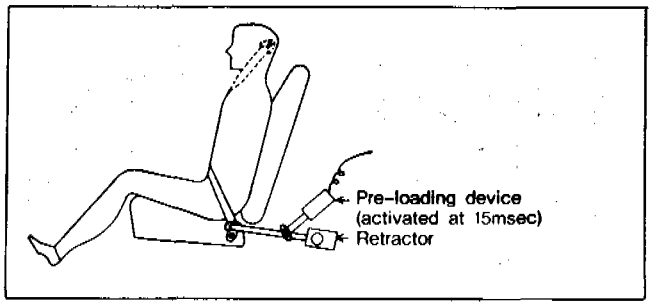

Figure 8. Schematic of pre-loading device installation.

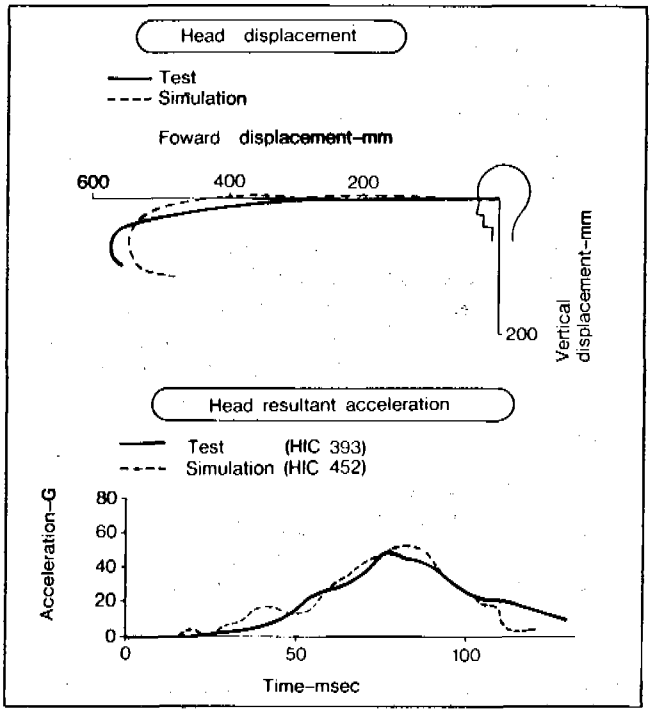

Figure 10. Comparison of the results between simulation and test (with pre-loading device).

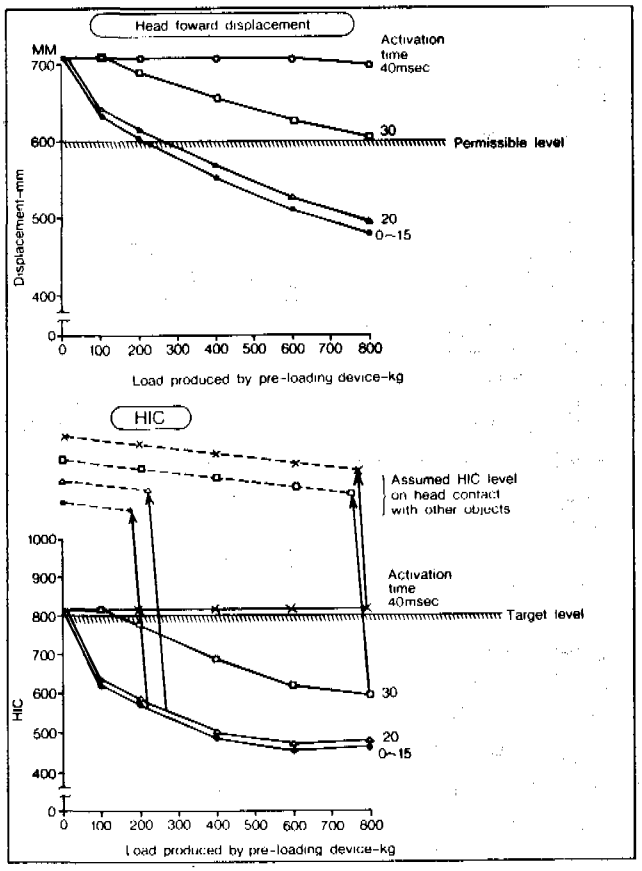

Figure 11. Influences of pre-loading device at 40 mph simulation.

However, there is restriction against the load parameter to keep the HIC and the head displacement under the respective permissible levels. Namely, it is said that the number of rib fractures increases as the load produced by seat belt increases, and there is an instance where rib fracture was suffered at as low a shoulder load as 200 kg or so, according to tests using human cadavers (5), and the higher load produced by inadvertent activation of the pre-loading device could lead to driver's error in vehicle operation. There is also restriction against the activation time to maintain the sensing reliability.

Thus, in the example cited, it is considered that the load produced by the pre-loading device should be held to below 220 kg. With this condition, the activation time is required to be less than 15 msec, as shown in Figure 11, to meet the target of both HIC and head displacement.

PERFORMANCE AT LOW SPEED

Computer simulation is executed on an impact velocity of, as an example, 25 mph, to observe the feasibility of the pre-loading device with the optimum parameters obtained at 40 mph. The sled acceleration profile for the above-mentioned 40 mph was rearranged to that for 25 mph as follows.

First, the acceleration profile at 36.3 mph, as shown in Figure 9, was doubly integrated with respect to time, resulting the force versus deformation characteristic. Then assuming one dimensional, one mass and one spring model whose spring rate is given by the abovementioned characteristics, the acceleration profile at 25 mph is obtained as response of the mass on impacting the model into the fixed barrier at 25 mph. Generally, the activation time of pre-loading device comes to be rather late as the impact velocity of the vehicle decreases. In this case, it is assumed to be 25 msec rather arbitrarily, since the precise value depends on the specific sensing device for the pre-loading device.

With this assumption and load produced by the pre-loading device to be 220 kg as before, a computer simulation is executed at 25 mph. It is demonstrated as the result that the pre-loading device is still effective in reducing HIC and head displacement at 25 mph, too, as shown in Figure 12, thus indicating that the parameters specified for 40 mph would have no adverse effects in low speed collisions.

SUMMARY

(1) A two dimensional, five mass mathematical model can be used effectively to estimate such response as HIC and head displacement occurring at actual impact test.

(2) The computer simulation is an effective tool to determine the optimum parameters of a pre-loading device with respect to activation time and load. This approach could be applicable to various types of seat belt system, anchorage locations which vary with vehicle geometric features, and vehicle body deformation characteristics.

(3) On the simulated 4-door front drive car presumed to suffer deformation at an impact velocity of 40 mph, the optimum parameters of the pre-loading device are proposed to be activation time of 15 msec and load of 220 kg.

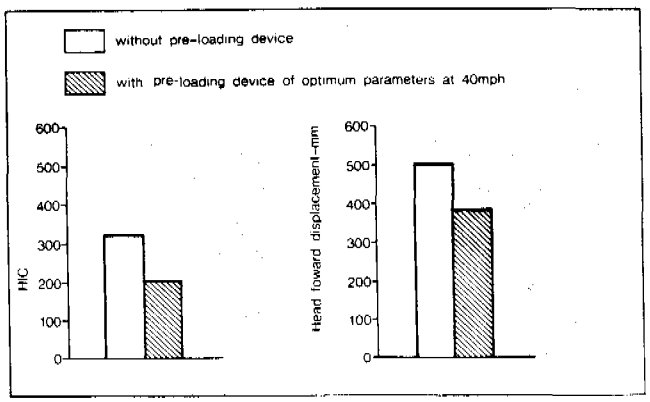

Figure 12. SWimulated effect of pre-loading device at 25 mph.

(4) The aforementioned optimum parameters obtained from the computer simulations seem to have no adverse effects at lower speed collisions and to be still effective in reducing HIC level and head displacement.

Thus it is observed that the pre-loading device is effective to the extent of a typical frontal collision studied. To put it into practical application, however, further extensive technical development has yet to be made, in addition of consumer acceptability, on such areas as elimination of occupant's uneasiness at activation of explosives, sensing reliability for the activation only when it is necessary, and ensuring reliability of the complex system.

ACKNOWLEDGEMENT

The authors wish to express heartful appreciation to related persons at Toyo Kogyo Co., Ltd. who extended valuable suggestion for this study.

REFERENCES

1. W. Reidelbach and H. Scholz, "Advanced Restraint System Concepts", SAE paper No. 790321, 1979.
2. R. P. Hubbard and D. G. McLeod, "Geometric, Inertial, and Joint Characteristics of Two Part 572 Dummies for Occupant Modeling", 21st Stapp Car Crash Conf., SAE Paper No. 770937, 1977.
3. B. M. Bowman, R. O. Bennett, D. H. Robbins and J. W. Becker, "MVMA Two-Dimensional Crash Victim Simulation, Version 4, Volume 1-3", HSRI, 1979.
4. D. C. Viano and C. C. Culver, "Test Dummy Interaction with a Shoulder or Lap Belt", 25th Stapp Car Crash Conf., SAE Paper No. 811017, 1981.
5. A. Fayon, C. Tarriere, G. Walfisch, C. Got and A. Patel, "Thorax of 3-Point Belt Wearers During a Crash (Experiments with Cadavers), 19th Stapp Car Crash Conf., SAE Paper No. 751148, 1975.

Mathematical Models for the Assessment of Pedestrian Protection Provided by a Car Contour

J. WISMANS and J. van WIJK
Research Institute for Road Vehicles TNO
Delft, The Netherlands

SUMMARY

Injuries sustained by pedestrians struck by the front of cars are dependent on the profile and the local stiffness characteristics of the vehicle. Mathematical Crash Victim models, if well-validated, could provide a suitable method for the assessment of pedestrian protection provided by different car contours.

In this presentation, first a review will be given of a number of existing pedestrian models along with the associated validation studies. On the basis of this review and results of recent accident analysis studies a series of pedestrian models with varying complexity were developed using the Crash Victim Simulation Program MADYMO.

The predictions of these models are compared with experimental results for two impact velocities and the reliability with respect to their complexity is discussed.

INTRODUCTION

Pedestrians are among the most vulnerable traffic participants. A pedestrian runs more than twice as high a risk of being fatally injured in a road accident as a car occupant. In recent years traffic safety research has concentrated more and more on the problem of pedestrian accidents.

Since the end of 1980 three research institutes: Bundesanstalt für Strassenwesen (BASt), Organisme National de Sécurité Routière (ONSER) and the Research Institute for Road Vehicles (IW-TNO) have co-operated in the field of pedestrian safety. The aim of this study is to propose a standardized test methodology that can be applied to pedestrian safety tests carried out for research or for compliance testing of passenger cars.

A part of this project was the formulation of a mathematical model of a pedestrian during an impact. Several advantages of mathematical models are the exact reproducibility of a simulation, the absence of measuring problems and the possibility to conduct sensitivity-analyses in a simple, rapid and inexpensive way.

This study was conducted with the MADYMO program package, developed at the Research Institute for Road Vehicles TNO, Delft, The Netherlands. A description of this package, along with several examples of applications can be found in (11). The main features of this package can be summarized as follows:

—a compact FORTRAN source which can be implemented on small computer systems;
—a 2D and a 3D option;
—a variable number of linkage systems;

—a set of standard force interaction routines;
—easy incorporation of user defined subroutines for specific force interactions and user defined output.

In this paper, first a brief review will be given of a number of existing pedestrian models along with the associated validation studies. On the basis of this review and results of recent accident analysis studies a series of three pedestrian models with varying complexity were formulated. The predictions of these models will be compared with experimental results with an Audi 100 for two impact velocities, namely 30 and 40 km/h.

REVIEW OF MATHEMATICAL PEDESTRIAN MODELS

In this section a literature review will be presented concerning existing mathematical models for the simulation of car-pedestrian collisions.

Table 1 summarizes the source and background of ten models that were analyzed. The models are numbered according to the numbers in the reference list. Four models are based on the CALSPAN CVS program. These models are not identical since different versions of this computer program were used and modifications were introduced by the users. The PRAKIMOD model is based on the MVMA-program.

In Table 1 the main characteristics of the models are summarized. A first distinction which can be made is between 2D and 3D models. This last type of models, in general, will be more realistic since the kinematics of a pedestrian impacted by a car are found to be of a three-dimensional nature. However, such a 3D model is much more complicated and in addition a lot of extra input data has to be defined.

A CVS-model consists of a series of rigid bodies, connected by hinge or ball-and-socket (3D) joints. The number of elements in the various models is included in Table 1.

In most of the models, the vehicle is represented by a number of straight line segments (2D) or planes (3D). In the PROMETHEUS 2 model, however, interconnected segments are used for the simulation of the vehicle contour. The position of these segments can be defined by means of an auxiliary program, which transforms the input parameters into a finite element model of the vehicle. The user can define the hood-contour by a skewed hyperellipse.

Most of the mathematical models for pedestrian collisions are limited to the impact of the pedestrian with the vehicle. Ground impact is not considered in these simulations. Reasons for this are (6):

—a meaningful simulation of the secondary impact is extremely difficult since inaccuracies in the simulation of the primary impact will strongly affect the pedestrian kinematics in the secondary impact;
—in the airborne phase the pedestrian has time for voluntary muscle action;

Table 1. Summary of ten pedestrian models.

Ref.	author/model	Year	2D/3D	Number of segments	Institute
1	Transportation Research Department	1971	2D	3	Cornell Aeronautical Laboratory (USA)
2	Glöcker	1973	2D	1	Institut für Kraftfahrzeuge, Technische Universität Berlin (Germany)
3	Kramer	1974	2D	3	Institut für Kraftfahrzeuge, Technische Universität Berlin (Germany)
4	Mac Laughlin	1974	2D	4	National Highway Traffic Safety Administration. U.S. Dept. of Transportation (USA)
5	Young, TTICVS	1975	3D	12	Texas Transportation Institute, Texas A&M University (USA)
6	Twigg, Prometheus 2	1977	2D	11	Boeing Computer Services Inc. (USA)
7	Fowler, Calspan 3-D CVS, version III	1976	3D	15	British Leyland Limited (Britain)
8	Padgaonkar, Calspan version III	1977	3D	15	Biomechanics Research Center, Wayne State University, Detroit (USA)
9	Lestrelin, Prakimod (MVMA)	1980	2D	8	Laboratoire de Physiologie et de Biomécanique de Peugeot S.A./ Renault (France)
10	Cotte, Calspan version III	1980	3D	15	Laboratoire de chocs et de Biomécanique ONSER (France)

—the simulation time must be increased from 200 ms to about 1000 ms resulting in a considerable increase of computer costs.

In addition it follows from accident analyses that the secondary impact in general causes less severe injuries than the primary impact (Ashton (12), Mackay (13)).

For the interaction between pedestrian and vehicle three types of contact models are used:

—in models 2 and 3 contact interaction is based on the classical theory of collisions between two rigid bodies. According to this theory the impact time is taken as zero. Consequently force and acceleration time histories during the impact phase cannot be evaluated by this type of model;

—in model 6 (PROMETHEUS 2) the vehicle contour is represented by an arbitrary number of interconnected segments;

—in the other models description of the contact is based on interactions between contact surfaces (lines, planes, ellipses, etc.) connected to the vehicle and the predestrian. Whenever a positive penetration between contact surfaces is detected, normal and friction forces are calculated. Force-penetration characteristics have to be defined and are based on measurements or assumptions. Realistic simulation of contacts between pedestrian and sharp edges (e.g., between lower leg and bumper) may cause problems in this type of contact models (7).

In most studies model predictions have been compared with experimental results in order to get an impression of the reliability of the models. Table 2 summarizes some of the test conditions used for validation of the various models. The last item of Table 2 is the type of data used for validation.

The degree of validation, however, differs strongly in the various studies. Some models are not validated at all (models 2 and 4); others are compared with several experiments for a number of conditions. The first column shows the pedestrian surrogate used in the test. Most researchers have concentrated on dummies, because these are a relative easily accessible source for model input data. Measurements of masses, moments of inertia, joint-torques, etc. easily and accurately can be carried out at dummies. Padgaonkar (8) has simulated cadaver experiments. One of the differences between his dummy- and cadaver-model was in the knee-joint: a hinge-type for the dummy and a ball and socket joint for the cadaver in order to admit lateral deflection.

The orientation of the pedestrian, in these tests, varies from frontal via oblique to lateral (see Table 2). Simulation of a lateral or oblique impact in general will be more difficult than a frontal impact, due to the more complex three-dimensional motions. Twigg, for instance, (model 6, 2D) observes that the elbow of the pedestrian can act as a lever to vault the torso up over the hood, thus reducing the injury incurred by the head and torso.

Table 2 also summarizes the cars which were used in

Table 2. Validation of the models.

Ref.	Pedestrian	Pedestrian orientation	Vehicle	Velocity (km/h)	Validation criteria
1	50th % male child dummy	Frontal	Ford Galaxie 1966	16	gross motion
2	—	—	—	—	—
3	50th % male	Frontal	—	36	gross motion throwing distance
4	—	—	—	—	—
5	6-yr Sierra dummy 5th % Sierra dummy female 95th % Sierra dummy male	Frontal Oblique	Mock-up	*	gross motion accelerations
6	Part 572 modified 6-yr child dummy	Lateral	Impala 1974, Test bucks	32	accelerations
7	Ogle OPAT	Lateral	Leyland cars SRV2 Marina	16,32	gross motion, accelerations
8	95th % Sierra dummy	Lateral Frontal	Chevrolet 1973	22,24) 30,39)**	gross motion, accelerations
9	50th % dummy	Frontal	Ford Fairlane Renault 5 Honda N360 Peugeot 204 Opel Kadett Peugeot 304 Citroën GS	16,28,33,40 36 43 40 45 22 43,48	trajectory head
10	ONSER 50	Frontal	Citroën Visa	20,25	gross motion, head impact

*Drop tests on mock-up. Drop height 0,4-0,8 m.
**In addition four cadaver tests and drop tests of Young (5).

the experiments as well as the impact velocity. The fact that different validation criteria are used prevents an adequate comparison of the reliability of the several models.

Most researchers stress in their conclusions the importance of the contact model. The contact model must be able to cope with the problem of edge-contacts, as well as inertial effects. Another crucial point is the description of the joints. Inelastic failure and dynamical effects (damping) must be taken in account. Both the contact and the joint-model must be based on realistic, preferably measured, input data.

MADYMO 2-DIMENSIONAL PEDESTRIAN SIMULATIONS

Based on the preceding literature review of existing pedestrian models and results of several recent accident analyses, a number of requirements were formulated for simulations of pedestrian-vehicle impacts with the general CVS program package MADYMO. The literature study did not show a clear relationship between the complexity of the different models (i.e., number of elements, 2D versus 3D) at the one side and their reliability at the other side. One of the aims of our study therefore was to get first a better insight in this problem. It was decided to develop several models with a differing complexity. Three models are presented which were formulated with the 2D option of MADYMO. In a future study (14) results of 3D-simulations will be presented.

The simulations are limited to the primary impact (pedestrian-car contact) and are concerned with lateral impacts, since this is the most frequent type of impact observed in pedestrian accidents (12). The three models have 2, 5 and 7 segments, respectively, as is shown in Figure 1. The same contact ellipses are attached to the 2- and 5-segment model. In the present models the arms are not incorporated as separate segments: a part of the mass of the arms is added to the mass of the thorax segments.

The input data set describing the pedestrian (e.g., the geometry, mass distribution and joint characteristics) are derived from a standard data set of a Part 572 50th percentile male dummy, which itself is based on a number of measurements conducted in our laboratory.

One of the most important aspects concerning the simulation of pedestrian accidents is the representation of the contacts between vehicle and pedestrian, especially for the edge-contacts. A special contact model was developed in which the external geometries of pedestrian and vehicle are simulated by hyperellipses. A hyperellipse is a general form of a standard ellipse and can be described by the following equation:

$$\left(\frac{|x|}{ea}\right)^n + \left(\frac{|x|}{eb}\right)^n = 1$$

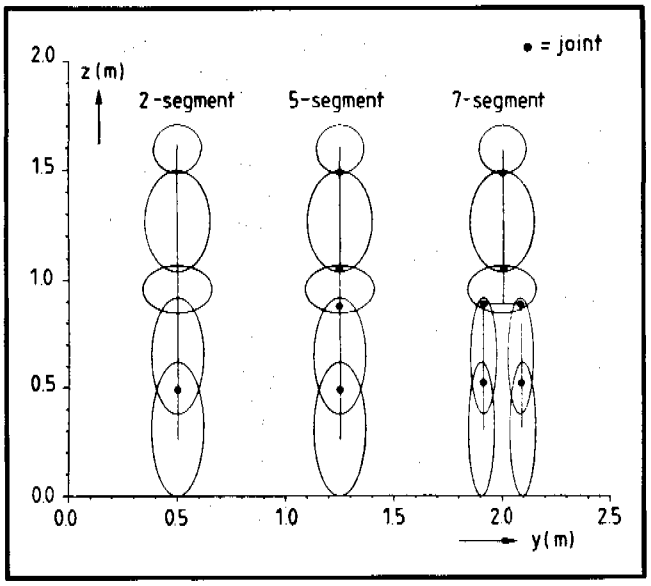

Figure 1. Geometry and contact-ellipses of resp. 2-, 5- and 7-segment model.

where ea and eb are the semi-axes of the hyperellipse and n the degree (see Fig. 2). If n = 2, this equation describes a standard ellipse; however, if n increases, the hyperellipse approximates more and more a rectangle as is shown in Fig. 2 for n = 8. This geometrical description is particularly of interest for the representation of the car and bumper geometry, since vehicle edges quite well can be approximated in this way. A more detailed description of hyperellipse contact models will be presented in reference (14).

The three models presented were applied to simulate a pedestrian impact with a vehicle of the type Audi 100. The geometry of this vehicle is represented by two hyperellipses: one for the bumper and one for the hood (see Fig. 3). The vehicle dimensions were determined from scale drawings and measurements.

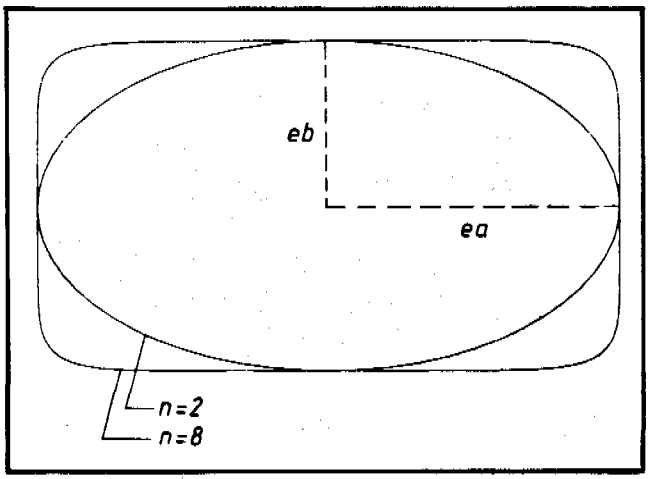

Figure 2. Hyperellipses with identical semi-axes, n = 2 and n = 8.

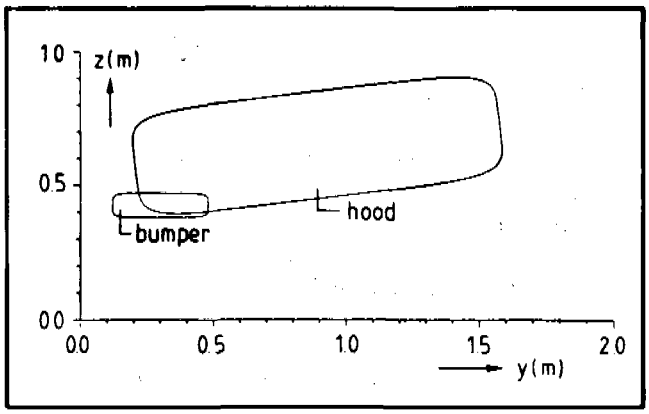

Figure 3. Geometry of Audi 100.

Dynamic force-deflection characteristics of the bumper, hood and hood edge of the Audi 100 vehicle were determined experimentally by the BASt (Bundesanstalt für Strassenwesen). Pendulum tests with a rigid wooden pendulum were used for the bumper and the hood edge. This pendulum was equipped with an accelerometer, while the vehicle deflection was measured with a linear transducer, mounted in the car. The pendulum mass was 10 kg for the bumper impact and 15 kg for the hood edge while the impact velocity was 25 km/h in these tests. For the hood instead of a pendulum test a drop-test was used. The impacting body was a rigid wooden sphere with a mass of 5.25 kg and an impact velocity of 30 km/h.

VALIDATION TESTS

The mathematical model results are compared with a number of dummy tests, which were conducted by the BASt. The dummy in these tests, a 50th percentile male, Part 572 was equipped with triaxial accelerometers in the head, chest and pelvis and uniaxial accelerometers in the knees and feet. Test velocities were taken 30 and 40 km/h and the car deceleration 6 m/s^2. At each impact velocity three tests were conducted.

The dummy position before impact is shown in Figure 4. This position was selected after several pretests. In these pretests it could be observed that in case of a pure lateral impact no direct head-hood contact occurs due to the stiff neck and shoulder assembly of the part 572 dummy. Since head-impact was desired in these tests the dummy torso was slightly rotated (25°) causing the dummy to rotate around its vertical axis during impact and resulting in a direct head impact. The geometry of the ellipses of the pedestrian model was selected in such a way that they approximate the projection of the geometry of the rotated dummy on the plane of simulation.

Experimental results of these tests will be presented in the next section together with mathematical model results.

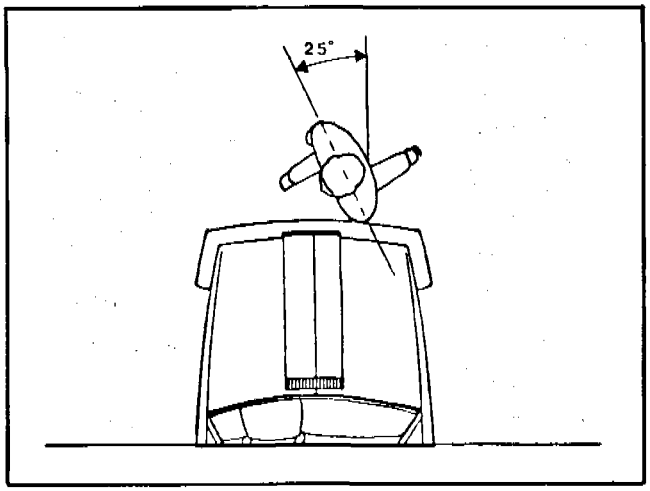

Figure 4. Dummy position at impact.

RESULTS

Figure 5 shows model predictions for the kinematics resulting from the 7-segment pedestrian model in a 40 km/h impact. A good agreement in general between model and experimental result could be observed. A comparison of predicted trajectories of the head, chest, pelvis and foot relative to the vehicle, resulting from the 2-, 5- and 7-segment model, is presented in Figure 6 (30 km/h impact) and Figure 7 (40 km/h impact). Locations of the head impact point on the hood predicted by the various models are summarized in Table 3. All models appear to predict this location within or close to the range of experimental results.

Table 3 includes model predictions and experimental results for the head impact velocity just before impact with the hood. Both the 5- and 7-segment model appear to predict too high values for this quantity compared to experimental observations.

Figure 8 presents model results together with experimental data for the knee, pelvis, chest and head accelerations in a 40 km/h impact. Results are given for the 2-, 5- and 7-segment model respectively. For the pelvis, chest and head, resultant linear accelerations are pre-

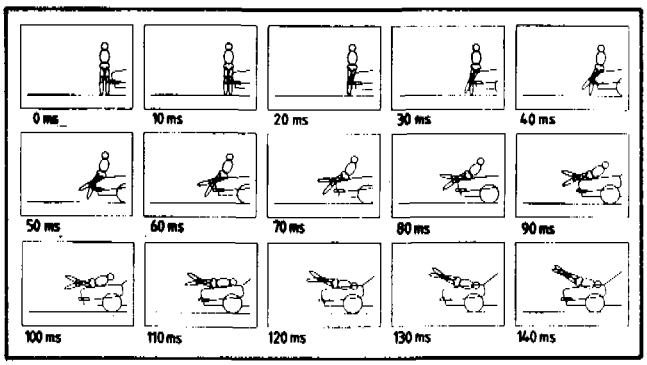

Figure 5. Kinematics of 7-segment model, v = 40 km/h.

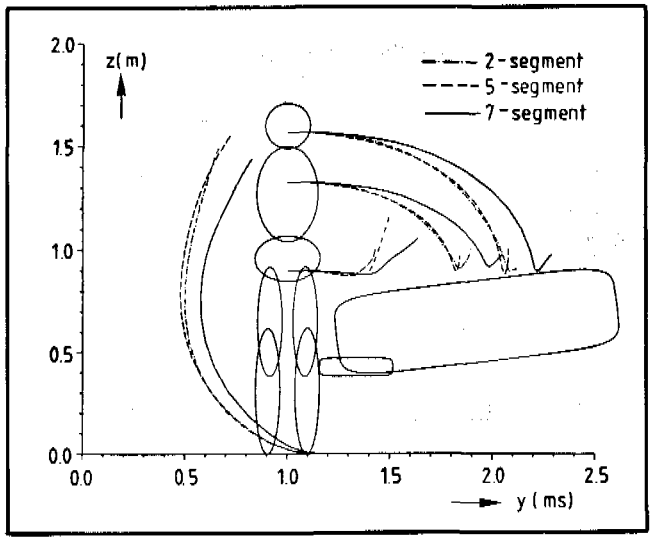

Figure 6. Trajectories of 2, 5 and 7 segment models, v = 30 km/h.

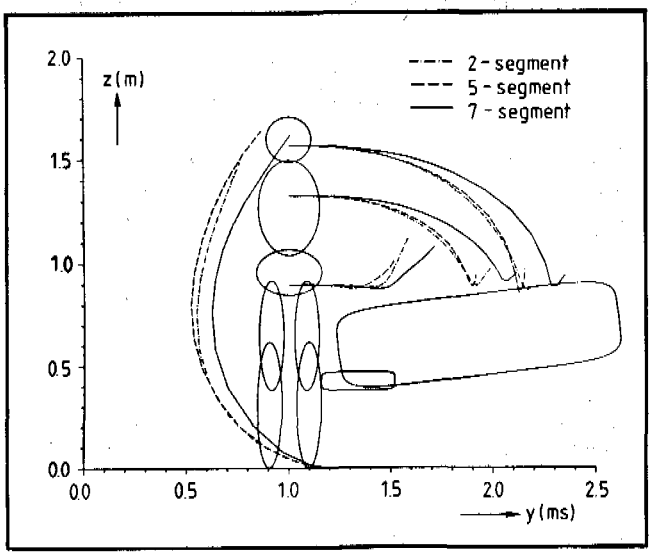

Figure 7. Trajectories of 2, 5 and 7 segment models, v = 40 km/h.

sented and for the knee joint the linear acceleration in lateral direction. It follows that the simple 2-segment model gives quite reasonable results for the acceleration-time histories (i.e., these accelerations appear to be in or close to the experimental corridors). Application of the 5-segment model does not result in better predictions for the knee and pelvis acceleration. A small improvement of the head and chest acceleration-time histories, however, can be observed particularly for $t < 20$ ms, where head and chest acceleration become smaller and more corresponding to the experimental observations. The peak head acceleration, however, becomes too high in this simulation.

Extension of the 5-segment model with 2 segments in order to represent the left and right leg separately in the model, results in a more realistic prediction of the knee accelerations. Also, the alignment between model and experimental head and chest accelerations appears to become more realistic now.

A comparison of bumper load-time histories for the 40 km/h impact, predicted by the 5- and 7-segment model, respectively, is shown in Figure 9. Due to the introduction of a second leg in the model, peak bumper loads are found to decrease by about 25%. Furthermore, the curve has two peaks. The bumper loads resulting from this model are more close to the results of experiments than results from the more simple models.

Accelerations predicted by the 2-, 5- and 7-segment models in a 30 km/h impact showed in general the same characteristics as in the 40 km/h impact. The agreement between model and experiment in this impact was found to be less, however, than in the more severe 40 km/h impact.

A limited sensitivity study was conducted to analyze the response of the 2-, 5- and 7-segment models to variations in some of the model input parameters. Two different series of variations will be presented here.

The first series concerns a change on the stiffness of the bumpers by +25% and −25% respectively. Results of these calculations are summarized in Table 4. It follows that the 3 models predict an almost identical relative

Table 3. Head impact velocity and head impact point for three models, along with experimental results.

	Model			Experimental
	2 segment	5 segment	7 segment	test-range
v = 30 km/h				
resultant head-impact velocity (m/s)	9.1	12.3	12.0	6.7-9.2
distance head-impact point/hood-edge (m)	.91	.90	1.02	0.82-1.00
v = 40 km/h				
resultant head-impact velocity (m/s)	12.7	16.6	15.8	11.2-12.5
distance head-impact point/hood-edge (m)	.96	.95	1.08	1.00-1.07

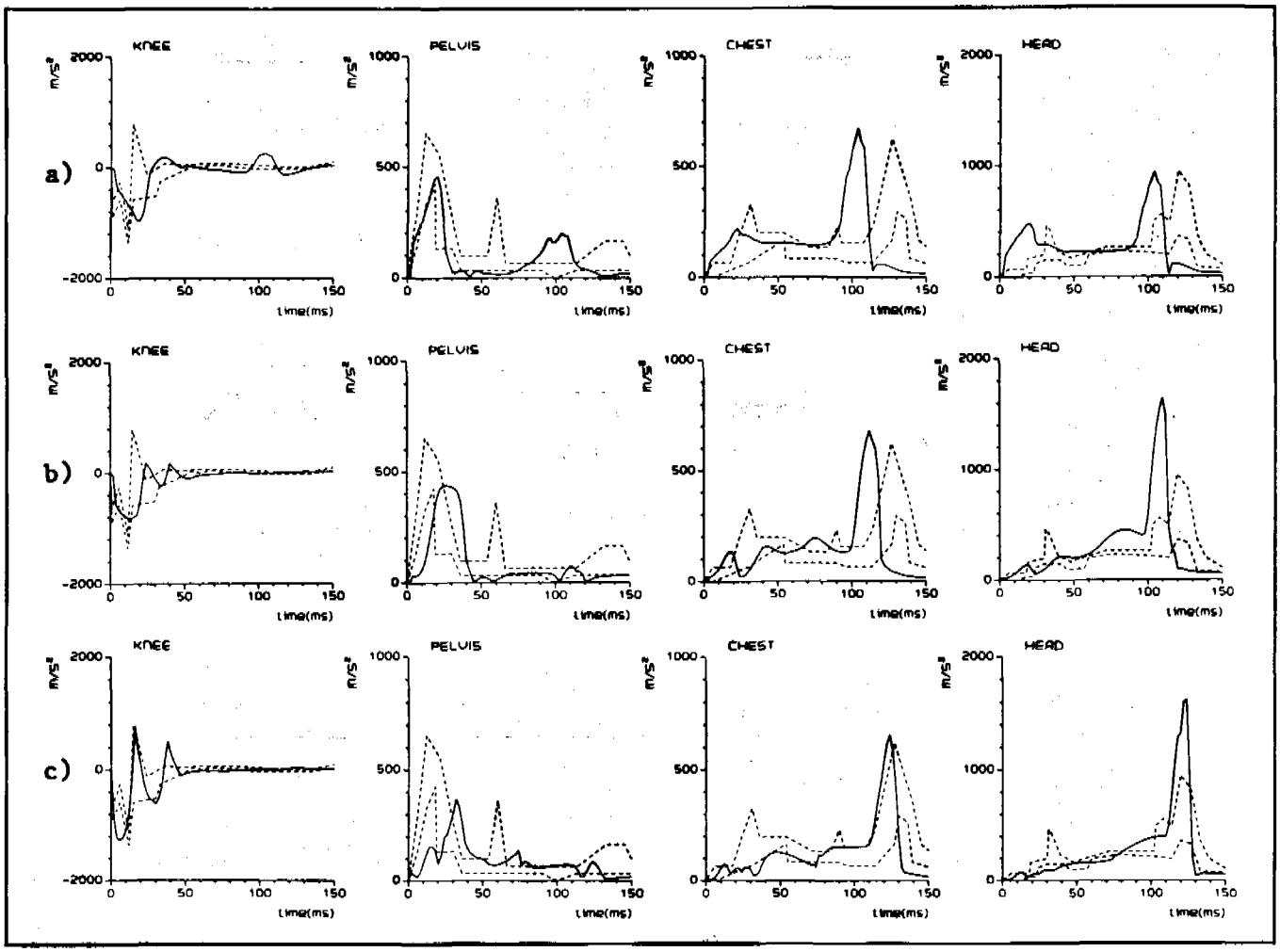

Figure 8. Accelerations of knee, pelvis, chest and head for a) 2-segment, b) 5-segment and c) 7-segment model (— = model, -- = experimental corridor) in a 40 km/h impact.

change in peak bumper loads. However, predictions for the relative change in accelerations of the impacted leg (i.e., foot and knee accelerations) are found to be strongly dependent on the number of elements in the model. In the models with a greater number of elements, the peak foot and knee accelerations are found to be much more sensitive to changes in the bumper stiffness.

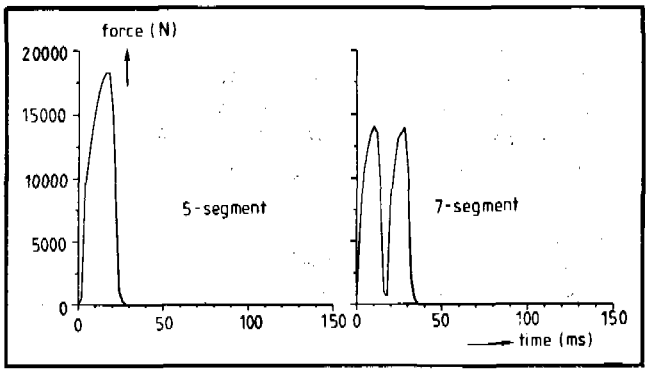

Figure 9. Bumper force for (a) 5-segment and (b) 7-segment model in a 40 km/h impact.

A second series of variations is concerned with the friction between foot and ground. In the reference simulation (Audi 100, 40 km/h impact), the friction coefficient was taken 0.7. Table 5 shows the results of a series of simulations in which the friction between ground and foot is omitted. Predictions of the three models for most of the output quantities are found to be close to each other. The influence of this variation in general is minor: bumper force and foot acceleration are somewhat lower and the knee acceleration becomes higher.

DISCUSSION AND CONCLUSIONS

Mathematical simulation of the highly complicated gross motion of the human body impacted by a vehicle has gained increasing importance in the past years. A brief literature review was given of various pedestrian models along with the associated validation studies. These models varied strongly in complexity: 2-dimensional models with the number of segments for the pedestrian varying between 1 and 11 as well as 3-

Table 4. Effect of bumper stiffness[1].

Bumper Stiffness Increased by 25%							
	Max. accelerations (Δ %)					Max. contact forces (Δ %)	
Model	foot	knee	pelvis	chest	head	bumper-(left) lower leg	hood edge-(left) upper leg
2 segment	3	2	−2	6	5	16	−30
5 segment	8	16	−10	−4	1	14	−2
7 segment	12	24	−1	−5	−3	17	−1
Bumper Stiffness Decreased by 25%							
	Max. accelerations (Δ %)					Max. contact forces (Δ %)	
Model	foot	knee	pelvis	chest	head	bumper (left) lower leg	hood edge-(left) upper leg
2 segment	−3	0	3	−2	−3	−17	40
5 segment	−5	1	13	−3	−4	−15	7
7 segment	−14	−26	−5	1	3	−15	0

[1] Changes with respect to reference simulation: a 40 km/h Audi 100 impact.

Table 5. Effect of ground friction[1].

	Max. accelerations (Δ %)					Max. contact forces (Δ %)	
Model	foot	knee	pelvis	chest	head	bumper-(left) lower leg	hood edge-(left) upper leg
2 segment	−13	2	−1	0	−1	−2	−1
5 segment	−5	4	−1	−5	−2	−1	1
7 segment	−6	2	0	−3	0	−1	0

[1] Changes with respect to reference simulation: a 40 km/h Audi 100 impact.

dimensional models having up to 15 segments were reported. In addition, methods for representation of the interaction between pedestrian and vehicle were found to vary considerably in these models. This literature study did not show a clear relationship between the complexity of the models and their reliability. One of the aims of our study therefore, was to get first a better insight into this problem.

A series of three 2-dimensional pedestrian models with 2-, 5- and 7-segments, respectively, was formulated using the general CVS program package MADYMO. The literature review showed that adequate description of the contact between pedestrian and vehicle is of crucial importance for a successful simulation. Particularly the pedestrian interactions with sharp vehicle edges (like the bumper and the hood) appeared to cause sometimes problems in the existing contact models. Therefore, within our project a more advanced contact model was developed in which the vehicle is represented by a number of hyperellipses as illustrated in Figure 3. This new contact model in MADYMO was found to perform very well for this type of applications. Extension of this contact model for incorporation in the 3-dimensional version of MADYMO is planned for the near future.

The three proposed pedestrian models were used to simulate a Part 572 dummy impacted at two different impact velocities (30 km/h and 40 km/h) by an Audi 100 vehicle. All three models were found to predict the head impact point location on the hood within or close to the experimental range of results. Predictions for the head impact velocity just before impact with the hood were too high (± 35%) in the 5 as well as the 7-segment model. Knee, pelvis, chest and head accelerations predicted by the various models were found in or close to the experimental corridor (Fig. 8). The observed differences between models and experiments may be due to the following reasons:

—The dummy in the experiments was slightly rotated before impact, causing the dummy to rotate around its vertical axis during the impact. In addition, the arms were found to interact with the hood. The effect of these aspects will be analyzed in future with a 3-dimensional pedestrian model.

—High speed films were used to determine the head impact velocity before impact with the hood. Due to 3-dimensional head motions and absence of adequate calibration procedures, this measurement might be rather inaccurate.

—Dynamic force-deflection characteristics were determined for the bumper, hood and hood edge. However, due to possible differences in impact velocities, shape of contact bodies, and location of the impact, the force-deflection characteristics in the actual dummy-vehicle impact may vary. Development of a contact model that accounts for geometric and velocity effects could considerably contribute to the improvement of the model's reliability. The sensitivity of the model to changes in the bumper stiffness (see Table 4) indicates the importance of an adequate description of the pedestrian-vehicle contact.

The influence of the complexity of the model (i.e., the number of model segments) can be summarized as follows: The reliability of the model if used for a lateral impact seems to be slightly improved if a greater number of segments is used to represent the pedestrian. The most significant changes are absence of an initial peak in head (and chest) accelerations if the number of segments increases from 2 to 5 and more realistic lower leg accelerations (and probably also bumper loads) if the number of segments is increased to 7.

In the next phase of this project, mathematical simulations for different car types are planned. In addition to adult dummy tests, also child dummy and cadaver experiments will be simulated. Further, it will be analyzed to what extent more complex models like a 15-segment 3D model can contribute to the reliability of the simulations. If the mathematical models then show reliable results for such different conditions, successful model application for the evaluation and improvement of pedestrian protection provided by different car contours might be expected.

REFERENCES

1. Transportation Research Department: "Research in Impact Protection for Pedestrians and Cyclists". Final NHTSA Contract Report, Cornell Aeronautical Laboratory, Buffalo, 1971.
2. Glöckner, H.: "Beitrag zur Simulation des Zusammenstosses Fahrzeug-Fussgänger". Automobil-Industrie, pp. 71–76, 1973.
3. Kramer, M.: "Ein einfaches Modell zur Simulation der Fahrzeug-Fussgänger Unfall". Automobiltechnische Zeitschrift 76, 3, 1974.
4. Mac Laughlin, T. F., Daniel, S.: "A Parametric Study of Pedestrian Injury". Proceedings of the 3rd International Congress on Automotive Safety, San Francisco, 1974.
5. Young, R. D., Lammert, W. F., Rose, H. E.: "Vehicle Exteriors and Pedestrian Injury Prevention, Vol. V, A 3-D Mathematical Simulation of a Crash Victim". Final NHTSA Contract Report, Texas Transportation Institute, Texas, 1975.
6. a. Twigg, D. W.: "PROMETHEUS 2—A User Oriented Program for Human Crash Dynamics". Final NHTSA Contract Report, Boeing Computer Services, Seattle, 1977.
   b. Twigg, D. W., Tocher, J. L.: "Pedestrian Model Parametric Studies, Vol. II". Final NHTSA Contract Report, Boeing Computer Services, Seattle, 1977.
7. Fowler, J. E., Axford, R. K., Batterfield, K. R.: "Computer Simulation of the Simulation of the Pedestrian—Development of the Contact Model". Proceedings of the 6th International Conference on Experimental Safety Vehicles, Washington, 1976.
8. Padgaonkar, A. J., Krieger, K. W., King, A. I.: "A Three-Dimensional Mathematical Simulation of Pedestrian-Vehicle Impact with Experimental Verification". Journal of Biomechanical Engineering, May 1977, pp. 116–123.
9. Lestrelin, D., Brun-Cassan, F., Fayon, A., Tarriere, C., Castan, F.: "PRAKIMOD: Mathematical Simulation of Accident Victims. Validation and Application to Car Pedestrian Collisions". Proceedings of the 8th International Conference on Experimental Safety Vehicles, Wolfsburg, 1980.
10. Cotte, J. P., Laurent, M.: "Improvement of a Mathematical Model to Study Pedestrian Safety". Proceedings of the 5th IRCOBI Conference on the Biomechanics of Impacts, Birmingham, 1980.
11. Wismans, J., Maltha, J., Wijk, J. J. van, Janssen, E. G.: MADYMO—A Crash Victim Simulation Computer Program for Biomechanical Research and Optimization of Designs for Impact Injury Prevention". AGARD Conference Proceedings, Cologne, 1982.
12. Ashton, S. J., Mackay, G. M.: "Car Design for Pedestrian Injury Minimisation". Accident Research Unit, University of Birmingham. Proceedings of the 7th International Conference on Experimental Safety Vehicles, Paris, 1979.
13. Mackay, G. M., Fonseka, C. P. de: "Some Aspects of Traffic Injury in Urban Road Accidents". Proceedings of the 11th Stapp Car Crash Conference, Los Angeles, 1967.
14. Wijk, J. J. van, Wismans, J., Maltha, J.: "MADYMO Pedestrian Simulations". To be presented at the SAE 1983 Winter Congress.

ACKNOWLEDGEMENTS

The authors wholeheartedly thank the BASt for conducting the experiments and Mr. L. Wittebrood for his efforts in running the MADYMO package.

Practical Vehicle Design for Pedestrian Protection

J. E. FOWLER and J. HARRIS
Austin Rover Group Ltd, BL Cars PLC, Cowley, Oxford
Transport and Road Research Laboratory, Crowthorne

3671

ABSTRACT

The objective of the study described in the paper is to determine the extent to which pedestrian protection can be provided by practical car design measures. The project examines the effects of vehicle impacts upon the six-year-old child and 50th percentile male adult.

Evaluation of vehicle designs primarily involves the use of the Calspan CVS computer program for pedestrian impact simulation. Computer models of dummies have been developed with the simulation method being validated against practical testing. Modifications have been carried out on the OGLE adult dummy to improve the performance of the leg in lateral impacts. Adduction of the hip joint has been increased and the knees have been given lateral compliance together with suitable torque characteristics. The results from tests and simulation show good correlation and give confidence in the modelling technique.

The influence of various front-end changes have been studied with computer simulation using a simplified vehicle representation.

INTRODUCTION

Pedestrians form a significant proportion of road accident casualties and therefore warrant an investigation to establish if vehicle design measures can mitigate injuries and reduce the costs incurred by society.

This paper describes the first stages of a 2½ year collaborative project between the UK Government and BL Cars PLC that studies simulated pedestrian impacts up to a speed of 40 km/h. Such an investigation should give car designers a better understanding of the interaction between changes in car design and the resulting change in severity of an impact with a pedestrian.

The project is based on computer simulation of pedestrian impact and examines the influence of car shape and structural stiffness on the kinematics, impact forces and accelerations imparted to adult and child pedestrian models. It is confined to the most important and predictable injury-producing phase of the pedestrian collision, namely, the impact between the pedestrian and the vehicle (1).

A computer simulation modelling technique was chosen since it facilitates the study of many different shapes and stiffnesses and gives complete repeatability, thereby enabling the effect of changes to a single component to be clearly resolved.

COMPUTER SIMULATION MODEL

For many years BL Cars have been using computer simulation techniques to study and optimise vehicle performance in terms of occupant and pedestrian protection (2), (3), (4). During this time, the Calspan Corporation's 3D Crash Victim Simulation Program has been a major tool (5), (6), (Figure 1). For the work reported here BL have made changes to the current version of the program (CVS III Version 20) to:

- improve the vehicle to victim contact model (7)
- output additional joint force data
- retain kinematic dummy plotting facility from version 15

The program has been extensively validated and an example of this is given in Section 6.

Dummy Models

The simulation models of the OGLE adult and child dummies have been developed from data derived from a comprehensive study of the two dummies. This included the establishment of:

- the location, axis of rotation and ranges of motion of each joint;
- the joint's stiffness and viscous properties, including the nature of the joint stops;
- the inertial characteristics of each body segment;
- the contact stiffness and energy recovery properties of each body segment;
- the external profile of each body segment.

For the project, the simulation of the adult dummy was modified to give increased limits of adduction at the hip and also lateral compliance of the knees (described in Section 3). The latter entailed the addition of an extra segment in each leg at the knee to enable the inclusion of a joint to provide the extra direction of knee movement.

The victim contact surface model is defined by ellip-

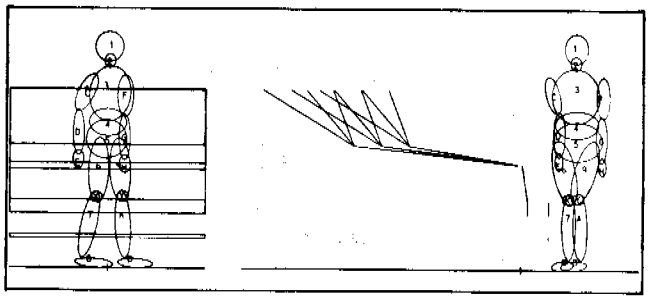

Figure 1. Computer simulation model.

soidal contact surfaces corresponding to each body segment and these were determined from the data. The stiffness characteristic of each segment was obtained by compressive tests between flat and curved rigid surfaces.

In the simulation program, contact forces can be generated between ellipsoids and vehicle panels, and are calculated as a function of penetration of the surfaces, with sliding friction forces generated to oppose any relative motion. Any such contact must therefore be defined in terms of the combined characteristics of the two surfaces involved as a tabular or analytical function (7).

Vehicle Model

The vehicle contact surface model consists of up to 30 rectangular plane panels. For a particular vehicle model, panels are chosen to represent the surfaces as required. The stiffness data are determined from component impact tests. Each significant area is impacted normal to its surface using an appropriate rigid form weighted according to the part of the body it represents, for example, the bumper would be impacted with a leg form and the windscreen by a head form.

Several impact speeds are used up to and including the speed to be used in the simulation. From these results each force versus deflection characteristic and the nature of the energy recovery and permanent distortion can be determined.

Program Operation

When setting up a full impact simulation model the contacts between each vehicle panel and the appropriate body segment ellipsoids are specified, and, using the available stiffness data, the mutual force deflection characteristics are derived. The output from the program is both by printout of simulation parameters and by post processor plotting of the dummy kinematics at selected time frames. In addition, it is possible to plot variables in a graphical format either against each other or against time, and to calculate relevant injury criteria. A BL modification makes it possible to printout the forces and torques at any joint in the geometric reference system of a segment as seen at any point within that segment. Additionally, the data are output in the same reference system as the vehicle. From these data and a knowledge of contacts with vehicle panels, it is possible to investigate segment bending moments. This is particularly useful when considering the lower limbs of an impacted pedestrian.

PEDESTRIAN DUMMIES

Although the project is based on computer simulation, it was necessary to conduct some experimental tests with dummies. Firstly, to validate the program and its input data, and secondly to provide occasional experimental 'reference points' to check for drift in the computer prediction that might occur after a wide range of parameter changes.

The dummies used as the standard for the pedestrian models were of OGLE design and manufacture, and represented a 50th percentile male adult, 1.76 m tall weighing 75 kg and a six-year-old child, 1.19 m tall weighing 21.5 kg. They were basically conventional vehicle occupant test devices, strengthened where appropriate and modified to allow the dummy to stand upright. All joints were torque loaded at 1 g.

The adult dummy also had additional modifications to the hip and knee joints as described below.

Hip Joint

In the human body, values of hip joint adduction of up to 40° have been reported (8). With the dummy in the required stance, the hip joint of the impacted leg was found to have no residual adduction. To represent the human characteristic more realistically, the hip joint of the impacted leg was modified to the maximum practical extent so that adduction was increased to 28° but at the expense of some abduction.

The leg on the non-impacted side was not modified; so both legs were able to swing relative to the torso for at least 25° in the direction of impact.

Both hip joints were fitted with compressible washers to reduce the severity of the shock loads when the joints reached the limits of their travel.

Knee Joint

Impact tests on cadavers (9), (10) have shown that the human knee will bend to a limited extent in the lateral direction. To reproduce this effect both knee joints were modified to permit rotation in both lateral directions, with friction plates added to give an adjustable but constant level of friction torque (Figure 2).

INJURY TOLERANCE LEVELS

Tolerance levels for the different body regions have been selected so that an assessment can be made of the relative safety potential of the car configurations studied.

They are based on quantities that can be measured from practical tests as well as computer simulation, and are acceleration of the head, thorax and pelvis, and bending moments in the leg.

Head, Thorax and Pelvis

The acceleration levels chosen, are at the lower end of the range known to be in common use, and are shown in Table 1.

However, to enable several vehicle profiles to be assessed simultaneously during the first stages of this study, a head impact velocity criterion was preferred to accel-

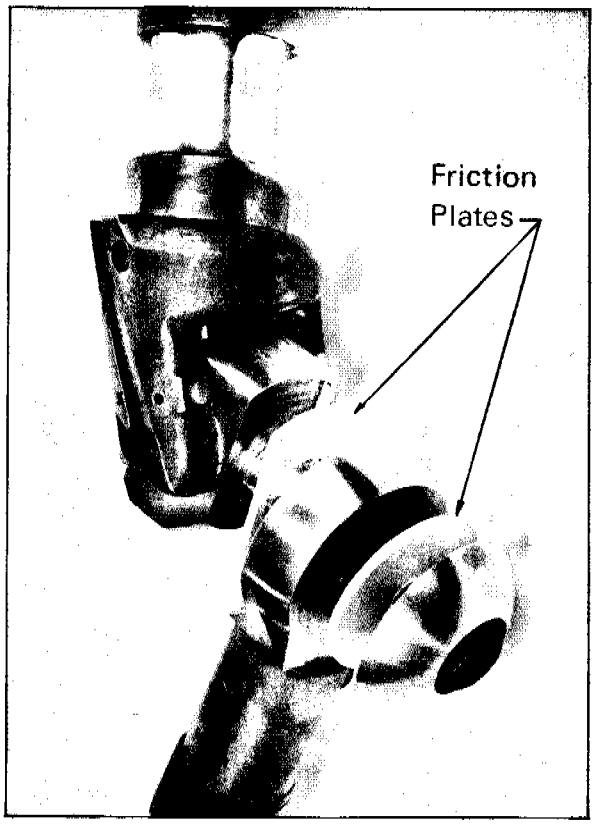

Figure 2. Modified adult knee.

eration. This was set at the maximum vehicle impact velocity of 11 m/s and represented the level of kinetic energy which might realistically be absorbed whilst maintaining an acceptable acceleration condition.

This relationship between energy absorption and maximum acceleration does not apply to the stiffest parts of the vehicle structure and so the head impact location was also considered in conjunction with its velocity.

The Leg

The aim of the research concerning the legs is primarily to save the knee from serious injury, and secondly, to reduce the risk of long bone fracture.

For the lower limbs it has been assumed that long bone fracture or knee injury results from either horizontal shear, crush or bending loads. The torsional failure mode has not been considered. However, it was found in early tests that to obtain an acceptable level of bending moment in the leg, the necessary low stiffness of the contacting car structure would reduce the risk of crush or shear failure. So, to simplify the assessment of injury, only bending moments are considered. Values of bending strength for the knee and long bones were not available and estimates have therefore been developed from existing data.

Table 1. Tolerance levels based on acceleration.

	Acceleration g for 3ms	HIC	SI
Head	80	1000	—
Thorax	60	—	1000
Pelvis	60	—	1000

The Long Bones

Estimates of long bone tolerance values have been obtained from published data on static bending tests in the anteposterior direction (11). There was claimed to be no significant difference in the ultimate strength of the bending breaking load in the lateral and the anteposterior direction. Consequently, the derived values have been used as a first estimate for bending in any direction.

Quoted values of ultimate deflection, ultimate specific deflection and bending breaking load have been used to calculate the following bending moments at fracture:

Femur		212Nm
Tibia	186Nm	214Nm
Fibula	28Nm	

A value of 200Nm has therefore been adopted for both the upper and lower leg. 200Nm has also been used for the child because no data were available.

Knee—Adult

To establish the tolerance limit of lateral compliance for the adult knee there were two parameters to be determined. The first was joint stiffness (represented by friction torque in the model) and the second, the magnitude of lateral rotation representing the tolerance limit.

For the lateral stiffness, comparative tests on cadavers and adult dummies (9) claimed that representative deformations of the dummy lower leg were seen when a short length of 12.5-mm-diameter threaded rod was inserted axially into the leg directly below the knee joint. In the model, a lateral friction torque of 200Nm at the knee joint would provide a similar resistance to that of the threaded rod.

Consequently, a lateral friction torque of 200Nm was adopted.

Because the friction torque setting in the knee joint was the same value as the bending moment tolerances adopted for the long bones, the leg model had a constant tolerance to applied bending moment over its entire length. The effect of this was that the leg tolerance level was most frequently exceeded at the point of impact. This is in agreement with accident studies (15) which found that leg injury most frequently occurred adjacent to the point of major impact.

For lateral rotation an angle of 6° was chosen to represent collateral ligament failure. This value was determined by utilising the work by Aldman et al. (14). By

taking the maximum reported elongation for the medical collateral ligament (7.2 mm) and the active distance of the ligament from the condyle (70 mm), an angle of 6° was produced.

Knee—Child

No attempt was made to determine a tolerance value for the child knee because of the infrequency of serious injury to the knees of children as noted in an appraisal of accidents investigated by Dr. S. J. Ashton (Birmingham University, Accident Research Unit). In this investigation, from a total of 83 accident cases of children ten years of age or younger, there were 24 cases of fractured long bone, 15 cases of minor surface injury at the knee and only 1 case of non-minor injury—a fracture of the tibial plateau rated at AIS 2. It was therefore assumed for this study that for the range of shapes and stiffnesses to be investigated, bending moment at the knee would be unlikely to cause serious injury.

IMPACT CONDITIONS

The following conditions applied throughout the project.

Dummy

The dummy was struck on the right hand side, with the right leg backward and the left leg forward to represent a walking stance. Both legs were straight and the full weight of the dummy was judged to be evenly distributed between the two legs at the moment of impact. The dummy was rotated 60° from a position directly facing the vehicle, as shown in Figure 3.

The left arm of the dummy was allowed to hang vertically down whereas the upper segment of the right arm was inclined rearwards at 30° to the vertical plane and the lower segment allowed to hang vertically down.

The torque settings for the joints were 1 g.

This stance was chosen for several important reasons:

- to avoid knee to knee impact
- to give a lateral impact to the lower limbs that is representative of typical accident conditions
- to improve the probability of head to vehicle contact without the shoulder striking in such a manner that it gives unrealistically high protection to the head
- to give a predictable trajectory, the dummy being inclined to rotate face down onto the vehicle.

Vehicle

The dummy was impacted on the centre line of the car at 40 km/h. This speed was considered to be the maximum at which pedestrian protection could be practicable.

The vehicle was braked at the instant of dummy contact with a nominal deceleration of 0,7g. The vehicle suspension was locked at normal running height to give repeatable impact conditions.

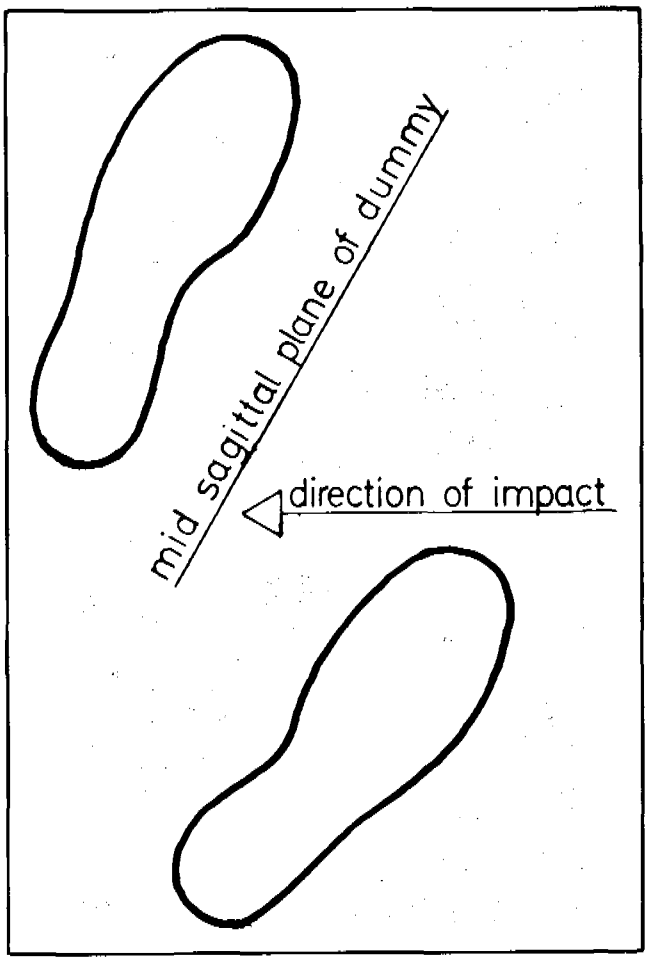

Figure 3. Pedestrian standing position.

COMPARISON BETWEEN EXPERIMENTAL TEST AND COMPUTER SIMULATION

Prior to the start of this project, it was essential to establish that computer simulation could accurately reproduce the results from practical tests. The simulation method was validated by comparing the results from high speed cine records of dummy impacts with post processor plots from the mathematical model. From these, one such adult comparison is presented to demonstrate the accuracy of the computer simulation, using the dummy and impact conditions described in Section 5. The results from the simulation and practical test are compared with respect to the kinematics (Figure 4), and head impact location and velocity (Table 2 and Figure 5).

Detailed analysis of the head plus a visual trajectory comparison of all the body segments was considered to

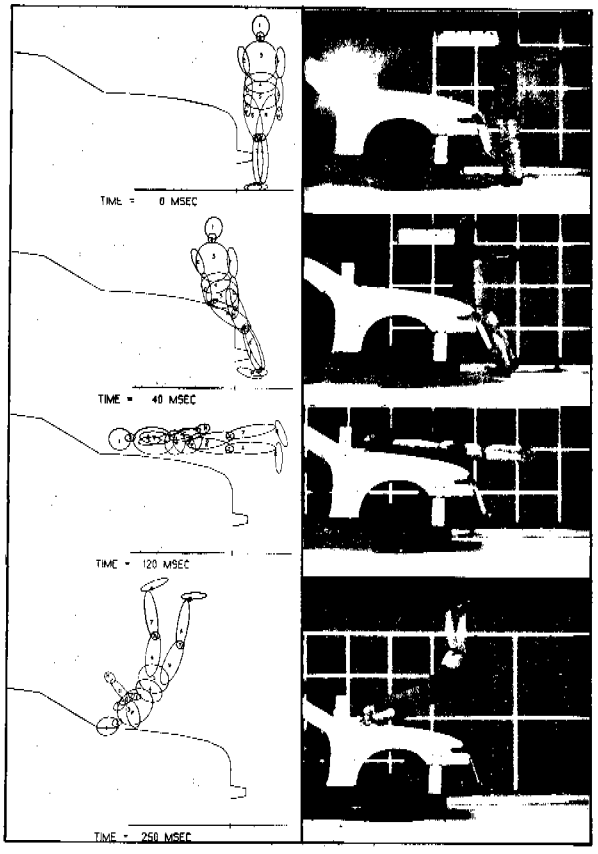

Figure 4. Kinematic validation.

be sufficient for final confirmation of the performance of the model. From these results, it was concluded that, in general, the correlation was good, especially during the critical periods of impact, e.g., head contact. It was considered sufficient for the computer predictions to be within the order of variation normally associated with nominally identical dummy tests (12). Consequently, the overall agreement in results, including those from numerous other validations, was such as to allow the project to proceed with confidence.

PARAMETRIC STUDY BY COMPUTER SIMULATION

This section describes the use of the computer program to evaluate the effect of various vehicle front-end profiles on impacted pedestrians. Since the project is ongoing, only the initial findings are discussed.

Vehicle Representation

A typical vehicle front was modelled by using a minimum number of flat planes to represent a simplified shape which nonetheless contained the most important features for pedestrian impact. The planes themselves were given idealised stiffness functions based upon those for current production vehicles.

Table 2. Summary of validation results—head.

	Simulation	Practical Test
Contact Time to Vehicle	122 ms	119 ms
Location Head to Vehicle		
—Horizontal	−1350 mm	−1425 mm
—Vertical	−560 mm	−585 mm
Resultant Head Impact Velocity	10,9 m/s	11,3 m/s
Head Impact Contact Angle (to horizontal)	72°	68°

Figure 6 shows the six panels or groups of panels used in the model. These represent the under-bumper region, bumper, grille, leading edge, bonnet and windscreen. To enable an extended amount of information to be gained from each run of the program, three bonnet lengths were modelled simultaneously, each having the same leading and trailing edge heights. Associated with each bonnet length was a group of three windscreens to which were given negligible stiffnesses. By this means the impact velocity of the head with each windscreen could be obtained. Where a radiused leading edge was investigated, a slightly

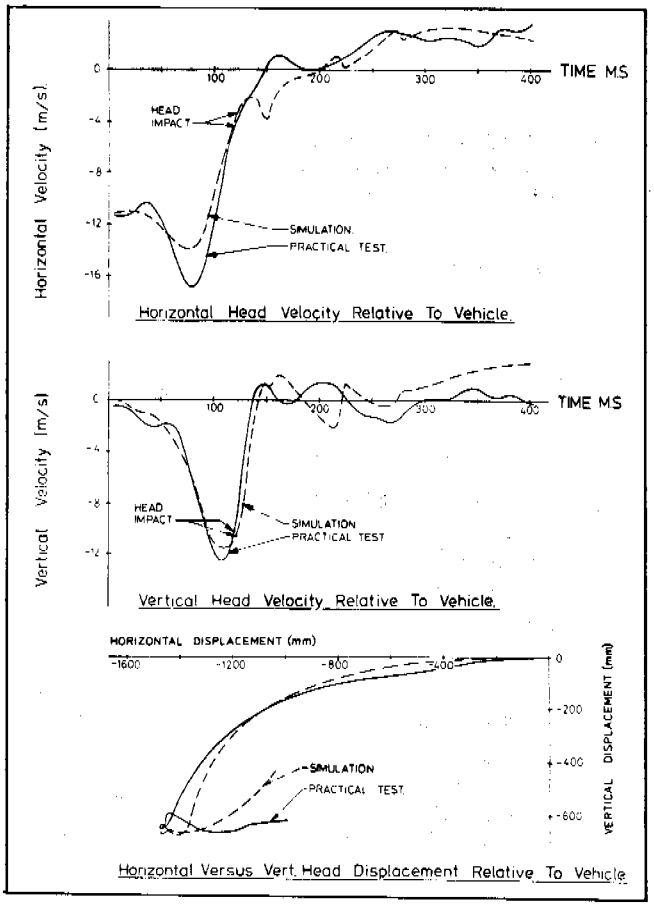

Figure 5. Head validation results.

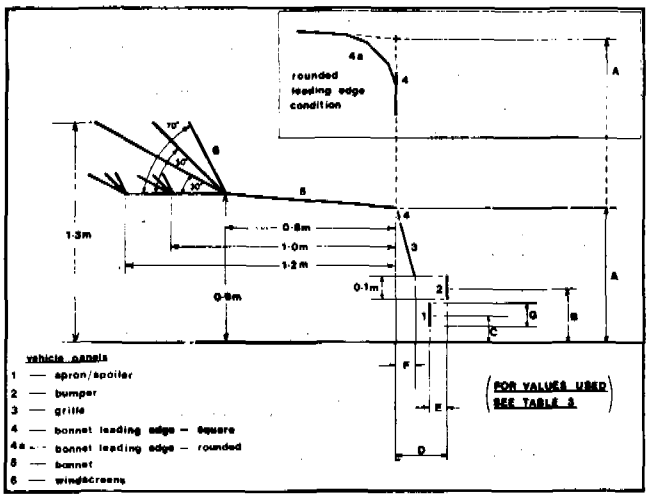

Figure 6. Vehicle simulation panels.

more complex model was used (Figure 6 inset). The three panels used to model the curvature operated in a dependent manner, the panel with the greatest contact with each segment being used at any one time.

Stiffness Characteristics

The idealised stiffness characteristics shown in Figure 7 describe forces normal to the vehicle panels. All reached a force plateau at which there was no limit on deflection (the stiffness of the understructure not being considered). By this means, necessary material crush depths could be assessed for each condition. Within the program, the stiffness for the interaction of each panel upon the relevant body segment was derived by combining their characteristics. For each combined stiffness, the permanent deflection and energy recovery were set to be constant proportions of the maximum values reached after impact.

Parametric Variables

Throughout the initial parametric study the bonnet trailing edge height and windscreens were maintained constant while the parameters under investigation were concentrated at the front face of the vehicle. Table 3 and Figure 6 summarise the type and extent of the variations. Since the total number of permutations for the parametric adjustments selected was extremely large, the choice of combinations had to be selectively based upon logical progression and a deepening understanding of the mechanics of the impacts. It became apparent that the three initial leading edge heights chosen displayed distinctive characteristics during pedestrian impact. Consequently, the approach adopted was to assess the effects of parametric change against each of these leading edge heights, using the primary run as the baseline. The comments in the following sections refer specifically to these simulations.

Adult Impact Response

To assist comparison of the different conditions, the period of impact has been divided into four phases as described in Figure 8. The length and timing of each phase varied depending upon the vehicle shape. Figure 9 summarises the results to date.

Low Leading Edge

Phase 1 tends to be at its longest with this profile because of the delay before leading edge contact. Consequently, a large proportion of the total energy imparted to the victim is transferred from the bumper. The knees undergo a high level of abduction and the lower legs are subjected to high bending moments with the localised impact close to the knee.

Phase 2 is short because the leading edge contact is only slight, its contribution being again close to the knee.

Phase 3 involves high rotational velocity with little thorax or arm contact with the bonnet. This trajectory is a consequence of the bumper and leading edge energies being centred on an area that is well below the overall centre of gravity of the victim.

Head contact (Phase 4) velocities are high due to the angular velocity of the whole body. All windscreens are contacted.

Medium Leading Edge

Phase 1 is shorter than for the low leading edge profile because of the earlier leading edge contact. The bumper therefore impacts less energy during this phase and while the bending moments in the lower legs are similar, knee abduction cannot reach as great an angle in the shorter time.

Phase 2 is initiated by the leading edge contacting the central region of the upper leg. The still considerable difference in speed between vehicle and victim means that the contact is severe and causes a high local bending

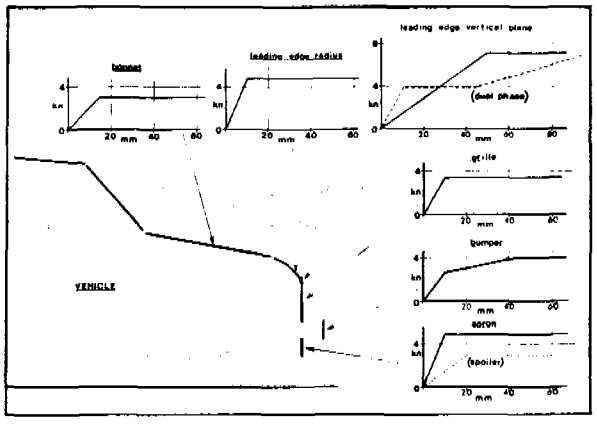

Figure 7. Simulation vehicle panel stiffness.

Table 3. Vehicle parametric variables.

RUN NUMBER		L1	L2	L3*	M1	M3*	M4	M5	M6	M7	M8	H1	H2	H3*	H4	H5	H6	H7
VEHICLE DIMENSIONS (mm) (SEE FIG. 6)	A	600	600	600	720	720	720	720	720	720	720	850	850	850	850	850	850	850
	B	450	350	450	450	450	450	450	450	350	450	450	350	450	450	450	450	350
	C	320	270	320	320	320	320	320	320	270	262	320	270	320	320	320	320	270
	D	150	150	150	150	150	250	350	150	150	150	150	150	150	250	350	150	150
	E	150	150	150	150	150	150	150	150	150	150	150	150	150	150	150	150	150
	F	0	0	0	0	0	100	200	0	0	0	0	0	0	100	200	0	0
	G	160	160	160	160	160	160	160	160	160	25	160	160	160	160	160	160	160
LEADING EDGE SHAPE (SEE FIG. 6)		⌐	⌐	⌐	⌐	⌐	⌐	⌐	⌐	⌐	⌐	⌐	⌐	⌐	⌐	⌐	⌐	⌐

(*) Dual Phase Leading Edge Stiffness – See Fig 7

moment. In addition, rapid angular motion of the upper leg puts the knee joint into severe abduction as the lower leg is being accelerated. This is in addition to that already imposed by the bumper during Phase 1. It is acknowledged that in a human victim, the knee injury would be greatly different if the upper leg was in fact broken.

Compared with the low leading edge, Phase 3 involves lower angular velocity of the torso because the leading edge is closer to the overall body centre of mass.

Head impact (Phase 4) velocities are close to the initial vehicle impact velocity but are less than those for the low leading edge case because of the reduced rotational velocity of the torso. Since the torso pivots about the leading edge, the impact sites are also less rearward.

High Leading Edge

Phase 1 is at its shortest for this configuration and there is only limited knee abduction before the leading edge contact, although the bending moments in the lower legs reach similar values to the other leading edge heights.

Phase 2 starts with the leading edge contacting the upper leg near to the hip at almost initial impact velocity (11 m/s). There is very little hip rotation because of the proximity of the impact and the force is transmitted almost directly into the pelvis; this also gives reduced upper leg bending moments. The consequence of this is that the hip joint is subjected to high forces and the pelvic region therefore sustains high accelerations. With a high bonnet there is a low rate of leg rotation about the leading edge, and therefore low inertial forces across the knee results in little abduction of this joint.

Phase 3 is controlled by the leading edge contact being close to the centre of body mass with the result that the rate of body rotation is low.

Phase 4 head impacts are well below the vehicle impact velocity as a consequence of the slow rotation rate. The contacts are only with the foremost group of windscreens.

Child Impact Response

The impact has again been divided into four phases as shown in Figure 10. Figure 11 summarises the child results to date.

Low Leading Edge

Phase 1 is again at its longest with this profile because of the delayed leading edge contact. As the bumper accelerates the upper leg, the inertia of the lower leg puts a bending moment across the knee. There is also a bending

moment at the site of impact due to the inertia of the whole leg.

Phase 2 is brief and involves a moderate contact with the leading edge.

Phase 3 involves the body flexing around the leading edge. The torso gains a high angular velocity constrained only by the stiffness of the hips. The impact velocity of the thorax with the bonnet is therefore high and results in a high chest deceleration.

Phase 4 continues from the previous phase with a head impact velocity just less than that of the vehicle.

Medium Leading Edge

Phase 1 is similar to that for the low leading edge but shortened by the earlier leading edge contact.

Phase 2 involves direct leading edge contact with the pelvis and this results in both high forces and accelerations.

Phase 3 is similar to that for the low leading edge except that it is the thorax and head which are rotating above the contact. The thorax contact velocity is low and both acceleration and rotation are small. The head rotation velocity is however affected by its inertia causing initial neck fluxion away from the vehicle only for the head to be rapidly accelerated forward when the neck recovers and the thorax decelerates.

Phase 4 therefore involves a head impact velocity which is only slightly below that of the vehicle.

High Leading Edge

Phase 1 is little affected by raising the leading edge although it is shortened slightly.

Phase 2 involves direct leading edge to thorax contact with resulting high chest accelerations.

Phase 3 is significantly different from those of previous profiles in that the torso does not rotate onto the bonnet, thus exacerbating the inertial effects upon the head and neck.

The head impact velocity (Phase 4) is low as most of the deceleration of the head is provided by the neck. For this reason, neck injury might well arise in real accidents of this type.

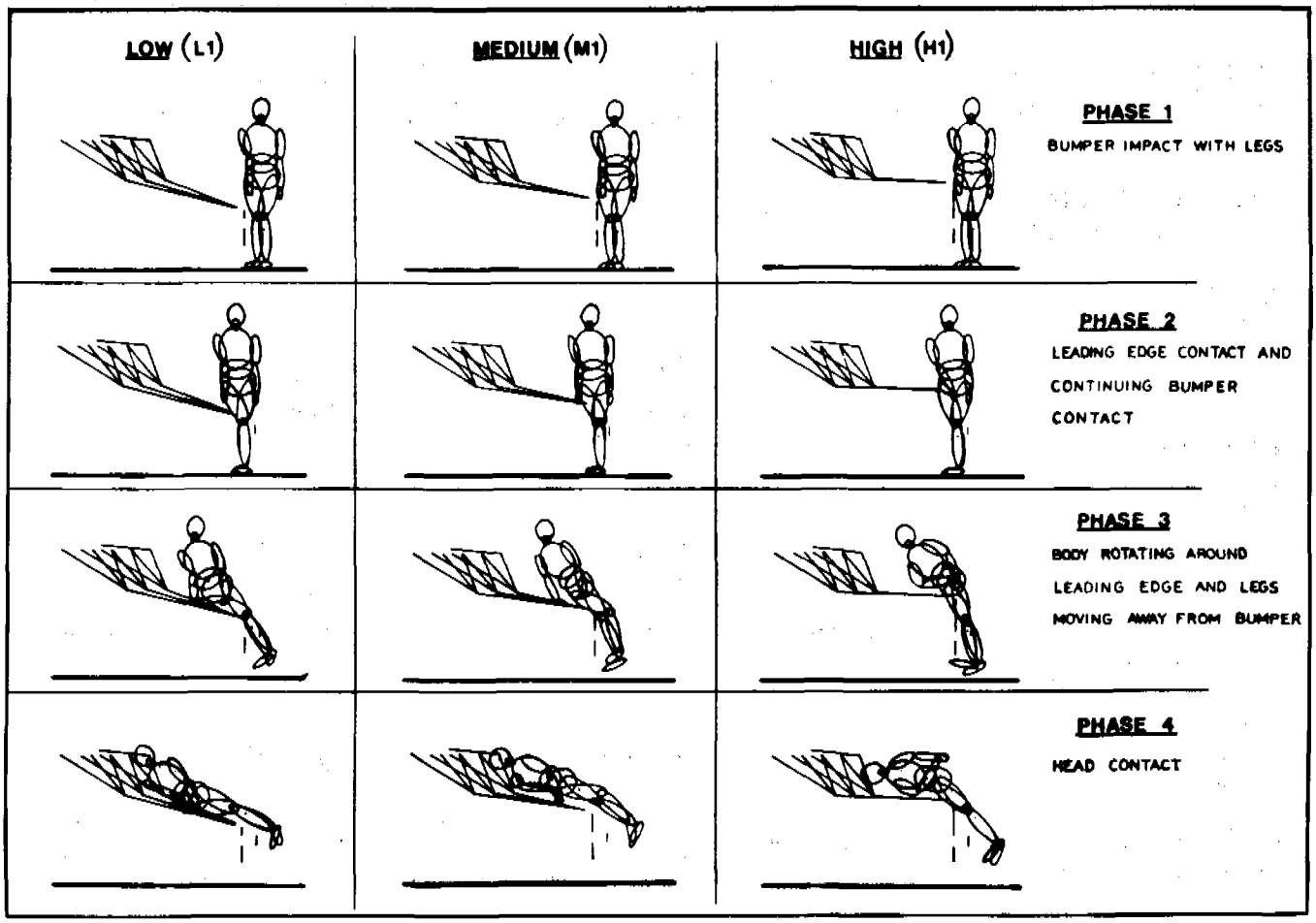

Figure 8. Adult impact phases for baseline profiles.

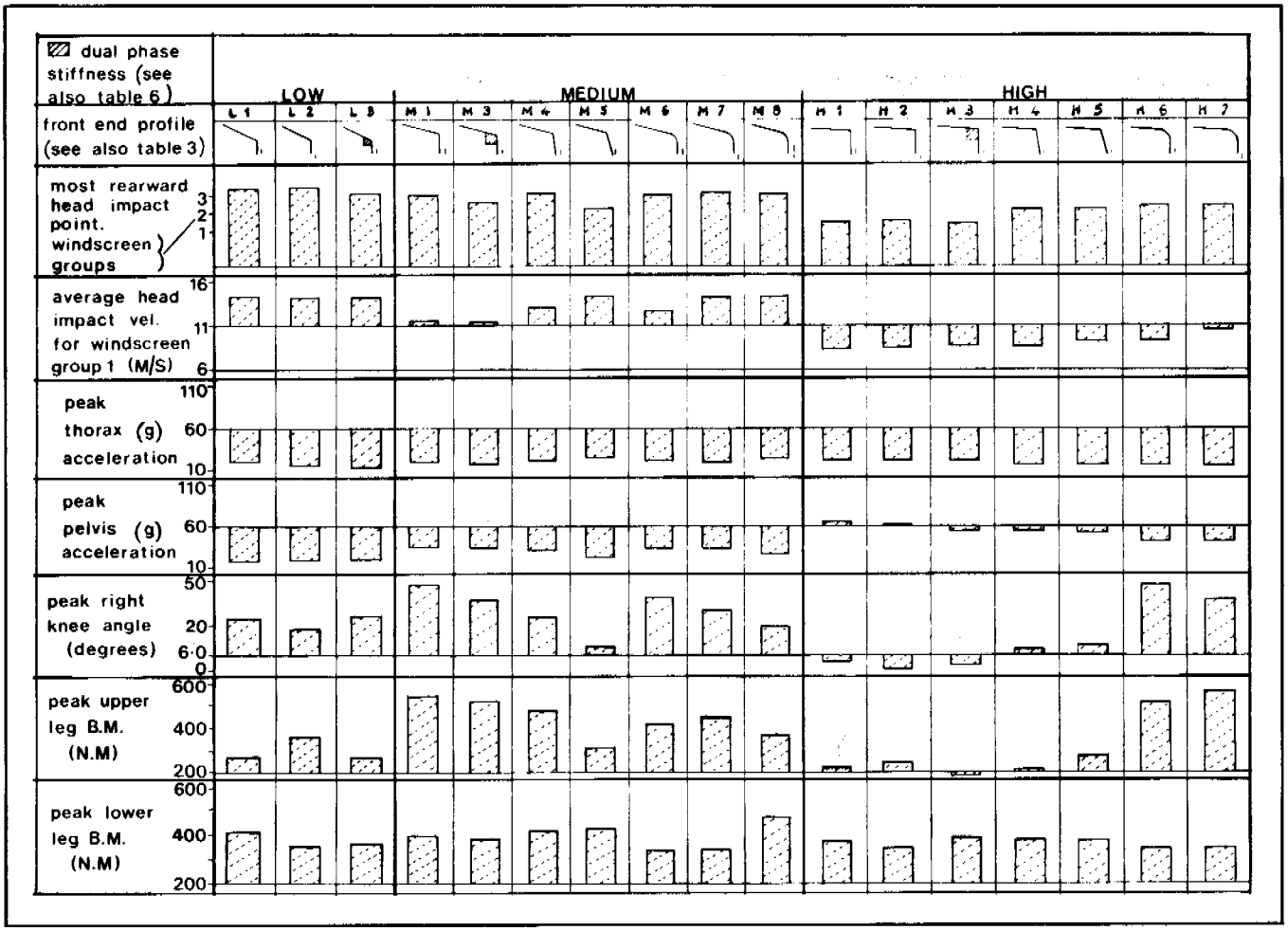

Figure 9. Parametric study results—adult. (Values related to applicable tolerance levels).

CONCLUSIONS

A mathematical model for the simulation of a pedestrian dummy has been described and its capability to effectively reproduce a car to dummy impact, demonstrated.

Tolerance levels for leg bending moments and lateral knee compliance have been determined and these have been used to assess the performance of various car shapes and stiffnesses, together with the generally accepted acceleration-based tolerance limits for head, thorax and pelvis.

A knee joint with limited lateral rotation, coupled with a constant frictional torque proved to be an effective method of representing the lateral flexibility of the knee.

The studies to date show the following general relationship between vehicle design and the resulting severity of impact to pedestrians at speeds of 40 km/h.

- A low leading edge profile has two major disadvantages. By concentrating most of its load input below the centre of gravity of the pedestrian high angular rotation is induced and this results in head impact velocities of greater magnitude than the initial vehicle impact speed. Secondly this concentration of load about the knee causes severe local injury.
- The medium leading edge profile has serious problems associated with adult leg and knee injuries and child pelvis acceleration. All the geometric changes to reduce these, increases the head impact velocities for the adult, but not for the child. Of the shapes considered, only the rounding of the leading edge reduced both upper and lower leg bending moments in the adult.
- A significant feature of the high leading edge is that both adult and child head impact velocities are consistently below vehicle impact speed. There are, however, problems associated with direct child thoracic and pelvis impact but these can be reduced by increasing the bumper lead.
- For the structural stiffnesses and leading edge heights

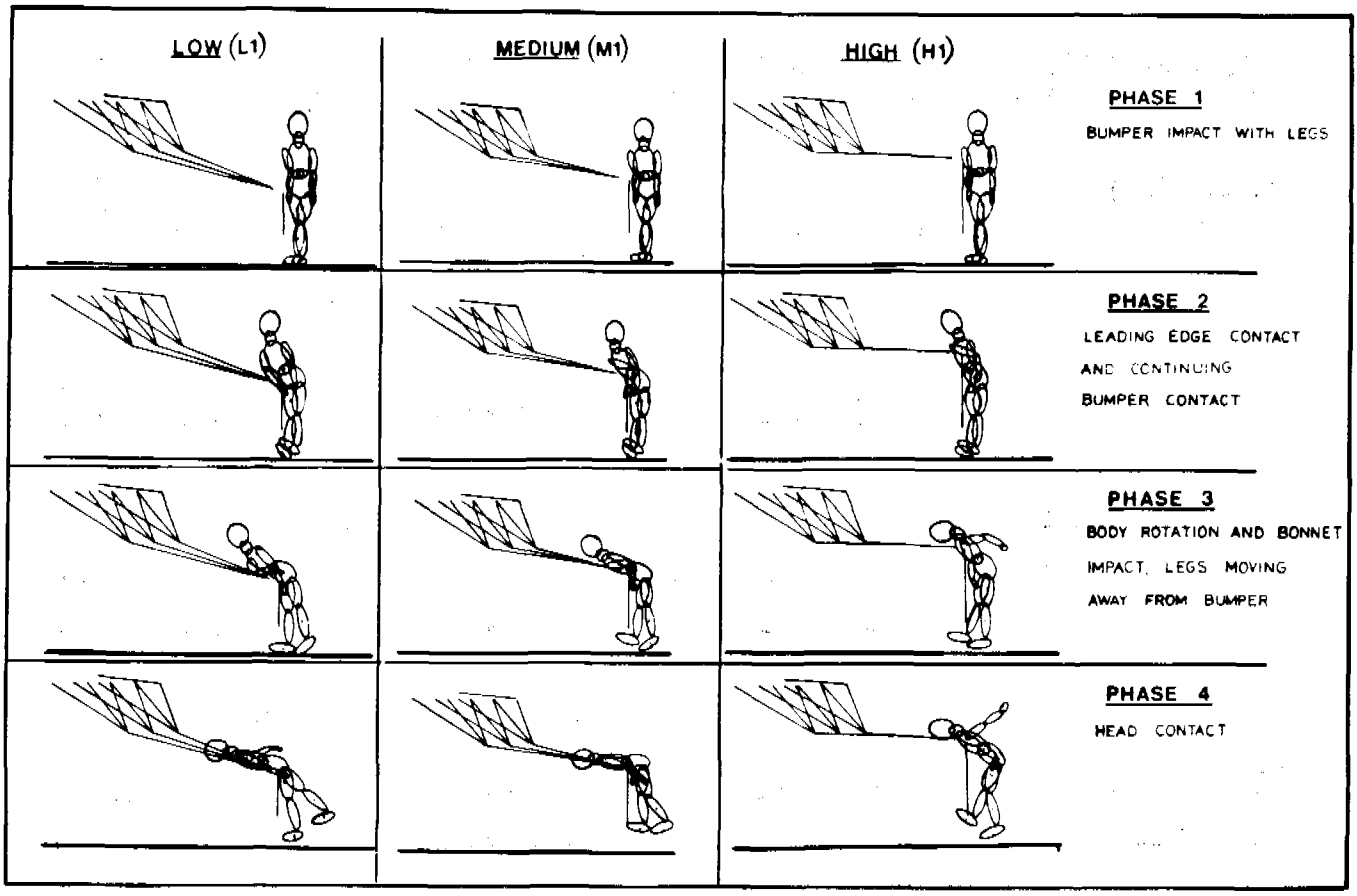

Figure 10. Child impact phases for baseline profiles.

studied, the resulting adult thoracic accelerations were always low and the pelvic accelerations only exceeded 60g for 3 milliseconds on two occasions.

The results to date suggest that further reductions in the severity of impact can probably be achieved with the medium to high leading edges. More detailed stiffness and geometric investigations will be conducted to study this possibility.

ACKNOWLEDGEMENTS

The authors would like to express their thanks to those who have contributed towards this project. Thanks are especially due to Mr. N. D. Grew, Mr. G. O. Davies and Mr. D. R. Gebbels of Austin Rover Group Limited.

REFERENCES

1. S. J. Ashton, G. M. MacKay, "Car Design for Pedestrian Injury Minimisation". Proc 7th Int Tech Conference on Experimental Safety Vehicles.
2. J. E. Fowler, K. F. Newman, "The use of Computer Simulation for the Design of Safer Vehicles". Proc I Mech E Conference—Progress Towards Safer Passenger Cars in the UK—1980.
3. W. E. Emmerson, J. E. Fowler, "Simulation of Frontal Vehicle Impacts". Proc I Mech E Conference—Vehicle Safety Legislation—Its Engineering and Social Implications—1973.
4. W. E. Emmerson, J. E. Fowler, "The Application of Computer Simulation in Vehicle Safety". Proc 5th Int Tech Conference on Experimental Safety Vehicles.
5. J. A. Bartz, "A Three-Dimensional Computer Simulation of a Motor Vehicle Crash Victim". Phase I—Development of the Computer Program, Cornell Aeronautical Laboratory 1971.
6. J. A. Bartz, F. E. Butler, "A Three-Dimensional Computer Simulation of a Motor Vehicle Crash Victim. Phase II— Validation Study of the Model, Cornell Aeronautical Laboratory 1972.
7. J. E. Fowler, R. K. Axford, K. R. Butterfield, "Computer Simulation of the Pedestrian Impact—Development of the Contact Model", Proc 6th Int Tech Conference on Experimental Safety Vehicles—1976.
8. J. A. Searle, C. M. Haslegrave, "Improvements in the Design of Anthropometric/Anthropomorphic

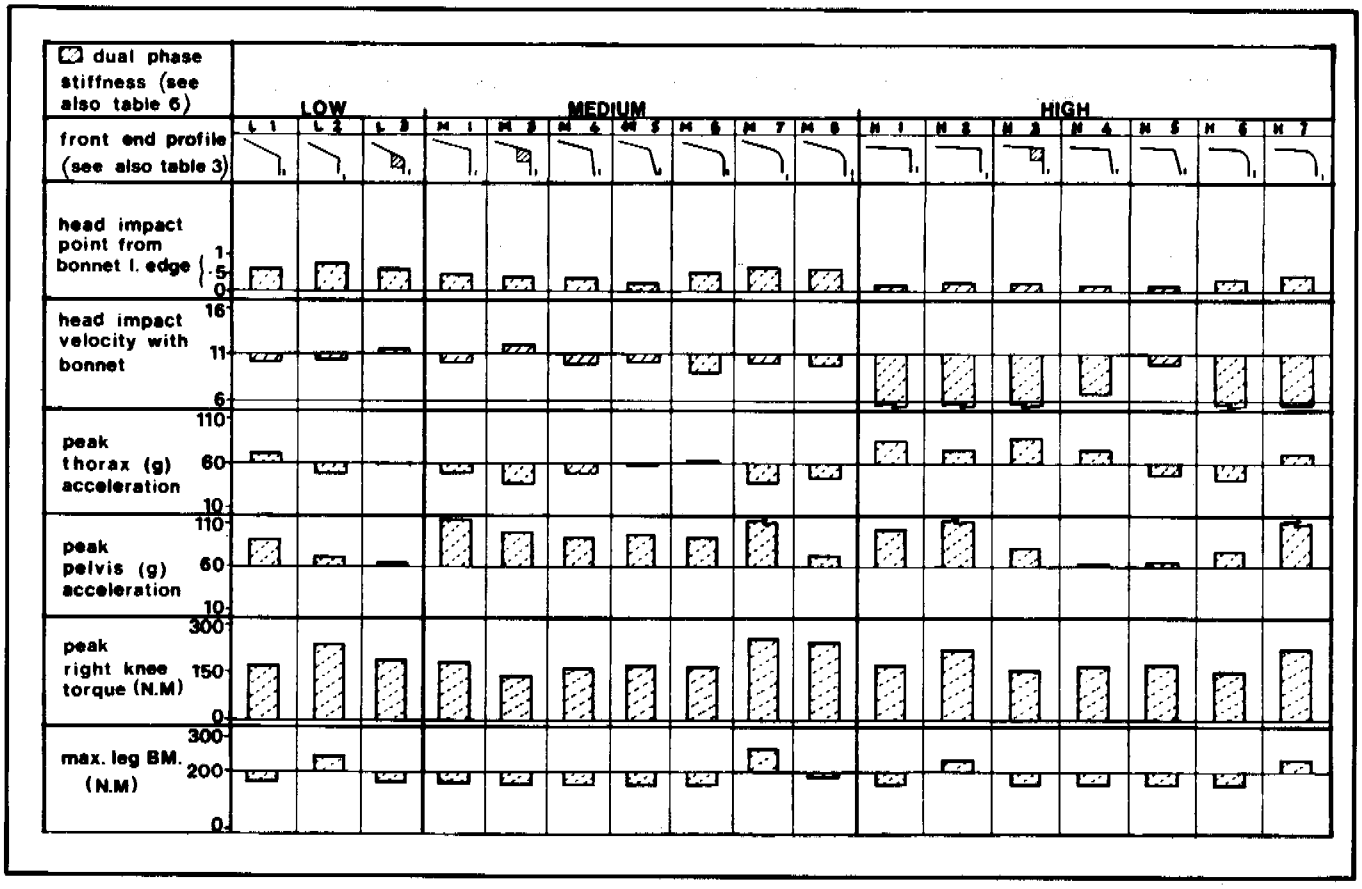

Figure 11. Parametric study results—child. (Values related to applicable tolerance levels).

Dummies", MIRA BULLETIN No. 5 1970 Sept/ Oct 10–2.

9. H. B. Pritz, "Comparison of the Dynamic Response of Anthropomorphic Test Devices and Human Anatomic Specimens in Experimental Pedestrian Impacts. Proc 22nd STAPP Car Crash Conference Ann Arbor USA October 1978.
10. B. Aldman, et al., "An Experimental model for the Study of Lower Leg and Knee Injuries in Car-Pedestrian Impacts", Proc 5th Int Conference on the Biomechanics of Impact IRCOBI Birmingham England September 1980.
11. Hiroshe Yamada, "Strength of Biological Materials", Baltimore 1970—The Williams and Wilkins Co.
12. Joint Biomechanical Research Project KOB—1982.
13. R. H. Eppinger, H. B. Pritz, "Development of a Simplified Vehicle Performance Requirement for Pedestrian Injury Mitigation", Proc of 7th Int Tech Conference on Experimental Safety Vehicles, Paris, June 1979.
14. B. Aldman, L. Thorngern, O. Bunketorp, B. Romanus, "An Experimental Model System for the Study of Lower Leg and Knee Injuries in Car Pedestrian Accidents", Proc of 8th Int Tech Conference on Experimental Safety Vehicles, Wolfsburg, Germany, October 1980.
15. S. J. Ashton, J. B. Pedder, G. M. MacKay, "Pedestrian Leg Injuries, The Bumper and other front structures", Proc 3rd International Conference Biokinetics of Impact, International Research Committee on Biokinetics of Impact, Lyon 1977.

Application of the Fiat Methodology for Characterizing Vehicle Structural Responses in Frontal Impacts

L. M. "MORRIE" SHAW
Arndt & Associates

CARL RAGLAND
National Highway Traffic Safety Administration

ABSTRACT

Over the past several years, Dynamic Science, Inc., under funding from Fiat Auto S.p.A., developed a methodology for evaluating vehicle crash compatibility. The ultimate goal was to provide compatibility characterization technology in the frontal, side, and rear impact environments. The result of this research has been extremely encouraging, providing accurate analysis and predictive capabilities, as well as justification of the methodology approach.

Because of the increasing concern for vehicle crash compatibility, the U.S. National Highway Traffic Safety Administration (NHTSA) acquired the Fiat Methodology in 1980. The NHTSA then increased the funding of an on-going program to apply the Fiat Methodology to a side impact research program. Frontal and side structural characterizations were used in the side impact analysis.

This paper summarizes the results from the above NHTSA research program emphasizing the applicability of the Fiat Methodology to the characterization of vehicle structural responses in frontal impacts. Validation of the frontal structure characterization is discussed and presented along with comparisons between predictive analysis and crash test results.

INTRODUCTION

For more than a decade automotive safety researchers have recognized the significance of vehicle crash compatibility in evaluating vehicle crashworthiness within the overall accident environment. This problem has become particularly evident in the United States due to the increasing number of small vehicles. During that period, however, the traditional measure of crashworthiness and compliance in frontal impacts has been and remains based on the rigid barrier SAE J 850a test. Researchers have voiced concern with regard to the limitations and ability of this test procedure for representing real world accidents. Some of the rigid barrier test limitations include:

- Is unable to simulate the great majority of automobile encounters
- Produces vehicle crashworthiness results which can deviate significantly from the traffic mix environment
- Overestimates the survival performance of smaller vehicles
- Underestimates the survival performance of larger vehicles.

These limitations have prompted researchers to study and recommend other testing and evaluative approaches which more closely represent the crash dynamics and structural interactions associated with traffic mix crash encounters. To effectively manage such a complex interactive evaluation, it would be necessary that efforts be concentrated on vehicle test and analysis techniques which consider all significant aspects of the crash environment.

In 1973, Fiat Auto S.p.A. and Dynamic Science, Inc. began formulation of test and analysis techniques for evaluation of vehicle crash compatibility. Since this initial formation, Dynamic Science, Inc., under funding from Fiat Auto S.p.A. developed a methodology for evaluating vehicle crash compatibility. The ultimate goal was to provide compatibility characterization technology in frontal, side and rear impact environments. The results of this research have been extremely encouraging—accurate analysis and predictive capabilities have been developed, as well as justification of the methodology approach.

Because of the increasing concern for vehicle crash compatibility, the U.S. National Highway Traffic Safety Administration (NHTSA) acquired the Fiat Methodology in 1980. The NHTSA then increased the funding of an on-going program (Reference 1) to initialize the applicability of the Fiat Methodology to side impact analysis. Both frontal and side structural characterizations were used in this study.

This paper summarizes the results from the above NHTSA research program emphasizing the applicability of the Fiat Methodology to the characterization of vehicle structural responses in frontal impacts. A companion paper, Reference 2, deals with the applicability of the Fiat Methodology to the characterization of side impacts, utilizing the frontal model characterizations presented herein.

FIAT METHODOLOGY APPROACH

Franchini (References 3 and 4) discussed and highlighted the Fiat Methodology in prior Experimental Safety Vehicles (ESV) conferences. However, it seems

appropriate to summarize the Fiat Methodology approach prior to presenting the results used for the NHTSA study.

The Fiat Methodology has resulted in new test and analysis approaches and techniques for evaluating vehicle-to-vehicle crash interactions. The research accomplished to date has resulted in the design and development of test hardware, test techniques, data analysis software and crash simulation software, along with validation of the basic methodology. Figure 1 flow charts the basic engineering approach and illustrates the coupling of experimental test data and analytical technology to define and characterize a vehicle's response to crash environments.

It was recognized from the beginning of the Fiat Methodology development effort that the results and analyses must be based on experimental data. As illustrated in Figure 1, the first step is a structural characterization test of the vehicle under the appropriate impact conditions. For our research, this was accomplished through the use of a test device developed to enhance structural data acquisition. The test device has been discussed and presented by Franchini in References 3 and 4 and consists of a 36-module load-measuring moving barrier fitted with energy-absorbing honeycomb blocks attached to each module. The purposes of the test device include:

1. Simulation of the structural interface interactions involved in vehicle-to-vehicle encounters,
2. Measurement of crash interface loads and deflections between the test device and vehicle being characterized, and
3. Simulation, as closely as possible, of inertia reactions associated with vehicle-to-vehicle impacts.

Of equal importance in the characterization test is the instrumentation of the vehicle being characterized. It must adequately define the structural dynamics and inertial reactions (including occupants, restraints, engine, suspensions, etc.) that characterize the vehicle's response to the crash environment. The vehicle instrumentation is dependent upon the impact mode (front, side, rear) and upon the vehicle's design configuration.

The second step of the Fiat Methodology was to develop analysis techniques which would permit characterization of a vehicle's structural response to a crash test environment. This was accomplished by developing a data processing software package referred to as Computer Program A. As illustrated in Figure 1, Program A accepts as input the kinematic and dynamic behavior obtained from the vehicle characterization test data, the vehicle parametric data, and analytical model configuration. The program then processes these data to define the necessary structural properties of the general lumped-parameter vehicle model which are required to reproduce the given kinematic input. The end product is an analytical model of the vehicle being characterized, using full-scale crash data.

The third step of the Fiat Methodology was to develop

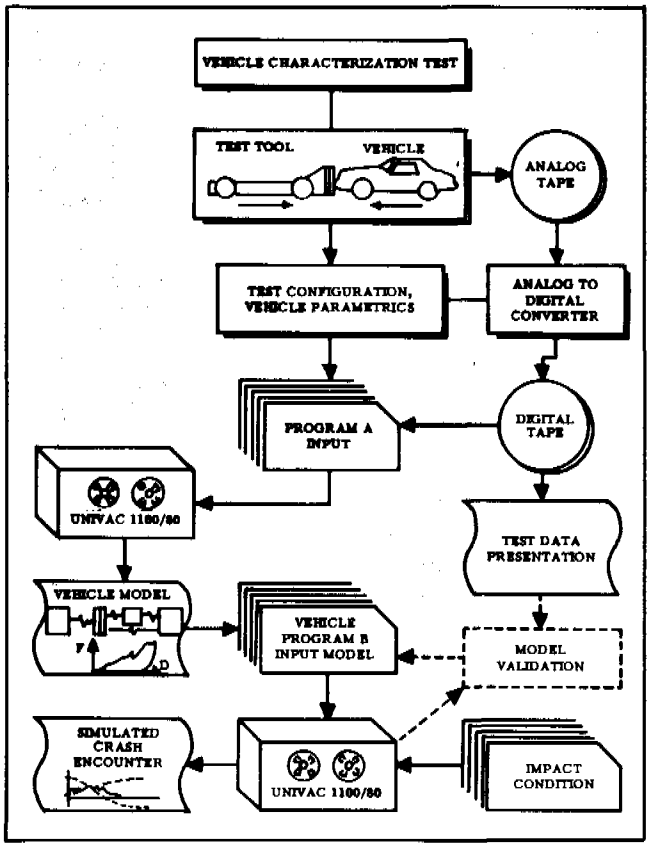

Figure 1. Fiat methodology approach.

techniques which simulate crash encounters between characterized vehicles. This was accomplished through the development of a software package referred to as Computer Program B. As illustrated in Figure 1, Program B accepts as input lumped-mass non-linear spring model representations such as defined by Program A output (or other desired impact conditions) and computes the crash response of the vehicles. Program B can also be used to check Program A output by simulating the vehicle characterization test, thus providing model validation and a means for model improvement.

Once a vehicle's model characterization has been validated, it can be used to study structural crash interaction with other characterized vehicle structures or barriers. A sufficient number of characterized vehicles representing the traffic mix environment could then provide a data base for evaluating an individual vehicle's structural crashworthiness compatibility with a traffic mix population environment.

FRONT STRUCTURAL CHARACTERIZATION

In the Fiat S.p.A.-sponsored Fiat Methodology development efforts, the Fiat 132 sedan was the primary evaluation vehicle. As a result, a considerable test data base

had been generated for that vehicle in both the frontal and side impact configurations. The Fiat 132 was consequently selected as the study vehicle for the NHTSA demonstration program (Reference 1). The Fiat 132 four-door sedan is a conventional front engine, rear wheel drive vehicle with a curb weight of approximately 2,380 pounds (1,080 kg).

The Fiat 132 front structures characterization effort is illustrated in Figure 2. It included full-scale characterization testing, computer data processing, model development, and model validation.

STRUCTURAL CHARACTERIZATION TEST

The front characterization test consisted of a head-on impact between the Fiat test tool (described in References 3 and 4) and a Fiat 132 Sedan. Table 1 summarizes the test conditions for this test. The Fiat 132 carried fully instrumented driver and right front passenger Part 572 dummies and extensive accelerometer instrumentation on all significant inertial masses. The test tool carried 36 load cells along with string potentiometers for measuring test tool honeycomb deflections and frame accelerometers.

Table 1. Fiat test tool to Fiat 132 frontal characterization test.

Fiat 132 Test Weight	2798 lb (1269 kg mass)
Test Tool Weight	4040 lb (1833 kg mass)
Closure Velocity	39.2 mph (63 km/h)
Impact Orientation	Head on with Aligned Centerlines

STRUCTURAL MODEL DEVELOPMENT AND VALIDATION

The data from the Fiat test tool-to-Fiat 132 frontal characterization test was processed through a Class 60 digital filter and input, along with the Fiat 132 parametric data and representative model configuration into Computer Program A. The output of Program A defined the interconnecting spring load deflection characteristics between the analytical model masses. For the Fiat 132 characterization test, the analytical model configuration, with respect to vehicle mass representations, is illustrated in Figure 3. This model incorporates both the Fiat 132 and Fiat test tool inertial representations.

The Fiat 132 model, along with the interconnecting spring characteristics and the analytical model of the Fiat test tool were input into Computer Program B and exercised under the impact conditions of the characterization test. This procedure validated the Fiat 132 analytical model by direct comparison of predicted and test results and provided an opportunity to fine tune the spring characteristics. It has been our experience that fine tuning, following the initial Program B validation run, is normally confined to improvements in the definition of the analytical spring unloading characteristics. This definition is extremely sensitive to data inaccuracies near the end of

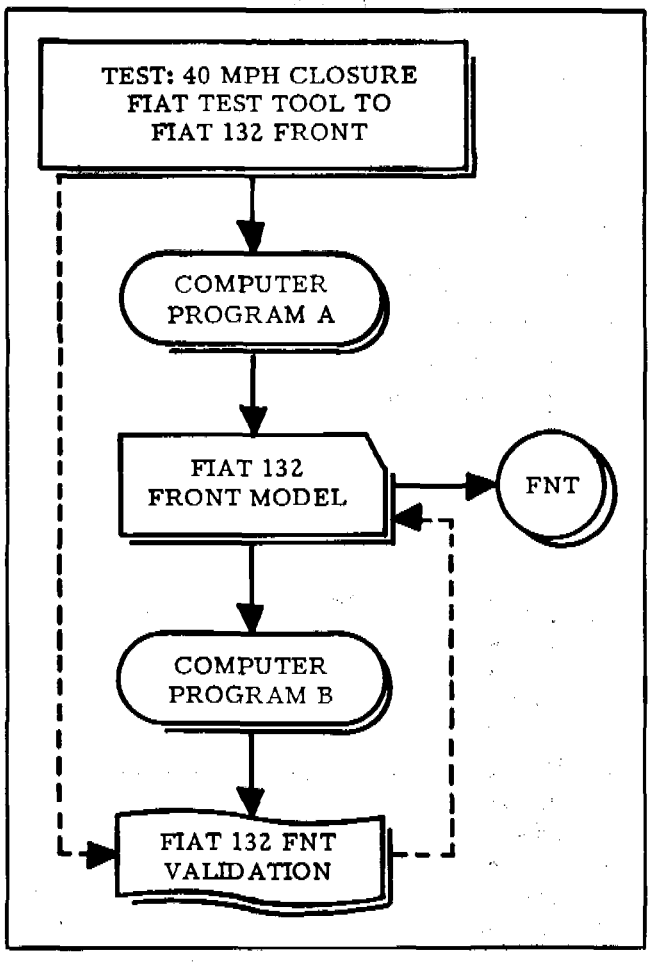

Figure 2. Flow chart of front structural characterization.

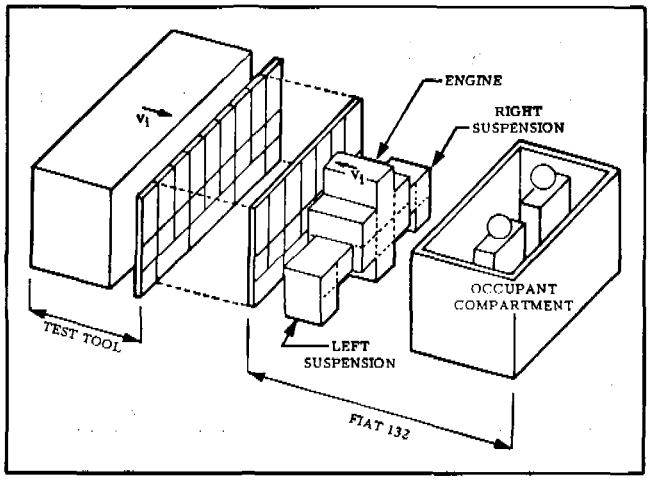

Figure 3. Model configuration for the Fiat front.

Table 2. Fiat 132 frontal model validation results summary

Parameter	Test Data	Simulation
Closure Velocity (mph)	39.2	39.2
Fiat 132 Weight (lb)	2798	2798
Test Tool Weight (lb)	4040	4040
Fiat 132 Velocity Change (mph)	24.5	26.2
Test Tool Velocity Change (mph)	17.4	17.4
Maximum Dynamic Mutual Crush (in.)	24.6	24.3
Fiat 132 Average Dynamic Crush (in.)	21.0	20.6

the crash pulse. Other fine tuning should not be necessary if test data retrieval is accurate.

The results of the Fiat 132 frontal model valiation are summarized in Table 2. Figure 4 compares the predicted response of the compartment of the Fiat 132 to the actual test data. Similarly, Figure 5 compares the predicted response of the test tool to the actual test data. Of particular interest in a frontal simulation is the ability to characterize the dynamics of vehicle components as well as structural responses. Figures 6 and 7 respectively compare Fiat 132 engine and left front suspension predicted responses to actual test results. The right front suspension response (not shown) was essentially the same as that shown in Figure 7 for the left front suspension. The results indicate excellent representation by the analytical model of the actual crash response of the vehicle. The Computer Program B input which provided these results consisted of a Fiat 132 frontal model and test tool model totaling 41 degrees of freedom.

VEHICLE-TO-VEHICLE PREDICTIVE CAPABILITY

The validated Fiat 132 frontal model was duplicated and both model sets were input into Computer Program B, along with the initial crash conditions of a Fiat 132

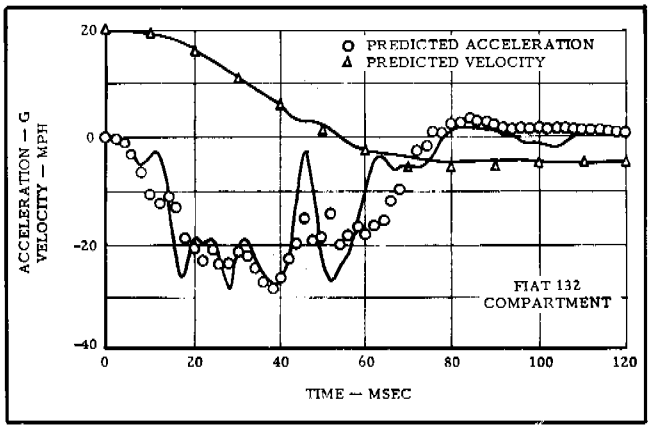

Figure 4. Comparison between predicted and test results for the Fiat 132 compartment—Fiat 132 frontal validation.

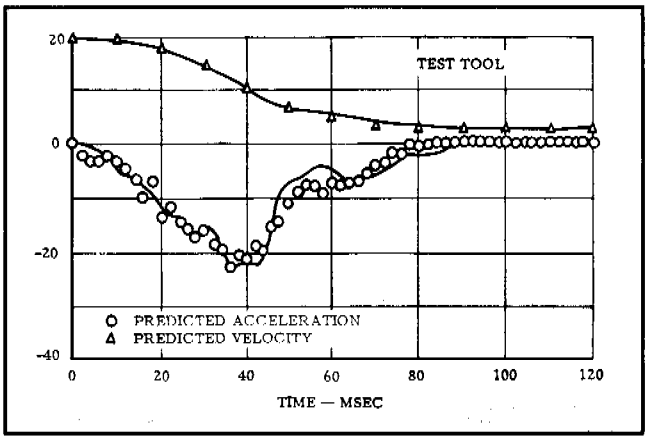

Figure 5. Comparison between predicted and test results for the Fiat test tool vehicle—Fiat 132 frontal validation.

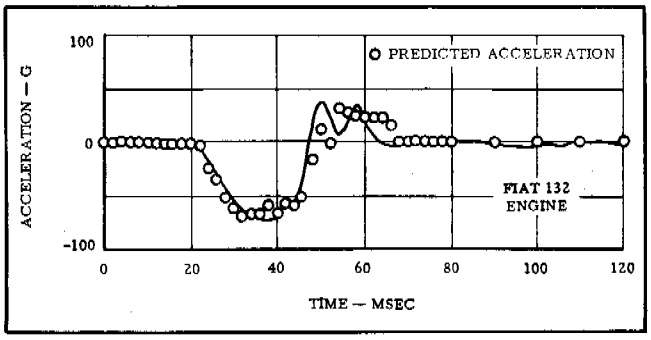

Figure 6. Comparison between predicted and test results for the Fiat 132 engine—Fiat 132 frontal validation.

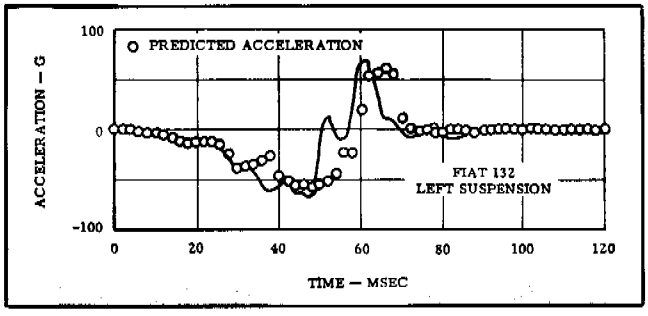

Figure 7. Comparison between predicted and test results for the Fiat 132 left suspension—Fiat 132 frontal validation.

front to Fiat 132 front crash test conducted at a closure velocity of 48.7 mph (78.4 km/hr) (Reference 5). This effort is illustrated in Figure 8. The resulting simulation provided 46 degrees of freedom, including both vehicle representations. Table 3 compares the predicted results to the actual test data. The vehicle analytical models were identical, therefore, producing exactly the same predicted responses. The crash test, however presents two identical

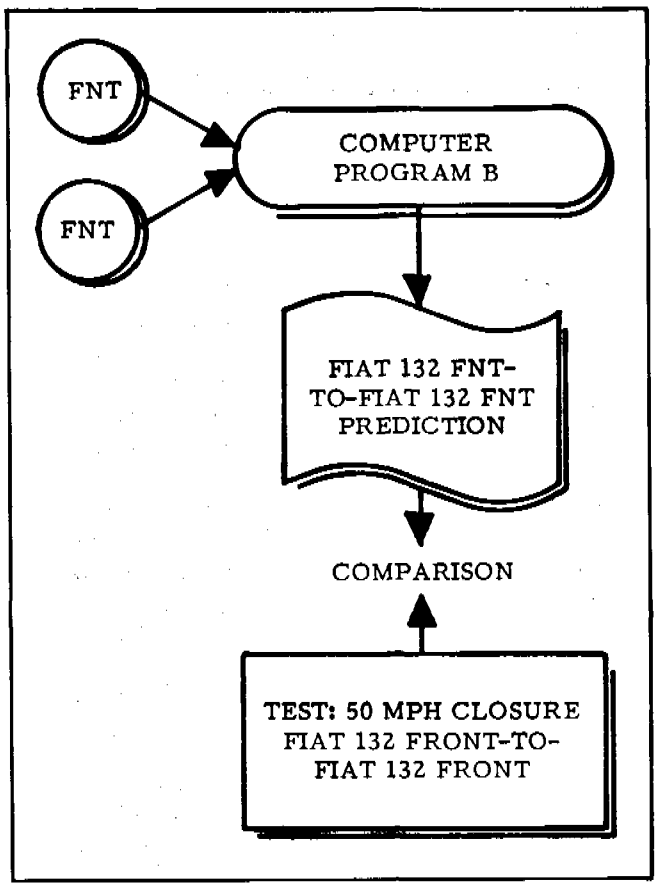

Figure 8. Flow chart for vehicle-to-vehicle prediction.

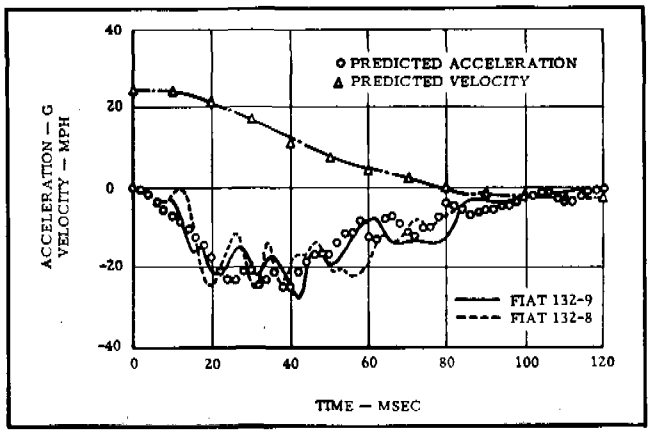

Figure 9. Comparison between predicted and test results for the Fiat 132 compartment.

vehicle models with corresponding responses representative of the real-world manufacturing and data acquisition tolerances. The Fiat 132 frontal model used was identical to that used in the validation analysis without adjustment of total vehicle mass differences.

Figure 9 compares the predicted Fiat 132 compartment response to the response accompanying each of the Fiat 132 test vehicles and Figure 10 compares the predicted engine response to the responses measured on each of the test vehicles. Figure 11 presents the predicted dynamic crush of the Fiat 132 models compared to the measured post-test residual crush for the test vehicles at bumper level.

Table 3. Fiat 132 front to front predicted crash results summary.

Parameter	Simulation	Test Data
Bullet Vehicle Weight (lb)	2798	2820
Target Vehicle Weight (lb)	2798	2826
Bullet Vehicle Velocity (mph)	24.4	24.4
Target Vehicle Velocity (mph)	24.4	24.4
Maximum Dynamic Mutual Crush		
—Integrated Acceleration (in.)	35.0	37.0
—Photography (in.)	N/A	34.0
Velocity Change at 100 msec (From Acceleration Data)		
—Bullet Vehicle (mph)	26.1	26.1
—Target Vehicle (mph)	26.1	27.0

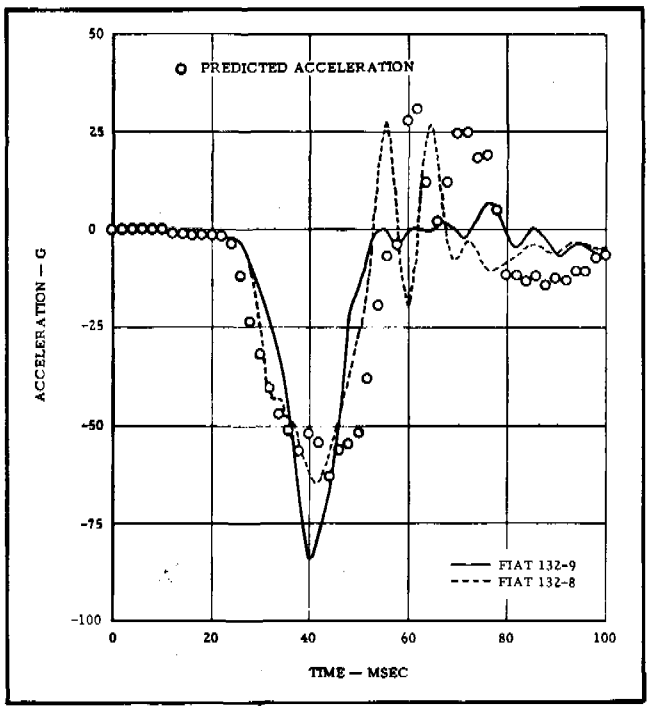

Figure 10. Comparison between predicted and test results for the Fiat 132 engine.

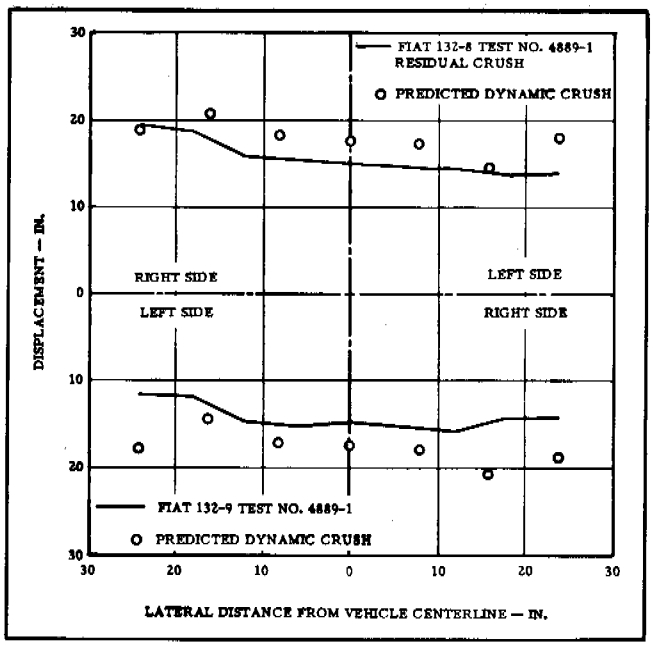

Figure 11. Comparison between simulated and test results for the Fiat 132 exterior crush at bumper level.

CONCLUSIONS

The objective of the Fiat Methodology is to provide a means by which vehicle interactions within a variety of crash environment can be determined with minimal testing. The applicability of the Fiat Methodology, test tool, and computer analysis procedures to the frontal head-on impact problem was demonstrated. The predicted results documented herein were well within the variability which can be expected when production vehicles are tested under identical conditions, using current instrumentation.

Early Fiat Methodology research revealed that the development of the predictive technology was evolutionary in nature—the achievement of a certain level of model sophistication resulted in improved modeling and characterization techniques. A great deal of the capabilities reported herein involved methodologies and upgraded computer programs which are presently proprietary to Fiat Auto S.p.A. Therefore, only the results of these analyses can be presented in this report.

The side impact model development on which the NHTSA program (Reference 1) focussed indicated that considerably more detail and capabilities, over and above the capabilities of the NHTSA versions of the Fiat Methodology, computer programs, were required to provide side impact characterization. Consequently, to maintain compatiblity between the frontal and side characterization programs, the frontal characterization model discussed herein also required this additional refinement.

Accuracy of the electronic test data is critical to the effective application of the Fiat Methodology. Significant time can be saved if the accuracy of the electronic test data is verified prior to its input into Program A. In addition, the vehicle characterization and model predictive accuracies can never be better than the test data used. As a result, the accuracies and refinement of the Fiat Methodology can be improved concurrently with improvements in instrumenation hardware and techniques. Furthermore, the use of the Fiat Methodology to evaluate a vehicle's crashworthiness is not fixed or dependent upon one evaluation condition or compliance environment. It is a methodology which is compatible with changing compliance criteria.

REFERENCES

1. Shaw, L. M., Knight, R. E. and Trudgen, A. C., "Application of the Fiat Methodology to Vehicle Side Impact", Report Number to be Assigned by the National Highway Traffic Safety Administration, Contract Number DOT-HS-8-01933, Modification Number 4, Dated September 1981.
2. Shaw, L. M., Ragland, C.,"Application of the Fiat Methodology for Characterizing Vehicle Structural Responses in Side Impact", Ninth International Technical Conference on Experimental Safety Vehicles, Kyoto, Japan, November 1 through 4, 1982.
3. Franchini, E., "Fiat Technical Presentation", Sixth International Technical Conference on Experimental Safety Vehicles, Washington, D.C., U.S.A., Pages 129 through 157, October 12 through 15, 1976.
4. Franchini, E., "Side Collision", Seventh International Technical Conference on Experimental Safety Vehicles, Paris, France, Pages 456 through 476, June 5 through 8, 1979.
5. "Data Submittal Report Entitled, Excerpts From an Existing Fiat Auto S.p.A. Report of Fiat 132 Front-to-Front Head-On Impact, Test Data for Task 1", Contract Number DOT-HS-8-01933, Modification Number 4.

3672

Influence of Occupant Seating Posture and Size on Head and Chest Injuries in Frontal Collision

TSUYOSHI AIBE, KUNIYUKI WATANABE,
TATSUMASA OKAMOTO and
TAKASHI NAKAMORI
Nissan Motor Co., Ltd.

ABSTRACT

The evaluation of vehicle occupant protection performance in a collision is generally based on the injury criteria. The seat is placed in the standard design position, using a 50th-percentile dummy, as represented in the FMVSS 208.

On the highway, however, vehicles are driven by individuals of various physical sizes and in various seat positions.

In this study, we have examined the relationship between injury level and occupant size or seating posture.

This paper presents examination results concerning forces acting on the chest and also on factors causing injury to the head.

TEST PROCEDURES

Test Equipment

In order to compare occupant injury levels in various conditions, we have conducted tests using a weight-drop type sled tester. This sled tester was considered to be a highly accurate reproduction when combined with a shock absorber, capable of producing a deceleration curve, simulating a 30-mph frontal barrier collision.

Figure 1 shows a schematic drawing of the test equipment. Figure 2 shows a deceleration curve caused by the combination of the weight-drop type sled and the shock absorber. Another deceleration curve produced by a 30-mph frontal barrier collision with a vehicle is also shown. This can be regarded as an actual simulation of the collision.

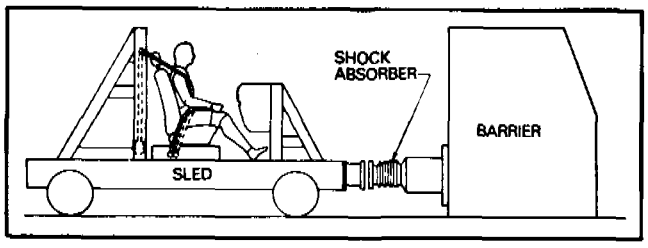

Figure 1. Test equipment.

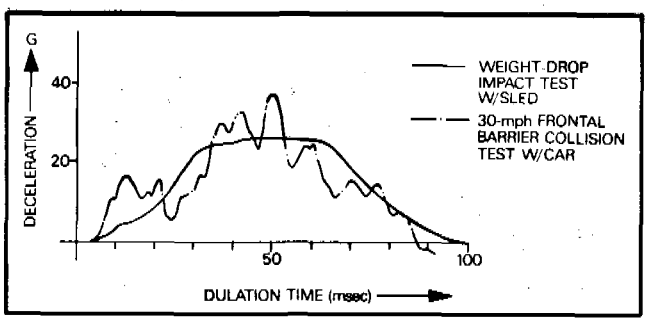

Figure 2. Deceleration curve.

Test Conditions

We conducted all sled tests with the same instrument panel, seats, seat belts, and seat belt anchorage points as found in an actual car.

To consider the influence of occupant body size, we used the following three types of dummies:

Table 1. Types of dummies.

	ABBR.	SIZE	Wt.(kg)	SITTING Ht.(cm)	REMARKS
1	M50	AMERICAN, MALE, 50th PERCENTILE	74.5	90.7	HYBRID II ALDERSON-MADE
2	M95	AMERICAN, MALE, 95th PERCENTILE	97.7	96.5	ALDERSON-MADE
3	F05	AMERICAN, FEMALE, 5th PERCENTILE	47.2	78.0	ALDERSON-MADE

Next, tests were conducted to examine the influence of occupant seating posture by setting up five points as shown in Figure 3. The seat slide was moved forward or rearward by 100 mm from the normal middle position. The seat back angle was set where the seat back was inclined forward or backward by 9 degrees from the normal middle position.

Using three different sized dummies to examine the relationship between injury levels and occupant sizes, a series of tests were carried out under the conditions shown in Table 2.

Next, to see what effect the seat slide positon had on

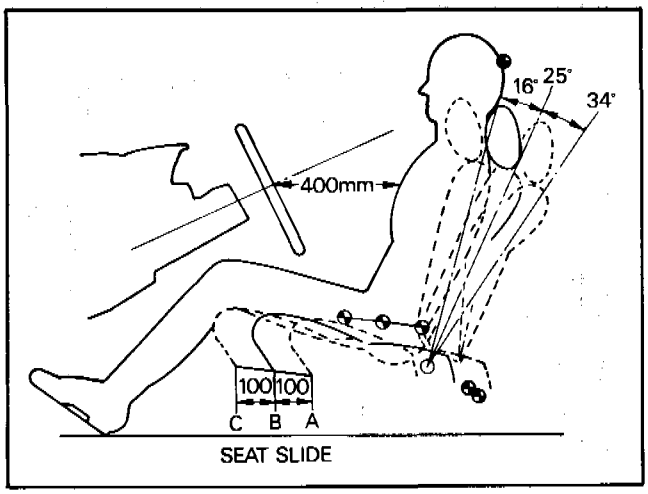

Figure 3. Positions of seat back and seat slide.

Table 2. Test condition (1).

SEAT SLIDE \ DUMMY / SEAT POSITION / SEAT BACK ANGLE	F05 DRIVER	F05 PASSENGER	M50 DRIVER	M50 PASSENGER	M95 DRIVER	M95 PASSENGER
A	1	2	3	4	5	6
B (25°)	7	8	9	10	11	12

Table 3. Test condition (2).

SEAT SLIDE \ DUMMY / SEAT POSITION / SEAT BACK ANGLE	M50 DRIVER	M50 PASSENGER	M95 DRIVER	M95 PASSENGER
A	③	④	⑤	⑥
B (25°)	⑨	⑩	⑪	⑫
C	⑬	⑭	⑮	⑯

Table 4.

SEAT SLIDE \ DUMMY / SEAT POSITION / SEAT BACK ANGLE	M50 DRIVER	M50 PASSENGER	M95 DRIVER	M95 PASSENGER
B, 16°	⑰	⑱	⑲	⑳
B, 25°	⑨	⑩	⑪	⑫
B, 34°	㉑	㉒	㉓	㉔

injury level, tests were conducted under conditions shown in Table 3.

To determine what effect the seat back angle had on the injury level, tests were conducted under the condition shown in Table 4.

Table 5.

SEAT BELT ELONGATION RATE \ DUMMY / SEAT POSITION	M50 DRIVER	M50 PASSENGER
STD WEBBING	⑨	⑩
15% MORE ELONGATING WEBBING	㉕	㉖

Finally, to determine the effect of the seat belt elongation rate on the injury level, tests were conducted under the same conditions as in Test Nos. (9) and (10), with the belt elongation itself increased by approximately 15 percent, as shown in Table 5.

RELATIONSHIP BETWEEN INJURY LEVEL AND OCCUPANT BODY SIZE

Figures 4 and 5 show the extent of injuries sustained by the head and by the chest, as a result of tests of Test Nos. (1) through (12) under the conditions shown in Table 2.

In Figures 4 and 5,

(1) The head injury level increases as the dummy size decreases, especially with the F05 which shows high injury levels, and

(2) The chest injury level also increases as the occupant size decreases.

Here, force applied to the dummy during a collision is shown in Figure 6. The difference in occupant size does not change the initial restraint caused by the seat belt.

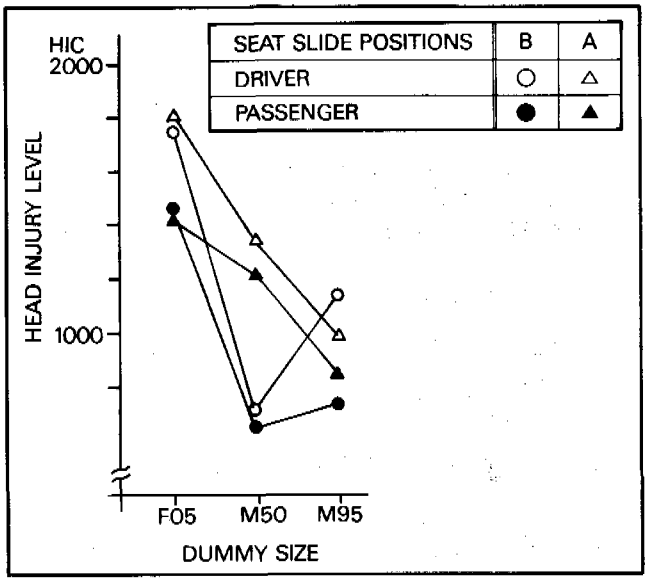

Figure 4. Head injury level.

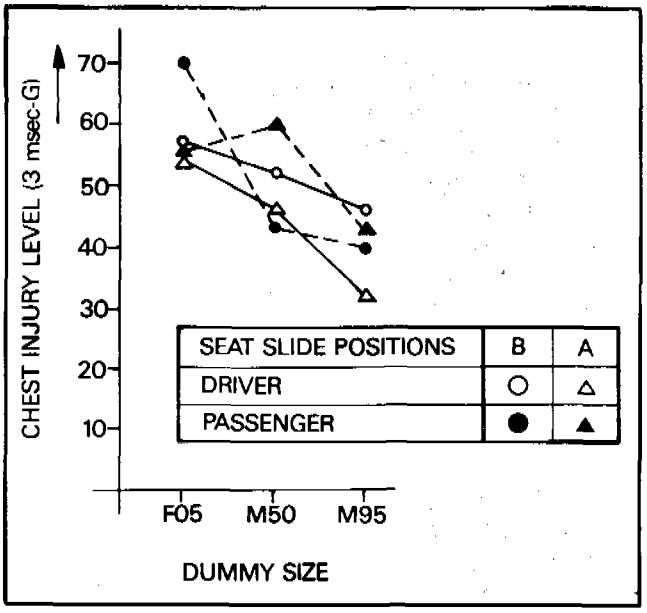

Figure 5. Chest injury level (3 msec-G).

After approximately 40 to 50 msec from the start of the collision, the chest becomes restrained by the shoulder belt, and after another 30 msec, the chest stops moving. Then, the head begins to pivot on the neck, and thus, the phenomenon caused by the collision comes to an end.

We examined the reason why, in a similar phenomenon, the tendencies shown in Figures 4 and 5 occur.

The chest is restrained by the shoulder belt. Our examination revealed, in each test case, that the relationship between the tension on the shoulder belt and the occupant weight was highly correlated as shown in Figure 7. Generally the substantial mass weight applied to the shoulder belt is said to account for 25 percent of the overall weight. The Substantial mass weight figured out from the belt tension and the deceleration G produced on the chest is shown in Table 6. This shows clearly that the substantial mass weight makes up approximately 25 percent of the overall weight.

The force produced on the chest can be calculated by

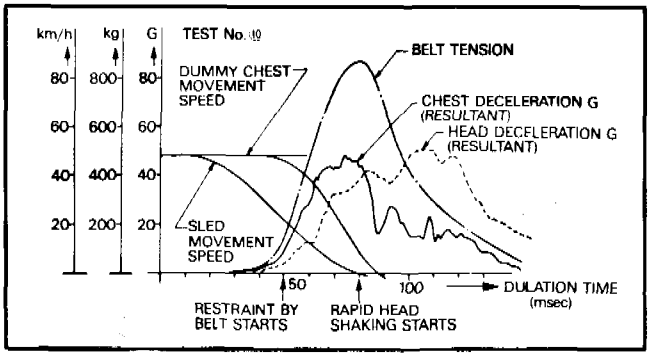

Figure 6. Phenomenon occurring on each part in collision.

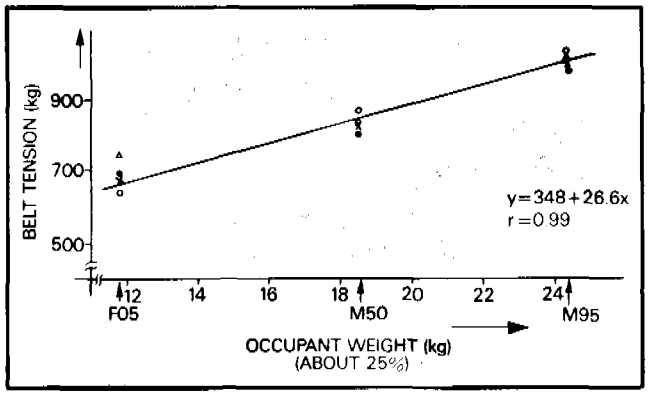

Figure 7. Relationship between occupant weight and belt tension.

using a simple equation. From the correlative equation in Figure 7, the following equation is formed:

$$F = WG \quad \ldots\ldots (1)$$

where F : Shoulder belt tension (kg)
W: Substantial mass weight (kg)
G: Deceleration produced on chest

$$F = 26.6W + 348 \quad \ldots\ldots (2)$$

From equations (1) and (2), the deceleration produced on the chest is expressed by the following equation:

$$G = \frac{348}{W} + 26.6 \quad \ldots\ldots (3)$$

From equation (3), it is found that the chest injury level is lowered in a reciprocal proportion to the dummy size and weight.

Table 6. Substantial mass weight applied to shoulder belt.

DUMMY SIZE	SEAT SLIDE POSITION	DUMMY SEATING POSITION	INITIAL STAGE			PEAK STAGE		
			Dec'n (G)	BELT TENSION (F)	SUBSTANTIAL Wt. (W)	Dec'n (G)	BELT TENSION (F)	SUBSTANTIAL Wt. (W)
F05	B	DRIVER	10	120	12	57	690	12.1
		PASSENGER	10	120	12	54	635	11.8
	A	DRIVER	–	–	–	70	810	11.6
		PASSENGER	10	140	14	57	670	11.8
M50	B	DRIVER	10	120	12	52	820	15.6
		PASSENGER	10	150	15	46	865	18.8
	A	DRIVER	10	180	18	43	840	19.5
		PASSENGER	10	180	18	60	830	13.8
M95	B	DRIVER	10	250	25	46	980	21.3
		PASSENGER	10	310	31	32	1,020	31.8
	A	DRIVER	10	280	28	40	1,010	25.2
		PASSENGER	10	350	35	43	990	23.0

	WEIGHT (kg)	SUBSTANTIAL MASS Wt. Av. (kg)	PERCENTAGE (%)
F05	47.2	12.2	25.8
M50	74.5	16.3	21.9
M95	97.7	25.1	25.7

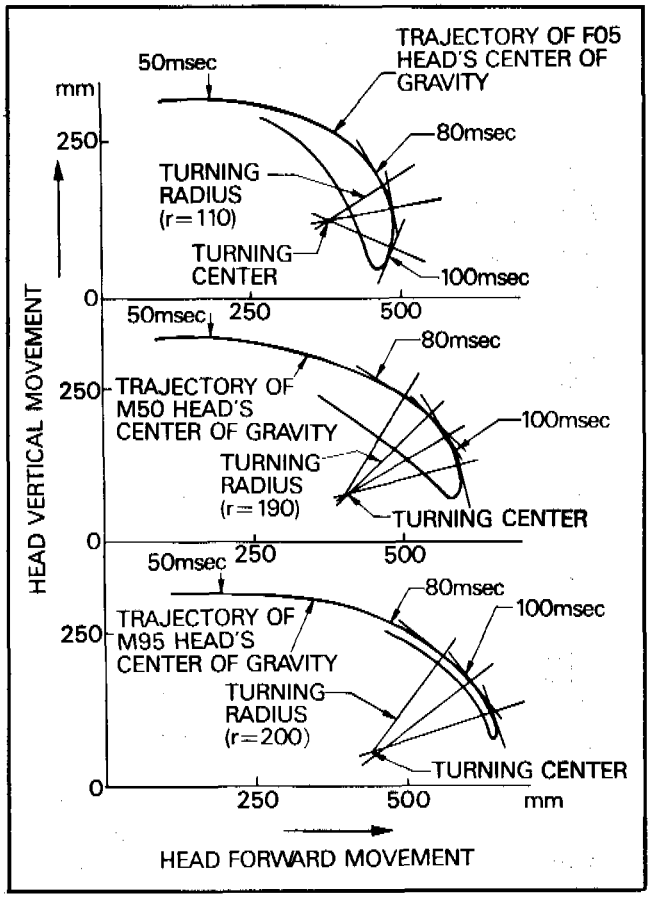

Figure 8. Head behavior by size.

Next, let's consider the influence of the dummy size on the head injury level. It is found that although the aforementioned chest deceleration influences the head injury, the dummy size has a more dominant effect.

That is, when the curve of deceleration produced on the head is looked at after a period of time, we can consider the phenomenon in the following two stages:

According to the deceleration curves in Figure 6,

(1) Approximately 80 msec after the initial collision, the deceleration on the chest reaches a peak. In the meantime, the head, affected by the chest, traces a large circular arc trajectory with the waist as a pivot, and thus, a peak at the first stage is reached.

(2) The chest stops moving after the peak of the first stage. The remaining speed energy on the head is absorbed by the head shaking motion. It has an extremely small turning radius, and uses the neck as a pivot. Centrifugal force generated by the head shaking motion produces the second-stage peak deceleration.

In this study, the level of head injury sustained by the F05 dummy is highly comparable to those cases of the M50 and M95 dummies. This is thought to be due to the second-stage peak mentioned above.

Figure 8 shows head behavior graphed according to dummy size. From the head behavior after the chest ceases to move (approximately 80 msec after the initial collision), the turning radius of the head shaking motion is measured to be equal to the values shown in Figure 8.

The difference of these turning radii of the head shaking motion was caused by the difference in the position of chest restraint by the shoulder belt.

Let's discuss the head turning radius. Changes in the early position of chest restraint by the shoulder belt, which is caused by the difference in occupant size, will have different effects on the attitude of the restrained dummy during a collision. As shown in Figure 9, the difference in restraint ranges from a rapid head shaking motion, with the neck as a pivot (F05 type), to a comparatively gentle head shaking motion with the neck turning with the twisting torso (M50 and M95 types).

As described above, it can be seen that the head injury level is largely influenced by the difference between the chest restraint position and dummy size, namely due to the difference in the head turning radius, even if the occupant compartment has no components to cause a secondary collision to the head.

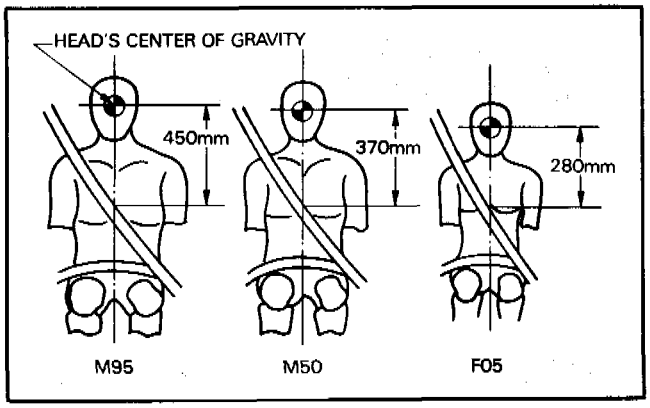

Figure 9. Restraint positions by size.

INFLUENCE OF SEAT SLIDE POSITION ON INJURY LEVEL

Figures 10 and 11 show the chest injury level and the head injury level as they relate to the position of the seat slide, with the following results:

(1) The chest injury level tends to increase as the seat slide is positioned rearward.

(2) The head injury level tends to increase as the seat slide is moved rearward. When the seat slide is positioned forward, a phenomenon can occur in which a secondary collision against the steering wheel, etc. becomes more severe and the injury level increases.

Hereupon, we examined the reason why we see increased deceleration on the chest when the seat slide is moved rearward.

Figure 12 is a comparison graph showing deceleration produced on the chest, belt tension and chest moving

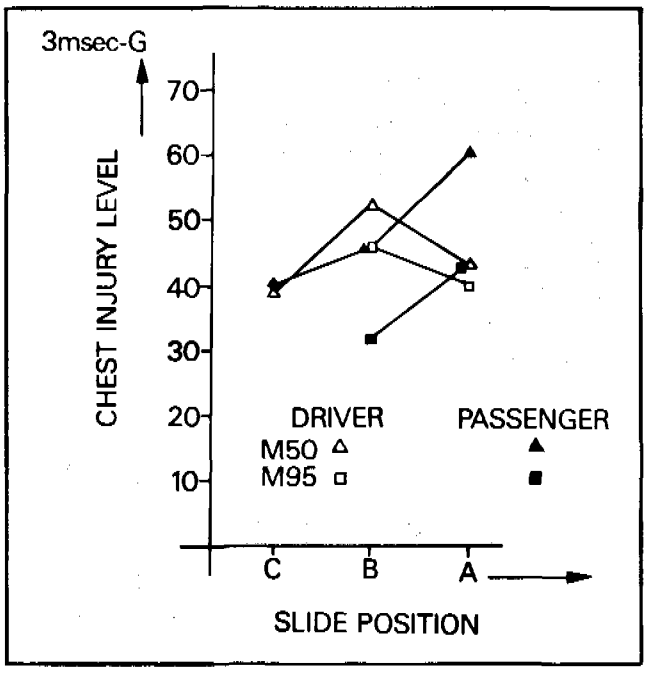

Figure 10. Seat slide position and chest injury level.

speed of Test Nos. (3), (9) and (13), when conducted using an M50 dummy.

The time when the shoulder belt begins to restrain the chest changes by 4 to 6 msec according to the position of the seat slide.

This difference in time influences the amount of tension produced on the shoulder belt and the rise of deceleration produced on the chest. On the other hand, an observation of the relative speed between the occupant's chest and the sled reveals that there is a difference of 4 to 5 km/h in relative speed due to variations in the time when the restraints begin.

It can be considered that a delay in initiating the seat

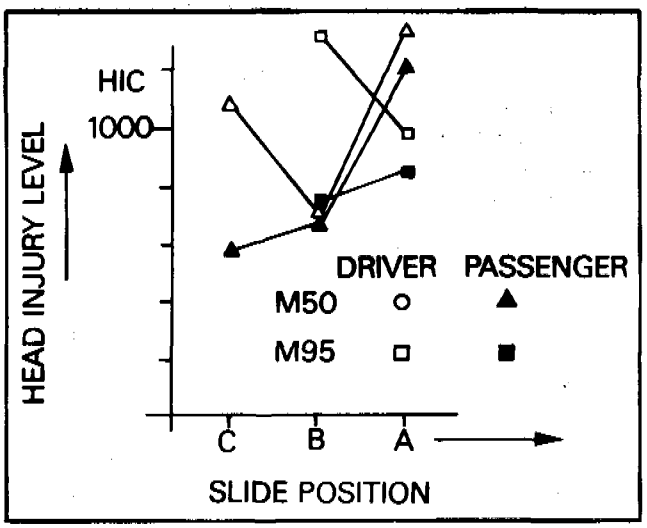

Figure 11. Seat slide position and head injury level.

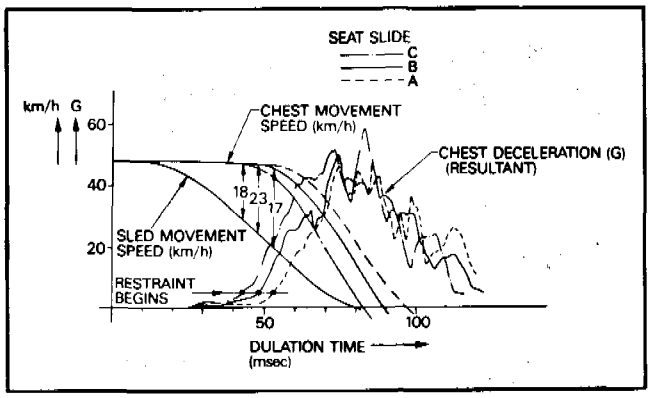

Figure 12. Results of tests by seat slide position.

slide rearward position restraint results in a lowered Ride-Down Effect, and thus leads to an increase in chest deceleration and in injury level.

INFLUENCE OF SEAT BACK ANGLE ON INJURY LEVEL

Figures 13 and 14 show changes in injury level, caused when the seat back angle was changed. The chest injury level rises slightly when the seat is inclined backward.

As clearly seen in Figure 14, the head injury level increases remarkably when the seat is inclined backward.

Figure 15 shows how deceleration acts on each part. The graph shows that a delay in chest restraint by the shoulder belt is caused in the same way as in the test conducted by changing the position of the seat slide.

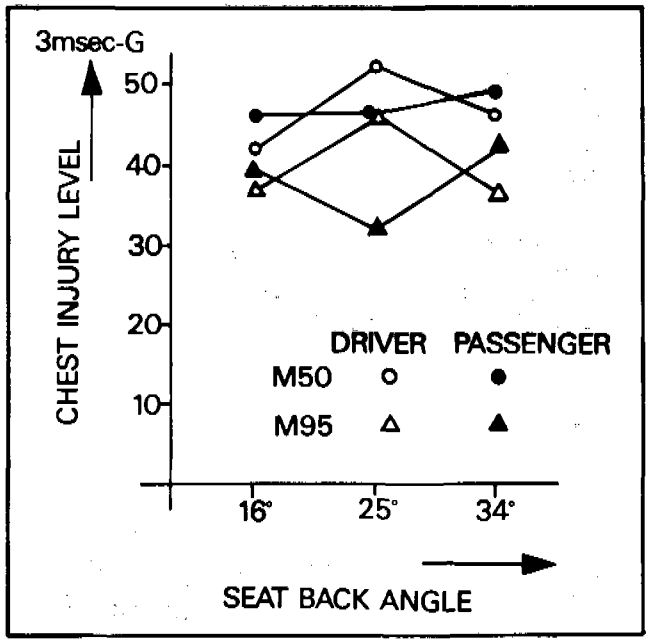

Figure 13. Seat back angle and chest injury level.

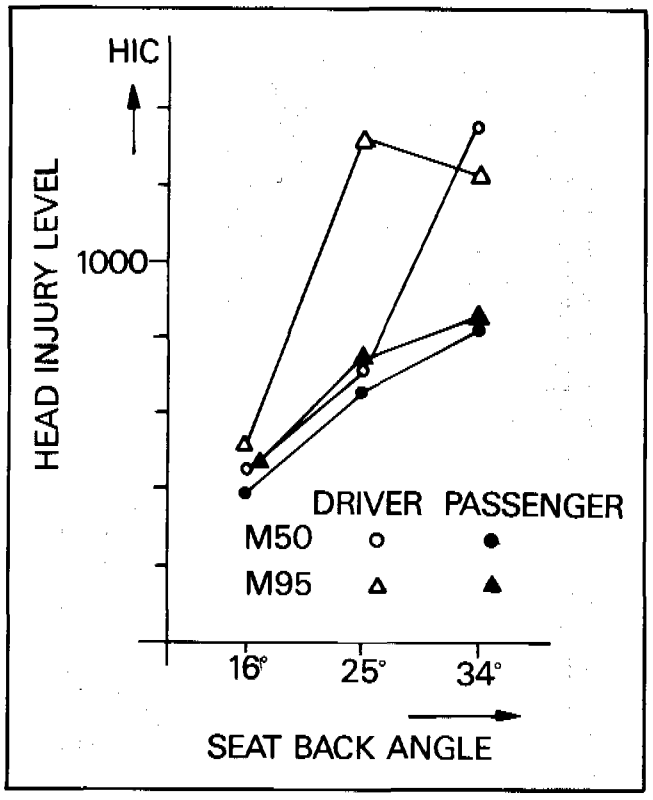

Figure 14. Seat back angle and head injury level.

FEMUR LOAD ACCORDING TO SEAT POSITION

Table 7 shows femur loads obtained in all the tests reported so far. As is clear in this table, even the heaviest femur loads are within 70 percent of the injury criteria provided in FMVSS 208, etc., and have no significant influence.

The level of the femur load is determined by whether or not the knees have collided with the instrument panel or the steering shaft, or by the severity of the knee collision.

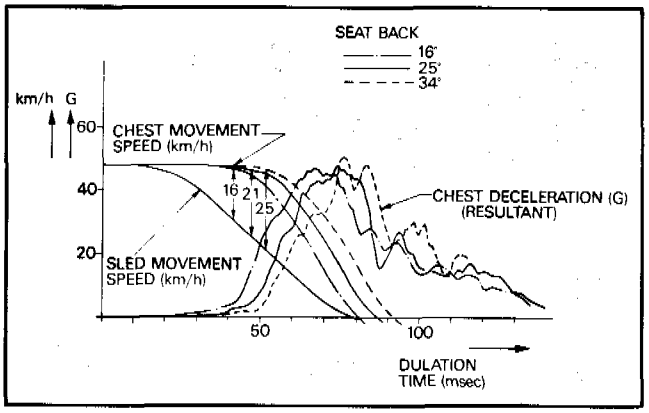

Figure 15. Results of tests by seat back angle.

Table 7. Femur load.

DUMMY	SEAT SLIDE	SEAT BACK ANGLE	DRIVER 0	DRIVER 50%	DRIVER 100%	PASSENGER 0	PASSENGER 50%	PASSENGER 100%
F05	B	25°						
	A	25°						
M50	C	25°						
	B	16°						
		25°						
		34°						
	A	25°						
M95	B	16°						
		25°						
		34°						
	A	25°						

RELATIONSHIP BETWEEN SEAT BELT AND OCCUPANT INJURY LEVEL

We have conducted an examination to find out the influence of the seat belt webbing elongation rate, when increased by 15 percent over the standard, on the behavior of the occupant.

Table 8 shows the increased amount of movement of each body part of the dummy when the seat belt webbing elongation rate is increased. From this it is seen that an increase in the webbing elongation rate leads to an increase in the amount of chest and pelvis movement, which is directly restrained by the seat belt.

Figure 16 shows the movement speeds of the sled and the dummy chest. It also shows the amount of tension acting on the shoulder belt. When the seat belt webbing elongation rate is increased, the chest movement speed is greatly delayed by 6 to 8 msec. Further, the seat belt gently raises the tension, and causes an 8 to 10 msec delay for the same tension and a 15 msec delay for the tension to reach a peak.

Table 8. Increased amount of movement of each part.

PART	DRIVER	PASSENGER
HEAD	107%	110%
CHEST	120%	136%
PELVIS	119%	123%

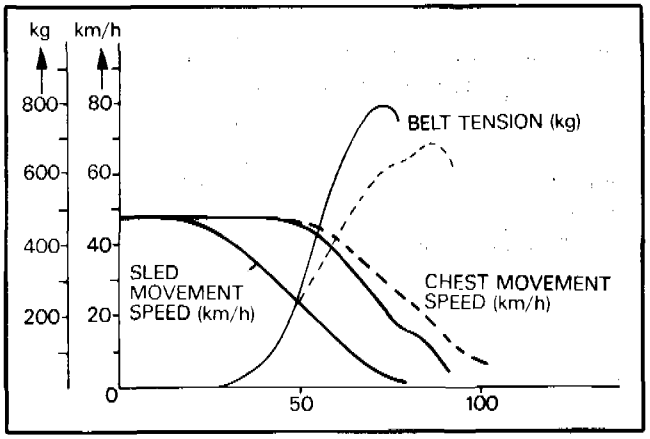

Figure 16. Movement speeds of sled and chest.

It follows from this that an increase in webbing elongation rate will somewhat ease the chest restraint and lower the injury level.

Figure 17 shows the behavior of the head. It is when the chest is restrained by the seat belt that an increase in seat belt webbing elongation rate begins to cause a difference in the head behavior. The head's forward movement is increased by as much as the chest restraint is loosened.

The head behavior in Figure 17 is sharply changed because the top of the head has collided with the upper side of the instrumental panel caused by an increased in forward movement. This phenomenon is very advantageous for decreasing the dummy injury level. It can be decreased by increasing the rate of the seat belt webbing elongation. For the head, however, this signifies that a secondary collision has occurred due to an increase in forward movement.

The length of seat belt webbing left on the retractor spool may cause injury to the occupant. Sufficient webbing is generally wound inside the seat belt retractor, so that the seat belt can be used in any seat position. Further, in order for the belt to restrain the dummy in a collision, a device is installed for immediately locking the retractor mechanism when a collision occurs, that is, Emergency Locking Retractor.

An examination of the movement of a tightly belted dummy in a collision was done. It was found that approximately 40 to 50 msec after the collision, the seat belt starts to restrain the dummy. In the meantime, the dummy moves forward approximately 100 mm.

The cause for this is thought to be that the seat belt webbing in the retractor is spooled out. Therefore, we conducted tests on the amount of spooled out seat belt webbing in the three stages of 400 mm, 800 mm and 1,100 mm. These are the lengths of webbing found on the retractors before the respective tests. Figure 18 shows the amount seat belt spooled out in the process of applying a 1,000 kg load.

Another phenomenon in Fig. 18 is that when 10 percent of the tension acting on the seat belt is produced, the amount of spooled out webbing covers approximately 70 percent of the maximum spooled out amount, and when 20 percent of the tension is produced, the amount of spooled out webbing covers approximately 75 to 80 percent of the maximum spooled out amount.

It follows from this that the amount of spooled out seat belt webbing will lead to a delay in the beginning of occupant restraint.

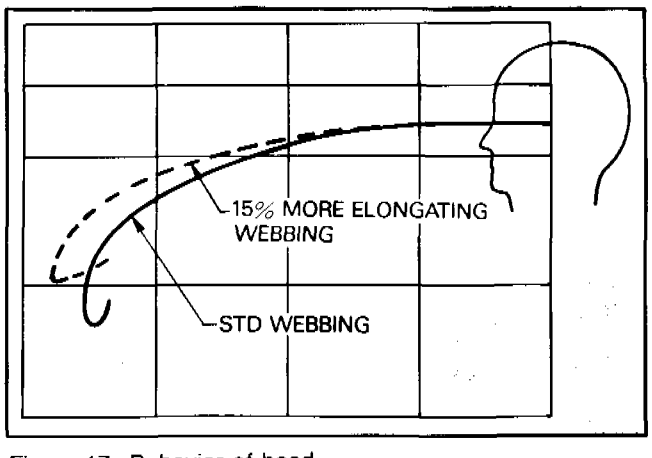

Figure 17. Behavior of head.

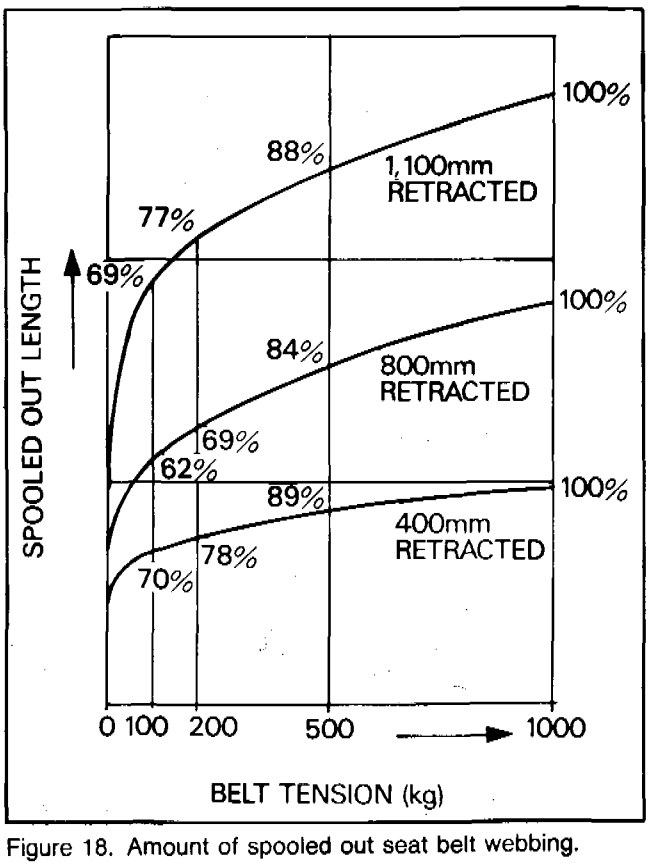

Figure 18. Amount of spooled out seat belt webbing.

CONCLUSIONS

As a result of this study, it is found that the occupant injury level varies largely according to occupant body size, seating posture, and the seat belt. That is,

(1) The larger the occupant body size, the less the injury level. Especially with the head injury level, it is found that when the occupant size is small, the head turning radius becomes small. Thus, the injury level is increased after completion of the chest movement, because the distance between the seat belt restraint point on the occupant and the head's center of gravity is short.

(2) The beginning of the chest restraint is delayed as the seat slide is moved rearward. Due to this lapse in time, the Ride-Down Effect is lowered, and thereby the injury level is increased.

(3) As the seat is inclined backward, the beginning of restraint is delayed as in the case of the seat slide position.

(4) When the seat belt webbing elongation rate is increased, the chest restraint is reduced and the injury level is lowered. However, the head forward movement is increased, and thus the danger of a secondary collision against the instrument panel, etc. is increased.

(5) Furthermore, it is certain that the spooled out webbing length from the seat belt retractor, even under a load equivalent to 100 kg, amounts to approximately 70 percent of the overall spooled out amount, thus leading to a delay in the beginning of restraint.

It is important to conduct evaluations under various conditions on the occupant restraint system used in the market. There are many subjects still to be examined; some of them are mentioned below:

(1) A quick restraint of the occupant by the seat belt immediately after a collision is effective in the sense of reducing the injury level. On the highway, people of various physical sizes are driving in various positions; thus, to cope with this, the seat belt should be improved in its fitting performance, taking its comfort and convenience into consideration.

(2) For evaluation of the occupant protection performance according to size, the performances and specifications of dummies should be realistic. This is a subject of development necessary to solve the present problems. There are some differences even in measurement data obtained by tests carried out in the same conditions. We would like to pursue our study for the development of a better occupant protection system.

(3) All of the tests were conducted using weight-drop sleds, in order to evaluate occupant protection systems in collisions. In actual collisions, however, complicated secondary collisions and various vehicle behaviors will come into play. For this reason, we should continue to analyze various factors affecting the comparison between weight-drop type sled and actual vehicle tests.

REFERENCES

1. Heinrich Hontshik, Egbert Müller and Gert Rüter, "Necessities and Possibilities of Improving the Protective Effect of Three-Point Seat Belts," SAE Paper 770933.
2. Murray Dance and Bert Enserik, "Safety Performance Evaluation of Seat Belt Retractors," SAE Paper 790680.
3. Roger P. Daniel, Kenneth R. Trosien and Burgess O. Young, "The Impact Behavior of Hybrid II Dummy," SAE Paper 751145.
4. L. M. Patrick, N. Bohlin and A. Anderson, "Three-Point Harness Accident and Laboratory Data Comparison," SAE Paper 741181.
5. David C. Herbert, John D. Scott and Christopher W. Corben, "Head Space Requirements for Seat Belt Wearers," SAE Paper 751164.
6. Rüdiger Weissner, "A Comparison of Advanced Belt Systems Regarding Their Effectiveness," SAE Paper 780414.